# DEDICATED TO DR. DR. HAIO HARMS ON THE OCCASION OF HIS 60TH BIRTHDAY

**If you want to build a ship, don't drum up the men to gather wood, divide the work and give orders. Instead, teach them to yearn for the vast and endless sea.**
(Antoine de Saint-Exupéry, *"The Wisdom of the Sands")*

When we chose this citation as the motto for this issue of the Lenzinger Berichte we had two reasons: It is a good motto for people doing research and development on wood and the products made from it.
Moreover, it inevitably crosses one's mind if asked to congratulate Haio Harms on the occasion of his sixtieth birthday. Since sixty years is a long time and Haio Harms is a person who does not spend his time idly, we will highlight only a few aspects of his (professional) life.
Haio Harms, born 1950, studied chemistry at the University of Vienna with the focus on physical chemistry. Since he deemed an education in natural sciences a little one sided he counterbalanced it by studying law. Needless to say that he finished both with a doctoral degree. He started his industrial career in the research department of the Lenzing AG in Austria in 1983 and worked for Lenzing AG for 25 years, holding management positions in Asia (Technical Director, then CEO of the Lenzing subsidiary P.T. South Pacific Viscose) and in Austria (amongst others: Head of Strategic Planning, Head of R&D, Head of Legal Services). He held the position of an Executive Vice President before he became managing director of the Kelheim Fibres GmbH in Kelheim, Germany.
In addition to his many managerial obligations he always found time to give passionate talks (he was one of the first to promote the wood refinery concept) at many occasions. Moreover he was/is lecturing at the universities of Graz and Leoben (both Austria), the University of Stuttgart (Germany) and at the Ecole des Mines de Paris (France).
He is a leading member of many organisations because of his leadership abilities and his resoluteness to promote and realise his ideas.

Past and present memberships are:

- advisor at the *Forschungskuratorium Textil* (Eschborn Germany);
- FP7-Theme 2 member of the Advisory Committee, DG Research, Brussels;
- value chain leader "Specialities and New Businesses" of the European *Forest*-Based Sector *Technology Platform* (*FTP*);
- member of the governing council of the European Technology platform for the Future of Textiles and Clothing;
- president of the Austrian Chemical Society; member of the senate and the board of trustees of the Christian Doppler Society (Vienna, Austria) and
- chairman of the board of the Competence Centre of Wood Composites and Wood Chemistry (Wood K plus) Linz, Austria.

He worked and works with many people and we asked a handful of them to contribute to this honorific article.

*Mr. Herbert Sixta, Professor of Chemical Pulping Technology, Helsinki University of Technology (TKK) and former colleague:*
I experienced Haio as a well-educated personality with a clear attitude and a sense of humour.
It was 1985 in Indonesia when I first met Haio on the occasion of a preliminary environmental assessment of SPV's viscose manufacture. I remember our open discussions and his effective support, which clearly contributed to a successful conclusion of our task.
Ten years later, when Haio was appointed as R&D director, I became a member of his team and our close collaboration started.
He immediately understood that successful research in an industrial environment of no or very little dedicated research at universities requires the initiation of own basic research and the close collaboration with international institutions. Within a very short time Lenzing's R&D succeeded in the participation of several EU projects in prominent and leading positions.
Finally, with the successful application of the two Christian-Doppler laboratories on "Pulp Reactivity" and "Textile and Fibre Chemistry in Cellulosics" the basis was created to initiate both basic and applied research on cellulose chemistry and technology, relevant for the current and future business of the company. With this initiative Haio managed to line-up with the pioneer times where so prominent researchers like Kleinert, Mark, Treiber, Kratky, Schurz, and Krässig contributed to Lenzing's research.
He continued his efforts in establishing highly funded fundamental and applied research when he realized the opportunity of the newly established funding programme KPLUS. He promoted the application of a wood chemistry programme tailored to Lenzing's needs, which was approved and realised within the Competence Centre of Wood Composites and Wood Chemistry (Wood K plus) in 2001 and successfully re-approved in 2008.

*Mr. Boris Hultsch, managing director of Wood K plus:*
Mr. Haio Harms has been a major player in the positive development of the Competence Centre of Wood Composites and Wood Chemistry because he is a man of vision and of high commitment to a chosen task, who also exercises due care for the important details. He is a reliable partner as the chairman of the board not only for the centre but also for its network. Our subjects *wood composites and wood chemistry* gained the proper place in the Austrian and European research communities owing to his tireless promotion in various bodies, work groups etc.

*Mr Bruno Lindorfer, managing director of the OÖ. Technologie- und Marketing-gesellschaft m.b.H. (TMG):*
Dear Haio,
it is a great honour for me having been asked to write some lines for you on the occasion of your 60th birthday! I have known you for approximately 15 years.
I met you at many conferences on R&D strategy and of course many many times in "our" CDG.
I do intentionally say "our" CDG, because I really feel, that persons like you, Prof. Krieger, Prof. Affenzeller, Dr. Hribnerik, and myself have not only been members of the CDG Senat and the CDG Kuratorium, but have really designed and formed the CDG over the years. What I always have admired and valued has been your clear logic of argumentation in research discussions, may the subjects be as difficult as IPR regulations between a CD-Lab, the university, and the industry partner. You have been the ultimate obstetrician ("Geburtshelfer") for the new *Rahmenvertrag* between the CDG and the

universities in 2007.
In addition to that you always kept your sense of humour (even after we had to tell you in 2003 that it had been decided, that LENZING was not admitted to join the Knet MET with its fibre solidification project).
You have been and will always remain an enthusiastic and igneous promotor of (application oriented) basic research and you are not becoming tired of pointing out the importance of both, basic research and applied R&D. I know you have been running on a high workload for many many years. Be it in Lenzing, in Indonesia, in Germany, or in the *Sensengasse* in Vienna.
So please take some time now and relax and celebrate your 60th Birthday with your family and close friends. I do wish you all the best! Bruno (Lindorfer - to distinguish from Bruno Hribernik)

*Mr Erich Leitner, managing director of the Austrian Chemical Society:*
At first glance he is one of the 1800 members of the Austrian Chemical Society, who started his membership early in his career. He came into focus when he participated in the working group for renewable raw materials, where he impressed the participants and the chairman by his charming way of clearly stating his position and his ability to represent the interest of his company in his unique style without neglecting the viewpoint of others.
These skills recommended him to be the best candidate for the presidency of the Society. It is important to mention that he received acceptance and support by the leading academic members, who normally are very critical of (not only) the scientific qualification of those, who do not continue their academic career at university.
So he managed the challenge by sacrificing a lot of his leisure time.
He has enormous energy to realize a project and to finalize it in a short time without pressuring others. He analyses a situation very fast, reacts flexibly, selecting the right words to convince people what's necessary and to set priorities to maximize the outcome of his actions. The following is a very typical example of his efficiency: the traditional *Monatshefte für Chemie* nearly collapsed due to inadequate actions by certain employees of the publishing house. Attempts to solve this problem by different interventions and discussions failed. Then he decided to intervene personally. He organized, even neglecting his own holidays, all the steps immediately necessary in order to make the future for this journal certain. Today the stage for further success is set.
One of his most admirable talents is his ability to be a careful listener and to integrate other's points of view into his concept in such a way as if it has been part of the plan right from the start. He respects every co-operative person and lets them know his appreciation. Very few can claim this character trait.
To sum up, the Society values his down-to-earth creativity: He is no dreamer, he's a man of action, he doesn't have a heavy hand. Like Saint-Exupéry who recommended, if one wants to build a ship one should not explain how to do it, but better one should awaken the yearning to sail over the sea – Haio Harms fosters enthusiasm in others in the same way. In addition he uses friendly encouragement to reach the goals. There are a lot of them to mention. He showed the path to renew the journal for members in the *Nachrichten aus der Chemie*. He started the active participation of Austrian neighbouring countries at the Austrian Chemistry Days and convinced the Austrian members to dare to use the language of science exclusively at those events. In addition during his presidency financial consolidation continues to proceed.
At least: How does he handle mistakes and difficulties of others? He never assigns blame. In every case he steps up to the plate and finds a solution. So working with

him and for him is always pleasant and productive.

*Mr. Andreas Kleinschmit von Lengefeld, manager of the Forest-Based Sector Technology Platform (FTP)*
From the beginning Haio Harms took a very active part in the set-up of the Forest-Based Sector Technology Platform (FTP) and its subsequent development. The implementation of the value added chain *Biorefinery/ Specialities/New Businesses* became a success because of his many years of experience and knowledge in this area.
A very important field of action, namely the cooperation within and the development of fractions of the forest-based sector has been initiated thanks to his invaluable work. Haio Harms stands out due to his great commitment, his diplomacy and ease on the international stage, and due to his ability to motivate.

*Ms Hedda Weber, area manager Wood K plus and former co-worker:*
There are so many things already said, which I assent wholeheartedly, that I will add just a few.
I worked with Haio Harms during his time as head of research at Lenzing. I experienced him as a man of great leadership abilities as well as a mentor. During this time span he was not only the head of research department he also led a small working group on innovative cellulosics. He set the general direction trusting that we will do the right things and hence he refrained from meddling. He challenged our ideas, results etc. but he refrained from nagging. During our meetings he brought forward many new ideas, which we of course felt free to challenge as well. In conclusion it was a very fruitful time for all of us.
Haio sparked my interest in wood (bio-) refineries and paved my way for entering the international wood refinery community.
Last but not least we very often had a good giggle since he has a splendid sense of humour.
Haio, all the best for the years to come and enjoy your birthday!
Hedda (on behalf of all of us)

Lenzinger Berichte 87 (2009) 1-10

# THE FOREST-BASED SECTOR VALUE CHAIN – A TENTATIVE SURVEY

**Alfred Teischinger**

University of Natural Resources and Applied Life Sciences (BOKU), Dept. of Material Sciences and Process Technology, Vienna, Austria and Kompetenzzentrum Holz GmbH (Wood K plus), Linz, Austria

Phone: (+43) 1 47654-4251; Fax: (+43) 1 47654-4295; E-mail: alfred.teischinger@boku.ac.at

**"Value chain" and "value added" are frequently used terms in management and economic policy. The paper provides a general overview on a value chain and some specific value added items are discussed in detail. Furthermore the European forest-based sector is introduced and structured into several value chains, specific data concerning the sector are provided and a process-based analysis of value added in the forest products industries are provided as well. Finally detailed information on the gross value added of the forest-based sector in Austria including the downstream branches is given. Finally the incoherent database of the sector is criticized.**

**Keywords:** *value chain, value added forest products, forest-based sector*

## Introduction

A value chain describes the full range of activities which are required to bring a product or service from conception, through the different phases of production (involving a combination of physical transformation and the input of various producer services), delivery to final consumer, and final disposal after use [1]. Each process step of the chain of activities gives the product more added value. The added value can be seen as the difference between expenses (materials etc.) to produce and the sales price of the product. The term "added value" of a production process is used in various forms also as discussed by [15].

The "value chain" is a concept from business management that was first described and popularized by Porter [2] in order to understand the behaviour of costs and the existing and potential sources of differentiation and categorizes the generic value-adding activities of an organization/enterprise. The five "primary activities" include: inbound logistics, operations (production), outbound logistics, marketing and sales (demand), and services (maintenance). The four "support activities" include: administrative infrastructure management, human resource management, technology (R&D), and procurement (figure 1).

The costs and value drivers are identified for each value activity. The value chain concept quickly made its way to the forefront of management thought as a powerful analysis tool for strategic planning and has been extended beyond individual organizations. What Porter first described for a single enterprise can also be applied to complete supply chains and distribution networks.

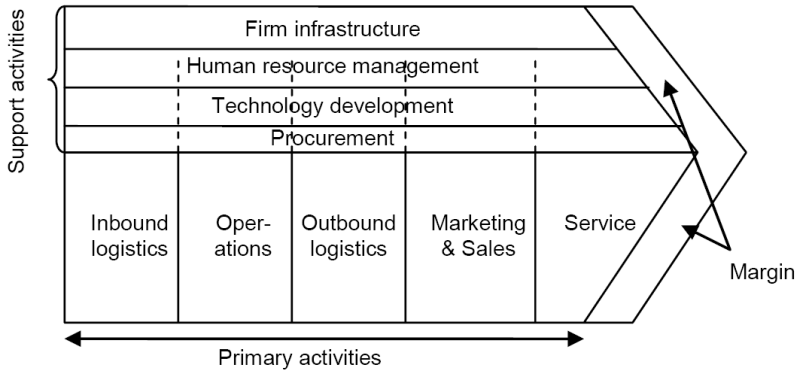


**Figure 1.** The generic value chain according to [2].

The delivery of a mix of products and services to the consumer will mobilize different economic factors, each managing its own value chain. The industry wide synchronized interactions of those local value chains create an extended value chain, sometimes globally. Porter terms this larger interconnected system of value chains the "value system".

Ritsch [3] analyzes the various forms of "value-adding processes" such as the value-adding chain and the value-adding network and provides a definition of terms such as value added, value chain and other inter-enterprise cooperation concepts. A general demonstration of a value-adding network, containing Porter's intra-enterprise value adding and the inter-enterprise value adding is given in figure 2.

This leads to the current understanding of a "Value Chain" as an alliance of consecutive collaborating enterprises (sometimes also referred to as "vertically collaborating") to achieve a more rewarding position on the market. Consecutive or sequential alignment means that companies are connected from one end of the primary production process (e.g. forestry), through processing, and possibly into the final marketing stages where customers purchase retail or consumer products.

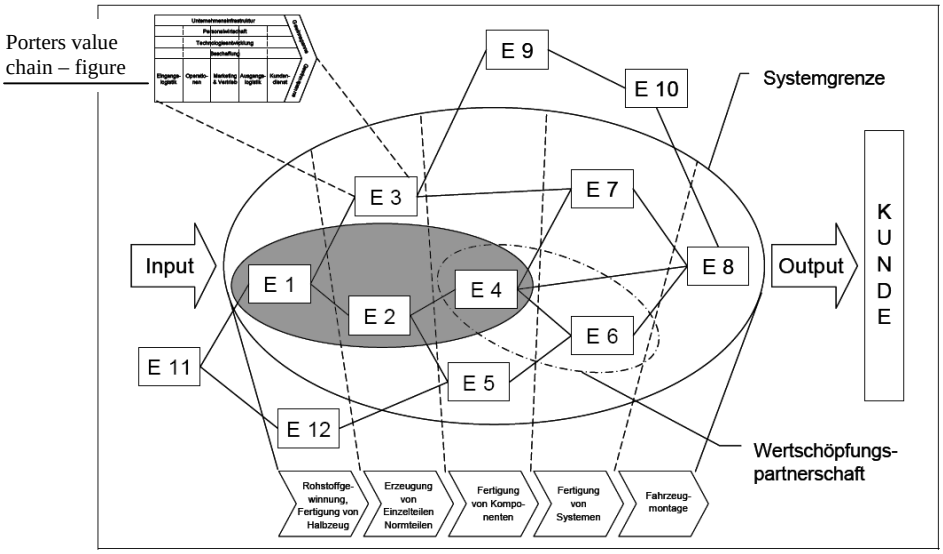


**Figure 2.** Example of a value adding network according to [3]. E = single enterprise within the network; Systemgrenze = boundary of the system; Wertschöpfungspartnerschaft = value-added partnership; Kunde = customer.

While companies in a value chain are legally independent operations, they become interdependent because they have common goals and work collaboratively to achieve them [4]. They work together over the long term discussion issues and troubleshooting problems, which also makes the difference to the traditional supply chain.
There are three general triggers for developing a value chain such as [4]:

- improving quality
- increasing system efficiency
- developing differentiated products

But there are also many other additional reasons why to build up, analyze and depict value chains such as politico-economic (e.g. basis for political decision), socio-economic (e.g. societal and ecological drivers) or technological reasons etc. Speaking about a value chain or a supply chain and their management is much of how to approach these concepts and is also beyond the scope of this paper. For a more detailed insight into this topic we refer to the relevant literature such as [4], [5] etc., but we also want to draw the attention to some critical thoughts about supply chain management given by [6]. Bretzke reveals the inherent shortcoming of these concepts and substantiates his claim for open, loosely coupled polycentric networks which exploit the benefits of a better mutual information about demand and capacities on the market.
An important step is to transform the value chain from a heuristic to an analytical concept, where the various activities in the chain – within firms and in the division of labour between firms etc. are subject to what Gereffi (cit. in [1]) has usefully termed governance. Governance ensures that interactions between firms along a value chain exhibit some reflection of organization rather than being simply random. Value chains are governed when parameters requiring product, process, and logistic qualification are set which have consequences up or down the value chain encompassing bundles of activities, actors, roles, and functions.
Concerning the concept of chain governance, Gereffi 1999 (cit. in [1]) has made the very useful distinction between two types of value chains. The first describes those chains where the critical governing role is played by a buyer at the apex of the chain. Buyer-driven chains are characteristic of labour intensive industries such as footwear, clothing, furniture and toys. The second describes a world where key producers in the chain, generally commanding vital technologies, play the role of coordinating the various links – producer-driven chains. Here producers take responsibility for assisting the efficiency of both their suppliers and their customers. Producer-driven chains are a reflection of the old "import substituting industrialization order", whereas buyer-driven chains are more attuned to the outward-oriented and networked production systems of the 21st century.

## Forest-based sector value chains

In order to understand an economic sector, specific data and information has to be provided. The forest-based sector is very complex and the boundaries of the sector have not been yet well defined which still makes great trouble in analyzing the sector. On the various levels (e.g. European and national level) different boundaries of the sectors are used (e.g. including the furniture production into the sector or not etc.) and therefore make a common sector documentation very difficult.

*Definition of the forest-based sector*
The Forest Sector Outlook Study [7] has defined the sector as to cover both, forest resources and the production, trade and consumption of forest products and services. Forest products include all the pri-

mary wood products manufactured in the forest processing sector (sawn wood, wood-based panels, paper and paperboard) and the main inputs or partly processed products used in the sector (round wood, wood pulp, wood residues and recovered paper). Secondary or value-added forest products (such as wooden doors, window frames and furniture) are not covered.
The EU-commission "Enterprise and Industry" comprises 35 different sectors of which one of them is the "forest-based industries sector" (http://ec.europa.eu/enterprise/forest_based/index_en.html).
There, the sector includes forestry, wood working, pulp & paper manufacturing, paper & board converting and printing. Wood furniture is part of a separate furniture sector (http://ec.europa.eu/enterprise/sectors/furniture/index_en.htm), but wood-based furniture contributes to the forest-based industry sector. This makes a precise documentation (statistics) of the forest-based sectors and its subsectors and value chains sometimes very difficult.
In 2004, the European Confederation of Woodworking Industries (CEI-Bois), the Confederation of European Forest Owners (CEPF) and the Confederation of European Paper Industries (CEPI) took the initiative to set up the "Forest-based sector Technology Platform" (FTP) (www.forestplatform.org). Very soon, key forest research organizations operating at the European level, such as the European Forest Institute (EFI, representing forest research) and Innovawood (for wood research) and further wood related institutions became actively involved in the FTP. The FTP, thus supported by key stakeholders from the entire forest-based sector, set the aim to define and implement a research and development agenda for the future. In the course of the process of establishing a common understanding and strategy for the future by means of an appropriate governance mechanism represented by a European "Technology Platform", the Forest-based Sector Technology Platform, again, the forest-based sector had to be defined.
The main targets of the chain governance are the development of a long-term strategic research and innovation process of the sector (expressed by a strategic research agenda, which has been developed by the input of about 1000 experts), further a co-ordination of education training, communication and lobbying at EU-level and the various national levels. A survey on the up-to-date activities of the FTP is given in [8].

*Forestry-wood value chains*
The whole forestry-wood sector is very complex and several value chains within the sector can be identified. In the process of formulating a strategic research agenda (SRA) experts in the FTP identified the following value chains in order to boost competitiveness across many facets of the forest based sector in order to develop innovative products and services for changing markets and consumer needs [9]:

- forestry
- wood products
- pulp & paper products
- bioenergy
- specialities (including the wood biorefinery concept)

Based on an implementation structure of the FTP (high level group, management, national support groups etc.) the momentum created, should be kept and further guided in order to achieve the targets which have been envisaged in the "Vision 2030" document [10] and the strategic research agenda (SRA).
Within the value chain "wood products" in the SRA, further chains can be identified, which are documented as the projects "living with wood" and "building with wood". These value and supply chains strongly refer to the Wood CEI-Bois Roadmap 2010 [11] and structures several chain such as the wood in construction

chain or the wood furniture and interior design chain. This Roadmap study was launched with the aim of:

- producing an updated analysis on key factors and challenges affecting the European woodworking industries,
- identifying the opportunities for the sector,
- describing the ideal position and
- producing an action programme for the European woodworking industries towards 2010

within the general vision of "Wood and wood products to become the leading material in construction and interior solutions by 2010".

The final aim of this Roadmap is the establishment of an action programme targeted to the industries, their associations and the authorities.

## Mapping the forest-based sector and mapping of various value chains

*The European forest-based sector*

The economic contribution of branches or sectors to the total economy can be measured by various indicators, generally by their respective gross value added. The European forest-based sector is acknowledged as one of the most prominent industrial sectors within Europe. The sectors main characteristics are shown in table 1 and a comparison to selected other industrial sectors is given in figure 3.

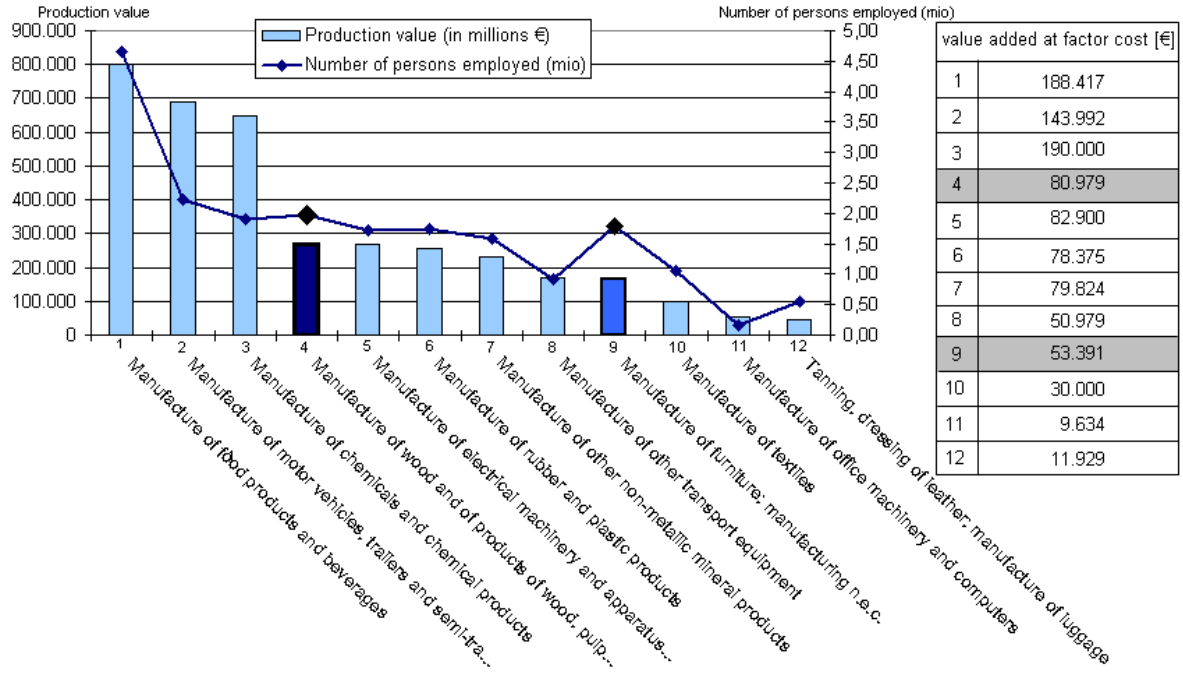


| | value added at factor cost [€] |
|---|---|
| 1 | 188.417 |
| 2 | 143.992 |
| 3 | 190.000 |
| 4 | 80.979 |
| 5 | 82.900 |
| 6 | 78.375 |
| 7 | 79.824 |
| 8 | 50.979 |
| 9 | 53.391 |
| 10 | 30.000 |
| 11 | 9.634 |
| 12 | 11.929 |

**Figure 3.** Key data of selected industrial sectors out of 35 sectors within the EU in 2007 [14]. The graph comprises industrial activities only. The table right provides the value added at factor cost for these sectors.

**Table 1.** Production and employment of the European forest-based sector in EU 25 for 2001 according to [12][1)] and the EU 27 for 2005 according to [13].

| | *PRODUCTION VALUE EUR BILLION* | *VALUE ADDED EUR BILLION* | *NUMBER OF EMPLOYEES* | *NUMBER OF ENTERPRISES* | *VALUE ADDED PER EMPLOYEE 1000 EUR*[2)] |
|---|---|---|---|---|---|
| Wood working | 103.5 | 32.4 | 1 188 400 | 190 600 | 27.3 |
| Manufacture of pulp, paper & paperboard | 73.2 | 23.5 | 254 300 | 2 300 | 92.2 |
| Converting | 76.8 | 23.7 | 487 400 | 16 200 | 48.6 |
| Printing | 103.5 | 43.5 | 1 038 500 | 125 600 | 41.9 |
| FBI[3)] total (2001) | 357.0 | 123.1 | 2 968 600 | 334 700 | 41.5 |
| FBI as percentage of total manufacturing | 6.7 | 8.0 | 8.7 | 15.4 | 81.3 |
| FBI (2005) | 380.0 | 115.7[4)] | 2 987 500 | 350 446 | 38.7 |

[1)] Based on different sources there are big differences in mapping the sector with respect to production value, number of employees and enterprises etc.

[2)] Note the big differences of value added per employee in the various branches, but also the labour-intensive branches such as wood working and printing. There are also big differences of indicators between the various countries such as "value added per employee" (derived from [13]) with more than € 60 000.- (BE, IE, AT, FI, SE) and less than € 10 000.- (BG, LV, LT, RO)

[3)] referred to „forest-based industries" (FBI) by name

[4)] Value added at factor cost

**Table 2.** Total value added by the production of various products from different raw materials (sawlogs, pulpwood, forest residues) expressed by different measures according to [15].

| | *SAWLOGS* | | | *PULPWOOD* | | | *FOREST RESIDUES* | | |
|---|---|---|---|---|---|---|---|---|---|
| | *PER UNIT PRODUCT* | *PER UNIT BIOMASS INPUT (A)* | *PER HA-YR* | *PER UNIT PRODUCT* | *PER UNIT BIOMASS INPUT (A)* | *PER HA-YR* | *PER UNIT PRODUCT* | *PER UNIT BIOMASS INPUT* | *PER HA-YR* |
| Ethanol (GJ) | -1.4 | -0.6 (-4) | -9 | 2.7 | 1.1 (7) | 11 | 3.4 | 1.3 | 10 |
| Methanol (GJ) | 2.0 | 1.3 (9) | 21 | 4.5 | 3.1 (20) | 30 | 4.8 | 3.0 | 24 |
| Dimethyl-ether/ DME(GJ) | 0.5 | 0.4 (2) | 6 | 3.0 | 2.1 (13) | 20 | 3.4 | 2.1 | 17 |
| Fischer-Tropsch-diesel (GJ) | -0.4 | -0.2 (-1) | -3 | 2.9 | 1.5 (10) | 15 | 3.4 | 1.6 | 13 |
| Pellets (GJ) | -1.0 | -0.9 (-6) | -14 | 0.8 | 0.8 (5) | 8 | 1.1 | 1.0 | 8 |
| Electricity (GJ) | -1.0 | -0.5 (-3) | -8 | 2.3 | 1.2 (8) | 12 | 2.8 | 1.3 | 11 |
| Co-generation heat & power (GJ) | 1.6 | 0.7 (5) | 12 | 5.2 | 2.5 (16) | 24 | 5.8 | 2.5 | 20 |
| Market pulp (t) | 191 | 5.3 (34) | 84 | 252 | 7.0 (45) | 69 | | | |
| Newsprint (t) | 186 | 12 (75) | 185 | 214 | 13 (86) | 132 | | | |
| LWC[1)] paper (t) | 449 | 34 (220) | 331 | 472 | 35 (230) | 348 | | | |
| Particleboard (m³) | 169 | 18 (120) | 283 | 185 | 20 (130) | 193 | | | |
| Sawn lumber (m³) | 222 | 17 (110) | 267 | | | | | | |
| Sawn lumber + particleboard (m³) | 318 | 24 (160) | 383 | | | | | | |
| Glued laminated beams (m³) | 1010 | 63 (400) | 990 | | | | | | |
| Glued laminated beams + particleboard (m³) | 1140 | 71 (460) | 1120 | | | | | | |

[1)]LWC … light weight coated paper

(A) …. Units of biomass input are GJ lower heating value for alls 3 raw materials. Input units of m³ ub (under bark) are also shown in parentheses for sawlogs and pulpwood

*A specific process-based analysis of added value in forest product industries*

As shown in table 1 the value added can be expressed by means of different indices such as the gross value added, the value added per employee etc. Sathre et al. [15] discuss several measurement indices that can be used to express the value added. Specifically for the forest-based industries he also refers to normalized indices such as output value per unit value of biomass input (€/€), which allows a better comparison of the products based on various input and output units (GJ for energy, m³ for sawlogs, tonnes for pulp and paper). Concerning the unique aspect of wood as biomass, it is appropriate to construct indices that evaluate the added value not only from the discrete industrial process, but also from a continuous flow of biomass outputs from the forest that, based on the productivity of a forest stand, can be calculated as added value per hectare-year etc. An extract of Sathre's approach of analyzing the production of 14 different industrial products (output products) using forest biomass as a primary input material is given in table 2.

It has to be emphasized that there are wood-based products and value chains beyond the scope of Sathre's studies, which exhibit an even higher value added. One example is the production of regenerated cellulose fibre in a fully integrated production plant (based on a "wood refinery concept of Lenzing AG") which is given by [16].

Based on a study of Pöyry Forest Industry Consulting (2006) (cit. in [17]) the Confederation of the European Paper Industries (CEPI) presented data on the value added in the European pulp and paper industries and the bioenergy sector in order to demonstrate the significantly higher value added and employment impact of the pulp and paper sector against the wood-bioenergy sector. The study and information on the comparatively low value added and employment impact of the bioenergy sector addressed decision and policy makers and was promoted in a press conference and press releases of CEPI.

*The gross value added of the forest-based sector in Austria*

In a comprehensive study [18] calculated the gross value added of the forest-based sector and the gross added value induced by the sector in downstream branches (figure 3). The figure also exhibits the problems of the definition of the forest-based sector (e.g. including the printing sector, excluding wood related construction industries and furniture etc.), which is discussed in detail by [18] and [19].

Besides the direct added value of the forest-based industries in Austria as shown in figure 3, [18] also calculated the induced added value of the forest-based sector. The downstream branches account for an induced added value of total 488 million Euro in 2004.

As shown in table 1 and several studies (e.g. [13]) the forest-based sector is one of the most prominent industrial sectors in the EU. But forests are much more than a mere source of wood, forests are ecosystems that contribute in many ways to the welfare and well-being of our societies by providing a broad range of ecological and societal benefits. It could also be shown in studies (summarized by [20]) that society as a whole and the single persons are aware of the multiple functions of forests, possibly due to the perceptions of forests as pristine, they are regarded as a symbol for true nature compared to urban or agricultural areas.

However, a number of studies (compiled by [20]) suggest that the general public is not satisfied with the overall condition of forests and people are concerned about forest health, loss of biodiversity, decrease in forest area etc.

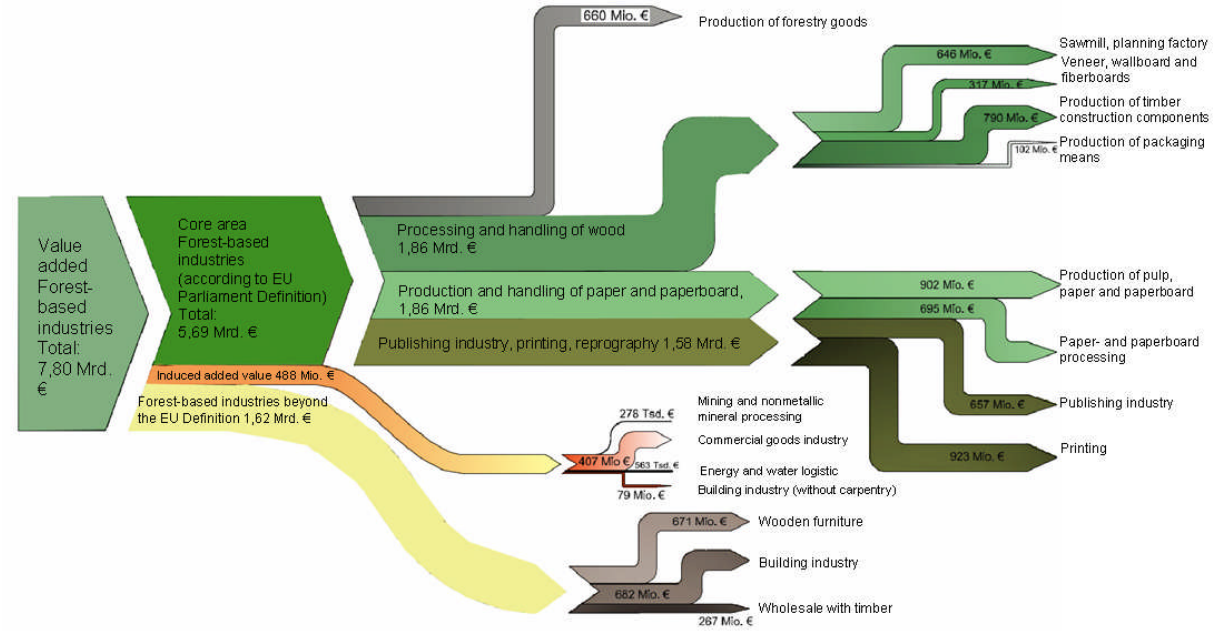


**Figure 4.** Value chain and added value of the forest-based sector in Austria in 2004 according to [18]. The different colours of the value streams account for different sectorial boundaries and statistic database (also compare [19]).
Green streams: account for the EU-statistics for the forest-based sector
Orange stream: induced value added in downstream branches
Yellow/grey streams: furniture, wholesale trade and wood-related construction sector which is accounted for the forest-based sector in Austria but not in the EU-statistics

*Public opinion and consumer attitudes towards the forest products and forest industries*

As modern value-chains are strongly consumer-driven, it is very important for the forest sector to have scientifically based information on current stakeholder attitudes and attitudes of the single consumer in order to anticipate threats and opportunities and to enable forward-looking decision-making in the sector.

The unique compilation of studies about the public opinion and consumer attitudes on the forest products and forest industries by [20] provides a comprehensive survey on the opinion and attitudes towards wood products structured in the perception of wood in general, labelling issues (namely FSC and PEFC), furniture, wood as a construction material, paper products, wood as energy source and forest industries in general.

Summing up the survey one can say that people are in favour of wood, but all stakeholders in the public sphere need reassurances that wood can be utilized reasonably while all other services of the forest ecosystem are sustained. It must be communicated that forest industries are committed to sustainability and environmentally sound processing. A core need of the sector is to gain and maintain the public´s trust and to demonstrate the importance of the sector as a whole.

## Conclusions

The European forest-based sector – which is in the main focus of the current paper – is one of the most important sectors in Europe if one considers its economic size but also its multifunctional impacts on society, environment and the role model for sustainable development as well.

However, no real impact factor exits,

combing the above mentioned multifunctional performances and contributions to society in order to compare the various industrial sectors. Despite of the fact that the sector is often regarded as low tech, there are many examples of high tech solutions based on the raw material wood. The SRA of the FTP is a strong sign for the innovation power of the sector (and so are the various research papers in the current issue of "Lenzinger Berichte, 2009)" which will play a key-role in providing materials and energy in a future post-petrol society.

Analyzing the many statistics and information about the forest-based sector one can see an incoherence in the presentation of the sector, namely the sectors boundaries, a common understanding what the sector comprises and the sector related performance data. In some cases even incorrect data is provided, a situation which has to be corrected/adjusted as soon as possible, the way it has been done at the national level by [21].

## Acknowledgements

I thank both, Mr. T. Stern (Competence Centre Wood K plus) and Mr. P. Schwarzbauer (BOKU) for their kind support and Mr. Stern for his support compiling figure 3.

## References

[1] Kaplinsky R, Morris M (2002) A handbook for value chain research. Prepared for the IDRC. The Open University Library's e-prints Archive (United Kingdom).

[2] Porter M E (1985/1998) Competitive advantage: creating and sustaining superior performance. Free press New York.

[3] Ritsch K (2004) Wissensorientierte Gestaltung von Wertschöpfungsnetzwerken, Dissertation, Technische Universität Graz.

[4] Anonymous (2004) Value Chain Guidebook. A process for value chain development. Agriculture and Food council of Alberta, Nisku, Alberta, Canada.

[5] Kannegiesser M (2006). Value chain management in the chemical industry. Physica Verlag Heidelberg

[6] Bretzke W-R (2006) SCM: Sieben Thesen zur zukünftigen Entwicklung logistischer Netzwerke. Supply Chain Management III/2006.

[7] Anonymous (2005a) European forest sector outlook study (main report), Geneva timber and forest study paper 20, United Nations, Geneva.

[8] Anononymous (2008) Forest-based sector technology platform. The first years. Forest-Based Sector Technology Platform. The European Forestry House, BE-1000 Brussels (www.forestplatform.org).

[9] Anonymous (2006a) Forest-based Sector Technology Platform – A strategic research agenda for innovation, competitiveness and quality of life. www.forestplatform.org.

[10] Anonymous (2005b). Vision 2030 – Innovative and sustainable use of forest resources. A technology platform initiative by the European forest-based sector. CEI Bois, CEPF, CEPI, Brussels.

[11] Wood CEI-Bois Roadmap 2010. http://www.roadmap2010.eu/ on 24.08.2009.

[12] Anonymous (2006b) Wood, paper and printing. Forest-based and related industries in the EU. European Commission, Directorate-General for Enterprise and Industry, Forest-based and related industries Unit, Brussels, European Communities 2006.

[13] Carlsson-Aubry C, Castronova J (2008) Forest-based industries in the EU-27. Eurostat Statistics in focus 74/2008, Luxembourg.

[14] EUROSTAT, 2009, Statistical Database, Structural Business Statistics, 27.8.2009 (compiled by T. Stern).

[15] Sathre R, Gustavsson L (2009) Process-based analysis of added value in forest product industries. Forest policy and economics. 11, 65-75.

[16] Harms H (2006) Hochleistungsmaterialien aus der chemischen Verarbeitung von Holz: Die Holz „Raffinerie“. In: Teischinger A (ed): Hochleistungswerkstoffe aus der Natur/High performance mater-ials from nature. LIGNOVISIO-NEN Bd. 14. Universität für Bod-enkultur Wien, p 27-34. ISSN: 1681-2808.

[17] Dworak O (2008) Wertschöpfung in der Papier- und Zellstoffindustrie. Nachwachsende Rohstoffe, No 47, p 4, ISSN 1993-1476.

[18] Neubauer F-J (2009) Die Wertschöpfung der österreichischen Forst und Holzwirtschaft inklusive nach gelagerter Branchen. Schriftenreihe des Instituts für Marketing und Innovation, Band 2, Universität für Bodenkultur Wien, ISSN 2074-1022.

[19] Schwarzbauer P (2008) Die österreichische Forst-, Holz- und Papierwirtschaft. Größenordnungen – Strukturen – Veränderungen. In: Teischinger A, Tiefenthaler B (2009) Ergebnisbericht des Projektes Technologie – Roadmap Holz in Österreich. LIGNOVISIO-NEN Band 23. Universität für Bodenkultur Wien. ISSN: 1681-2808 (www.map.boku.ac.at/lignovisio-nen.html).

[20] Oberwimmer R (2007) Public opinion/consumer attitudes on forest products and forest industries in the UNECE Region. Master Thesis. University of Natural Resources and Applied Life Sciences (BOKU), Vienna, Austria.

[21] Teischinger A, Tiefenthaler B (2009) Ergebnisbericht des Projektes Technologie – Roadmap Holz in Österreich. LIGNOVISIO-NEN Band 23. Universität für Bodenkultur Wien ISSN: 1681-2808 (www.map.boku.ac.at/lignovisio-nen.html).

Lenzinger Berichte 87 (2009) 11-15

# IMPACT OF FUNGAL ACTIVITY ON VOC EMISSIONS FROM PINE WOOD PARTICLES

**Daniel Stratev[1,2], Thomas Ters[3], Cornelia Gradinger[1,2], Kurt Messner[2], and Karin Fackler[2]**

[1] Competence Centre for Wood Composites and Wood Chemistry – Wood Kplus, Linz, Austria
[2] Institute of Chemical Engineering, Vienna University of Technology, Vienna, Austria
[3] BOKU, Department of Material Sciences and Process Engineering, University of Natural Resources and Applied Life Sciences, Vienna, Austria

phone: (+43) 01 58801 17241; Fax: (+43) 01 58801 17249; E-mail: karin.fackler@tuwien.ac.at

**The influences of selected fungal strains on the emissions of volatile organic compounds from pine sapwood particles were investigated. Volatiles were measured during incubation and after heat sterilization using SPME-GC/FID. Secondary VOC emissions, namely short chain aldehydes like hexanal were completely inhibited by all fungi investigated throughout the incubation period. After heat sterilization hexanal emissions could be detected again in some samples. One fugal strain looks promising for possible industrial applications.**

**Keywords:** *pinewood;* Pinus sylvestris*; VOC emissions; sapwood; SPME;* Diplodia sp., Hypocrea pilulifera*;* Ophiostoma piliferum*;* Phlebiopsis gigantea; Sphaeropsis sapinea; Trichoderma sp.*; hexanal; terpenes; sesquiterpenes; toluene.*

## Introduction

The development of the consumer protection legislation in the industrialized countries has led to the introduction of standards and methodologies for the measurement of volatile organic compound (VOCs) emissions from end products [1-4]. These kinds of regulations concern to a great extend the building and housing industry in which the end consumer is normally not involved in choosing the quality of the materials used. The cited norms thus are supposed to additionally assure the protection of the consumer's health.

The emissions of VOCs from materials under normal conditions depend on their content of substances with low evaporation enthalpies, but can also depend on the content of easily degradable or oxidizable substances, which can also form volatile compounds.

Pinewood is a widely used raw material for the production of building products. The typical VOCs, emitted from pinewood products, are terpenes of the resin and aldehydes, which are concerned to be products of the autoxidation of unsaturated fatty acids and their derivates [5].

It is known that certain wood inhabiting fungi can degrade and mineralize wood extractives while growing on wood. This effect has been tested and applied to solve pitch problems in the pulp and paper industry [6].

In this work, we describe a two-stage experiment, in which it was examined, how preselected fungal species influence the VOC emissions of pinewood strands during their growth on wood, and after

heat sterilization of the incubated wood samples. The results from the first stage of the experiment are of importance for the determination of the biochemical interactions of the living organisms with the wood; the second stage results characterize the industrial application potential for reducing VOC emissions of the fungi used in this work.

## Materials and methods

*Fungal strains:*
Cartapip® 97 (*Ophiostoma piliferum*) - albino strain, related to *Ophiostoma ulmi*, used in biopulping for the pitch control in pulp mills [6];
Rotex® (*Phlebiopsis gigantea*) - strain used as biocontrol organism against root rot, caused by *Heterobasidion annosum* [7];
LC3 (*Hypocrea pilulifera*) - albino strain of the mold fungus *Trichoderma*, used as biocontrol organism against *Sphaeropsis sapinea*, causing sapstain of pinewood [8];
W16 (*Sphaeropsis sapinea*) - fast growing ascomycete, causing sapstain of pinewood.
Fungi were pre-incubated on malt extract agar (MEA) for one week before use. Pine sapwood particles <2mm were prepared by milling at 12000 rpm in a Retsch ZM200 ultracentrifugal mill. A gamma-ray sterilization method (25.5 kGy/min; EN ISO 9001:2000) was chosen for sterilizing the particles in order to avoid possible VOC profile changes which occur after thermal pre-treatment of pinewood [9, 10]. 0.4 g (dry weight) of wood particles filled in 20 ml headspace vials were inoculated.
The inoculums were prepared by mixing one well overgrown MEA plate from each fungal strain for 25 sec in 150 ml distilled water using a Waring® blender. The overall moisture content of the wood-inoculum mixture was calculated to be approximately 200%.
VOCs collected from these vials were measured for a period of 28 days during the incubation (stage 1), and for another 28 days after a thermal sterilization of the vials by 105°C (stage 2). Headspace vials were put in an incubator at 25°C and were purged every 48 hours with 60 ml air through two 0.45 µm sterile cellulose IWAKI filters (
Figure 1). The VOC measurements for stage 1 were always made directly before air rinsing using a manual SPME (solid phase micro extraction) fiber holder equipped with a 75 µm CAR/PDMS fiber (Supelco). The fiber was exposed to the headspace for 30 min at 25°C. For stage 2 the headspace vials were hermetically sealed and no air purging occurred. The fiber was introduced to an Agilent 6890N GC/FID equipped with a 30 m DB5 (0.25 mm x 0.25 µm) column using helium as carrier gas. The injector temperature was set to 270°C. The oven program started at 40 °C for 4 min and raised to 320 with 5°C/min. The qualitative determination of volatile substances was carried out through measurement of control wood samples on another GC, equipped with a MS detector using the same column and followed by a Kovats-Index calibration.
GC analysis of the acetone extracts (ASE) of the samples during both experimental stages was carried out additionally; results are not shown in this work.

**Figure 1.** Incubation of fungal inoculated particles in SPME vial.

## Results and discussion

*VOCs during fungal growth (Stage 1)*
Each microorganism changed the VOC emission profile during incubation in a typical way. All fungi completely suppressed the emission of hexanal during the whole first stage (Figure 2). It was interesting, that the hexanal emissions revived after sterilization of the treated samples (stage 2); however to a different extent for each sample type.

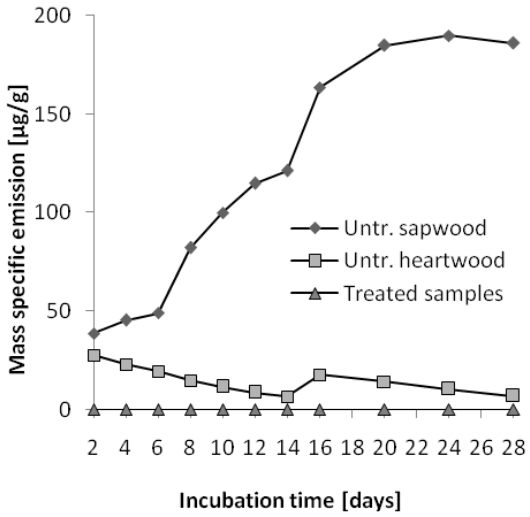


**Figure 2.** Hexanal emissions during fungal growth on pine sapwood particles.

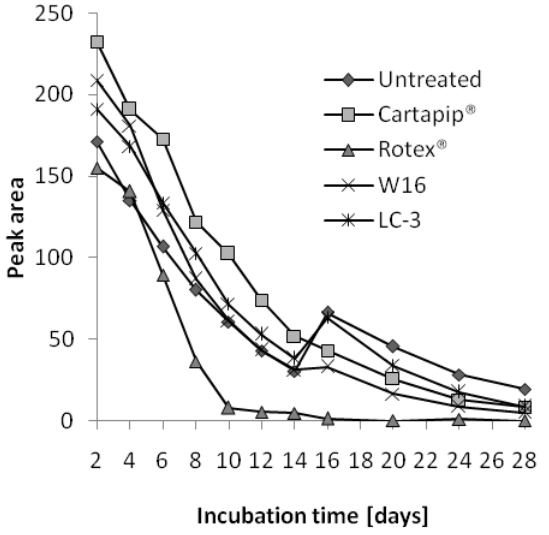


**Figure 3.** Monoterpene emissions during fungal growth on pine sapwood particles.

Other typical characteristics of the treated samples were the rapid reduction of the monoterpene emissions and the increase in toluene emissions after day 4 for Rotex® (Figures 3 and 4) as well as the 20-fold increase of the emissions in the 1300-1560 (Kovats index) region for Cartapip® (Figure 5). Although the last substances were not identified, it can be assumed that they belong to sesquiterpenes, which have Kovats retention indexes in the same region.

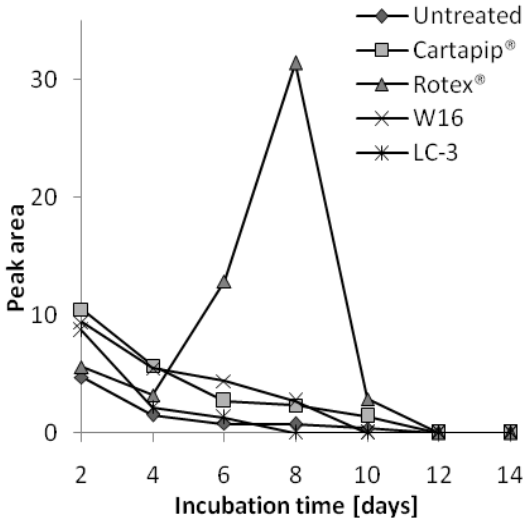


**Figure 4.** Toluene emissions during fungal growth on pine sapwood particles.

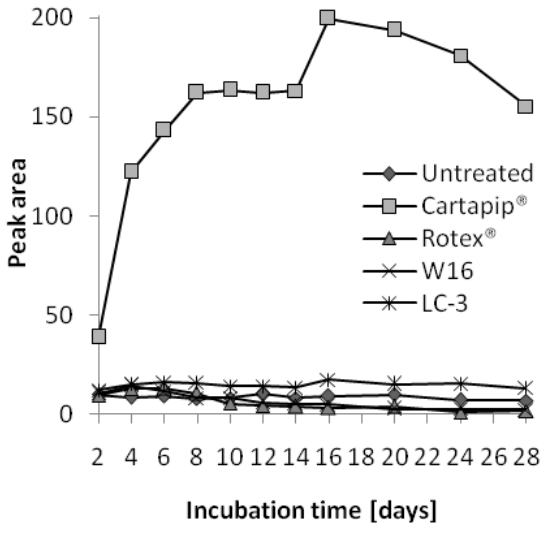


**Figure 5.** Sesquiterpene emissions during fungal growth on pine sapwood particles.

*VOCs after sterilization (Stage 2)*
After heat sterilization for 3 hours at 105°C (filters and lids were removed), the vials were sealed and two subsequent emission measurements were made in 14 days intervals.
Hexanal was the substance which made more than 85% of the chromatographic peak surfaces in the C7-C16 (VOC) region. Terpenes concentrations were too low to be quantified properly. Therefore only the hexanal emission is shown in figure 6.
Samples treated with Cartapip® and Rotex® showed a tangible reduction in their mass specific hexanal emissions compared to the untreated samples. W16 treated samples however, emitted more hexanal than the control sample. LC-3 treated samples emitted equal (to controls) amounts during the first 2 weeks and less during the following 2 weeks.

## Conclusions

The growth of fungi on/in pine wood particles leads to a shift in the typical VOC emission profile of the treated samples. Some of the emitted substances are stable enough over longer periods and could therefore possibly be used as biological markers (sesquiterpenes for *Ophiostoma sp*.).

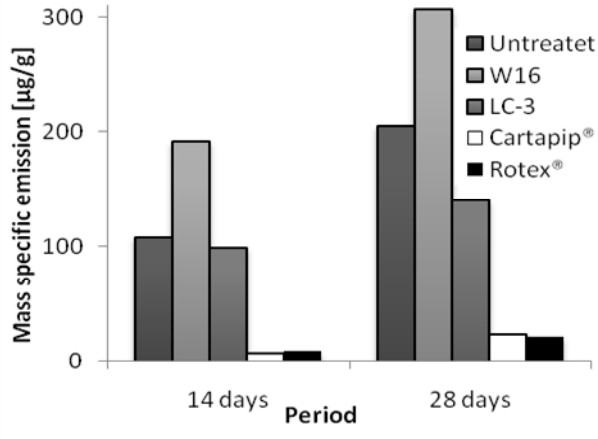


**Figure 6**. Hexanal emissions from fungal treated and thermal sterilized pine sapwood particles.

These substances may probably be also involved in symbiosis between bark beetles and associated fungal organisms [11] for recognizing infected trees.
The total suppression of hexanal emissions during fungal growth on pinewood particles is a phenomenon which deserves further validation and research.
During their life-cycle, microorganisms degrade and utilize many substances, which can be responsible for VOC emissions. Such compounds are e. g. lignin, hemicelluloses, and glycerides of unsaturated fatty acids or unsaturated fatty acids alone. Among the fungi investigated in this study, only Rotex®, a well known white rotter, is capable of degrading lignin. However, the analysis of the acetone extract from Rotex® treated pine strands (not shown), indicates that Rotex® also completely degrades glycerides and unsaturated fatty acids. The ability of *Phlebiopsis sp*. to degrade pitch components has already been described by [12]. Except for lignin degradation, the above statement is also true for Cartapip®[6]. However, the industrial application of Rotex® and Cartapip®, especially under unsterile conditions (e. g. wood yard), may be limited due to their slow growth rates [8, 13] and the degradation of structural wood components (Rotex®). LC-3 and W16 showed higher growth rates; however, glycerides and unsaturated fatty acids were degraded at lower extends (not shown); explaining the higher hexanal emissions in the samples treated with these fungi. W16 was reported to accumulate unsaturated fatty acids in its cell walls [14], which can be the reason for the higher hexanal emissions of W16 treated wood strands compared to the control.
From the industrial point of view, fungal treatment of pine wood for the reduction of VOC emissions of wood products is possible and makes sense when suitable growth conditions can be achieved at the corresponding industrial scale at economic reasonable prices. Such conditions are for

example appropriate incubation temperature, humidity and air supply and availability of time- and timber yard resources. The microorganism of choice must also be characterized by its high growth rate, in order to be competitive with the softwood inhabiting ubiquitous *Diplodia pinea* (*Sphaeropsis sapinea*), which causes excessive blue staining during wood storage. From the three possible alternatives examined in this work (Cartapip®, Rotex®, LC-3) only LC-3 was proven to be an efficient *Sphaeropsis sapinea* antagonist; however its VOC-reducing capabilities were not that pronounced.

## References


[1] Umweltbundesamt Deutschland, Ausschuss zur gesundheitlichen Bewertung von Bauprodukten AgBB, 2008.

[2] California department of health services, Reducing occupant exposure to volatile organic compounds (VOCs) from office building construction materials, 1996.

[3] Ministry of Land Infrastructure and Transport Tokyo, Building Standard Law on Sick House, 2003.

[4] ISO 16000-9, Determination of the emission of volatile organic compounds from building products and furnishing - Emission test chamber method, 2006.

[5] Risholm-Sundman M., Lundgren M., Vestin E., Herder P., Emissions of acetic acid and other volatile organic compounds from different species of solid wood, Holz Als Roh-Und Werkstoff 56 (1998) 125-129.

[6] Farrell R.L., Blanchette R.A., Brush T.S., Hadar Y., Iverson S., Krisa K., Wendler P.A., Zimmerman W., Cartapip(TM): a biopulping product for control of pitch and resin acid problems in pulp mills, Journal of Biotechnology 30 (1993) 115-122.

[7] Greig B.J.W., Inoculation of pine stumps with Peniophora gigantea by chainsaw felling, European Journal of Forest Pathology 6 (1976) 286-290.

[8] Cornelia Gradinger, Tsilla Boisselet, Daniel Stratev, Thomas Ters, Kurt Messner, Karin Fackler, Biological control of sapstain fungi: From laboratory experiments to field trials, Holzforschung (Ahead of Print (ISSN Print 0018-3830)).

[9] Manninen A.-M., Pasanen P., Holopainen J.K., Comparing the VOC emissions between air-dried and heat-treated Scots pine wood, Atmospheric Environment 36 (2002) 1763-1768.

[10] McGraw G.W.H., Richard W.; Ingram, Leonard L., Jr.; Canady, Catherine S.; McGraw, William B., Thermal degradation of terpenes: camphene, Δ-carene, limonene, and α-terpinene, Environmental Science & Technology 33 (1999) 4029-4033.

[11] Klepzig K.D.S., D.L., Bark Beetle-Fungal Symbiosis: Context Dependency in Complex Associations, Symbiosis 37 (2004) 189-205.

[12] Dorado J., Claassen F.W., van Beek T.A., Lenon G., Wijnberg J.B.P.A., Sierra-Alvarez R., Elimination and detoxification of softwood extractives by white-rot fungi, Journal of Biotechnology 80 (2000) 231-240.

[13] Stratev D., Einfluss von Pilzen auf die Qualität von Kiefernholz: Biokontrolle, Harzabbau und Emissionskontrolle, Institut für Verfahrenstechnik, Umwelttechnik und Technische Biowissenschaften, TU-Wien, Vienna, 2008.

[14] A. Moret M.N., Fr. García, C. Montón, Caracterización de aislados de *Sphaeropsis sapinea* (Fr.) Dyket Sutton mediante cromatografía de gases, Boletín de sanidad vegetal. Plagas 21 (1995) 371-376.

Lenzinger Berichte 87 (2009) 16-25

# FORMATION OF INSOLUBLE COMPONENTS DURING AUTOHYDROLYSIS OF *E. GLOBULUS*

**Moritz Leschinsky [1], Hedda K.Weber [1], Rudolf Patt [2], and Herbert Sixta [3]**

[1]Kompetenzzentrum Holz GmbH, A-4021 Linz, Austria
[2] Chemical Technology of Wood, Hamburg, Germany
[3]Lenzing AG, Department ZF, A-4860-Lenzing, Austria

Phone: (+43) 07672-701-3963 E-mail: m.leschinsky@lenzing.com

**Autohydrolysis reactions of lignin leading to the formation of insoluble components and scaling during water prehydrolysis and during handling of the prehydrolysate were studied. Scaling represents a major problem for the extraction of valuable hemicellulose degradation products from the prehydrolysate.**
**Various lignin fractions isolated from autohydrolysis experiments were extensively characterised. In addition, lignin mass balances were established.**
**During autohydrolysis, lignin is degraded to a significant extent through cleavage of aryl-ether bonds resulting in a significant reduction of the molecular weight. Some of the dissolved lignin degradation products remain soluble in the prehydrolysate, while degradation products characterised by a higher molecular weight precipitate upon cooling. Exposure of water prehydrolysates to 170°C leads to the formation of highly condensed precipitates characterised by an increased molecular weight. These precipitates, denoted as PT-fraction, form scaling on the reactor wall. Condensation reactions of soluble and insoluble lignin degradation products dissolved in the prehydrolysate were identified as the origin of the PT-fraction.**

**Keywords:** *autohydrolysis, lignin degradation, residual lignin, MWL, NMR, prehydrolysis kraft pulping, biorefinery*

## Introduction

Dissolving pulps are pure cellulose pulps with an extremely low content of hemicelluloses and lignin. In contrast to paper pulps, hemicelluloses have to be removed during the production of dissolving pulps. This results in low pulp yields of 30 to 40% based on wood, depending on the wood species, the production process and the purity grade of the pulp. The hemicelluloses, which are dissolved together with the lignin in the spent liquors of the production processes, are normally combusted for power generation. However, the approximate calorific value of hemicelluloses of about 14 MJ/kg is low compared to that of about 25 MJ/kg for lignin. Therefore, the hemicelluloses should be used as a source for valuable products. As an example, the dietetic sweetener xylitol is produced on the basis of hardwood hemicelluloses. Also Acetic acid and furfural are products that are formed during acid degradation of hardwood xylan. The Lenzing AG is a representative for the commercial use of hardwood hemicelluloses by selling

xylose, which is the starting product for xylitol. Acetic acid and furfural are extracted from the spent liquors of dissolving pulp production. [1].

Two different processes are used for the production of dissolving pulps from wood: the prehydrolysis kraft (PHK) process and the acid sulphite process. The acid sulphite process is the dominant process for dissolving pulp production. . However, the PHK process has numerous advantages compared to the acid sulphite process, and PHK pulping, particularly of hardwoods, is gaining importance [2, 3]. Nevertheless, recovery of dissolved hemicelluloses is not possible so far. The selective removal of hemicelluloses during the PHK process is achieved through autohydrolysis of the wood chips prior to kraft cooking. During this prehydrolysis step, 15-30% of the dry matter of hardwoods, depending on the intensity of the treatment, is dissolved. At present, steam prehydrolysis conducted at a low liquor to wood ratio is state of the art. The dissolved material is neutralised with alkaline cooking liquor subsequent to steam prehydrolysis and then displaced from the digester [2, 4]. The neutralisation step results in a complete degradation of the dissolved carbohydrates and the neutralisation liquor is combusted. If a water prehydrolysis conducted at a higher liquor to wood ratio is applied without subsequent neutralisation, the resulting prehydrolysate contains important amounts of xylan degradation products but also substantial amounts of lignin [5-7]. The prehydrolysate could represent a rewarding source of carbohydrates. However, insoluble components precipitating from the prehydrolysate tend to form deposits that pose major difficulties during handling and processing of the hydrolysate [8-11]. Measures to handle the scaling and deposition problems have to be developed to allow for the recovery of the valuable hemicellulose degradation products,. Therefore, a better knowledge about the origin and behaviour of the insoluble components contained within the prehydrolysate is required. The most important results of a study investigating the composition of the insoluble components, the reason for their formation and their behaviour are summarized in this paper. The results have previously been published in detail in a series of publications [12-15].

## Experimental

Autohydrolysis experiments were carried out with extractive-free *E. globulus* wood chips with a particle size between 2.50 and 3.55 mm in a Parr reactor station equipped with mechanical stirring and a reactor volume of 450 ml. The reaction was carried out at a water to wood ratio of 5:1 and at 170°C. When attaining the desired reaction time, the prehydrolysate was withdrawn in an isothermal phase separation step and transferred into a second reactor. In general, the prehydrolysate and the wood residue were immediately cooled. In one particular experiment, denoted as “temperature treatment” (TT), the prehydrolysate was separated from the wood at a P-factor of 650 and then further treated under prehydrolysis conditions until a total P-factor of 1570 was attained. The black resinous precipitate formed during this particular experiment on the reactor wall was dissolved in acetone/water (5:1) and denoted as PT-fraction.

In each experiment, insoluble lignin degradation products were isolated from the prehydrolysate by centrifugation (I-fraction) and soluble degradation products were extracted with ethylacetate (Et-O-Ac extract) (Figure 1). Lignin from the original wood and from the wood residues after autohydrolysis was isolated as milled wood lignin (MWL). The lignin fractions were characterised by sugar analyses, methoxy group determinations, elemental analyses, SEC, and quantitative NMR-spectroscopy of the acetylated samples.

The experimental setup, the isolation of lignin fractions and the analytical procedures are described in detail in [15]. Quantification of lignin for the purpose of mass balances was based on Klason lignin and acid soluble lignin determination as described in [13].

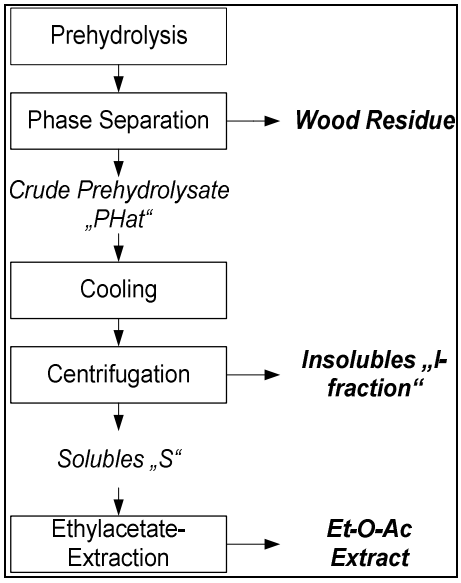


**Figure 1.** Scheme of different fractions obtained from the prehydrolysis experiments.

## Results and Discussion

The insoluble components (I-fraction) contained within the water prehydrolysate were identified as relatively pure lignin. I-fractions obtained from autohydrolysis experiments conducted at 170°C and at a P-factor of 600 showed FTIR spectra that were almost identical to those of lignin isolated from native *E. globulus* wood. Qualitative characterisation using 2D NMR HSQC spectroscopy revealed that the I-fraction contained all structural features typical for native lignin. In addition, some other structural features were found, which were not present in the native lignin that was used as a reference [12]. Subsequently a detailed study of the reactions of lignin under autohydrolysis conditions typical for the PHK process in order to identify the reasons for the formation of insoluble components during water prehydrolysis. . All lignin containing fractions formed during water prehydrolysis were isolated and characterised in order to fully understand the reactions occuring during the autohydrolysis:
Lignin contained in the wood residue was isolated as MWL, soluble lignin was extracted with EtOAc from the hydrolysate and the I-fraction was isolated by centrifugation., MWL was isolated from the native *E. globulus* wood as the reference lignin. These four lignin fractions were then investigated in detail.

*Characterisation of Lignin Fractions*
Native lignin. MWL was isolated from the native wood yielding 46% based on the Klason lignin content. Comparison of analysis results of this MWL with recent literature data on eucalypt lignins revealed significant differences. The content of methoxy groups and of β-O-4 bonds was 140 and 35 per 100 phenylpropane units, respectively [14, 15]. These values were clearly lower than the literature values for eucalypt lignins published by Capanema et al. [16] and Evtuguin et al. [17]. Presumably, differences in the extraction procedure of the wood prior to lignin isolation were responsible for the discrepancy between these values. In the papers cited, wood was extracted with boiling 0.3% NaOH to remove tannins. During this treatment, a portion of lignin rich in guaiacyl and hydroxyphenylpropane units is also removed [18]. For the present investigation, only a mild extraction with acetone/water (9:1) was performed. We tried to avoid changes of the lignin structure and its reactivity so that we could draw clear conclusions concerning the autohydrolysis process. The differences between our values and those reported in the literature may also be explained by the presence of residual amounts of polyphenolic impurities and an alkali-soluble lignin fraction rich in guaiacyl and hydroxyphenylpropane units in MWL isolated from sources not subjected to

alkaline pre-extraction. However, the amounts of primary and secondary aliphatic hydroxyl groups and phenolic hydroxyl groups found in the native MWL are in agreement with values published for E. grandis MWL (Capanema et al. 2005).

Prehydrolysed lignin fractions. FTIR spectra of all lignin fractions isolated from the same water prehydrolysis experiment conducted at P-factor 670 showed the typical lignin bands in the fingerprint region. A yield of 1.4% (based on wood) of the I-fraction was obtained and 1.3% (based on wood) of the EtOAc extract. The amount of the EtOAc extract corresponded well to the concentration of soluble lignin in the prehydrolysate as determined by UV/Vis spectrometry. It was concluded that the extraction was efficient. Comparison of the FTIR spectra of the prehydrolysed lignin fractions to the spectrum of native lignin revealed that prehydrolysis initiated changes in all lignin fractions.

All prehydrolysed lignin fractions exhibited a higher carbon content and lower oxygen and hydrogen contents compared to native lignin. This was attributed to condensation reactions and to the elimination of hydroxyl groups. Quantitative NMR spectra confirmed an increased degree of condensation of the aromatic ring and a reduced content of aliphatic hydroxyl groups in all prehydrolysed lignin fractions. All prehydrolysed lignin fractions had an increased content of phenolic hydroxyl groups, indicating the occurrence of cleavage reactions of the aryl-ether bonds of lignin during prehydrolysis. In addition, all fractions showed a reduced content of β-O-4 bonds, compared to native lignin.

The cleavage reactions resulted in a molecular weight reduction of all fractions compared to native lignin. SEC revealed a slight but significant reduction in molecular weight of the lignin from the residual wood. The EtOAc extract was composed of low molecular weight lignin degradation products, containing substantial amounts of monomers. The I-fraction comprised components with a molecular weight between MWL and EtOAc extract. The SEC chromatogram of I showed strong overlapping with both, MWL and EtOAc extract (Figure 2).

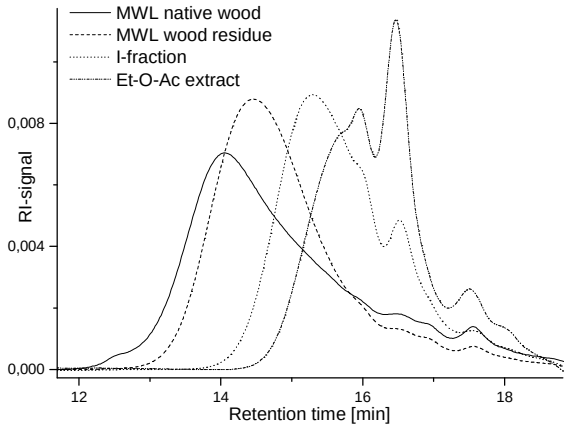


**Figure 2.** SEC chromatograms of the different lignin fractions obtained from native wood and from water prehydrolysis at 170°C and a P-factor of 670.

The results of SEC were in agreement with the content of β-O-4 bonds and phenolic hydroxyl groups in the lignin fractions. The low molecular weight EtOAc extract showed the lowest content of β-O-4 bonds and the highest one in phenolic hydroxyl groups. The I-fraction contained intermediate amounts of β-O-4 and phenolic hydroxyl moieties, while the MWL isolated from the wood residue had the highest content of β-O-4 bonds and the lowest one of phenolic hydroxyl groups. Thus, although an increased degree of condensation was found in all prehydrolysed lignin fractions by NMR, prehydrolysis resulted in a reduced molecular weight of all fractions compared to native lignin. It was concluded that degradation reactions prevailed over condensation reactions at P-factor 670. The chemical structure of condensation products could not be identified using NMR spectroscopy. Condensation of Cα of

the phenylpropane side chain with the aromatic ring resulting in diphenylmethane structures is often assumed to occur under acidic conditions [19, 20]. However, no diphenylmethane structures could be detected in any of the investigated lignin fractions.

The FTIR spectrum of the EtOAc extract indicated a high content of carbonyl groups. Using NMR spectroscopy, syringaldehyde and sinapaldehyde were detected as the major products in this fraction, which was otherwise a complex mixture of various lignin degradation products. Syringaldehyde and sinapaldehyde are reaction products, which are typical for a homolytic reaction mechanism during cleavage of β-O-4 bonds [21]. In the EtOAc extract and in the I-fraction, an increased amount of β-β (resinol) structures was detected. Resinol structures are typical reaction products of radical coupling reactions of reaction intermediates which are formed during the homolytic cleavage of β-O-4 bonds. Based on the presence of these typical reaction products, it was concluded that homolytic cleavage of β-O-4 bonds occurs during water prehydrolysis.

In conclusion the lignin underwent extensive degradation reactions and structural changes during water prehydrolysis at a P-factor of 670 [15]. Lignin degradation products were dissolved in the prehydrolysate only in small amounts due to their limited solubility in the acidic aqueous medium. Low molecular weight products remained in solution, while products with a higher molecular weight precipitated upon cooling, forming the I-fraction. The main reaction of lignin during water prehydrolysis was the homolytic cleavage of aryl-ether bonds. Condensation reactions also occurred, but the cleavage reactions prevailed.

*Influence of Autohydrolysis Intensity on the Chemical Structure of Lignin Fractions*

The intensity of autohydrolytic treatments strongly influences the reactions of lignin. Fast cleavage reactions prevail in the beginning of the reaction, whereas, slower condensation reactions result in a molecular weight increase at increasing autohydrolysis intensities [22]. These consecutive reactions lead to an optimum autohydrolysis intensity with maximum lignin removal in subsequent pulping stages. This optimum was attained at a P-factor of approximately 700 during PHK pulping of *E. urograndis* [23]. The changes in the lignin composition and functionality at prehydrolysis intensities higher and lower than this optimum were also examined for the following reasons:

- It should be clarified if carbohydrate degradation products contribute to the condensation reactions.
- It has been published that scaling problems increase under extensive prehydrolysis conditions.
- It was unclear if the lignin degradation products dissolved in the hydrolysate undergo condensation reactions resulting in an increased molecular weight.
- No quantitative information on the extent of lignin degradation and on the chemical structure of lignin degradation products formed during water prehydrolysis has been published yet.

Therefore, lignin fractions were isolated from water prehydrolysis experiments at P-factors of 320, 670 and 1540 and compared to each other [14]. The most important findings are:

The content of carbohydrate impurities in the MWL isolated from the wood residues was reduced with increasing P-factor. This was attributed to the progressive cleavage of the bonds between lignin and carbohydrates. The content of methoxy groups in the MWL fractions was

independent of the P-factor. It was concluded that sugar degradation products did not contribute to the MWL and that no demethoxylation reactions occurred during water prehydrolysis. Quantitative NMR spectroscopy revealed that the substitution pattern of the aromatic ring in the residual lignin changed with increasing prehydrolysis intensity. Protons were replaced and the degree of condensation increased, whereas oxygen substitution did not change to a significant extent. Strong lignin degradation was evident in the decrease in molar amount of β-O-4 bonds. Compared to native lignin, the β-O-4 content halved after treatment at a P-factor of 1540. Primary and secondary hydroxyl groups showed a similar trend and their content was also reduced by 50%. At the same time, the content of phenolic hydroxyl groups doubled. The progress of the most significant structural changes in MWL during prehydrolysis is given in Figure 3.

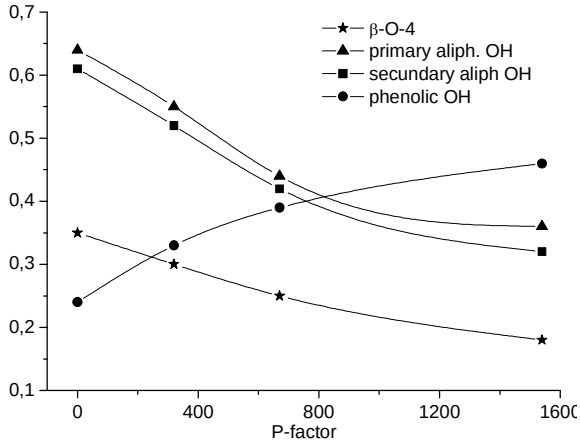


**Figure 3.** Development of the abundance of selected functional groups in the MWL as a function of the prehydrolysis intensity.

The important decrease in aliphatic hydroxyl groups in residual lignin after autohydrolysis is mainly responsible for the deactivation of the sulphonation reaction in subsequent acid sulphite processes, since these groups represent the reactions sites in lignin for sulphonation.
SEC of the MWL fractions showed a slight but significant decrease of the molecular weight with progressing prehydrolysis intensity. Obviously, in the residual lignin isolated from the wood residues as MWL, degradation reactions prevailed over condensation reactions, even at P-factor 1540. The reduced reactivity towards kraft and organic solvent delignification occurring at these high P-factors could not be explained by the structural changes of residual lignin observed in this study.
The I-fraction was obtained in a maximum yield at P-factor 670. The slightly reduced yield of I-fraction at P-factor 1540 was attributed to its reprecipitation on the wood surface. The molecular weight distribution of the I-fraction was independent of the prehydrolysis intensity. Even at P-factor 1540, no contribution of furfural condensation products could be detected, since the methoxy group content remained constant. However, the I-fraction was subjected to the same kind of reactions as the residual lignin in the wood: With increasing prehydrolysis intensity, progressive elimination of aliphatic hydroxyl groups and β-O-4 bonds occurred, as well as progressive increase in phenolic hydroxyl groups. Concurrently, the degree of condensation increased considerably. The molecular weight distribution of the I-fraction was only slightly affected by the altering P-factor: A minor reduction in the molecular weight was observed with increasing autohydrolysis intensity. The β-O-4 cleavage reactions observed in the I-fractions should lead to a considerable decrease in molecular weight which is not the case. Thus the condensation reactions must counterbalance the degradation reactions. As will be discussed later, high molecular weight components that are formed by condensation reactions from the I-fraction precipitate on the wood surface. The fact that the molecular weight distribution of the I-fraction does not significantly change, regardless to the changes in its chemical structure, proves

that precipitation of the I-fraction during cooling of the hydrolysate is due to its high molecular weight. The yield of the EtOAc extract increased with increasing P-factor. A decreasing methoxyl group content indicated the progressive incorporation of non-lignin products in this fraction. This could be attributed to increasing contents of HMF. In contrast to furfural, HMF is not removed during vacuum evaporation of the EtOAc extract. The concentration of syringaldehyde increased when the reaction time was extended. Sinapaldehyde and resinol structures had maximum concentrations at P-factor 670.

*Amount and Origin of Dissolved Lignin*

Material balances based on Klason lignin and ASL (acid soluble lignin) determinations should reveal what amount of lignin is dissolved at P-factors of 300, 600 and 1500 during the water prehydrolysis process [13]. The material balances confirmed that the I-fraction was maximum at P-factor 600 and was reduced at a higher P-factor of 1500 (Table 1). The bulk of lignin remained soluble in the prehydrolysate and in the wash filtrate even after centrifugation. With rising P-factor, the amount of ASL in the wood residue (WR) was clearly reduced, while the amount of soluble lignin in the hydrolysate was slightly increased. The amount of ASL, which was removed from the wood, corresponded well to the amount of soluble lignin detected in the hydrolysate. It was concluded that ASL contained in the native wood was progressively dissolved during water prehydrolysis. This portion of lignin remained dissolved after cooling and centrifugation of the hydrolysate.

At P-factors of 300 and 600, Klason lignin dissolved only sparingly - about 5-6% of the primary lignin content in the wood. This amount corresponded well to the I-fraction. It was concluded that the I-fraction resulted from dissolution of part of the Klason lignin. This is in agreement with the structural features and the polymeric character of the I-fraction, which clearly demonstrate its origin as a degradation product of native lignin.

At P-factor 1500, a slight increase in the amount of Klason lignin in the wood residue was observed. This increase can partly be explained by the reprecipitation of part of the I-fraction on the wood surface. Condensation reactions of dissolved lignin, of sugar degradation products and of polyphenolic extractives might also contribute to this increased Klason lignin value.

The usual removal of extractives prior to the determination of Klason lignin and ASL values given in Table 1, using soxhlet extraction with ethanol and toluene was omitted. The reason is that a substantial part of the lignin contained in the wood residue dissolves in organic solvents after autohydrolysis. Removal of this solvent soluble lignin portion would considerably falsify the results. Consequently soxhlet extraction was also omitted prior to analysis of the native wood to obtain comparable results. The Klason lignin and ASL contents determined after soxhlet extraction are given in parentheses in Table 1 for comparison.

**Table 1.** Mass balances of lignin.

| P-factor | Klason lignin in wood/WR | ASL in wood/WR | I-fraction | Soluble lignin in hydrolysate + wash filtrate | Total Lignin |
|---|---|---|---|---|---|
| 0 | 243 (229)* | 52 (48)* | - | - | 294 (277)* |
| 300 | 231 | 19 | 11 | 32 | 293 |
| 600 | 230 | 15 | 13 | 35 | 292 |
| 1500 | 239 | 11 | 11 | 36 | 296 |

All values given in g per kg of the original wood; * Soxhlet extraction prior to analysis

*Formation of Condensed Lignin Precipitates*

The worst scaling problems occur in continuous prehydrolysis digesters [8, 11]. Continuous prehydrolysis results in a permanent contact of the prehydrolysate with the inner surface of the digester. It might be expected that storage of prehydrolysates in tanks at high temperature also leads to the formation of scaling problems. One of the main objectives of this study was to identify the origin of the scaling problems. Scaling occurs on any surface available. It was useful to study the formation of scaling in the absence of wood, because the wood represents an additional surface where scaling can take place. Scaling on the wood surface is difficult to distinguish from the wood itself. Hence, to study scaling formation, prehydrolysates were treated under prehydrolysis conditions in the displacement reactor after the phase separation step.

The resinous precipitates deposited on the reactor wall after temperature treatment of the hydrolysate had a similar chemical structure as the I-fraction and were, hence, identified as another form of lignin degradation products [12]. The resinous precipitates (PT-fraction) were characterised by a drastically increased molecular weight compared to the lignin degradation products isolated from a prehydrolysate without TT. This led to the conclusion that the PT-fraction was a condensation product of lower molecular weight lignin degradation products dissolved in the hydrolysate. The molecular weight distribution was broad and components with a molecular weight similar to the I-fraction were included in the PT-fraction as well as components with a higher molecular weight than the native MWL (Figure 4). The molecular weight distribution of the I-fraction was not affected by the TT.

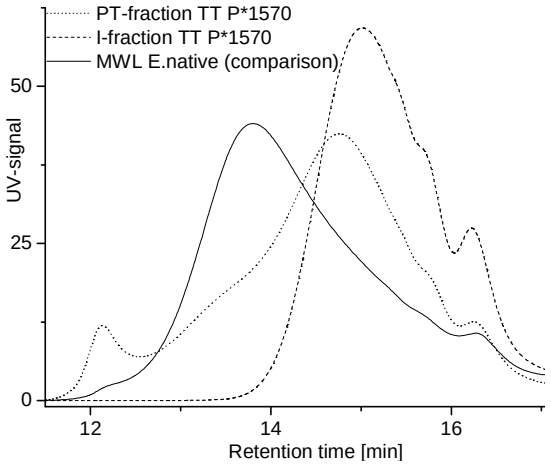


**Figure 4:** SEC chromatograms of the fractions isolated after temperature treatment of prehydrolysates. TT P* denotes the sum of a P-factor of 650 and TT-factor of 920.

The methoxyl group content of 18.3% was only slightly lower than that of native lignin. Thus, contribution of furfural to the formation of PT was considered to be of minor importance. Structural characterisation of PT using NMR spectroscopy posed a problem. Due to the high molecular weight the resolution of the spectra was low. A curved baseline in quantitative $^{13}C$ spectra impaired quantification of most lignin moieties. Only the hydroxyl groups could be quantified. Comparison to an I-fraction obtained under similar autohydrolysis conditions revealed similarities [14]. In this case NMR spectroscopy could not assist in elucidating chemical pathways.

Leschinsky et al. [12] studied the formation of resinous precipitates by means of carbon balances by varying the duration of the temperature treatment.. It was revealed that prolonged TT led to increasing amounts of PT-fraction. Surprisingly, the amount of I-fraction, which was separated by centrifugation from the hydrolysate subsequent to TT, remained constant over the course of the treatment. Due to the similar chemical structure, it was expected that the PT-fraction is formed by condensation of I-fractions, resulting in a reduced amount of

I-fraction. The increasing formation of PT-fraction was reflected by a drop in the carbon content in the soluble part of the hydrolysate and it was concluded that soluble lignin degradation products are transformed into insoluble components.

## Conclusions

During autohydrolysis, lignin is degraded to a significant extent through cleavage of aryl-ether bonds resulting in a significant reduction of the molecular weight. As a result of these cleavage reactions, the degraded lignin is characterised by a drastically increased content of phenolic hydroxyl groups and a reduced content of aliphatic hydroxyl groups. Evidence for the occurrence of a homolytic cleavage mechanism was found. Condensation reactions change the substitution pattern of the aromatic ring.

As a result of the degradation reactions, lower molecular weight lignin degradation products are dissolved in relatively small amounts due to their low solubility in the acidic aqueous prehydrolysate. Some of the dissolved lignin degradation products remain soluble in the prehydrolysate, while degradation products characterised by a higher molecular weight precipitate upon cooling.

The dissolved lignin degradation products are highly reactive. At high prehydrolysis intensities and during storage of prehydrolysate at elevated temperatures, condensation of the dissolved lignin leads to the formation of resinous precipitates characterised by an increased molecular weight. Further research is focused on the control of the formation of these high molecular weight lignin deposits and on the purification of prehydrolysates.

## Acknowledgements

Financial support was provided by the Austrian government, the provinces of Lower Austria, Upper Austria and Carinthia as well as by the Lenzing AG. We also express our gratitude to the Johannes Kepler University, Linz, the University of Natural Resources and Applied Life Sciences, Vienna, and the Lenzing AG for their in kind contributions.

## References

[1] H.K. Weber. in Biorefining for the Pulp and Paper Industry 2008.

[2] H. Sixta and A. Borgards, Das Papier 53 (1999) 220-234.

[3] A. Borgards and H. Sixta, Mitteilungen der Bundesforschungsanstalt für Forst- und Holzwirtschaft 222 (2006) 23-30.

[4] W. Peter and A. Lima, Lenzinger Berichte 78 (1998) 28-32.

[5] M. Fasching, A. Griebl, G. Kandioller, A. Zieher, H. Weber and H. Sixta, Macromolecular Symposia 223 (2005) 225-238.

[6] M.A. Kabel, H.A. Schols and A.G.J. Voragen, Carbohydrate Polymers 50 (2002) 191-200.

[7] L. Mozolová, E. Golis and L. Sutý, Sammelschrift der Arbeiten der Chemisch-technologischen Fakultät der Slowakischen technischen Hochschule (1977) 217-221.

[8] G. Annergren, Å. Backlund, J. Richter and S. Rydholm, Tappi Journal 48 (1965) 52-56.

[9] J. Hojnos, Papír a Celulóza 42 (1987) 69-75.

[10] C. Stanciu, Celuloza si Hirtie 23 (1974) 1-23.

[11] P. Szalai and J. Bella, Papir a Celulóza 40 (1985) 185-188.

[12] M. Leschinsky, R. Patt, and H. Sixta. in Pulp and Paper Conference 2007, Vol. Fiber modifications and brightening, pp. 7-14, Helsinki 2007.

[13] M. Leschinsky, H. Sixta and R. Patt, Bioresources 4 (2009) 687-703.

[14] M. Leschinsky, G. Zuckerstätter, H.K. Weber, R. Patt and H. Sixta, Holzforschung 62 (2008) 653-658.
[15] M. Leschinsky, G. Zuckerstätter, H.K. Weber, H. Sixta and R. Patt, Holzforschung 62 (2008) 645-652.
[16] E.A. Capanema, M.Y. Balakshin and J.F. Kadla, Journal of Agricultural and Food Chemistry 53 (2005) 9639-9649.
[17] D.V. Evtuguin, C. Pascoal Neto, A.M.S. Silva, M.R.M. Domingues, F.M.L. Amado, D. Robert and O. Faix, J. Agric. Food Chem. 49 (2001) 4252-4261.
[18] C.P. Neto, D. Evtuguin and P. Paulino. in 9th International Symposium on Wood and Pulping Chemistry, Vol. Poster Presentations, pp. 78.1-78.4, Montreal 1997.
[19] M. Funaoka, T. Kako and M. Kubomura, Bulletin of the Faculty of Bioresources, Mie University 6 (1991) 27-36.
[20] K. Kratzl and J. Gratzl, Holzforschung und Holzverwertung 12 (1960) 8-14.
[21] S. Li and K. Lundquist, Nordic Pulp and Paper Research Journal 15 (2000) 292-299.
[22] J.H. Lora and M. Wayman, Tappi 61 (1978) 47-50.
[23] H. Sixta. in (Sixta, H., ed.) Handbook of Pulp, WILEY-VCH, Weinheim 2006, pp. 325-365.

Lenzinger Berichte 87 (2009) 26-38

# NEW GENERATION KRAFT PROCESS

**Herbert Sixta[1] and Gabriele Schild[2]**

[1]Department of Forest Products Technology, Helsinki University of Technology, Vuorimiehentie 1, 02015 Espoo, Finland
[2]Kompetenzzentrum Holz GmbH, St.-Peter-Str.25, 4021 Linz, Austria

**Kraft pulping offers a very efficient lignin removal and the production of fibers with high strength properties. Transforming kraft pulping into biorefinery concepts is, however, very challenging because the hemicelluloses and other carbohydrates are degraded into low molecular weight hydroxyl-carboxylic acids which are very difficult to recover as pure substances. Quite recently, we have proposed the concept of multifunctional alkaline cooking which allows the selective removal of short-chain carbohydrates by pre- and post-treatment processes.**

**In this study aqueous pre-hydrolysis and pre-alkaline extraction was applied to *Eucalyptus globulus* wood followed by kraft and Soda-AQ pulping of the pre-extracted wood chips. The results showed that alkaline pre-extraction prior to Soda-AQ pulping largely preserves the pulp yield, while a substantial amount of xylan can be extracted in polymeric form during this pre-step. The resulting unbleached pulp revealed characteristics indicating an alternate use as paper and dissolving pulp. Water pre-hydrolysis prior to kraft or Soda-AQ cooking contributed to a yield increase of approximately 20% relative to carbohydrate yield of dissolving pulp production. The removal of hemicelluloses after alkaline pulping by means of cold caustic extraction (CCE) allows the production of high yield dissolving pulps also equally applicable as paper and dissolving pulps. The resulting xylan-containing lye has been recycled to Soda-AQ pulping contributing to a 2-4% yield increase by xylan-reprecipitation. Alternatively, it has been demonstrated that the CCE-lye can be purified efficiently by ultrafiltration while the rather pure and high molecular weight xylan is concentrated in the retentate for further use.**

**The results indicated that biorefinery concepts can be realized for kraft pulping by adopting the proposed multifunctional alkaline pulping concept.**

**Keywords:** *Kraft pulp, biorefinery, xylan, CCE*

## Introduction

Chemical pulping serves as the most suitable basis for translating the wood-refinery concept into practice. A key element here is the close integration of chemical pulp manufacture with the production of different building block chemicals. Kraft pulping has developed as the principal cooking process, accounting for more than 90% of the chemical pulps. It accommodates a variety of wood species, recovers and reuses all pulping chemicals, and the fibers show excellent paper making properties. However, the existing technology is limited to the production of only one product, namely paper grade pulp, and in most cases no economically feasible technologies are available to isolate and purify valuable

products from the degradation of wood components, particularly from the degradation of hemicelluloses which are identified as a group of chemicals that could serve as an economic driver for a biorefinery.
Dissolving pulp production experiences a significant growth rate, particularly due to a marked upturn in viscose staple demand since 2001. This development has led to a tight supply/demand position for dissolving pulps of all different grades. Substantial investments in new production capacity will be necessary to meet the increasing demands for dissolving pulps.
The state-of-the-art dissolving pulp technologies, Visbatch® and VisCBC, combine the advantages of displacement technology and steam prehydrolysis [1]. They are characterized by their short cover-to-cover times, low energy requirements and very homogeneous and high product quality.
However, the current practice of steam prehydrolysis followed by a neutralization step prevents the recovery of valuable carbohydrate degradation products. At present, water prehydrolysis kraft pulping is not commercially utilized because of high investment and energy costs of a water prehydrolysis step and, more importantly, due to the expensive waste disposal of the prehydrolyzate caused by the formation of sticky precipitates [2, 3].

Much effort is currently undertaken to investigate the possibilities of integrating water pre-hydrolysis into alkaline pulping concepts to realize biorefinery concepts[4-8]. Other methods for hemicelluloses extraction comprise near neutral aqueous solutions at elevated temperature [9] and alkaline pre-extraction at moderate temperatures [10]. The latter has shown that hemicelluloses can be removed prior to pulping in a reasonable amount, while the pulp yield is almost not affected.
Quite recently, we have suggested an extended alkaline pulping concept, the multifunctional alkaline cooking process, which allows the production of a broad range of pulp grades and the recovery of sugar-based products following the principle of resource efficiency [11, 12]. This concept provides the basis for the production of a new low cost technology for the manufacture of dissolving pulps of all possible grades ranging from low to very high alpha pulps parallel to the production of a high-yield paper grade pulp. The high molecular weight hemicelluloses isolated by cold caustic extraction may be utilized either as a pure carbohydrate source for the conversion to building block chemicals or as an additive for paper pulp production to improve both yield and fibre-fibre bonding capability.

Alternatively, the concept of multifunctional alkaline cooking allows the removal of short-chain carbohydrates also by either autohydrolysis or alkaline pre-extraction. Again, both approaches permit the alternate production of dissolving and paper grade pulps. At the same time the removed extracts give access to a sugar-rich feedstock in a broad range of molecular weight depending on the pre-treatment intensity.

The presented study pursues a comparative evaluation of this multifunctional alkaline cooking process, a new generation kraft process, aiming at different hemicelluloses isolation processes integrated with alkaline cooking for the parallel or alternate production of high-purity dissolving and high-yield paper grade pulps using *Eucalyptus globulus* as a wood source.

## Experimental

### Wood chips

*Eucalyptus globulus* wood chips from plantations in Uruguay, supplied by ENCE, were used for all pulping experiments. The fraction >7 mm was used after a laboratory screening according to standard method SCAN CM 40:94. The

average characteristics of the screened wood chips were as follows (table 1):

**Table 1.** Characterization of *Eucalyptus globulus* wood.

| | |
|---|---|
| Klason lignin | 22.7 % |
| acid soluble lignin | 4.7 % |
| cellulose | 42.4 % |
| galactoglucomannan (GGM) | 2.2 % |
| xylan | 17.0 % |
| arabinan | 0.4 % |
| rhamnan | 0.1 % |
| total uronic acids | 4.8 % |
| acetone extractives | 0.6 % |
| ash | 0.4 % |
| moisture content | 31.6 % |

The xylan content was corrected assuming that 60% of the linkages between 4-*O*-methylglucuronic acid (MGA) and the xylan backbone survive the primary and secondary hydrolysis step [13]. Total uronic acids were calculated from 2.4% MGA, 1.9% galacturonic acid and 0.5% glucuronic acid.

## Cooking Experiments

The pilot plant trials were carried out in a 10-L digester with forced liquor circulation according to the general CBC concept[14]. According to the CBC process principle, all the process-related liquors, such as the impregnation and cooking liquors are prepared already in the tank farm using different tank-to-tank circulation loops.

In total, six different cooking concepts were investigated:

| | |
|---|---|
| K | Kraft |
| SAQ | Soda-AQ |
| E-SAQ | Alkaline pre-extraction followed by Soda-AQ cooking |
| SAQH | Soda-AQ cooking with xylan-enriched lye originating from CCE treatment |
| PH-K | prehydrolysis-Kraft |
| PH-SAQ | prehydrolysis-Soda-AQ |

The effective alkali concentration (EA) in the cooking liquor was kept constant at about 30 g/L (27 – 31 g/L) for all cooks expect for SAQH pulping, where EA was stepwise reduced to 10 g/L to study the effect on xylan-reprecipitation. EA of the impregnation liquor for K, SAQ and SAQH pulping was kept constant at 15 g/L. Likewise, the P-factor of 600 for PH-K and PH-SAQ cooks as well as the cooking temperature at 160ºC for all cooks were kept constant. For SAQ cooking dispersible anthraquinone(AQ), Baycel AQ from Kemira Chemie, in a concentration of 0.5 g/L was added to the white liquor and to the cooking liquor corresponding to a dosage of approximately 0.15 % odw.

Alkaline pre-extraction is carried out with pure white liquor, EA = 2.5 mol/L at 90º for one hour according to the process scheme outlined in Figure 1.

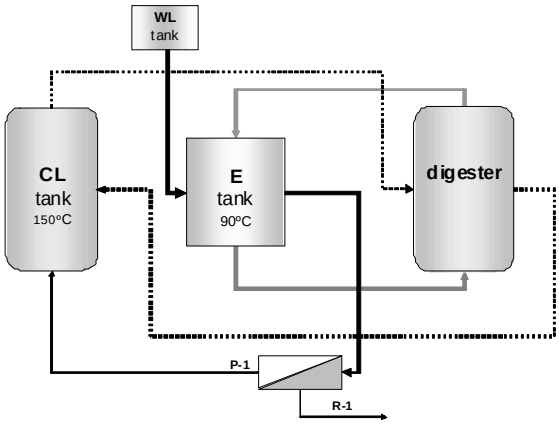


**Figure 1.** Flow sheet of alkaline pre-extraction followed by alkaline cooking, CL: cooking liquor, E: extraction liquor, WL: white liquor, R-1: retentate from membrane filtration, P-1: permeate from membrane filtration.

SAQH cooking was carried out with CCE-lye as alkali source. Starting with pure CCE-lye, the displaced cooking liquor from the previous cook was utilized as cooking liquor of the subsequent cook after having adjusted the target EA concentration by means of CCE-lye.

## Methods

### *Carbohydrate analysis*

The neutral sugar monomers were determined by anion exchange

chromatography (AEC) with pulsed amperometric (PAD) detection after a total hydrolysis with $H_2SO_4$ according to [15], while the uronic acids were quantified by methanolysis [16].

***Conventional pulp analysis***

The well-washed pulps were screened using a flat screen with 0.15 mm slots. All analyses were performed according to standard Tappi-, ISO- and SCAN standards.

***Membrane filtration***

The laboratory-scale filtration equipment Memcell from KCS Osmota equipped with a plunger pump was used for the ultrafiltration of the CCE-lye (Figure 2).

**Figure 2.** Bench-scale pressure-driven membrane system Memcell.

The ultrafiltration membrane UP010 from Microdyn-Nadir was applied in the flat-sheet crossflow cell with a 44 mil parallel spacer resulting in an active membrane area of 80 cm². The cut-off of this alkali stable polyethersulfone membrane is 10 kDa. The temperature was kept constant at 40 °C by heating the 7L-feed-vessel. The pressure before the membrane was varied between 200 and 800 kPa. The applied flow rate was in the range of 1 to 3 L/min.
Two process modes were applied. The permeate was either collected in a separate container during the concentration mode or led back into the feed reservoir in the closed circuit mode, while the retentate was always recycled back to the feed vessel.

The new membrane was purged with NaOH before the experimental operating started to ensure hydrophilicity of the membrane. The equipment was flushed with deionized water until neutral pH and cleaned in two steps after each experiment. First, the membrane was cleaned with an Ultrasil 2 solution from Henkel-Ecolab with addition of the enzyme Novozym 342 from Novozymes at 50 °C for 60 min followed by a thoroughly rinsing with water. The second step comprises a cleaning with Ultrasil 11 with the same procedure as in the first step. The pure water flux was determined at 40 °C, a flow rate of 2 L/min and a pressure of 300 kPa before and after cleaning to evaluate irreversible fouling.

## Results and discussion

Kraft and SODA-AQ cooking, in case of hardwood, represent the core process step within the multifunctional alkaline cooking process, responsible for efficient delignification. Following the principle of this novel cooking concept, the selective removal of hemicelluloses may be achieved by two alternative pre-treatments, autohydrolysis (PH) and alkaline pre-extraction (E) or by a post-extraction step, cold caustic extraction (CCE). Contrary to mere alkaline cooking, the chemical structure of the removed short-chain carbohydrates is largely preserved. Hemicelluloses show a polymeric form in the E-extract and the CCE-lye, an oligomeric and monomeric form in the autohydrolysate. The recycling of the CCE-lye containing high molecular weight hemicelluloses to paper pulp cooking allows xylan enrichment of paper pulps as will be demonstrated later. The effect of the pre- and post-treatment steps on both the processability and the resulting pulp properties will be exemplified in the following:

***Cooking performance***

One target of the novel cooking concept is also to reduce sulfidity in kraft cooking or even to completely replace it by anthraquinone (AQ) or other sulfur-free additives. Therefore, we put emphasis on the comparative evaluation of the K and SAQ cooking performance both based on CBC process technology. The effect of H-factor on total yield was quite comparable for both cooking concepts which is in good agreement with the results obtained by other authors [17]. Alkaline pre-extraction, however, resulted in a slightly lower yield following the same dependency on H-factor than the reference pulping processes (Fig 3).

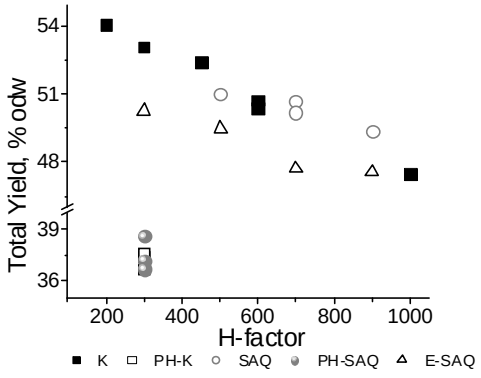


**Figure 3.** Total yield versus H-factor for modified alkaline pulping with constant cooking conditions.

The lower yield of the E-SAQ pulps may be attributed to lower xylan content as a result of the pre-extraction with highly concentrated sodium hydroxide solution (≥ 2 mol/L) at moderate temperature (≤ 90ºC). Under these conditions the wood structure opens up through swelling and a substantial part of the accessible xylan dissolves in polymeric form. In addition, alkaline pre-extraction serves as a perfect impregnation step, and as a result, the amount of reject is very low. Figure 4 shows that delignification was also positively affected by this pre-extraction step.

The delignification rate in SAQ pulping was slightly lower than that of K pulping which confirms the results obtained by some authors using other hardwood species [17] but is in contradiction to that of other authors. S.B. Vitta, for example, reported a higher delignification rate in SAQ pulping as compared to K pulping using sweetgum [18].

The reason for this discrepancy might be found in variations in the lignin structure among different hardwood species and in different effective concentrations of AQ in the cooking liquor. The formation of substantial amounts of hexenuronic acid (HexA) is one drawback of alkaline cooking of Eucalyptus species. No difference in the HexA content of pulps as a function of H-factor exists between K and SAQ pulps. In contrast, the alkaline extraction prior to SAQ pulping (E-SAQ) results in a substantial decrease in HexA formation. This seems to be quite logical since substantial amounts of xylan are removed during the pre-extraction step. However, the ratio of HexA-to-xylan in the E-SAQ pulps (1.8) is lower than that in the SAQ pulps (2.1) which indicates that the early xylan removal impedes the HexA formation to some extent. Figures 3 and 4 also confirm the low yield of autohydrolyzed pulps (PH-K and PH-SAQ) as well as their low kappa number and HexA content at comparatively low H-factor.

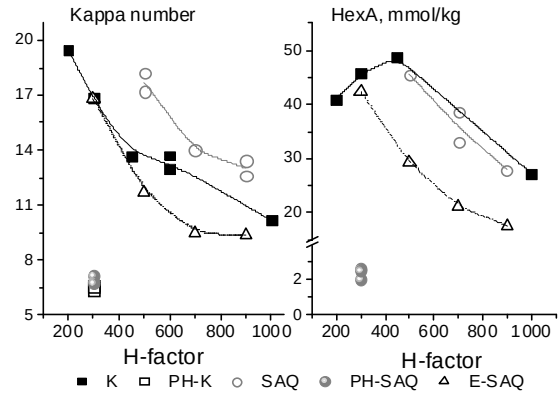


**Figure 4.** Kappa number and HexA content versus H-factor for modified alkaline pulping. All conditions except H-factor were kept constant.

The residue in 18 wt% sodium hydroxide solution, denoted as R18 content, relates to the high-molecular weight polysaccharide fraction in a pulp. At the same level of hemicelluloses, alkaline pulps generally show a significantly higher R18 content than sulfite pulps. This can be explained by the higher molecular weight of the hemicelluloses and the much lower amount of degraded cellulose in pulps from alkaline pulping. In addition, the reducing ends of alkaline pulps have been converted to aldonic acid endgroups, resisting alkali-induced degradation reactions to some extent. Processes in which dissolving pulps are subjected to steeping in aqueous solutions of high sodium hydroxide concentrations (18-25 wt%) such as viscose and etherification process, have gradually increased their process temperature to more than 50ºC during the last decades. Thus, the alkali resistance measured at 20ºC (DIN 54355) does not any more reflect the yield of the conversion products since the alkali resistance decreases with temperature as demonstrated in Figure 5.

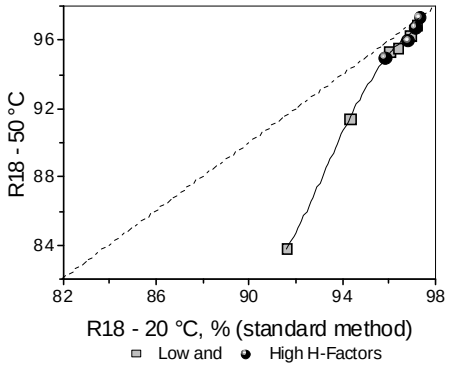


**Figure 5.** Relationship between alkali resistances in 18 wt% NaOH determined at 20º and 50ºC, exemplified for Eucalyptus globulus kraft pulps.

In this particular example the effect of temperature between 20º and 50ºC on alkali resistance diminishes beyond an R18 content of 96%.

The results depicted in Figure 6 show that the R18 content of K pulps increases with increasing H-factor. This can be partly explained by a progressive decarboxylation of the uronic acid side chains of the xylan parallel to the removal of the lignin. This renders the xylan less soluble in sodium hydroxide solution. Although the xylan content may be kept constant, it contributes to higher alkali resistance. The high pulp viscosity denotes another reason for the high R18 contents of the SAQ pulps.

However, the SAQ pulps follow the same trend at a higher level of R18 content. A further, substantial increase in R18 can be achieved through the alkaline pre-extraction step as shown for E-SAQ pulps. Values beyond 95% indicate their suitability as dissolving pulps without further refinement provided that not too much of this alkali resistance is lost during the viscosity adjustment and bleaching operations in subsequent process steps. Also for these pulps a certain relationship applies between the carboxylic group content and the R18 value.

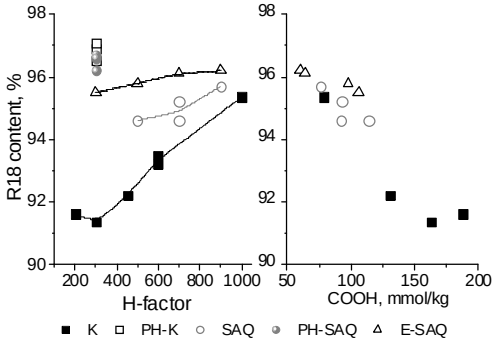


**Figure 6.** Relationship between R18 content (20ºC), H-factor and carboxylic groups for K-, SAQ-, E-SAQ and PH-K and PH-SAQ pulps from Eucalyptus globulus.

The effect of CCE-lye as alkali source on SAQ cooking has been studied in some preliminary tests applying the CBC cooking concept. Although the impregnation and the cooking liquor were not yet in equilibrium conditions, the addition of xylan-containing lye clearly contributed to higher pulp yield due to an increase in xylan content. This is demonstrated in Figure 7, where xylan and

total yield are related to H-factor at different levels of effective alkali concentration of the cooking liquor. The relationship is not very clear since on the one side prolonged cooking conditions may result in an increased cellulose yield loss, but on the other side it may contribute to an increase in xylan re-precipitation, particularly at low EA concentration.

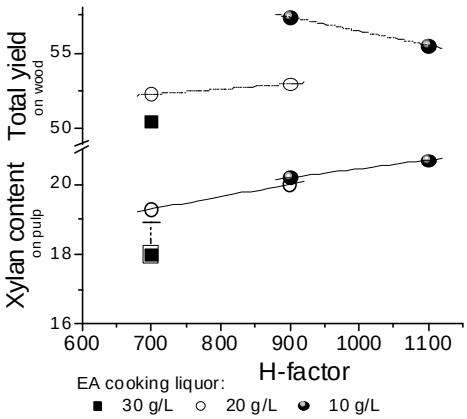


**Figure 7.** Xylan content and total yield of unbleached SAQH pulps from Eucalyptus globulus.

Autohydrolysis prior to alkaline cooking to produce high-purity dissolving pulps resulted in a substantial yield loss as indicated above. No differences in pulp yield at given kappa number and delignification rate between PH-SAQ and PH-K pulps have been observed, which is accordance with the published literature [19]. Figure 8 reveal boxer plots representing repetition cooks with different liquor-to-wood ratios during autohydrolysis ranging from 1.4 to 3.5 as the only changes in process conditions.
While no differences between PH-K and PH-SAQ pulps were visible for pulp yield and kappa number, the former showed slightly higher R18 and lower xylan contents than the latter. The differences in R18 are, however, small and might not be statistically significant. In contrast, the xylan content is clearly higher in PH-SAQ pulps than in PH-K pulps reflecting the efficient stabilizing effect of AQ.

The objective to replace vapour phase by water phase autohydrolysis is to allow the isolation of sugar degradation products such as mono- and oligo-sugars, furfural and/or acetic acid. Provided that the problems associated with the formation of sticky precipitates caused by degraded lignin products can be solved, a substantial fraction of the degraded hemicelluloses may be isolated and converted to valuable products [2, 3, 20].

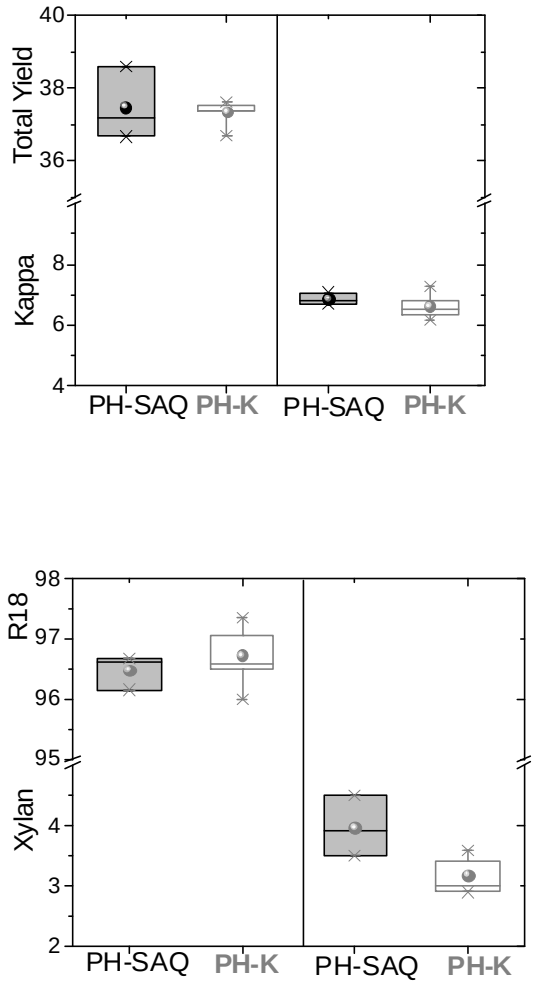


**Figure 8.** Kappa number, total yield, R18 and xylan contents of unbleached PH-K and PH-SAQ pulps from Eucalyptus globulus.

Actually, the amount of recoverable autohydrolysis products depends on the liquor-to-wood ratio as demonstrated in Figure 9. A compromise between the liquor-to-wood ratio and the recoverable

amount of sugar products has to be found to minimize process costs, particularly energy costs.

In case of *Eucalyptus globulus* wood, a liquor-to-wood ratio of about 1/0.55-1/1.53 = 1.1 g*ml$^{-1}$ has to be exceeded to receive free liquor to be discharged from the digester.

Figure 9 shows that a liquor-to-wood ratio of about 2.5:1 may be sufficient, because it offers a disproportionately high recovery rate.

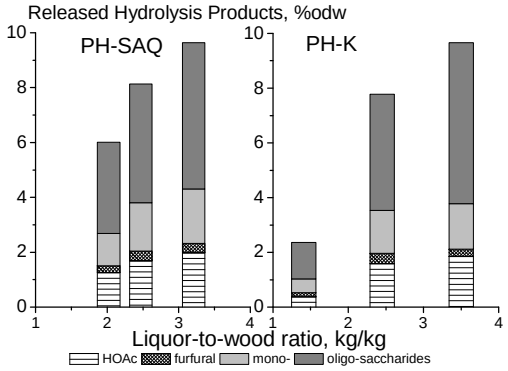


**Figure 9.** Recoverable amounts of hydrolysis products derived from autohydrolysis of Eucalyptus globulus at a P-factor 600 prior to both K and SAQ pulping.

**Table 2.** Characterization of unbleached Eucalyptus globulus pulps from continuous batch cooking (CBC) following the concept of multifunctional cooking. For comparison, the key properties of an acid Mg based sulfite dissolving pulp (MgS) are included.

| Parameters | Units | Kraft | SAQ | E-SAQ | SAQH | PH-SAQ | PH-K | MgS |
|---|---|---|---|---|---|---|---|---|
| | | paper pulps | | | | dissolving pulps | | |
| Total yield | % | 51,2 | 50,7 | 50,3 | 53,0 | 37,2 | 37,4 | 46,1 |
| Kappa number | - | 14,6 | 14,0 | 16,8 | 16,2 | 6,8 | 6,3 | 8,8 |
| HexA-kappa number | - | 4,0 | 2,8 | 3,6 | 3,5 | 0,2 | | |
| Brightness | %ISO | 41,3 | 41,8 | 39,2 | 34,8 | 45,2 | 41,2 | 59,3 |
| Viscosity | mL/g | 1240 | 1115 | 1090 | 1160 | 1125 | 1065 | 900 |
| R18 | %odp | 91,9 | 95,2 | 95,5 | 93,9 | 96,7 | 97,1 | 91,4 |
| Xylan | % odp | 18,4 | 17,4 | 16,9 | 20,1 | 3,5 | 2,9 | 5,3 |
| Copper number | % | 0,5 | 0,7 | 0,9 | 0,9 | 0,7 | n.d. | 1,9 |
| carboxylic group | µmol/g | 147 | 93 | 106 | 122 | 39 | n.d. | 54 |
| Degree of beating at 4500 rev | °SR | 73 | 50 | 52 | 69 | 38 | 37 | n.d. |
| Opacity at 4500 rev | | 91 | 96 | 96 | 93 | 99 | 99 | n.d. |
| Tensile stiffness index at 4500 rev | kNm/g | 8,0 | 7,0 | 7,0 | 7,3 | 5,1 | 4,9 | n.d. |
| Tensile stiffness index at 30°SR | N*m/g | 5,6 | 6,4 | 5,9 | 5,1 | 4,5 | 4,8 | n.d. |
| Tear index at 4500 rev | mN*m²/g | 6,2 | 6,6 | 6,5 | 6,1 | 3,35 | 3,52 | n.d. |
| Elastic modulus at 4500 rev | GPa | 5,9 | 4,7 | 4,6 | 5,2 | 3,2 | 3,0 | n.d. |
| Zero span tensile index at 4500 rev | Nm/g | 138 | 138 | 124 | 107 | 92 | 94 | n.d. |

## Unbleached pulp properties

The concept of multifunctional alkaline cooking allows the manufacture of five different pulp grades using the same core process for delignification either kraft (K) or Soda-AQ (SAQ). On the basis of the latter concept, a comparative evaluation of four different unbleached pulp grades comprising E-SAQ, SAQH, PH-SAQ and SAQ processes has been conducted using *Eucalyptus globulus* as the wood source.

So far, the CCE post-extraction has been extensively tested on a commercial TCF bleached *Eucalyptus globulus* pulp only. However, the results of these investigations are excluded from the comparative evaluation of pulp properties because of differences in the cooking and downstream processes.

The unbleached pulp properties including paper making properties are listed in table 2.

The SAQ and E-SAQ pulps are characterized by a high R18 content, slightly lower xylan content as compared to K and SAQH pulps, and behave more resistant to beating which is also reflected by low tensile stiffness and high tear index. As expected, the prehydrolyzed pulps show high cellulose purity and in turn inferior paper making properties. Figure 10 illustrates the beatability of pulps in more detail.

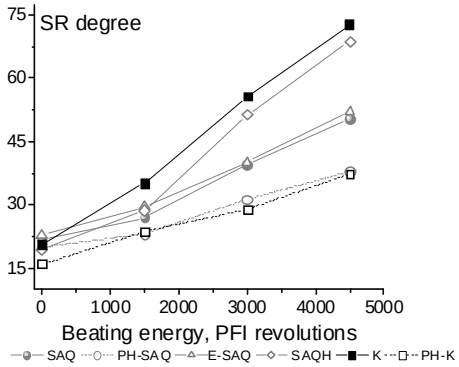


**Figure 10.** Freeness in ºSR as a function of beating energy in terms of PFI revolutions for Eucalyptus globulus pulps as listed in table 2.

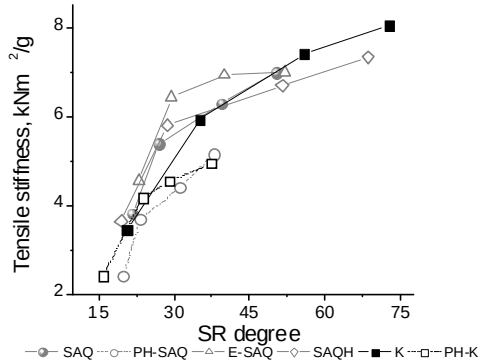


**Figure 11.** Tensile stiffness index as a function of freeness in ºSR for Eucalyptus globulus pulps as listed in table 2.

The beating performance can be classified into three categories: the first category comprises the PH-K and the PH-SAQ pulps which are highly resistant to beating due to the lack of hemicelluloses necessary for cross-linking, the second category of pulps with moderate beatability is represented by the SAQ and E-SAQ pulps and the third category of pulps is characterized by easy beatability and represented by the K and SAQH pulps showing the highest hemicellulose contents. Surprisingly, the development of the tensile stiffness index experiences the highest increase at low beating energy for the E-SAQ pulp followed by the hemi-rich SAQH pulp (Figure 11). This means that the E-SAQ pulp shows the highest tensile stiffness index at a freeness of 30ºSR which is surprising and has to be confirmed in further trials.

## Membrane separation process

The cost-effective separation and purification of the alkali-extracted hemicelluloses is a prerequisite to establish economically viable biorefinery concepts. The technology of choice is a pressure driven membrane separation process such as ultra- or nanofiltration.

For demonstration, bench-scale experiments have been conducted using CCE-lye as a feed substrate. Due to an average molecular weight of the extracted xylan higher than 15 kDa, the use of ultrafiltration membranes ensures high efficiency and selectivity. In Table 3 the CCE process, the resulting CCE-lye and the pulp before and after CCE-treatment are characterized.

**Table 3.** Characterization of the CCE process applied to a commercial TCF bleached Eucalyptus globulus kraft pulp and the CCE-treated pulp resulted thereof.

| | | Pulp | CCE-treatment | | Pulp |
|---|---|---|---|---|---|
| **Parameter** | | **K** | Lye | filtrate | **K-CCE** |
| **CCE** | | | | | |
| conditions | | | | | |
| consistency | | 10 | | | |
| time | min | | 30 | | |
| temperature | °C | | 30 | | |
| concentrations | | | | | |
| NaOH | g/L | | 90,1 | 81,2 | |
| Beta-cellulose | g/L | | 0,0 | 19,1 | |
| xylan* | % of beta | | | 77,1 | |
| Mw | kDa | | | 17,7 | |
| Mn | kDa | | | 9,3 | |
| Gamma-cellulose | g/L | | 0,0 | 1,4 | |
| **Pulp** | | | | | |
| Yield | % od | 100,0 | | | 82,8 |
| Viscosity | ml/g | 820 | | | 900 |
| R10 | % od | 87,9 | | | 97,9 |
| R18 | % od | 91,5 | | | 98,7 |
| Xylan | % od | 19,1 | | | 5,7 |

* too low value since determined by HPLC-PAD after two-step hydrolysis

The chosen ultrafiltration set-up allows for achieving high hemi-to-NaOH ratios in the concentration mode while maintaining a reasonably high flux up to about 20 $Lm^{-2}h^{-1}$ (table 4).

The hemi-to-NaOH ratio may be further increased by a subsequent diafiltration process to improve the economic feasibility of xylan precipitation and purification.

**Table 4.** Ultrafiltration performance using CCE-lye as feed for both the closed-circuit and the concentration modes. CCE-lye originated from CCE-treatment of a commercial TCF bleached Eucalyptus globulus kraft pulp. VCF: volumetric concentration factor.

| Parameter | | V C F | | |
|---|---|---|---|---|
| | | 1,0 | 3,0 | 3,4 |
| Feed | | | | |
| NaOH | g/L | 79,4 | 79,4 | 79,4 |
| hemicellulose | g/L | 18,5 | 18,5 | 18,5 |
| flux | $L/m^2.h$ | | 19,5 | 15,4 |
| Permeate | | | | |
| NaOH | g/L | 77,8 | 76,7 | 78,4 |
| hemicellulose | g/L | 1,2 | 0,9 | 0,8 |
| Retentate | | | | |
| NaOH | g/L | 77,8 | 78,3 | 80,3 |
| hemicellulose | g/L | 22,0 | 52,2 | 67,4 |
| Yield | % | | 96,9 | 97,1 |
| hemi-to-NaOH ratio | | 0,28 | 0,67 | 0,84 |

## Material balance

Multifunctional alkaline pulping aims at maximizing the carbohydrate yield derived from the respective wood source and providing a platform for alternating or parallel production of high-yield dissolving and paper grade pulps. In addition, the extracted hemicelluloses should be recovered in a form where they could be either transferred to a parallel line for high-yield paper pulp manufacture or utilized as a source for the conversion to products of high added value.

Based on lab trials, the sugar components in both product and process streams have been carefully quantified. The yield loss during an ECF bleaching sequence, O-D-E-H-D for dissolving and O-D-E-D for paper pulps, has been considered in the calculation of the material balance of the pulps. All the results shown in table 5 are related to bone dry wood.

Considering the hemicelluloses present in the E-extract, E-K pulping results in a 9% higher carbohydrate yield as compared to K-pulping, the reference case for paper pulping (Table 5). This is quite marginal if one considers the recovery rates of the sugar components in the E-extract being only about 50-70%. On the other side, the added value of the E-K concept could be somewhat increased if the resulting pulp can be utilized for certain dissolving pulp applications. The situation is different for the dissolving pulp case: if the amount of sugars in the water hydrolysate (PH) is considered, the carbohydrate yield increases by about 20% compared to the PH-K pulp, which represents the reference dissolving pulp. Currently this pulp is produced by vapour phase prehydrolysis only. The carbohydrate yield can be further increased when dissolving pulp is produced according to the K-CCE concept. There the yield increase applies to both pulp (+17%) and xylan (+20%) as additional product. The latter can be used as an additive for high-yield paper pulp manufacture or as raw material source for the conversion to polymeric (film), oligomeric (XOS as food additive) and monomeric material (xylose, xylitol) or highly functionalized building block chemicals.

Please note, that for an economic evaluation one has to consider that the isolation, purification and conversion processes are connected with significant yield losses.

At this stage of the project it is not possible to predict an economic efficiency of the proposed multifunctional alkaline pulping process yet. However, it is quite clear that profitability can be achieved only if the (new) pulp products meet the market requirements from the quality point of view and prices for the sugar-based products can be realized which are equal to or higher than the pulp prices.

**Table 5.** Carbohydrate balance of ECF-bleached Eucalyptus globulus kraft pulps following the concept of multifunctional alkaline pulping.

| Sugars<br>% od | Wood | K | K-CCE | CCE | Total | PH-K | PH* | Total | E | E-K | Total |
|---|---|---|---|---|---|---|---|---|---|---|---|
| Cellulose | 414 | 406 | 405 | 0 | 405 | 348 | 1 | 349 | 0 | 398 | 398 |
| Xylan | 161 | 88 | 19 | 66 | 85 | 12 | 57 | 69 | 37 | 82 | 119 |
| Acetyl | | | | | | | 9 | | 21 | | |
| GGM | 25 | 2 | 1 | 0 | 1 | 1 | 8 | 8 | 2 | 2 | 4 |
| others | 76 | 6 | 1 | 4 | 6 | 1 | 1 | 11 | 0 | 6 | 27 |
| **Total** | **676** | **503** | **425** | **71** | **496** | **362** | **76** | **438** | **60** | **488** | **548** |

* recoverable prehydrolysate only

## Conclusions

1. The study confirmed that pre- and post-treatments to alkaline pulping, representing the key elements of multifunctional alkaline cooking, allow the production of modified paper and dissolving pulps with promising properties. The chemical structure of the extracted hemicelluloses is largely preserved and constitutes a valuable source for the conversion to sugar-based products.

2. Cooking performance of Soda-AQ was quite comparable to kraft cooking. As expected, higher beating resistance, lower tensile stiffness and elastic modulus constituted once again the disadvantageous paper making properties of the Soda-AQ pulp over the kraft pulp.

3. However, no differences in both processability and pulp properties between Soda-AQ and kraft were observed in case of prehydrolysis-alkaline pulping.

4. Contrary to autohydrolysis, alkaline pre-extraction showed only a minor effect on pulp yield. It also accelerated the delignification rate, lowered the HexA formation and, after Soda-AQ pulping, resulted in a surprisingly high R18 content which might qualify for some interesting dissolving pulp applications.

5. The use of CCE-lye as alkali source for Soda-AQ pulping clearly contributed to higher pulp yield due to xylan retention. The resulting paper making properties were indicative for a hemicellulose-rich pulp.

6. Efficient separation of xylan from strong alkaline solution by means of ultrafiltration has been demonstrated in bench-scale experiments. It was shown that reasonably high flux could be maintained even at high volumetric concentration factors.

7. Material balances indicate substantial advantages in carbohydrate yield for certain mill cases. However, it is too early to speculate on the economic feasibility of the proposed concept of multifunctional alkaline pulping.

## Acknowledgements

Financial support was provided by the Austrian government, the provinces of Lower Austria, Upper Austria and Carinthia as well as by the Lenzing AG.

## References


[1] W. Wizani, A. Krotscheck, J. Schuster and K. Lackner, *Viscose production process. Verfahren zur Herstellung von Viskosezellstoffen*, in *WO9412719 PCT Pub.* **1994**: Germany.

[2] M. Leschinsky, G. Zuckerstätter, H. K. Weber, R. Patt and H. Sixta, *Effect of autohydrolysis of Eucalyptus globulus wood on lignin structure. Part 2: influence of autohydrolysis intensity.* Holzforschung, **2008**. **62**(6): p. 653-658.

[3] M. Leschinsky, G. Zuckerstätter, H. K. Weber, R. Patt and H. Sixta, *Effect of autohydrolysis of Eucalyptus globulus wood on lignin structure. Part 1: comparison of different lignin fractions formed during water prehydrolysis.* Holzforschung, **2008**. **62**(6): p. 645-652.

[4] M. S. Tunc and A. R. P. van Heiningen, *Autohydrolysis of mixed southern hardwoods: effect of P-factor.* Nordic Pulp & Paper Research Journal, **2009**. **24**(1): p. 46-51.

[5] S.-H. Yoon, K. Macewan, and A. van Heiningen, *Hot-water pre-extraction from loblolly pine (Pinus taeda) in an integrated forest products biorefinery.* Tappi Journal, **2008**. **7**(6): p. 27-32.

[6] S.-H. Yoon and A. R. P. van Heiningen, *Kraft pulping and papermaking properties of hot-water pre-extracted loblolly pine in an integrated forest products biorefinery.* Tappi J. FIELD Full Journal Title:Tappi Journal, **2008**. **7**(7): p. 22-27.

[7] M. S. Tunc and A. R. P. van Heiningen, *Hemicellulose Extraction of Mixed Southern Hardwood with Water at 150 DegC: Effect of Time.* Industrial & Engineering Chemistry Research, **2008**. **47**(18): p. 7031-7037.

[8] M. S. Tunc and A. R. P. van Heiningen, *Hydrothermal dissolution of mixed southern hardwoods.* Holzforschung, **2008**. **62**(5): p. 539-545.

[9] A. R. P. van Heiningen and M.S. Tunc, *Influence of operation conditions on the extraction yield of hemicellulose from mixed southern hardwood.* Abstracts of Papers, 229th ACS National Meeting, San Diego, CA, United States, March 13-17, **2005**: p. CELL-209.

[10] W. W. Al-Dajani and U.W. Tschirner, *Pre-extraction of hemicelluloses and subsequent kraft pulping. Part I: alkaline extraction.* Tappi Journal, **2008**. **7**(6): p. 3-8.

[11] H. Sixta, A. Promberger, A. Borgards and R. Möslinger, *Method for producing a type of pulp*. **2007**, (Lenzing Aktiengesellschaft, Austria). WO 2007128026. p. 48pp.

[12] H. Sixta, A. Promberger, A. Borgards and R. Möslinger, *Method for producing a type of pulp*. **2007**, (Lenzing Aktiengesellschaft, Austria). WO 2007128024. p. 50pp.

[13] J. M. Genco and N. Busayasakul, *Hemicelluloses retention during kraft pulping.* Tappi, **1990**: p. 223-233.

[14] H. Sixta, A. Potthast and A.W. Krotschek, *Chemical pulping processes.* Handbook of Pulp, **2006**. **1**: p. 109-509.

[15] H. Sixta, N. Schelosky, W. Milacher, T. Baldinger and T. Röder, *Characterization of alkali-soluble pulp fractions by chromatography*. in *11th ISWPC*. **2001**. Nice, France.

[16] T. Vuorinen and R. Alén, *Carbohydrates*, in *Analytical Methods in Wood Chemistry, Pulping and Papermaking*, E. Sjöström and R. Alen, Editors. **1999**, Springer: Heidelberg. p. 38-75.

[17] J. M. MacLeod, B. I. Fleming, G. J. Kubes and H. I. Bolker, *The strengths of kraft-AQ and soda-AQ pulps. Bleachable-grade pulps.* Tappi, **1980**. **63**(1): p. 57-60.

[18] S. B. Vitta, *Delignification kinetics and pulping characteristics of SODA-AQ and SODA-THAQ pulping of sweetgum,* in *Department of Wood and Paper Science*. **1979**, NCSU: Raleigh.

[19] C. K. Lin, *Prehydrolysis-alkaline pulping of sweetgum wood*. **1979**, North carolina State University: Raleigh, NC 27650, USA.

[20] M. Leschinsky, H. Sixta and R. Patt, *Detailed mass balances of the autohydrolysis of Eucalyptus globulus at 170 DegC.* BioResources, **2009**. **4**(2): p. 687-703.

Lenzinger Berichte 87 (2009) 39-48

# THE ELUCIDATION OF CELLULOSE SUPRAMOLECULAR STRUCTURE BY $^{13}$C CP-MAS NMR

**Gerhard Zuckerstätter[1], Gabriele Schild[1], Petra Wollboldt[1], Thomas Röder[2], Hedda K. Weber[1], and Herbert Sixta[3]**

[1]Kompetenzzentrum Holz GmbH, St.-Peter-Str.25, 4021 Linz, Austria
[2]Lenzing AG, 4860 Lenzing, Austria
[3]Department of Forest Products Technology, Helsinki University of Technology, Vuorimiehentie 1, 02015 Espoo, Finland

**$^{13}$C CP-MAS NMR spectroscopy is a well-established method to determine the supramolecular structure, the morphology, the domain sizes, and the crystallinity of cellulose. These molecular properties strongly influence the chemical, physical, and mechanical characteristics of a cellulose material and are, thus, of interest to the cellulose industry. We review current opinions and NMR methodologies towards the extensive characterisation of celluloses in the native solid-state. Physical models are presented that aid in the interpretation of parameters accessed via NMR spectroscopy. Methodological advantages and limitations are highlighted and discussed with respect to the available information content, quantification, accuracy, and sample history.**

**Keywords:** *Cellulose, $^{13}$C CP-MAS NMR, morphology, crystallinity, fibril size*

## Introduction

The supramolecular structure of cellulose has been at the core of interest to the pulp, paper and fibre industry for decades. The organisation of the cellulose chains within the investigated material significantly influences its physical and chemical properties. Therefore, an enhanced understanding of cellulose morphology is essential to improve cellulose reactivity, processability and mechanical strength. Extensive research led to a detailed and quite consistent picture of cellulose structures at the molecular and supramolecular level. In the late 1950s a two-phase model was presented [1], assuming low ordered (*amorphous*) and highly ordered regions (crystalline) within solid state cellulose, which is supported by experimental evidence available today. [2-3]. The distribution and relative quantities of these regions strongly influence the interaction between reactants and cellulose. Further, it was shown that cellulose may exist in several different crystallographic forms, whereas for us the most interesting forms are cellulose $I_\alpha$, $I_\beta$ and II [4-7]. Interchanges between these can also be afforded by thermal and/or chemical treatment, e.g. pulping [8], alkalisation or dissolution and regeneration, however, cellulose $I_\beta$ is the thermodynamically more stable phase compared to cellulose $I_\alpha$ and the

transformation of cellulose I to cellulose II is considered largely irreversible.

Several analytical techniques were employed to study the morphology of cellulose. In 1937 Meyer and Misch [9] determined the unit cell dimensions of cellulose via X-ray diffraction. Later wide-angle X-ray scattering (WAXS) was established as the standard method for the determination of crystallinity, morphology and orientation [2]. Approaches relying on WAXS calibration, such as FT-IR and Raman spectroscopy have been used extensively, too [10-11]. Another well-established method for cellulose morphology determination is solid-state $^{13}C$ CP-MAS NMR spectroscopy [12-13]. The "felt" magnetic field of a given nucleus in a solid NMR sample is additionally influenced by the static magnetic fields of precessing neighbouring spins. The surrounding supramolecular structure, i.e. "packing" thus leads to variations in the chemical shift of the nuclei. The solid-state $^{13}C$ CP-MAS NMR spectrum of cellulose exhibits easily separable resonances from crystalline and less-ordered domains for the C4 and C6 atoms in the anhydroglucose unit (AGU). The cellulose C4 signal is particularly well resolved and stretches over a wide chemical shift range from about 79 to 91ppm. Early, the two dominating signals at about 89 and 84 ppm were attributed to crystalline and non-crystalline components, respectively [4]. A quick and simple estimation of cellulose crystallinity was achieved by signal integration. Later, Larsson et al. [13] and Newman et al. [12, 14] established more detailed assignments and routines for the deconvolution of signal components contributing to both crystalline and less-ordered (fibril surface) domains.

## Materials and Methods

The herein displayed spectra were acquired on either a generic cotton linters sample (cellulose I), Lenzing viscose fibres or Tencel fibres (both cellulose II).

Unless stated differently ca. 300mg of pulp are placed into a 2 mL Eppendorf tube, soaked with de-ionized water and equilibrated for at least 2 hours. The wet cellulose is then directly transferred and tightly stuffed into a 7mm zirconium oxide magic angle spinning (MAS) rotor. If the available sample amount does not allow for filling the rotor completely, PTFE inserts are used (centre packing). The water content of the sample inside the rotor is approximately 40-60% by weight, i.e. saturated. Cellulose II samples (i.e. regenerated fibres) are normally measured in an air-dry state.

Solid-state $^{13}C$ CP-MAS NMR measurements are conducted on a Bruker Avance DPX300 NMR spectrometer, operating at 75.46 MHz $^{13}C$ resonance frequency. The spectrometer is equipped with a 7 mm $^{1}H$/BB MAS probe, and the typical sample spinning speed is 4 kHz. NMR measurements are performed at room temperature (T = 26°C) and typically involve the following acquisition parameters: acquisition time 41 ms, cross-polarization (CP) contact time 1ms, repetition interval 3 s, 1024 accumulations, total acquisition time 53 min. Adamantane is used as an external chemical shift reference ($\delta[^{13}C]$= 29.5 ppm for the methylene signal). The acquired FIDs are multiplied with an exponential window function using a line broadening of 5 Hz prior to Fourier transform. Zero-order phase correction and sinusoidal baseline correction yield the final spectrum, which is then exported as x-y dataset for analysis into Microsoft Excel.

## Results and Discussion

*Cellulose I morphology, degree of order and crystallinity*

Solid-state $^{13}C$ CP-MAS NMR spectroscopy yields valuable information on cellulose morphology, its degree of order and crystallinity. However, the

separation of these three concepts proves sometimes difficult [12, 15]. One early and relatively straightforward approach in cellulose NMR analysis was the definition of a crystallinity index $CrI_{NMR}$ [%] [16-18], analogous to that used with X-ray diffraction. It is expressed as the crystalline fraction of cellulose in a given sample:

$$CrI_{NMR}\,[\%] = A_{cryst.}/(A_{cryst.}+A_{non\text{-}cryst.})\times 100\% \quad [Eq.1]$$

$A_{cryst.}$ and $A_{non\text{-}cryst.}$ denote the crystalline and non-crystalline signal areas in quantitative cellulose $^{13}C$ CP-MAS NMR spectra [Figure 1]. Commonly, the well-separated AGU C4 resonance is utilized for analysis. Crystalline and non-crystalline contributions are determined by either integration of peak areas using fixed integration limits or by signal deconvolution. The usual deconvolution procedure is the fitting of two Gaussian (sometimes Lorentzian-shaped) lines of fixed centre position and also fixed width. The integration tends to overestimate the narrower crystalline peak in contrast to the signal deconvolution described above. Another method of the determination of crystallinity of cellulose was recently described: Park et al. [19] subtract an amorphous cellulose standard spectrum from the sample $^{13}C$ CP-MAS NMR spectrum. The remaining crystalline signal contribution as a fraction of the total signal yields the crystallinity index $CrI_{NMR}$. This method shows results comparable to other methods for pure cellulose samples, but has not been proved on pulp samples so far.

Newman et al. [12] showed that the assignments of crystalline and non-crystalline resonances at 89 and 84ppm are not always consistent with relaxation analysis. Although crystallinity indices obtained from X-ray and NMR measurements are often in good agreement, deviations for microcrystalline contributions were observed [20]. These are attributed to signal overlap in the less-ordered region, where also crystallite surface signals were detected.

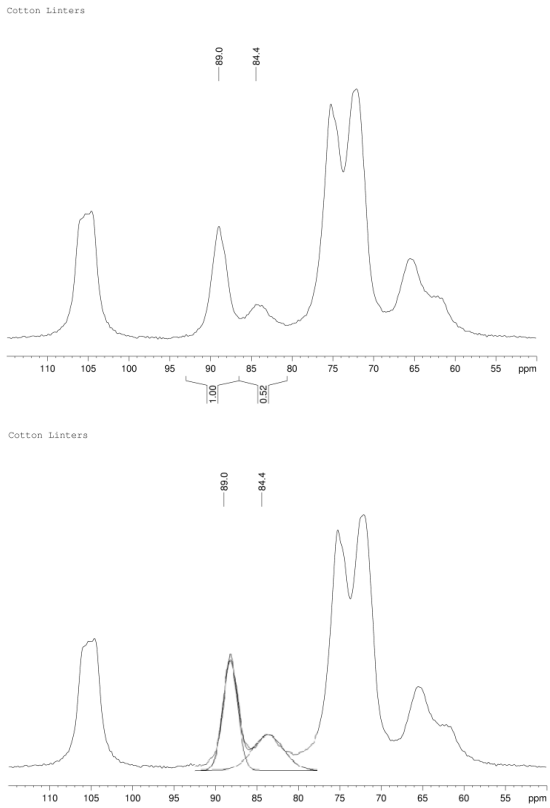


**Figure 1**. Cellulose I (cotton linters) $^{13}C$ CP-MAS NMR spectrum, showing integrated (top) and deconvoluted (bottom) AGU C4 signal areas from crystalline (89ppm) and less-ordered (amorphous; 84ppm) sample portions. Typical integration limits are: 93.0-86.5ppm for crystalline material and 86.5-80.6ppm for amorphous material.

A sophisticated approach towards cellulose I crystallinity, but also morphology analysis in general was published by Larsson and co-workers [21]. This methodology uses three Lorentzian and four Gaussian lines to fit the experimental spectrum in the cellulose C4 region [Figure 2]. Additional resonances attributed to hemicelluloses are commonly added. The signal assignment includes separate lines for crystalline cellulose $I_\alpha$, $I_\beta$, and a mixed cellulose $I_{\alpha+\beta}$ peak, a so-called para-crystalline signal, as well as resonances attributed to accessible (AFS) and inaccessible fibril surfaces (IAFS). The terms inner-crystalline, para-crystalline, accessible and inaccessible

fibril surfaces are best explained by a 2x2 fibril aggregate model [Figure 3].

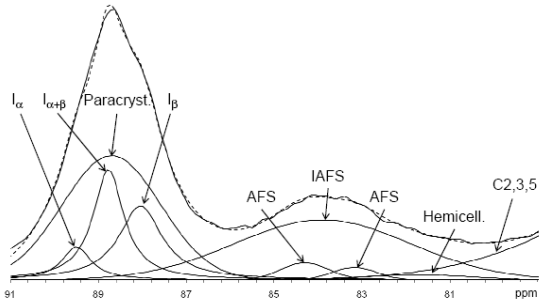


**Figure 2.** Deconvolution of an experimental native cellulose (cotton linters) $^{13}C$ CP-MAS NMR spectrum according to Larsson et al. [13]. A total of eight Gaussian and Lorentzian lines of fixed position and width (FWHM) are adjusted in height, such that their sum (dotted line) fits the experimental spectrum.

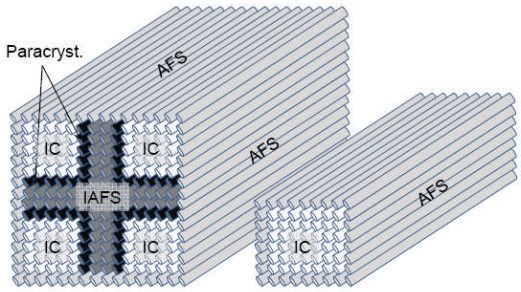


**Figure 3.** Larsson's and Wickholm's models for 2x2 fibril aggregates (left) and cellulose fibrils (right) [13, 21]. IC = inner-crystalline cellulose ($I_\alpha$, $I_\beta$, $I_{\alpha+\beta}$), Paracryst. = para-crystalline cellulose, IAFS = inaccessible fibril surfaces, AFS = accessible fibril surfaces.

Notably, Larsson assigns the broad resonance between about 79 and 86 ppm – previously denoted as non-crystalline or less-ordered cellulose – exclusively in terms of material located at the fibril surfaces. The para-crystalline signal contribution – situated within the crystalline region – is termed a "well-ordered in-core structure, not accessible to solvents" [13, 21], but is not assumed to be (truly) crystalline. While the exact nature of this species remains unknown, it seems apparent, that it is not identical to either cellulose $I_\alpha$ or $I_\beta$. Consequently, Larsson et al. do not explicitly define a crystallinity index analogous to that used in the two-site integration or deconvolution routines. Nocanda et al. [22] define the degree of crystallinity C [%] in the following way:

$$C[\%] = \frac{(I_\alpha+I_\beta+I_{\alpha+\beta})\times 100\%}{(I_\alpha+I_\beta+I_{\alpha+\beta}+\text{Paracryst.}+\text{AFS}+\text{IAFS})} \quad \text{[Eq.2]}$$

Note, however, that crystallinities obtained in this way are usually much lower than those determined with WAXS and other methods. It is our belief that the "well-ordered" para-crystalline cellulose form also contributes to the crystalline cellulose portion, in a more general sense. In our laboratory C [%] is thus defined as:

$$C[\%] = \frac{(I_\alpha+I_\beta+I_{\alpha+\beta}+\text{Parachutist.})\times 100\%}{(I_\alpha+I_\beta+I_{\alpha+\beta}+\text{Parachutist.}+\text{AFS}+\text{IAFS})} \quad \text{[Eq.3]}$$

Apart from cellulose morphology, the fibril aggregate model [Figure 3] provides also estimates of lateral fibril and fibril aggregate dimensions from the C4 fitting analysis, which are remarkably consistent with e.g. electron microscopy results. From Figure 3 it is apparent, that the fraction of fibril surface area relates to the lateral size of a fibril or fibril aggregate. Wickholm et al. [21] define this fibril surface area fraction q as:

$$q_{fibril} = \frac{(\text{AFS} + \text{IAFS})}{(I_\alpha+I_\beta+I_{\alpha+\beta}+\text{Parachutist.}+\text{AFS}+\text{IAFS})} \quad \text{[Eq.4a]}$$

$$q_{aggregate} = (\text{AFS})/(I_\alpha+I_\beta+I_{\alpha+\beta}+\text{Parachutist.}+\text{AFS}+\text{IAFS}) \quad \text{[Eq.4b]}$$

q is related to the lateral fibril aggregate size according to:

$$q = (4n - 4) / n^2 \quad \text{[Eq.5]}$$

Here, n is the number of glucan chains along one side of the fibril (aggregate). Introducing q into Eq.5 and solving for n, the lateral fibril (aggregate) dimension can be computed using a conversion factor of 0.57 nm width per glucan chain [21].

Larsson's deconvolution routine further yields information about the hemicelluloses content of the investigated material. From our studies it seems, that accuracy and precision of hemicelluloses quantification are limited: Hemicelluloses are partly resistant to acid hydrolysis as a preparatory treatment [21]. Thus, only signals contributing to the accessible fraction of hemicelluloses can be identified and quantified. Furthermore, signals of

hemicelluloses are partly overlapped with the inaccessible fibril surface resonance, are sensitive to spectral phase and baseline correction, and also to the fitting of the neighbouring, large C2, 3, 5 peak. Published AGU C4 fits are further quite inconsistent with respect to the number, position and width of used hemicelluloses resonance lines. In general, one has to beware of over-interpretation.

*Cellulose II*

Larsson's fibril aggregate and signal deconvolution models focus on cellulose I analysis mainly of wood pulp, cotton linters and other native cellulose. Only relatively small amounts of cellulose II occur within the sample after pulping and bleaching. Resonance positions published by Newman et al. [14] can be used in a line shape analysis for larger cellulose II contents in alkaline treated samples or regenerated fibres. Again, signal contributions from inner-crystalline and crystallite-surface material have been assigned. However, Newman et al. [14] define no (analogues to) para-crystalline and inaccessible fibril surfaces signals. Therefore, the direct application of Larsson's deconvolution and analysis routine for cellulose II characterisation seems questionable [23]. Under the assumption of a fibril, rather than a fibril aggregate model [Figure 3], no inaccessible fibril surfaces need to be considered. The broad featureless resonance roughly between 79 and 86 ppm may then be attributed to amorphous or disordered cellulose. Ibbett et al. [24] have analysed regenerated (i.e. cellulose II) fibres using signal deconvolution [Figure 4] and spin relaxation edition. Less- or partially ordered contributions (at surfaces) are interpreted in terms of increased rotameric freedom of the C5-C6 bond in the AGU, with respect to crystalline forms. Signal contributions in the region between 79 and 85ppm are assigned to fully disordered cellulose, i.e. exhibiting variable C5-C6 and glycosidic bond angles.

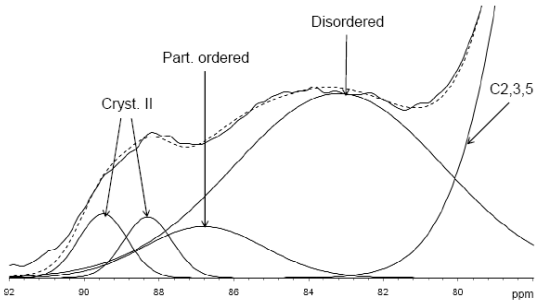


**Figure 4.** Deconvolution of an experimental cellulose II (Lenzing viscose) $^{13}C$ CP-MAS NMR spectrum according to Ibbett et al. [24]. A total of four Gaussian lines of fixed position and width (FWHM) are adjusted in height, such that their sum (dotted line) fits the experimental spectrum.

There exist several methods to determine cellulose I vs. II ratios in various types of samples [Figure 5]. Differences between these techniques mainly refer to their quantification and resolution abilities, also with respect to the absolute amount of cellulose I or II present. Larsson et al. quantify smaller amounts of cellulose II in pulps by analysis of the AGU C1 resonance [Figure 5 A]. Only one line is added for cellulose II in the deconvolution routine, which probably does not sufficiently reflect the structural diversity of this species. However, for smaller amounts of cellulose II (about 4-10%) Larsson's C1 fit yields useful absolute quantities. For larger cellulose II contents, it proves better to analyse C6 line shapes according to Newman's assignments [Figure 5 B]. Here, the resonances for crystalline cellulose I and II are well-separated. Overlapping signals from cellulose I surface signals hamper, however, the reliable quantification of smaller cellulose II amounts. A similar quick and quite reliable estimate for larger cellulose II contents is obtained by C6 crystalline vs. surface cellulose I plus cellulose II integration and deduction of the cellulose I surface signals as retrieved from C4 integration [Figure 5 C].

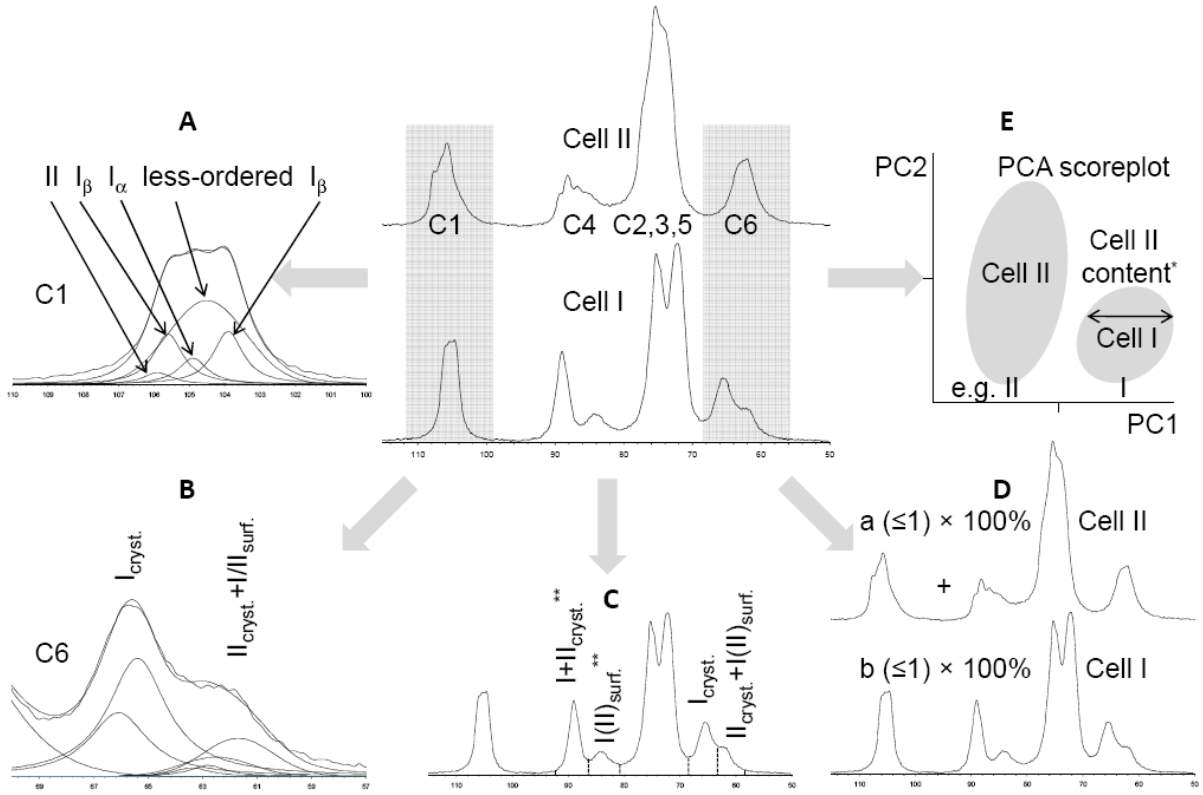


**Figure 5.** Some Cellulose I vs. II quantification methods. A shows the cellulose AGU C1 deconvolution method as described by Larsson et al. [13]. The AGU C6 deconvolution in B and the integration method in C base on Newman's assignment [14]. Fink's weighted addition of 100% cellulose I and II spectra [25-27] is visualised in D. The PCA analysis [8] of cellulose I and II spectral datasets is shown in E.

Two, more specialized cellulose II quantification methods have been established by Fink et al. [25-27] and Lennholm et al. [8] [Figure 5 D and E]. The previous of both uses the weighted addition of 100% cellulose I and 100% cellulose II spectra, such that the sum of both spectra fits the experimental data. Due to signal overlap between crystalline and less-ordered portions of both species implicit assumptions regarding the (ideally identical) degrees of order of both 100% species are made. This limits the accuracy of the method, and restricts its applicability to samples with a relatively well-known history. Another type of cellulose II content analysis in pulps utilizes principal component analysis (PCA). Although it is not a quantitative method, PCA uniquely allows one to establish a relative ranking of low-cellulose II pulps with respect to their cellulose II content.

*Wet-state NMR analysis*

The line-shape analyses of cellulose according to Larsson et al. [13] or Newman et al. [12, 15] require wet-state NMR measurements to enhance spectral resolution [Figure 6]. Significant differences in the apparent crystallinity (i.e. the ratio between crystalline and less-ordered components at 89 and 84ppm) are observed whereas the resolution of spectral features is notably increased. The actual mechanism and reason for the observed line narrowing and relative crystalline signal enhancement remain, however, largely unknown. Park et al. suggest, that amorphous components become more ordered upon hydration. Another reasonable explanation could be the partial suppression of signals associated to solvent accessible domains. This may be caused by their differential relaxation properties with respect to water inaccessible cellulose crystallites.

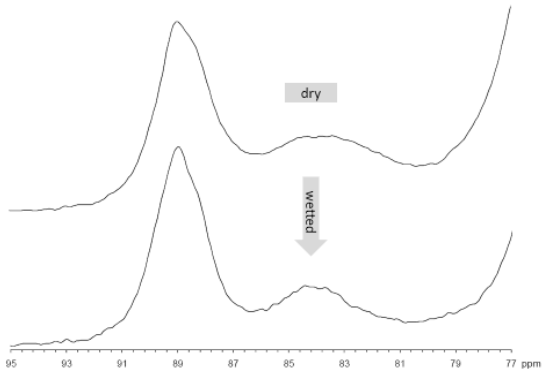


**Figure 6.** Effect of wet-state vs. dry-state cellulose $^{13}C$ CP-MAS NMR measurement on the example of cotton linters. Note the decrease in apparent crystallinity, i.e. the ratio of crystalline vs. less-ordered cellulose signals.

*Sample representativity*

NMR spectroscopy is – similarly to WAXS and Raman/FT-IR – a bulk analysis tool. The recorded signal represents the average of responses from all (cellulose) molecules within the effective receiver coil volume. This is certainly an important criterion when analysing inherently heterogeneous (natural) compounds, such as cellulose, Nowadays typical MAS rotors used for solid-state NMR analyses of cellulose have outer diameters of 7 mm or rather 4 mm, sometimes even less resulting in sample volumes that range from 350 µl down to <80µl. Therefore, we have to address the issue of sample representativity (not only for NMR characterizations) upon interpreting small variations in e.g. cellulose morphology. The reproducibility of solid-state NMR analyses on identical samples proved to be excellent, however the results for different samples from the same charge of cellulose material may significantly vary [14]. The careful evaluation of the representativity by double or triple measurements on different samples of the same specimen is highly recommendable.

*Sample history*

The history of a sample, i.e. age, drying, storage conditions, etc. plays an important role in the investigations of cellulosic material. We have noticed major variations in sample morphology upon drying: A dried and rewetted sample did not yield the same analysis results as the corresponding never-dried sample. This may originate from hornification involving a re-orientation and re-ordering of cellulose chains upon dehydration or from ageing, - admittedly a very slow process - which might cause changes in crystallinity, i.e. a slowly continued crystallization of less-ordered domains towards a lower energy crystalline state. Consequently larger variations in sample history should be avoided to enhance the reproducibility and comparability of the results from the analyses of cellulose samples.

## Conclusions

The importance of $^{13}C$ CP-MAS NMR spectroscopy for the morphological characterization of cellulose materials dramatically increased over the past 10 years. The development of sophisticated techniques played a major role in analysing complex resonance patterns and line shapes by signal deconvolution.. Today a single solid-state NMR experiment of cellulose yields quantitative information about:

a) The distribution of crystalline cellulose $I_\alpha$, $I_\beta$, II, and other polymorphs,
b) Lateral fibril and fibril aggregate dimensions,
c) The crystallinity of the investigated material, and
d) Hemicelluloses and other organic matter (e.g. lignin) content

It is mainly the versatility of the method, but also its compatibility with physical modelling, which has aided its widespread and well-established use today. NMR results provide a reasonable basis towards the investigation and interpretation of structure-properties relationships. The latter are of primary importance in the

directed industrial development of improved cellulosic materials.
Several questions in the field of the NMR spectroscopy of cellulose remain open. There still is room for improvement concerning the current interpretations of the morphological nature of cellulose still. Advanced models of the structure of regenerated cellulose may be required. Also the interactions between cellulose and solvents -particularly water – and their impact on the structure of cellulose deserve further investigation. Multidimensional correlative solid-state NMR may also provide insight into the interfaces of cellulose and lignin or cellulose and hemicelluloses in wood, which may assist in its processing.
The development of more sensitive hardware equipment, new and enhanced experiments, and also spectral analysis techniques will further increase the acceptance and application of NMR spectroscopy in the field of cellulose characterization. To us, the story of cellulose NMR is just at its beginning and we are looking forward to new and exciting future developments.

## Acknowledgements

Financial support was provided by the Austrian government, the provinces of Lower Austria, Upper Austria and Carinthia as well as by the Lenzing AG.. We also express our gratitude to the Johannes Kepler University, Linz, the University of Natural Resources and Applied Life Sciences, Vienna, and the Lenzing AG for their in kind contributions.

## References

[1] J.W.S. Hearle, Fringed-fibril theory of structure in crystalline polymers, J. Polymer Sci. 28 (1958), 432-435.

[2] P.H. Hermans and A. Weidinger, X-ray studies on the crystallinity of cellulose, *J. Polymer Sci.* 4 (1949) 135-144.

[3] R. Evans, R.H. Newman, U.C. Roick, I.D. Suckling and A.F.A. Wallis, Changes in cellulose crystallinity during kraft pulping. Comparison of infrared, X-ray diffraction and solid state NMR results, Holzforschung 49 (1995) 498–504.

[4] D.L. VanderHart and R.H. Atalla, Studies of microstructure in native celluloses using solid-state $^{13}C$ NMR, Macromolecules 17 (1984) 1465-1472.

[5] J.J. Cael, D.L.W. Kwoh, S.S. Bhattacharjee, S.L. Patt, Cellulose crystallites: a perspective from solid-state $^{13}C$ NMR, Macromolecules 18 (1985) 819-821.

[6] A. Isogai, M. Usuda, T. Kato, T. Uryu, R.H. Atalla, Solid-state CP/MAS $^{13}C$ NMR study of cellulose polymorphs. Macromolecules 22 (1989) 3168-3172.

[7] A. Sugiyama, R. Vuong, H. Chanzy, Electron diffraction study on the two crystalline phases occurring in native cellulose from an algal cell wall. Macromolecules 24 (1991) 4168-4175.

[8] H. Lennholm, T. Iversen, Estimation of Cellulose I and II in Cellulosic Samples by Principal Component Analysis of $^{13}C$ CP/MAS-NMR-Spectra, Holzforschung 49 (1995) 119-126.

[9] K.H. Meyer, L. Misch, Positions des atomes dans le nouveau modéle spatial de la celulose, Helv. Chim. Acta 20 (1937) 232-244.

[10] T. Röder, J. Moosbauer, M. Fasching, A. Bohn, H.-P. Fink, T. Baldinger, and H. Sixta. Crystallinity determination of native cellulose -comparison of analytical methods, Lenzinger Berichte 86 (2006), 85-89.

[11] T. Baldinger, J. Moosbauer, and H. Sixta. Supermolecular structure of cellulosic materials by Fourier Transform Infrared Spectroscopy (FT-IR) calibrated by WAXS and 13C NMR, Lenzing Berichte, 79 (2000) 15 - 17.

[12] R.H. Newman, L.M. Davies, P.J. Harris, Solid-State $^{13}C$ Nuclear Magnetic Resonance Characterization of Cellulose in the Cell Walls of Arabidopsis thaliana Leaves, Plant Physiol. 111 (1996) 475-485.

[13] P.T. Larsson, K. Wickholm and T. Iversen, A CP/MAS $^{13}C$ NMR investigation of molecular ordering in celluloses. Carbohydr. Res. 302 (1997) 19-25.

[14] R.H. Newman, T.C. Davidson, Molecular conformations at the cellulose-water interface, Cellulose 11 (2004) 23-32.

[15] D.S. Himmelsbach, F.E. Barton, D.E. Akin, Comparison of responses of $^{13}C$ NMR and NIR diffuse reflectance spectroscopies to changes in particle size and order in cellulose, Appl. Spectrosc. 40 (1986) 1054-1058.

[16] R.H. Newman, M.-A. Ha, L.D. Melton, Solid-state $^{13}C$ NMR investigation of molecular ordering in the cellulose of apple cell walls, J. Agric. Food Chem. 42 (1994) 1402-1406.

[17] F. Horii, A. Hirai, R. Kitamaru, Cross-polarization/magic angle spinning $^{13}C$-NMR study: molecular chain conformations of native and regenerated cellulose, ACS Symp. Ser. 260 (1984) 27-42.

[18] T. Liitiä, S.L. Maunu, B. Hortling, Solid State NMR Studies on Cellulose Crystallinity in Fines and Bulk Fibres Separated from Refined Kraft Pulp, Holzforschung 54 (2000) 618-624.

[19] S. Park, D.K. Johnson, C.I. Ishizawa, P.A. Parilla, M.F. Davis, Measuring the crystallinity index of cellulose by solid state $^{13}C$ nuclear magnetic resonance, Cellulose 16 (2009) 641-647.

[20] H. Sterk, W. Sattler, A. Janosi, D. Paul, H. Esterbauer, Einsatz der Festkörper $^{13}C$-NMR-Spektroskopie für die Bestimmung der Kristallinität in Cellulosen, Das Papier 41 (1987) 664-668.

[21] K. Wickholm, P.T. Larsson, T. Iversen, Assignment of non-crystalline forms in cellulose I by CP/MAS $^{13}C$ NMR spectroscopy, Carbohydr. Res. 312 (1998) 123-129.

[22] X. Nocanda, P.T. Larsson, A. Spark, T. Bush, A. Olsson, M. Madikane, A. Bissessur, T. Iversen, Cross polarisation/magic angle spinning $^{13}C$-NMR spectroscopic studies of cellulose structural changes in hardwood dissolving pulp process, Holzforschung 61 (2007) 675–679.

[23] H. Zhang, H. Zhang, M. Tong, H. Shao, X. Hu, Comparison of the structures and properties of lyocell fibres from high-hemicellulose

pulp and high α-cellulose pulp, J. Appl. Pol. Sci. 107 (2008) 636-641.

[24] R.N. Ibbett, D. Domvoglou, M. Fasching, Characterisation of the supramolecular structure of chemically and physically modified regenerated cellulosic fibres by means of high-resolution Carbon-13 solid-state NMR, Polymer 48 (2007) 1287-1296.

[25] B. Philipp, H.-P. Fink, J. Kunze, K. Frigge, NMR-spektroskopische und Röntgen-diffraktometrische Untersuchun-gen zur Wechselwirkung zwischen Cellulose und Natronlauge, Annalen der Physik 1985, 42 (1985) 507-523.

[26] J. Kunze, H.-P. Fink, Charakterisierung von Cellulose und Cellulose-derivaten mittels hochauflösender Festkörper-$^{13}$C-NMR-Spektroskopie, Das Papier 53 (1999), 753-764.

[27] J. Kunze, A. Ebert, H.-P. Fink, Characterization of cellulose and cellulose ethers by means of $^{13}$C NMR spectroscopy, Cellul. Chem. Technol. 34 (2000) 21-34.

Lenzinger Berichte 87 (2009) 49-59

# A MULTISTAGE MARKETING SURVEY FOR WOOD-BASED DIETARY FIBRE ADDITIVES

**Tobias Stern[1], Stefan Weinfurter,[2] and Peter Schwarzbauer[1,2]**

[1]Kompetenzzentrum Holz GmbH, A-4021 Linz, Austria
[2]University of Natural Resources and Applied Life Sciences, Vienna, Austria

Phone: (+43) 1 47654 – 3581; Fax: (+43) 1 47654 - 3562; E-mail: t.stern@kplus-wood.at

**Wood is widely used as a raw material for the production of food additives and ingredients, but consumers are hardly aware of that. The value-added chain of wood-based dietary fibre additives from producers to consumers has not been investigated as a whole, before. A business survey and a consumer survey were implemented to analyse the value-added chain. To research the market, interviews were conducted in companies producing, processing, or trading within the dietary fibres market, based in German speaking countries. A questionnaire survey was carried out among Austrian consumers to investigate beliefs and knowledge of wood-based food additives. To improve market potential, results suggest that makers of wood-based dietary fibre products apply multistage marketing approaches, such as "Ingredient Branding," and that they provide consumers with additional information (e.g. by health claims, communication labels) on wood-based food additives, because consumer attitudes towards wood-based food additives are predominantly positive.**

**Keywords:** *multistage marketing, consumer, survey, market assessment, wood-based food additives*

## Introduction

Wood is widely used as a raw material for the production of food additives and ingredients [1], [2]. Probably the most well known of these additives is cellulose [3]. In food, cellulose is mostly used as a thickener or binding agent. Many modified cellulose derivates, e.g. carboxymethyl cellulose, are employed as emulsifying agents or stabilisers in food products.

Another widespread and very traditional example of food ingredients derived from trees is gum arabic [4]. These exudates of African Acacia species (Acacia senegal) mainly consist of arabinogalactan, a polysaccharide and hemicellulose. To date gum arabic has been mainly used in the food industry as a thickener. It has recently been found useful as well, as a dietary fibre additive in functional foods. In 1874 Haarmann found that lignin from spruce bark juice could be used to create vanillin [5]. Today lignosulphonate derived from wood within the pulping process is one source for the commercial production of vanillin, which is used as a flavouring agent in food and other industries [6], [7]. The vanillin obtained by this process is the same chemical substance that creates the vanilla aroma when using original vanilla beans. The introduction of this process paved the way for the use of vanilla aroma as a bulk ingredient in the food industry [8].

Probably the most recent example of a wood-based food ingredient is phythosterol used as a supplement in margarine [9],

[10], [11] to lower cholesterol levels in humans. Phytosterols are usually extracted from either soy beans or tall oil, which is a by-product of the pulping process.
Some of these ingredients, such as the sweetener xylitol [12], are the result of time-consuming, complex production processes, which make it hard to identify them as wood-based products.
Most of the wood-based food additives serve to improve the mechanical attributes of food, such as stabilising, binding, dispersing or emulsifying. Some impact the taste of food (sweetening and flavouring); others provide health effects (e.g. cholesterol-lowering phytosterols or prebiotics like gum arabic). These health effect providing additives are relatively new and their markets can be described as dynamic and fast growing [13].
Exceptionally successful products in this context are sugar-free chewing gums with xylitol, such as Orbit from Wrigleys. Another well known example is the cholesterol-lowering margarine Benecol from the Finnish company Raisio Benecol. In 2002 the company reported €843 million sales, mainly derived from the phytosterol-containing margarine [14].
Although references regarding the sales volumes of functional food products are mentioned in the literature quite frequently, they often lack important contextual information, such as the market scope. Consequently, it is not surprising that the published figures show a wide range of variability. The Leatherhead Food Research Association published a report in 1996 estimating the global functional food market at about $6.6 billion in 1994 [15]. Half of this dollar amount was considered the Japanese market's share. Hilliam referred to forecasts expecting the market to reach $17 billion in 2000 [15]. In contrast, Holzapfel and Schillinger estimated a market volume of $75 billion in 2001 [16]. Hilliam mentioned a worldwide market reaching $33 billion in 2000 of which the U.S. market share was estimated to account for about 50 percent of the total [13]. When reviewing the functional food market, it is very important to note that this sector is one of the very few growing submarkets within the food industry, along with convenience and organic food.

## Research Question

Although the use of wood as a raw material in the food industry is quite common, it has rarely been the subject of research or of public interest. In contrast to this lack of publicity it is a topic of high strategic interest for the wood processing industry, e.g. for the development of wood bio-refinery concepts [17], [18]. In order to bridge the gap between existing information and potential strategic meaning, we investigated the following overall research question:

*How to market wood-based dietary fibre products along the added value chain in the food sector?*

## Conceptual Framework

A comprehensive way to investigate charge materials or ingredients markets needs to address the complete value added chain (see figure 1) from producers to consumers in the sense of a multi-stage marketing approach [19].

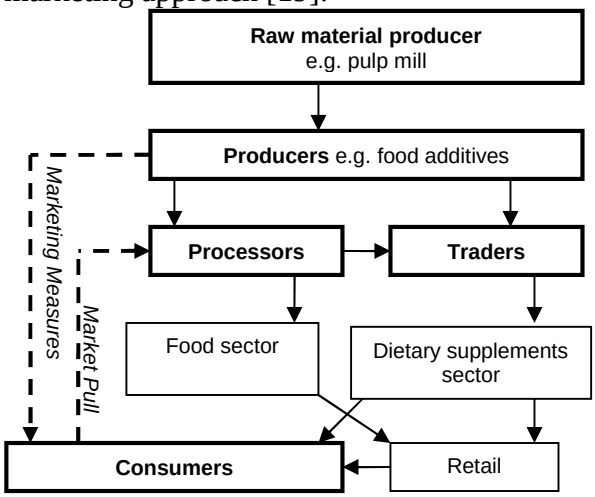


**Figure 1.** Value added chain of wood-based food additives as investigated within this study. The broken arrows on the left indicate a possible "Pull Strategy" by creating demand in a lower market stage.

The multi-stage marketing approach is a concept aiming at following a so called "pull strategy" which tries to create demand for the relevant product from market stages beyond the market stage directly supplied by a producer [19], [20], [21].
The following example shall illustrate that: Personal computers (PCs) need to include some processor chip. Although the PC producer (e.g. HP, Dell) will be the buyer of these processor chips a producer of such chips (e.g. Intel) may find it worthwhile to target advertisement towards final users of PCs. These consumers may ask at the retailer for personal computers with an Intel processor inside. Consequently, the PC producer will be "pulled" to use Intel processors in order to satisfy customer needs. A common tool to reach such a situation is "Ingredient Branding" which is frequently implemented by use of communication labels indicating a certain ingredient to be part of the product (e.g. "Intel inside").
A major issue when applying such strategies is the understanding of power (influence) and interest (attitude) of all relevant market stages [19]. In order to generate such an understanding across different market stages it is necessary to integrate business to business and consumer research (see figure 2).

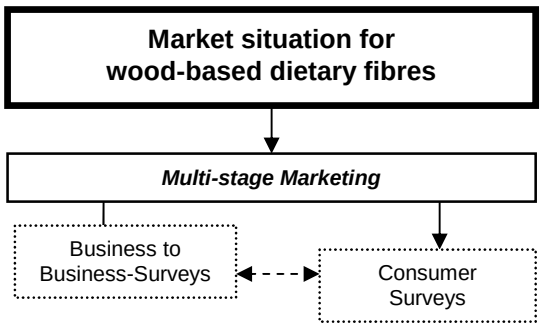


**Figure 2.** Conceptual framework of the study

On the business-to-business level market power can be measured by analysing the size and number of companies in the market, their market position and the relations between them [20], [22]. Their interest in using certain raw materials or ingredients can be analysed in context with product characteristics (e.g. price, technical properties).
At the consumer level market impact and attitudes towards certain products must be investigated on a more psychological level. Attitudes are one of the most common theoretical concepts in social sciences and have a long tradition, especially in marketing research. General theoretical attitude models consist of a cognitive and an affective component [23], [24] explaining the attitudes. In this study we used pre-knowledge and belief as cognitive and affective components stating that those will have a major impact on attitude (see hypothesis 1 - H1 in figure 3). In addition cognitive response analysis (CRA) was employed. CRA is based on the idea that people confronted with new information will try to connect that with their existing knowledge [25].

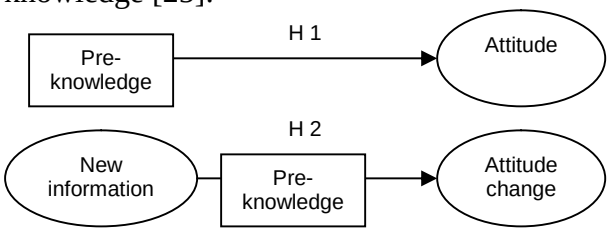


**Figure 3.** Theoretical model of the consumer survey.

Furthermore connecting new and existing information may create thoughts (ideas, etc.) that are different from the new information as well as from the original knowledge. The interaction of new information and existing knowledge therefore is of superior importance for attitudinal change (see hypothesis 2 - H2 in figure 3). The theory of cognitive dissonance [26] for example states that new information conflicting with what is known will be neglected by consumers.

**Table 1.** The study's business and consumer surveys.

| | Business survey | Consumer survey |
|---|---|---|
| **Population base** | *Companies producing, trading or processing dietary food additives* | *People responsible for food purchasing within their households* |
| **Sampling** | *all companies operating in Germany, Austria and Switzerland* | *non-probability sampling of Austrian households* |
| **Sample size** | *123 companies of which 80 responded* | *210 consumers* |
| **Data collection** | *telephone interviews* | *personal interviews* |
| **Questions** | *26 questions addressing Porter's (1985) five competitive forces* | *18 questions on knowledge, information intake and attitude regarding wood-based food additives* |

## Methods

Two separate surveys, a business survey and a consumer survey were employed to analyse the value-added chain of wood-based dietary fibre additives (table 1).

### *The Business Survey*

Companies producing, processing, or trading within the dietary fibres market and operating in German speaking countries were targeted for the business survey. Of a total of 123 companies, 22 were classified as producers, 43 as trading companies, and 58 as processors. Most of these companies were based in Germany (66). Others were headquartered in Switzerland, Austria, USA, France, the Netherlands, Italy, Japan and Belgium. The survey was conducted via telephone interviews. In the case of producing and trading companies, the survey focused on sales representatives, whereas in the case of processors, product development and marketing divisions were contacted. The questionnaire consisted of three parts relating to the following topics: products and activities, market developments and meaning of the sector, and statistical data of the company and respondent.

Of the total 123 companies contacted, a group of 43 firms declined to cooperate in the survey, which resulted in a response rate of around 65%. A higher proportion of the respondents came from representatives of companies based in Austria, whereas their German counterparts were most likely to refuse participation. This may be a result of the fact that many of the representatives from Austrian companies and Austria-based subsidiaries were graduates from the university at which the study was carried out.

About 82% of the producing companies took part in the survey, whereas just 60% of the processors did so (traders matching the average value). This discrepancy may reflect different levels of motivation. The overall response rate can be considered as comparably high. When possible, data concerning annual turnover and number of employees was collected separately for companies not taking part in the survey to acquire information concerning "non-response-bias". The response rate of the largest companies (over €10 billion turnover), that were mainly in processing, was very low (33%). Companies of this size are quite rare (only six in the total population of the survey). The motivation to take part in the survey for these very big companies may be lower since they may have lower need to share their market information with potential competitors. Nevertheless, for companies with more than 10,000 employees, a response rate of about 56% was achieved.

Overall, the 80 companies interviewed are more or less representative of the total population. Differences between the

population base and the participants should be expected to result from the lack of bigger processors. Analyzing the market situation with the specific products in mind, the weakness of missing larger processors, is partly compensated by the higher share of cooperating companies in the earlier market stages (the producers and traders) providing the information sought.

***The Consumer Survey***

Consumer data were collected through a face-to-face survey with 210 Austrian consumers. All the respondents were responsible for all or part of food purchasing within their households, which is reflected in an uneven gender distribution. All respondents were selected through non-probability sampling and were personally interviewed at home [27]. Common socio-demographic characteristics such as age, gender, size of household or place of abode (rural or urban) were questioned for reference regarding the representativeness of the sample (see table 2).

**Table 2.** Socio-demographic characteristics of the consumer sample (n=210) in comparison to the Austrian population according to Statistik Austria [28], [29]

| | Sample | Population |
|---|---|---|
| **Age** | | |
| **<25** | 31.6% | 28.1% |
| **25-35** | 17.9% | 12.7% |
| **36-45** | 20.5% | 16.8% |
| **46-55** | 19.0% | 13.2% |
| **56-65** | 6.1% | 12.3% |
| **66-75** | 3.4% | 8.7% |
| **>75** | 1.5% | 8.2% |
| **Gender** | | |
| **Female** | 61.2% | 51.8% |
| **Male** | 38.8% | 48.2% |
| **Person per household** | | |
| **1** | 9.1% | 34.1% |
| **2** | 26.4% | 28.4% |
| **3** | 28.5% | 16.6% |
| **4** | 20.2% | 13.4% |
| **>4** | 15.7% | 7.4% |

Slight differences appeared between the sample and the overall Austrian population. Female respondents for example were over-represented with 61% compared to 52% in the population [28], [29] (this is probably due to actual shopping behaviour). At the same time, older respondents and single households were under-represented compared to the Austrian average [28], [29].

The fact that the sample did not strictly match the Austrian average has to be taken into account when interpreting the results of the survey. It may be concluded that the sample – at least to some extent – is not statistically representative for the Austrian population.

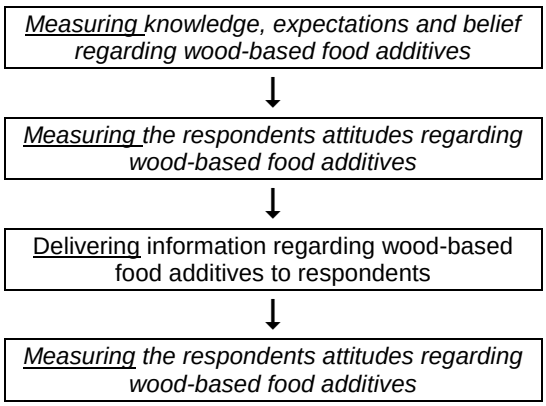


**Figure 4.** Consumer survey design including three types of measurement and a section providing the respondent with additional information.

To acquire information on the respondents' beliefs and knowledge (first box in figure 4) the interview started by asking what kind of raw materials were commonly used for the production of food additives. Then respondents were asked if they knew any wood-based food additives and to provide an example in case of a positive answer. Respondents who did not know food additives from wood were told about the most common examples of such additives (e.g. cellulose) and what they were used for.

Thereafter (second box in figure 4) the respondents were asked to rate wood-based food additives on a five-point scale

(Likert-type) ranging from very good to very bad. The respondents were also asked in an open question if wood-based food additives caused concerns in their minds.
During the next phase of the interview (third box in figure 4), respondents were told that vanilla aroma was one of the most important flavours worldwide with an annual consumption of 12,000 tonnes, of which only 40 tonnes came from the original herb. Consequently the respondents were asked if they knew that vanilla aroma was regularly produced from wood lignin to meet demand. Primarily, the intention of this question was not to receive an answer but to transfer additional information.
Subsequently, (forth box in figure 4) respondents were probed to unveil if their attitudes had changed during the interview. They were asked to evaluate wood-based food additives on a five-point scale once again.
Finally socio-demographic data concerning gender, age, job, household size and place of abode were collected.

**Business Survey Results**
When analysing the market power in a business to business environment it is necessary to distinguish between the producers, traders and processors (see figure 5). Size of producing firms ranges from four employees to about 120,000. All companies except the largest one have less than 10,000 employees.

For trading firms, a different situation can be observed (see figure 5). In this case the number of employees ranges from 3 to 19,500 with 61% of the companies employing less than 100 employees. Within the trading companies there are two subgroups, one employing more than 4,000 people the other employing less than 300.
With regard to the number of employees, the greatest range can be found in the processing stage, ranging from four to about 234,000. Twenty seven percent of these firms have 100 employees or less, while the largest 10% have more than 50,000. The processing stage seems to be the most balanced but also the most powerful.
Industry growth has been found a key factor in the observed market, especially in food industries. The respondents estimated an annual growth of 11.4%, which makes this market one of the fastest growing in the food industry.

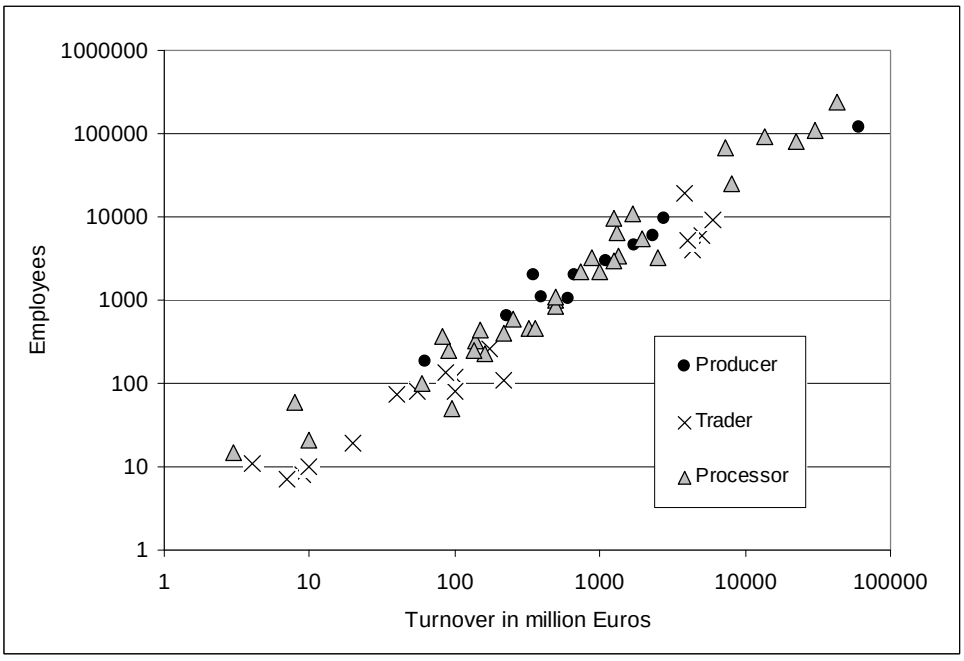


**Figure 5.** Annual turnover and number of employees of the firms (n=63).

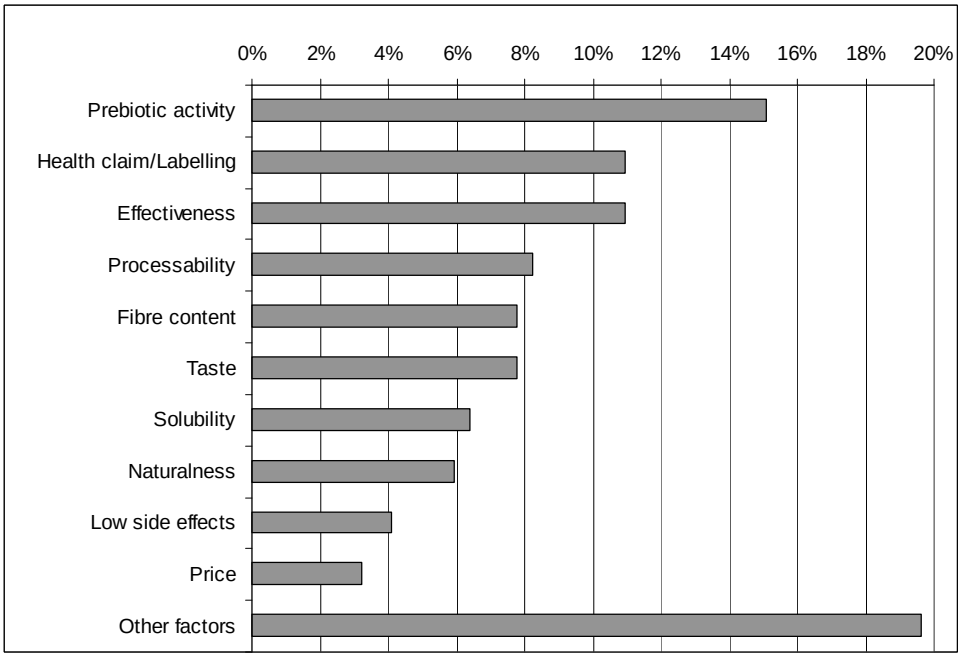


**Figure 6.** Frequency of product characteristics mentioned in the business survey as most important selling/buying issues (n=219).

The survey identified two different kinds of wood-based products in the dietary fiber market, cellulose-based products and hemicelluloses-based products (gum arabic and arabinogalactan). While the latter was identified in all market stages including processors, the former were mentioned only in the producing and the trading stage. The survey results identified prebiotic activity, labelling of approved health claims and high efficiency as the three most often mentioned competitive factors (see figure 6).

According to our results, cellulose-based products completely lack competitiveness in that they do not possess prebiotic activity, approved effects or health claims. In contrast, the health benefits and claims of gum arabic and arabinogalactan are approved and their producers created certain trade names and communication labels (e.g. brandings, trade names, logos). Due to their effectiveness and technical properties (e.g. solubility), these products are able to compete with dominant products (Fructooligosaccharide and Inulin), although their estimated market share within the analyzed firms is comparable low (about 6.2%). The price ratio between these two product groups is 1 to 1.89, indicating arabinogalactan and gum arabic to be nearly twice as expensive as the dominating products. Consequently, the producers of arabinogalactan and gum arabic tend to focus on certain niche applications (e.g. soft drinks, dietary supplements) that value the exclusivity, technical attributes, and/or the effects of their products.

In general, the survey confirmed that dietary fibre additives are complex products depending on their approved health claims that need to be communicated successfully to the consumer. Consequently, these products require multistage marketing approaches, such as “Ingredient Branding” in particular [30].

**Consumer Survey Results**

The results of the consumer survey indicate that approximately 12 to 14 % of respondents had some knowledge of wood-based food additives (so called “Experts”).

In general the respondents’ attitude towards wood-based food additives was

positive compared to food additives in general. The results indicate a clear link between pre-knowledge and attitude regarding wood-based food additives. Respondents who had some knowledge of wood-based food additives (see "experts" group and black bars in figure 7) showed more positive attitudes specifically in contrast to those who had wrong information or wrong ideas about wood-based food additives (e.g. sawdust to be used in strawberry yogurt, bread and sausages) (see "misbeliever" group and black bars in figure 8). Using the chi-square test, significant differences (n=210; $X^2$=31.552; df=12; p<0.01) between the knowledge groups and their evaluation of wood-based food additives were found (see black bars in figure 7).

The additional information provided on wood-based food additives generally lead to significant more positive attitudes (Wilcoxon signed rank test, Z=-3.660; p<0.01) about wood-based food additives.

On the basis of different kinds of knowledge or belief the impact of pre-knowledge on the effect of additional information can be observed (see grey bars in figure 7). As shown in figure 7, the evaluations of all knowledge groups were more closely bunched at the end of the interview (compare black bars with grey bars). At this stage no significant difference between the groups was found (n=210; $X^2$=11.884; df=8; p=0.160) in terms of the evaluations of wood-based food additives. Despite notable improvements, the "Misbelievers" still provided the worst evaluation. The greatest improvement was found in case of the "Uninformed" (no pre-knowledge or belief) group, whereas evaluations of "Experts" and the "Believers" showed insignificant changes.

These results indicate that it is easier to improve the evaluations of those respondents who had no or just a vague idea about wood-based food additives than those who already had an idea, be it right or wrong. This result is in a way convergent with the theory of cognitive dissonance [26] and confirmation bias [31] as some respondents probably blocked the intake of the offered but dissonant

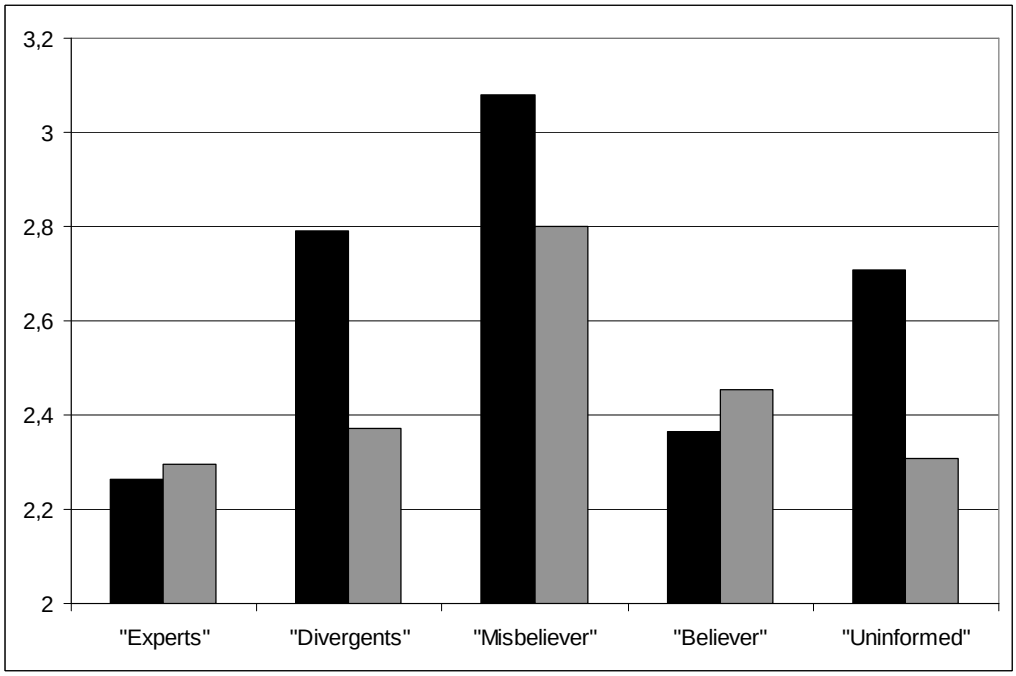


**Figure 7.** Mean evaluations on the five point Likert-scale from very good (1) to very bad (5) of wood-based food additives by respondents of the five defined knowledge groups at the beginning (black) and the end of the interview (grey) (n=210).

information. Those respondents who had a wrong idea, still showed a relative higher willingness to improve their evaluation than those who were confirmed in their knowledge and hence had no reason to change their evaluation at all.
It can therefore be concluded that the provision of additional information (e.g. by health claims, communication labels) on wood-based food additives would improve their marketing potential. As the positive effect of additional information was stronger in the case of respondents with no conceptions or beliefs, it would appear important for the industry to run proactive information campaigns.

## Conclusions

In the functional food sector some large multinational processing companies were identified as key stage possessing most of the market power. They defined prebiotic activity, labelling of approved health claims and high efficiency as important product attributes.
Hence raw material producers need to address these processing industries explaining which advantages their products will have to them for successful marketing in this sector.
Although consumers are not a typical key stage in this context their potential to act either as a major barrier or a potential "gate keeper" has been found notable. As only a relatively small group of consumers (about 10 to 12%) have been found to have a critical attitude towards wood-based food additives, it is unlikely that they will become a market barrier. Due to the fact that most consumers do not have any firm knowledge or attitude towards wood-based food additives so called „Ingredient Branding" could be utilized to create demand in sense of a "pull strategy".
The food sector is a very little known application area for wood-based products which can be derived from celluloses, hemicelluloses, lignin or extractives. In light of increasing utilization of side streams in various wood processing industries e.g. the wood bio-refinery, application areas in food, cosmetic or pharmaceutical industries become more and more interesting for research and industries.

## Acknowledgements

Financial support was provided by the Austrian government, the provinces of Lower Austria, Upper Austria and Carinthia as well as Lenzing AG. We also express our gratitude to the University of Natural Resources and Applied Life Sciences, Vienna, and the Lenzing AG for their in-kind contributions.

## References

[1] Stern, T., (2009), Wood for food: The situation of wood-based products in the market for dietary fiber additives – A branch-analysis approach, Forest Products Journal, 59(1-2):19-25.

[2] Stern, T., Haas, R. and Meixner, O., (2009), Consumer acceptance of wood-based food additives, British Food Journal, 111(2):179-195.

[3] Slavin, J.L. and Marlett, J.A. (1980), Influence of refined cellulose on human bowel function and calcium and magnesium balance, American Journal of Clinical Nutrition, 33:1932-1939.

[4] Mocak, J., Juraseka, P., Phillips, G.O., Varga, S., Casadei, E., and Chikemai, B.N., (1998), The classification of natural gums. X. Chemometric characterization of exudate gums that conform to the revised specification of the gum arabic for food use, and the identification of adulterants, Food Hydrocolloids, 12:141-150.

[5] Krammer, G.E., Weckerle, B., Brennecke, S., Weber, B., Kindel, G., Ley, J., Hilmer, J.M., Reinders, G., Stöckigt, D., Hammerschmidt, F.J., Ott, F., Gatfield, I., Schmidt, C.O. and Bertram, H.J., (2006), Product-oriented flavor research: Learnings from the past, visions for the future, Molecular Nutrition & Food Research, 50(4-5):345-350.

[6] Priefert, H., Rabenhorst, J. and Steinbüchel, A., (2001), Biotechnological production of vanillin, Applied Microbiology and Biotechnology, 56:296–314.

[7] Lewis, R.J., (1989), Food additives handbook, Van Nostrand Reinhold, New York.

[8] Bütehorn, U. and Pyell, U., (1996), Micellar electrokinetic chromatography as a screening method for the analysis of vanilla flavourings and vanilla extracts, Journal of Chromatography A, 736(1-2):321-332.

[9] de Graaf, J., de Sauvage Nolting, P.R.W., van Dam, M., Belsey, E.M., Kastelein, J.J.P., Haydn Pritchard, P. and Stalenhoef, A.F.H., (2003), Consumption of tall oil-derived phytosterols in a chocolate matrix significantly decreases plasma total and low-density lipoprotein-cholesterol levels, British Journal of Nutrition, 88:479–488.

[10] Wolfreys, A.M. and Hepburn, P.A., (2002), Safety evaluation of phytosterol esters, Part 7, Assessment of mutagenic activity of phytosterols, phytosterol esters and the cholesterol derivative, 4-cholesten-3-one, Food and Chemical Toxicology, 40:461–470.

[11] Maki, K.C., Shinnick, F., Seeley, M. A., Veith, P.E., Quinn, L.C., Hallissey, P.J., Temer, A. and Davidson, M.H., (2003), Food Products Containing Free Tall Oil-Based Phytosterols and Oat ß-Glucan Lower Serum Total and LDL Cholesterol in Hypercholesterolemic Adults, The American Society for Nutritional Sciences Journal of Nutrition, 133:808-813.

[12] Nigam, P. and Singh, D., (1995), Processes for Fermentative Production of Xylitol – a Sugar Substitute, Process Biochemistry, 30,(2):117-124.

[13] Menrad, K., (2003), Market and marketing of functional food in Europe, Journal of Food Engineering, 56:181-188.

[14] Dustmann, H., (2004), Analyse und Evaluierung der Auswirkungen des Angebots und der Nachfrage nach funktionellen Lebensmitteln auf die Ernährungsindustrie sowie auf vor- und nachgelagerte Stufen der Wertschöpfungskette, Dissertation, Technische Universität München, Munich.

[15] Hilliam, M., (1998), The Market for Functional Foods. International Diary Journal, 8:349-353.

[16] Holzapfel, W.H. and Schillinger, U., (2001), Introduction to pre- and probiotics, Food Research International, 35:109-116.

[17] Goldstein, I.S., (1981), Chemicals from biomass: present status, Forest Products Journal, 31(10):63-68.

[18] Willfor, S., Sundberg, K., Tenkanen, M., and Holmbom, B., (2008), Spruce-derived mannans - A potential raw material for hydrocolloids and novel advanced natural materials, Carbohydrate Polymers, 72(2):197-210.

[19] Rudolph, M., (1989), Mehrstufiges Marketing für Einsatzstoffe: Anwendungsvorausetzungen und Strategietypen, Europäische Hochschulschriften, Reihe 5, Peter Lang Verlag, Frankfurt am Main.

[20] Backhaus, K., (1990), Investitionsgütermarketing, 2. Auflage, Verlag Franz Vahlen,

München.
[21] Pförtsch, W.A. und Müller, I., (2006), Die Marke in der Marke, Bedeutung und Macht des Ingredient Branding, Springer Verlag, Berlin.
[22] Porter, M. E.,(1985), Competitive Advantage: Creating and Sustaining Superior Performance, The Free Press, New York, NY.
[23] Fishbein, M. and Ajzen, I., (1975), Belief, attitude, intention and behaviour, an introduction to theory and research, Addison-Wesley, Reading, UK.
[24] Trommsdorff, V., (1993), Konsumentenverhalten, Kohlhammer-Edition Marketing, Stuttgart.
[25] Petty, R. E., Ostrom, T. M., and Brock, T. C., (1981), Cognitive responses in persuasion, Erlbaum, Hillsdale, NJ.
[26] Festinger, L., (1957), A theory of cognitive dissonance, Row Peterson, Evanston, IL.
[27] Verbeke, W., (2005), Consumer acceptance of functional foods: socio-demographic, cognitive and attitudinal determinants, Food Quality and Preference, 16:45-57.
[28] Statistik Austria, (2005), Demographisches Jahrbuch 2004, Statistik Austria, Vienna.
[29] Statistik Austria (2006), Einkommen, Armut und Lebensbedingungen – Ergebnisse aus EU-SILC 2004, Statistik Austria, Vienna.
[30] Venkatesh, R. and Mahajan, V., (1997), Products with branded components: An approach for premium pricing and partner selection, Marketing Science, 16(2):146-165.
[31] Jonas, E., Schulz-Hardt, S., Frey, D. and Thelen, N., (2001), Confirmation bias in sequential information search after preliminary decisions: An expansion of dissonance theoretical research on selective exposure to information, Journal of Personality and Social Psychology, 80(4):557-571.

Lenzinger Berichte 87 (2009) 60-67

# ISOLATION OF HEMICELLULOSES FROM BIRCH WOOD: DISTRIBUTION OF WOOD COMPONENTS AND PRELIMINARY TRIALS IN DEHYDRATION OF HEMICELLULOSES

**Lidia Testova[1], Kati Vilonen[2], Henna Pynnönen[3], Maija Tenkanen[3], and Herbert Sixta[1]**

[1]Department of Forest Products Technology, Helsinki University of Technology.
[2]Department of Biotechnology and Chemical Technology, Helsinki University of Technology.
[3]Department of Applied Chemistry and Microbiology, University of Helsinki.

**General aspects of autohydrolysis at varied temperatures, treatment intensities and liquid-to-wood ratios were investigated. Overall solid balance of the selected samples was determined using gravimetrical methods. Analytical methods for carbohydrates and lignin were used to represent componential mass balance. Water hydrolysis activates lignin by homolytic cleavage which results in partial transfer to the hydrolysates in the form of dissolved and dispersed lignin while parts of the residue reveal an increased solubility in acetone. The amount of acetone soluble matter increases with P-factor and decreasing liquor-to-wood ratio. Moderate autohydrolysis, representing a P-factor of about 200, which might be suitable for subsequent paper pulp production releases sugar components in an amount of about 6-7% on wood, while this value increases up to 12% and more when autohydrolysis conditions are applied, P-factor ~ 800, which are typical for dissolving pulp production.**

**Preliminary dehydration studies with glucose as model substance at 160°C over $ZrO_2$ and $TiO_2$ catalysts have been conducted. The objective is to develop a low-cost process for the manufacture of hydroxymethylfurfural (HMF) from C6-sugars, preferably glucose and mannose. It has been shown that $ZrO_2$ is slightly more effective in catalyzing isomerisation to fructose, while $TiO_2$ was more active in dehydration. However, both catalysts exhibit not enough acidic sites to catalyze the overall reaction effectively.**

**Keywords:** *birch wood, hemicellulose, lignin*

## Introduction

High dependence on imported oil and declining fossil fuels reserves, environmental concerns of today and struggle for markets give modern bio-based industry a driving force for development of the Biorefinery concept which implies complete utilization of all biomass processing streams in the most efficient and beneficial way. For the existing pulp and paper mills this means not only improvement of the conventional processes but also introduction of new ones targeting at derivation of additional products with high added value. One of such possibilities is isolation and conversion of wood hemicelluloses into valuable products.

HemiEx is a project focusing on the selective extraction of hemicelluloses from hardwood species in connection with alkaline pulping and study of different chemical aspects of the process. The project scope includes investigation of

hemicelluloses isolation methods i.e. water prehydrolysis and alkaline pre-extraction prior to and novel solvents extraction subsequent to alkaline pulping. The sugar fraction of the extracts is then separated from other wood degradation products by means of membrane separation technology before it is converted to furanic compounds and xylose-based food additives. As regards pulp production, both dissolving and paper pulps are aimed at. The effect of pretreatment conditions on papermaking properties of pulp will also be investigated.

## Background

Hardwoods are rich in pentosans. The main component of hardwood pentosans is glucuronoxylan in which bonds between xylose units are easily hydrolysable. Birch wood contains up to 28% of pentosans most of which is acidic glucuronoxylan [1, 2]. Cleavage of acetyl groups present in hemicelluloses chains during water treatment at elevated temperatures facilitates acidic hydrolysis and decreases pH of the liquid fraction to 3-4 [3].

The most significant reaction taking place in autohydrolysis is hydrolytic cleavage of xylan and its dissolution in the liquid phase in the form of xylooligosaccharides (XOS) and xylose. Final hydrolysate composition depends on the treatment intensity. At some point formation of xylose degradation products (furfural, HMF and unknown products) increases and sugar yield decreases [4]. Cellulose is much less affected by the cleavage of glycosidic bonds than xylan due to its crystalline structure [5]. Lignin undergoes depolymerization and repolymerization in acidic conditions [6]. Cleavage of lignin β-O-4 bonds results in the formation of reactive phenolic species initiating the formation of precipitates which are difficult to process. Formation of reactive lignin structures is also followed by recondensation decreasing lignin reactivity in the subsequent treatment [7].

Prehydrolysis of wood in acidic environment is not a new process. It was developed for production of dissolving pulps in order to eliminate polysaccharides with low degree of polymerization. Water and diluted acid prehydrolysis were replaced by steam pretreatment due to technical difficulties caused by formation of precipitates. Unfortunately, utilization of separated sugars was not given any attention at that time due to the above mentioned problem.

Hydrolysate liquids offer a source of monosaccharides to be utilised in the production of renewable based fuel and chemical compounds. One interesting reaction route to fuel and chemical compounds is the production of furfural (F) and hydroxymethylfurfural (HMF) from pentose and hexose sugars. However, a low-cost and large scale production process satisfying also requirements of sustainability is needed. The main challenge is to obtain high selectivity together with high conversion. This requires continuous separation of formed products to prevent their further reactions to acids and polymeric condensation products [8].

In this paper preliminary results on birch wood (*Betula verrucosa*) autohydrolysis under different conditions and distribution of main wood components in wood residue and hydrolysate after autohydrolysis are presented, which also, includes some results from the studies of acid catalysed dehydration reaction.

## Experimental

### Autohydrolysis

Birch chips used for the investigation were delivered frozen, screened [9] and stored in the freezer until shortly before the experiments. Dry matter content was determined on defrosted chips [10].

Autohydrolysis was performed in a rotating batch oil-bath digester with eight bombs of 220 ml each. Prehydrolysis factor (P-factor) based on Arrhenius equation combining the effect of time and temperature similarly to H-factor in kraft pulping was used as a measure of prehydrolysis intensity [11].

Investigated intensities were in the total range of P-factors from 50 to 1500 at two temperatures of 150ºC and 170ºC at liquor-to-wood (L:W) ratios 4:1 and 8:1. After completion of autohydrolysis bombs were cooled rapidly in cold water. Wood residue was washed manually using washing bags immediately after complete cooling of the bombs at the temperature of 70°C. Yield of wood residue was measured. Wood residue, hydrolysates and wash filtrates were stored for further measurements and analyses. Gaseous fraction was not collected.

**Dehydration reactions with model compounds**

Dehydration experiments were carried out in a 70 ml stainless steel batch reactor, stirred with magnetic rod and heated with an electric oven. Studied reaction temperatures varied between 100 and 180°C. $TiO_2$ and $ZrO_2$ were used as acidic catalysts in water solution having pH 7. As substrates both glucose and xylose were used to follow dehydration reactions.

**Analytical methods**

Basic analysis was performed on the selected sample series (solid phase and hydrolysates). Solid phase (raw wood and wood residue) was air-dried and ground with the Wiley mill. Samples were analyzed for ash content [12]; acetone soluble matter content measurement (ASM) was followed by determination of [13] Klason lignin, acid soluble lignin (ASL) content [14]. Preparation of structural carbohydrate samples was carried out according to the NREL procedure [14] but analysis and quantification of carbohydrates was carried out with Agilent series 1100 HPLC with RID using the column Phenomenex Rezex Monosaccharide RHM H+ ion exchange column which allowed quantification of only glucose and xylose monosugars. Same analytical method was used also with the samples from dehydration reaction.

Measurement of dry solids concentration in hydrolysates and wash filtrates was performed using the procedure similar to the standard SCAN-N 1:61 [15] and involved drying of a sample in the oven at 105 °C. Insoluble hydrolysate fraction was separated from liquid fraction by centrifugation for 20 minutes at 8000 revolutions per minute. Liquid fraction was analyzed for carbohydrates composition with methanolysis and GC [16], acetic acid was quantified using Megazyme Acetic Acid kit K-ACET before and after releasing the acetic acid Solubilized lignin was quantified from UV spectra at wavelength 205 nm [17]. Content of separated insoluble fraction, which is assumed to be mainly composed of lignin [18], was determined gravimetrically. Componential analysis was not performed on the wash filtrates; calculations were based on the assumption that concentrations of hydrolysates and liquid remaining in the wood residue before washing are equal.

**Results and discussion**

**Autohydrolysis and overall mass balance**

Preliminary autohydrolysis trials were carried out at different conditions with a broad range of P-factors. Figure 1 represents yields of wood residue after autohydrolysis treatment at two temperatures and liquid-to-wood ratios. The fairly good agreement of the results obtained at 150ºC and 170ºC confirms the validity of the P-factor concept. Two dissolution stages are clearly observed.

**Table 1.** List of samples selected for componential analysis.

| Sample code | P-factor | Time at target temp., min | Temp., °C | Liquid-to-wood ratio | Sample code | P-factor | Time at target temp., min | Temp., °C | Liquid-to-wood ratio |
|---|---|---|---|---|---|---|---|---|---|
| 150-100-4:1 | 100 | 48 | 150 | 4:1 | 170-200-4:1 | 200 | 17 | 170 | 4:1 |
| 150-200-4:1 | 200 | 97 | | | 170-500-4:1 | 500 | 47 | | |
| 150-400-4:1 | 400 | 197 | | | 170-1000-4:1 | 1000 | 97 | | |
| 150-600-4:1 | 600 | 297 | | | 170-1500-4:1 | 1500 | 147 | | |
| 150-100-8:1 | 100 | 48 | | 8:1 | 170-750-8:1 | 750 | 72 | | 8:1 |
| 150-200-8:1 | 200 | 97 | | | 170-1000-8:1 | 1000 | 97 | | |
| 150-400-8:1 | 400 | 197 | | | 170-1250-8:1 | 1250 | 122 | | |
| 150-600-8:1 | 600 | 297 | | | 170-1500-8:1 | 1500 | 147 | | |

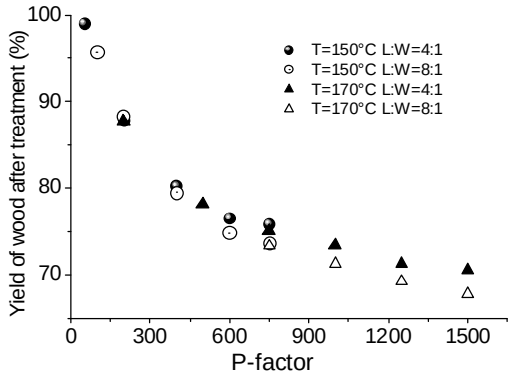


**Figure 1:** Wood yield after autohydrolysis at different temperatures and L:W ratios.

Dissolution rate of wood components is high at the first stage in the range of P-factors from 0 to 400 associated with the dissolution of highly branched hemicelluloses. Further dissolution occurs at lower rate. Final yield loss at highest investigated P-factor was 30% and 32% with liquid-to-wood ratios 4:1 and 8:1, respectively. Intensities higher than P-factor 750 were not investigated at 150 °C due to very long treatment duration (more than 6 hours). Furthermore, at higher liquid-to-wood ratios lower wood residue yields are observed due to facilitation of hydrolysis products transfer from the cell wall into the bulk liquid with lower concentration.

A selection of the conditions for further investigation was made to cover the P-factor range for potential production of paper and dissolving pulp grades as depicted in Table 1.

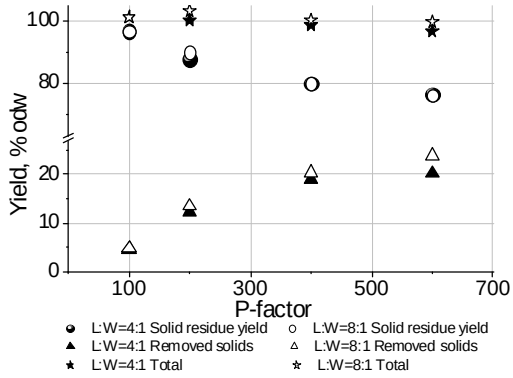


**Figure 2**: Overall solid mass balance for autohydrolysis at the temperature 150 °C.

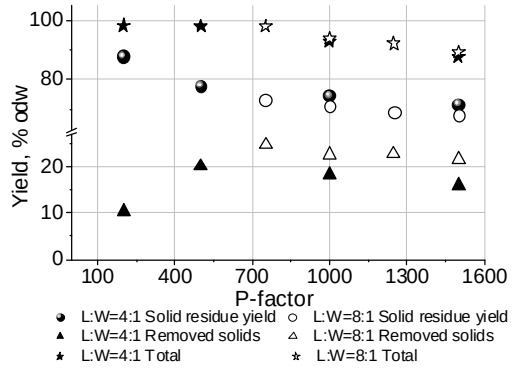


**Figure 3:** Overall solid mass balance for autohydrolysis at the temperature 170 °C.

Figures 2 and 3 represent overall autohydrolysis mass balance calculated as total of wood residue yield, dry solids concentration in hydrolysates and wash filtrates and total concentration of acetyl

groups in hydrolysates to compensate for evaporation of acetic acid while measuring dry solids concentration.

Total mass balance for low P-factors is quite close to 100 percent whereas trials with high P-factors demonstrate decrease in total balance. At the same time, decrease of dry solids concentration with increased P-factor is observed. One of the explanations is an increase of dissolved wood components decomposition with increased treatment intensity and possible subsequent volatilisation. Another reason is obviously the limitation of the dry solids concentration measurement method. Measurement of total organic carbon (TOC) is therefore required to obtain more reliable concentration values [18].

**Componential mass balance**

Preliminary analysis of selected wood samples was carried out. Tables 2.1 and 2.2 represent available data describing distribution of wood components in wood residue and hydrolysates.

Lignin content in solid phase was estimated as total of Klason lignin, acid soluble lignin and acetone soluble matter (including acetone soluble substances of initial wood). Formation of highly reactive lignin causes dissolution to large extent at the stage of acetone extraction. The resulting value decreases due to partial transfer of wood lignin to the hydrolysates in the form of dissolved and precipitated lignin. [6, 19]

Wood residue carbohydrates content was determined only as total glucan and xylan. Expected decrease of xylan content is seen as increase in xylan content in hydrolysates. However, total xylan in wood residue and hydrolysate decreases with increased intensity of autohydrolysis which can be explained by formation of furfural and other xylose degradation products which have not been quantified so far. Xylan content in hydrolysates decreases with autohydrolysis intensity due to formation of xylose degradation products. Higher liquid-to-wood ratio allows better dissolution of carbohydrates in liquid per unit wood weight as mentioned above.

Total componential balance is below 100 percent, which can be justified by the following: not all products were quantified in hydrolysates, solid residue carbohydrate composition is not complete, gaseous phase was not collected.

**Dehydration studies**

Monosaccharides isomerization and dehydration reactions were investigated in 10% glucose solutions in water (pH 7) at the temperature 160 $^{o}$C over $TiO_2$ and $SiO_2$ catalysts. Especially in the case of glucose, isomerization plays an important role, because fructose, an isomer of glucose, is clearly more reactive in dehydration. From the samples taken as a function of time it can be seen that the isomerization reaction is preferred over the dehydration reaction to HMF, which is assumed to happen via fructose (shown in Figure 4). Also other products in addition to fructose and HMF like levulinic and formic acids resulting from HMF degradation reactions were detected, but not quantified yet. At higher reaction temperature, above 160 $^{o}$C, the black precipitate, so called humins, were also formed as a condensation product from both glucose and furanic compounds.

From the experimental results it can be concluded $TiO_2$ is a little bit more active in dehydration, while $ZrO_2$ is more effective in catalyzing isomerization. Based on the characterization experiments of Watanabe *et al.* [20] it was concluded that $TiO_2$ has more acid sites on its surface, which explains its higher dehydration activity. On contrary, ZrO2 has more basic sites promoting higher isomerization activity. However, both catalysts had too low acidity to catalyze reaction effectively.

**Table 2.1.** Componential mass balance: raw wood and autohydrolysis at 150°C.

| Sample | Raw wood | PF100 4:1 | PF200 4:1 | PF400 4:1 | PF600 4:1 | PF100 8:1 | PF200 8:1 | PF400 8:1 | PF600 8:1 |
|---|---|---|---|---|---|---|---|---|---|
| **Wood residue** | **93.4** | **92.5** | **76.7** | **71.3** | **70.4** | **91.7** | **85.5** | **77.1** | **76.4** |
| Lignin and ASM | 26.0 | 24.9 | 24.7 | 23.6 | 25.1 | 24.9 | 23.9 | 24.0 | 24.2 |
| Klason lignin | 19.1 | 17.2 | 16.2 | 15.2 | 14.4 | 17.5 | 16.6 | 15.4 | 14.9 |
| ASL | 4.5 | 4.4 | 3.3 | 2.1 | 1.6 | 3.9 | 3.1 | 2.3 | 1.8 |
| ASM | 2.4 | 3.3 | 5.2 | 6.2 | 9.1 | 3.5 | 4.2 | 6.3 | 7.5 |
| Carbohydrates | 67.4 | 67.5 | 52.0 | 47.7 | 45.3 | 66.8 | 61.6 | 53.1 | 52.2 |
| Glucan | 38.8 | 40.1 | 34.8 | 35.1 | 34.8 | 38.8 | 40.3 | 38.6 | 40.0 |
| Xylan* | 28.6 | 27.4 | 17.3 | 12.6 | 10.5 | 28.0 | 21.3 | 14.5 | 12.2 |
| **Hydrolysate** | **-** | **4.3** | **10.7** | **17.3** | **19.3** | **5.2** | **12.5** | **19.6** | **22.5** |
| Carbohydrates | - | 2.1 | 6.2 | 10.9 | 11.0 | 3.0 | 7.4 | 10.7 | 12.7 |
| Xylan** | - | 1.2 | 4.5 | 8.6 | 8.6 | 1.5 | 4.9 | 8.0 | 9.7 |
| Acetic acid | - | 0.5 | 1.4 | 2.4 | 2.5 | 0.4 | 1.3 | 2.4 | 3.0 |
| Lignin | - | 1.8 | 3.2 | 4.0 | 5.8 | 1.8 | 3.9 | 6.5 | 6.7 |
| Solubilized lignin | - | 1.5 | 2.5 | 2.7 | 2.9 | 1.4 | 3.0 | 3.5 | 3.1 |
| Insoluble fraction | - | 0.2 | 0.6 | 1.3 | 2.8 | 0.4 | 0.9 | 2.9 | 3.6 |
| **Total** | **93.4** | **96.8** | **87.5** | **88.6** | **89.7** | **96.9** | **98.0** | **96.7** | **98.9** |

**Table 2.2.** Componential mass balance: autohydrolysis at 170°C

| Sample | PF200 4:1 | PF500 4:1 | PF1000 4:1 | PF1500 4:1 | PF750 8:1 | PF1000 8:1 | PF1250 8:1 | PF1500 8:1 |
|---|---|---|---|---|---|---|---|---|
| **Wood residue** | **83.7** | **74.7** | **73.0** | **70.0** | **67.2** | **65.3** | **63.5** | **62.0** |
| Lignin and ASM | 24.4 | 24.9 | 25.6 | 27.6 | 23.1 | 23.3 | 22.7 | 22.4 |
| Klason lignin | 16.1 | 14.1 | 13.0 | 11.5 | 13.6 | 12.9 | 11.8 | 11.4 |
| ASL | 3.3 | 1.9 | 1.2 | 0.9 | 1.4 | 1.5 | 1.2 | 1.1 |
| ASM | 4.9 | 8.9 | 11.3 | 15.2 | 8.2 | 8.9 | 9.7 | 9.9 |
| Measured carbohydrates | 59.3 | 49.8 | 47.4 | 42.4 | 44.1 | 42.0 | 40.8 | 39.6 |
| Glucan | 38.3 | 38.1 | 38.9 | 36.0 | 35.4 | 34.6 | 34.5 | 33.8 |
| Xylan* | 20.9 | 11.7 | 8.5 | 6.4 | 8.6 | 7.5 | 6.4 | 5.8 |
| **Hydrolysate** | **9.2** | **17.8** | **16.8** | **15.1** | **21.5** | **25.4** | **26.2** | **23.2** |
| Carbohydrates | 5.3 | 10.9 | 10.8 | 8.9 | 12.2 | 12.4 | 11.9 | 11.2 |
| Xylan** | 3.7 | 8.5 | 8.5 | 6.8 | 9.6 | 9.7 | 9.3 | 8.6 |
| Acetic acid | 1.2 | 2.4 | 2.7 | 2.9 | 3.0 | 3.1 | 3.3 | 3.5 |
| Lignin | 2.7 | 4.5 | 3.4 | 3.4 | 6.4 | 9.9 | 11.0 | 8.5 |
| Solubilized lignin | 2.0 | 2.7 | 2.4 | 2.9 | 3.0 | 3.1 | 5.9 | 6.0 |
| Insoluble fraction | 0.6 | 1.8 | 1.0 | 0.5 | 3.3 | 6.8 | 5.1 | 2.5 |
| **Total** | **92.9** | **92.5** | **89.8** | **85.1** | **88.7** | **90.7** | **89.7** | **85.2** |

* Value based on xylose monosugar content, may also include other monosaccharides

** Xylan as monosaccharides and oligosaccharides only

Of course the increase in reaction temperature also increases the activity, but at the same time selectivity is decreased. The amount of basic sites is more complicated. With hexoses basic sites are needed for isomerization but they also catalyzed unwanted side reactions, for example condensation of HMF and glucose. One way to prevent the further reaction of formed furfural and hydroxymethylfurfural is the continuous separation during the reaction [8].

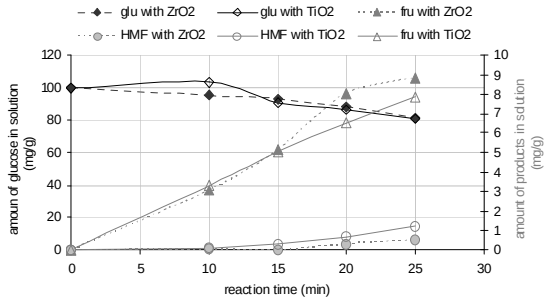


**Figure 4:** Comparison of the glucose reaction and the formation of products with two tested catalysts $ZrO_2$ and $TiO_2$

## Conclusions

1. Autohydrolysis of birch wood allows dissolution of considerable amounts of wood components, mainly xylan, but high intensities promote degradation of carbohydrates in the solution and involve long treatment duration. Selection of intensities should be made according to the pulp grade to be produced, but composition of the resulting hydrolysate should also be taken into account.

2. High liquid-to-wood ratios facilitate transfer of hydrolysis products from the cell wall to the bulk liquid but as concentration of carbohydrates in such hydrolysates is considerably lower, a compromise in liquid-to-wood ratio should be found for energy-efficient processing of hydrolysates.

3. Autohydrolysis involves lignin alteration with formation of highly reactive phenolic species in wood residue, partial lignin dissolution in the hydrolysate and isolation in the form of insoluble precipitate. Significant amount of altered lignin dissolves in organic solvents

4. Obtained material balances are more accurate at lower treatment intensities due to increased formation of not quantified compounds at higher intensities. More detailed componential analysis of wood residue and hydrolysates shall be carried out.

## Acknowledgements

Firstly, we would like to acknowledge TEKES, Andritz Oy, Danisco Sweeteners Oy,
Oy Metsä-Botnia Ab, Stora Enso Oyj, UPM Kymmene for financial support of the project. We also express gratitude to Helena Moring for experimental work and Mikhail Iakovlev for analytical support and discussions.

## References

[1] Nikitin, V.M., Obolenskaya, A.V., Shchegolev,V.P. (1978) “Khimiya drevesiny i tsellyulozy (Chemistry of Wood and Cellulose)”, Moscow, Lesn. Prom, 82-83.

[2] Hagglund, E. (1951) “The chemistry of wood”. New York, Academic Press, Inc., 350-355.

[3] Brasch, B. J., Free, K. W. (1965) “Prehydrolysis-kraft pulping of Pinus radiata grown in New Zealand”, *Tappi* 48(4), 245-248.

[4] Tunc, M.S., van Heiningen, A. (2008). “Hydrothermal dissolution of mixed southern hardwoods”, *Holzforschung* 62, 539-545.

[5] Tunc, M.S., van Heiningen, A. (2008). ”Hemicellulose extraction of mixed southern hardwood with water at 150 °C: Effect of time”, *Industrial and Engineering Chemical Research* 47, 7031-7037.

[6] Lora, J. H., Wayman, M. (1978) “Autohydrolysis-extraction: a new approach to sulfur-free pulping”, *Tappi* 61(12), 88-89.

[7] Leschinsky, M., et al., “Effect of autohydrolysis of Eucalyptus globulus wood on lignin structure. Part 2: Influence of autohydrolysis intensity.” *Holzforschung*, 2008. 62(6), 653-658.

[8] Roman-Leshkov Y., Barrett C.J., Liu Z.Y., Dumesic J.A. (2007) “Production of dimethylfuran for liquid fuels from biomass-derived carbohydrates” *Nature* 447, 982-986.

[9] SCAN-CM 40:01, “Wood chips for pulp production. Size distribution”.

[10] SCAN-CM 39, “Wood chips for pulp production − Dry matter content”.

[11] Sixta, H. (2006) “Multistage kraft pulping”, *Handbook of pulp, H. Sixta, ed.*, WILEY-VCH, Weinheim, 325-365.

[12] NREL/TP-510-42622, “Determination of Ash in Biomass”.

[13] SCAN-CM 49:03, “Content of acetone-soluble matter”.

[14] NREL/TP-510-42618, “Determination of Structural Carbohydrates and Lignin in Biomass”.

[15] SCAN-N 1:61, “Dry matter in sulphite spent liquor”.

[16] Sundberg, A., Sundberg, K., Lillandt, C. and Holmbom, B. (1996) ”Determination of hemicelluloses and pectins in wood and pulp fobres by acid methanolysis and gas chromatography” *Nordic Pulp and Paper Research Journal* 4, 216-219.

[17] TAPPI. (1991) “UM 250. Acid soluble lignin in wood and pulp”, *TAPPI Useful Methods*.

[18] Leschinsky, M., Sixta, H., Patt, R. (2009) “Detailed mass balances of the autohydrolysis of Eucalyptus globulus at 170 °C”, *BioResources* , 4(2), 687-703.

[19] Lora, J.H., Wayman, M. (1978) “Delignification of hardwoods by autohydrolysis and extraction” *Tappi*, 61(6) 47-50.

[20] Watanabe M., Aizawa Y., Iida T., Nishimura R., Inomata H. (2005) “Catalytic glucose and fructose conversion with $TiO_2$ and $ZrO_2$ in water at 473 K: Relationship between reactivity andacid-base property determined by TPD measurement” *Appl.Cat. A: General* 295, 150-156.

Lenzinger Berichte 87 (2009) 68-78

# SYNTHESIS OF 4-*O*-METHYL GLUCURONIC ACID

**Georg Sixta[1], Wilhelm Herok[1,2], Clemens Gruber[1], Hedda K.Weber[2], Herbert Sixta[3,4], and Paul Kosma[1]**

[1]University of Natural Resources and Applied Life Sciences, Department of Chemistry, A-1190 Vienna, Austria
[2]Kompetenzzentrum Holz GmbH, A-4021 Linz, Austria
[3]Lenzing AG, A-4860-Lenzing, Austria
[4]Helsinki University of Technology, Department of Forest Products, Helsinki, Finland

Phone: (+43) 1-47654-6055; Fax: (+43) 1-47654-6059; E-mail: paul.kosma@boku.ac.at

**4-*O*-Methyl glucuronic acid is an important constituent of hardwood xylans, and undergoes various chemical transformations upon cooking and bleaching processes, e.g. leading to the formation of hexenuronic acid under alkaline conditions. For kinetic studies of these degradation reactions, pure reference material for HPLC-analysis has been prepared utilizing three different educts. TEMPO-oxidation of methyl 4-*O*-methyl-β-D-glucopyranoside afforded the corresponding glucuronide derivative, which was hydrolyzed with trifluoroacetic acid to afford 4-*O*-methyl glucuronic acid in low yield. Alternative approaches were elaborated from either benzyl- or allyl-protected glucopyranosides *via* selective introduction of benzyl protecting groups at position 2 and 3, followed by tritylation and methylation at position 4, respectively. Detritylation and chromium(VI)-promoted oxidation afforded the glucuronic acid derivatives, which were converted into the corresponding benzyl ester derivatives. De-O-allylation of the allyl glycoside was accomplished under Pd(II) catalysis and hydrogenolysis of the benzyl groups under controlled conditions finally afforded the target compound in good overall yields.**

**Keywords:** *beech wood xylan, hexenuronic acid, 4-O-methylglucuronic acid, synthesis, oxidation*

## Introduction

Hard wood polysaccharides contain substantial amounts of 4-*O*-methyl-D-glucopyranosyluronic acid (MeGlcA) linked to the xylan backbone in an α-anomeric linkage [1]. The 4-*O*-methyl ether substituent is responsible for the β-elimination reaction under alkaline conditions leading to the formation of 4-deoxy-β-L-*threo*-hex-4-enopyranosyluronic acid (HexA) in Kraft pulps [2]. HexA contributes to the kappa number of pulps, consumption of bleaching chemicals as well as to brightness reversion [3-5]. Both acid constituents contribute to the overall charge of pulps and fibres and lead to the redeposition and sorption of xylans onto the fibre [6,7]. The ratio of MeGlcA and HexA in pulps and fibre products, the formation of the latter component and degradation of both constituents during cooking, bleaching and alkaline ripening is thus a major analytic task for process monitoring, which has not been fully solved thus far [8]. For ongoing kinetic studies, pure samples of MeGlcA were needed as reference samples for HPLC

analysis. The synthesis of MeGlcA has mainly been performed in the second half of the 20th century in low yields. Only limited information was reported on the purity and structural integrity of the synthesized material, which is prone to several side reactions depending on the reaction conditions applied for the final deprotection and purification steps [9,10]. Thus, in many cases, the synthesis of methyl glycosides as well as various esters of MeGlcA have been reported, since these are amenable to chromatographic purification [11]. This communication describes the preparation and full spectroscopic characterization of free MeGlcA starting from methyl, benzyl and allyl glucosides, respectively.

## Experimental

*General methods*

General methods were as described recently [12].

*Benzyl α/β-D-glucopyranoside (**1**)*

To a solution of anhydrous D-glucose (30.0 g, 167 mmol) in 170 mL of BnOH was added 1.67 g $H_2SO_4$-silica. The solution was stirred at 75 °C for 24 h. To purify the product, the reaction mixture was applied directly onto a column of silica gel (EtOAc) to give 22.0 g (81.4 mol, 49 %) of **1** as a syrup.

*Benzyl 4,6-O-benzylidene-β-D-glucopyranoside (**2**) and benzyl 4,6-O-benzylidene-α-D-glucopyranoside (**3**)*

To a solution of **1** (17.33 g, 61.1 mmol, α:β~5:1) in 200 mL of dry acetonitrile was added 35 g of $NaHSO_4$-silica. $PhCH(OMe)_2$ (39.0 g, 256 mmol) was added and stirred overnight at rt. After 16 h, $Et_3N$ (25.3 g, 250 mmol) was added and stirring was continued for 30 min. The reaction mixture was filtered through Celite and concentrated *in vacuo*. Flash chromatography on silica gel (2:3 *n*-hexane–EtOAc) afforded **2** (2.74 g, 7.64 mmol) as the higher running anomer. An analytical amount of the product was recrystallized from EtOH; mp 163-164 °C $[\alpha]_D^{20}$ +58 (*c* 1.0, $CHCl_3$); $R_f$ 0.44 (2:7 *n*-hexane–EtOAc); $^1$H NMR ($CDCl_3$): δ 7.52-7.25 (m, 10H, Ar), 5.54 (s, 1H, PhC*H*), 4.94 (d, 1H, $J_{gem}$ 11.6 Hz, PhC$H_2$), 4.64 (d, 1H, $J_{gem}$ 11.6 Hz, PhC$H_2$), 4.50 (d, 1H, $J_{1,2}$ 7.7 Hz, H-1), 4.37 (dd, 1H, $J_{6a,5}$ 4.9, $J_{6a,6b}$ 10.5 Hz, H-6a), 3.85-3.78 (m, 2H, H-6b, H-3), 3.61-3.53 (m, 2H, H-2, H-4), 3.46 (ddd, 1H, $J_{5,4}$ 9.6, $J_{5,6b}$ 9.6 Hz, H-5); $^{13}$C NMR ($CDCl_3$): δ 137.12 and 136.87 ($C_{arom., quart.}$), 129.47-126.46 ($C_{arom., C-H}$), 102.31 (C-1), 102.14 (Ph*C*H), 80.76 (C-4), 74.78 (C-2), 73.33 (C-3), 71.72 (Ph*C*$H_2$), 68.87 (C-6), 66.66 (C-5); ESI-TOFMS: *m/z* calcd for $[C_{20}H_{22}O_6+NH_4]^+$: 376.1755. Found: 376.1750.

Further elution of the column gave **3** (9.83 g, 27.44 mmol) corresponding to a total yield of 55 %. An analytical amount of the product was recrystallized from EtOH; mp 161.5-162 °C; $[\alpha]_D^{20}$+100 (*c* 1.0, $CHCl_3$); $R_f$ 0.29 (2:7 *n*-hexane–EtOAc); $^1$H NMR ($CDCl_3$): δ 7.45-7.17 (m, 10 H, Ar), 5.46 (s, 1H, PhC*H*), 4.94 (d, 1H, $J_{1,2}$ 3.9 Hz, H-1), 4.71 (d, 1H, $J_{gem}$ 11.7 Hz, PhC$H_2$), 4.50 (d, 1H, $J_{gem}$ 11.7 Hz, PhC$H_2$), 4.16 (dd, 1H, $J_{6a,5}$ 4.6, $J_{6a,6b}$ 10.1 Hz, H-6a), 3.89 (dd, 1H, $J_{3,2} = J_{3,4}$ 9.3 Hz, H-3), 3.79 (ddd, 1H, $J_{5,4}$ 9.8, $J_{5,6b}$ 9.8 Hz, H-5), 3.66 (dd, 1H, H-6b), 3.57 (dd, 1 H, H-2), 3.44 (dd, 1H, H-4), 2.69 (s, 1H, 3-OH), 2.18 (dd, 1H, $J_{2\text{-}OH,H\text{-}2}$ 9.9 Hz, 2-OH); $^{13}$C NMR ($CDCl_3$): δ 137.17 and 136.82 ($C_{arom., quart.}$), 129.42-126.45 ($C_{arom., C-H}$), 102.07 (Ph*C*H), 98.30 (C-1), 81.07 (C-4), 72.94 (C-2), 71.86 (C-3), 70.39 (Ph*C*$H_2$), 69.04 (C-6), 62.88 (C-5); ESI-TOFMS: *m/z* calcd for $[C_{20}H_{22}O_6+NH_4]^+$: 376.1755. Found: 376.1748.

Upon further elution of the column with EtOAc, 6.80 g of **1** (25.2 mmol, 39 %) was recovered.

*Benzyl 2,3-di-O-benzyl-4,6-O-benzylidene-α-D-glucopyranoside (**4**)*

4.716 g of **3** (13.2 mmol) was dissolved in 55 mL of dry DMF and stirred at 0 °C. 1.95 g NaH (60% suspension in oil, 48.7 mmol) was added in small portions. BnBr (3.5 mL, 29.3 mmol) was added and the ice bath was removed. After 3 h TLC (8:1 *n*-hexane–EtOAc) showed complete conversion and 4.5 mL of 2-propanol was added and stirring was continued for 1 h. The solution was diluted with 200 mL EtOAc and extracted three times with 250 mL of water. The combined aqueous phases were extracted with 100 mL of $Et_2O$. The combined organic phases were dried over $MgSO_4$ and concentrated *in vacuo*. The residue was purified on a column of silica gel (15:2 *n*-hexane–EtOAc) to yield 6.633 g (12.32 mmol, 94 %) of **4**. An analytical sample was recrystallized from *n*-hexane/EtOAc, mp 138-139 °C (*n*-hexane/EtOAc), $[\alpha]_D^{20}$ +23 (*c* 1.0, $CHCl_3$); $R_f$ 0.38 (3:1 *n*-hexane–EtOAc); $^1$H NMR ($CDCl_3$): δ 7.45-7.15 (m, 20 H, Ar), 5.47 (s, 1H, PhC*H*), 4.85 (d, 1H, $J_{gem}$ 11.2 Hz, PhC$H_2$), 4.77 (d, 1H, $J_{gem}$ 12.2 Hz, PhC$H_2$), 4.75 (d, 1H, $J_{1,2}$ 3.5 Hz, H-1), 4.67 (d, 1H, $J_{gem}$ 12.0 Hz, PhC$H_2$), 4.66 (d, 1H, $J_{gem}$ 12.3 Hz, PhC$H_2$), 4.51 (d, 1H, $J_{gem}$ 12.1 Hz, PhC$H_2$), 4.51 (d, 1H, $J_{gem}$ 12.1 Hz, PhC$H_2$), 4.13 (dd, 1H, $J_{6a,5}$ 4.8, $J_{6a,6b}$ 10.1 Hz, H-6a), 4.03 (dd, 1H, $J_{3,2} = J_{3,4}$ 9.3 Hz, H-3), 3.83 (ddd, 1H, $J_{5,4}$ 9.9, $J_{5,6b}$ 9.9 Hz, H-5), 3.61 (dd, 1H, H-6b), 3.53 (dd, 1H, H-4), 3.49 (dd, 1H, H-2); $^{13}$C NMR ($CDCl_3$): δ 139.00, 138.35, 137.59 and 137.15 ($C_{arom., quart.}$), 129.06-126.20 ($C_{arom., C-H}$), 101.41 (Ph*C*H), 96.77 (C-1), 82.41 (C-4), 79.46 (C-2), 78.87 (C-3), 75.51 (Ph*C*$H_2$), 73.64 (Ph*C*$H_2$), 69.54 (Ph*C*$H_2$), 69.21 (C-6), 62.82 (C-5); Anal. Calcd for $C_{34}H_{34}O_6$: C, 75.82; H, 6.36. Found: C, 75.84; H, 6.29.

*Benzyl 2,3-di-O-benzyl-α-D-glucopyranoside (**5**)*

To a stirred solution of **4** (6.067 g, 11.3 mmol) in 100 mL of MeOH, 33 mL of 0.5 M aq HCl was added and the mixture was heated under reflux. After 3 h another 20 mL of 0.5 M HCl was added. After 5 h the solution wass cooled to rt, 5 g $NaHCO_3$ was added and the reaction mixture was stirred for 20 min. The solution was extracted three times with 100 mL of $CHCl_3$. The combined organic phases were washed with brine (150 mL), dried over $MgSO_4$ and concentrated *in vacuo*. Purification by column chromatography (1:1 *n*-hexane–EtOAc) gave 4.365 g (9.7 mmol, 86 %) of **5**. An analytical sample was recrystallized from *n*-hexane/EtOAc, mp 110-111 °C; $[\alpha]_D^{20}$ +66 (*c* 1.0, $CHCl_3$); $R_f$ 0.41 (2:7 *n*-hexane–EtOAc); $^1$H NMR ($CDCl_3$): δ 7.43-7.24 (m, 15H, Ar), 5.04 (d, 1H, $J_{gem}$ 11.5 Hz, PhC$H_2$), 4.84 (d, 1H, $J_{1,2}$ 3.5 Hz, H-1), 4.71 (d, 1H, $J_{gem}$ 11.7 Hz, PhC$H_2$), 4.71 (d, 1H, $J_{gem}$ 11.7 Hz, PhC$H_2$), 4.63 (d, 1H, $J_{gem}$ 11.9 Hz, PhC$H_2$), 4.55 (d, 1H, $J_{gem}$ 12.2 Hz, PhC$H_2$), 4.54 (d, 1H, $J_{gem}$ 11.8 Hz, PhC$H_2$), 3.86 (dd, 1H, $J_{3,2}$ 9.2 Hz, H-3), 3.75-3.66 (m, 3H, H-5, H-6), 3.54 (dd, 1H, $J_{4,3} = J_{4,5}$ 9.3 Hz, H-4), 3.49 (dd, 1 H, H-2); $^{13}$C NMR ($CDCl_3$): δ 138.95, 138.15 and 137.26 ($C_{arom., quart.}$), 128.78-128.06 ($C_{arom., C-H}$), 95.75 (C-1), 81.53 (C-3), 79.98 (C-2), 75.53 (Ph*C*$H_2$), 72.89 (Ph*C*$H_2$), 71.20 (C-5), 70.66 (C-4), 69.43 (Ph*C*$H_2$), 70.66 (C-6); Anal. Calcd for $C_{27}H_{30}O_6$: C, 71.98; H, 6.71. Found: C, 71.94; H, 6.70.

*Benzyl 2,3-di-O-benzyl-6-O-trityl-α-D-glucopyranoside (**6**)*

To a solution of **5** (4.056 g, 9.0 mmol) in 30 mL of dry pyridine, 3.0 g (10.8 mmol) of TrCl was added and stirred at 100 °C. After 3 h, 300 mg (1.08 mmol) TrCl was added. TLC (2:1 *n*-hexane–EtOAc) showed complete conversion after 4.5 h. After cooling to rt, toluene (approximately 20 mL) was added until no further precipitation of pyridinium chloride was observed. The mixture was filtered, diluted with 200 mL of toluene and extracted with

1 L of 0.03 M $NaHCO_3$ solution. The aqueous phase was re-extracted with 200 mL toluene. The combined organic phases were extracted with 500 mL of 0.03 M aq $NaHCO_3$ solution, dried over $MgSO_4$ and concentrated *in vacuo*. Silica gel chromatography (4:1 *n*-hexane–EtOAc) afforded 6.202 g of **5** (9.0 mmol, 99 %); $[\alpha]_D^{20}$ +31 (*c* 1.1, $CHCl_3$); $R_f$ 0.49 (2:1 *n*-hexane–EtOAc); $^1$H NMR ($CDCl_3$): δ 7.49-7.15 (m, 30H, Ar), 4.98 (d, 1H, $J_{gem}$ 11.3 Hz, PhC$H_2$), 4.89 (d, 1H, $J_{1,2}$ 3.7 Hz, H-1), 4.78 (d, 1H, $J_{gem}$ 12.2 Hz, PhC$H_2$), 4.75 (d, 1H, $J_{gem}$ 11.3 Hz, PhC$H_2$), 4.66 (d, 1H, $J_{gem}$ 11.9 Hz, PhC$H_2$), 4.60 (d, 1H, $J_{gem}$ 12.0 Hz, PhC$H_2$), 4.56 (d, 1H, $J_{gem}$ 11.8 Hz, PhC$H_2$), 3.85 (dd, 1H, $J_{3,2}$ 9.2, $J_{3,4}$ 9.2 Hz, H-3), 3.83-3.77 (m, 1H, H-5), 3.57 (ddd, 1H, $J_{4,5}$ 9.3 Hz, $J_{4,4\text{-}OH}$ 2.2 Hz, H-4), 3.54 (dd, 1 H, H-2), 3.35-3.23 (m, 2 H, H-6), 2.26 (d, 1 H, $J_{4\text{-}OH,4}$ 2.5 Hz, 4-OH); $^{13}$C NMR ($CDCl_3$): δ 144.06 ($C_{arom., quart., trityl}$), 139.02, 138.35 and 137.31 ($C_{arom., quart., benzyl}$), 128.98-127.21 ($C_{arom., C\text{-}H}$), 95.10 (C-1), 86.94 ($C_{quart., trityl}$), 81.93 (C-3), 79.87 (C-2), 75.74 (Ph*C*H$_2$), 72.88 (Ph*C*H$_2$), 71.66 (C-4), 70.51 (C-5), 68.90 (Ph*C*H$_2$), 63.88 (C-6); ESI-TOFMS: *m/z* calcd for $[C_{46}H_{44}O_6+NH_4]^+$: 710.3476. Found: 710.3478.

*Benzyl 2,3-di-O-benzyl-4-O-methyl-6-O-trityl-α-D-glucopyranoside (**7**)*

4.00 g of **6** (5.77 mmol) was dissolved in 40 mL of dry DMF and stirred at 0°C. 0.670 g NaH (60% suspension in oil, 16.7 mmol) was added in small portions, then 1.6 mL (10.4 mmol) MeI was added, the ice bath was removed and stirring was continued. After 2 h, 2 mL of dry MeOH was added at 0 °C and stirring was continued for 30 min at rt. The mixture was poured onto 300 mL water and extracted with 100 mL EtOAc twice. The combined organic phases were extracted with water (300 mL), brine (100 mL) and dried over $MgSO_4$. Column chromatography (5:1 *n*-hexane–EtOAc) afforded **7** in 97% yield (3.953 g, 5.59 mmol); $[\alpha]_D^{20}$ +52 (*c* 1.1, $CHCl_3$); $R_f$ 0.56 (2:1 *n*-hexane–EtOAc); $^1$H NMR ($CDCl_3$): δ 7.51-7.19 (m, 30H, Ar), 4.92 (d, 1H, $J_{1,2}$ 3.8 Hz, H-1), 4.92 (d, 1H, $J_{gem}$ 10.7 Hz, PhC$H_2$), 4.78 (d, 1H, $J_{gem}$ 10.7 Hz, PhC$H_2$), 4.76 (d, 1H, $J_{gem}$ 12.2 Hz, PhC$H_2$), 4.71 (d, 1H, $J_{gem}$ 12.0 Hz, PhC$H_2$), 4.61 (d, 1H, $J_{gem}$ 12.2 Hz, PhC$H_2$), 4.60 (d, 1H, $J_{gem}$ 12.0 Hz, PhC$H_2$), 3.90 (dd, 1H, $J_{3,2}$ 9.3 = $J_{3,4}$ 9.3 Hz, H-3), 3.71 (ddd, 1H, $J_{5,6a}$ 2.0, $J_{5,6b}$ 4.1, $J_{5,4}$ 10.1 Hz, H-5), 3.58 (dd, 1H, H-2), 3.39 (dd, 1H, H-4), 3.35 (dd, 1H, $J_{6a,6b}$ 9.9 Hz, H-6a), 3.28 (s, 3H, $CH_3$-O), 3.08 (dd, 1H, H-6b); $^{13}$C NMR ($CDCl_3$): δ 144.22 ($C_{arom., quart., trityl}$), 139.01, 138.55 and 137.30 ($C_{arom., quart., benzyl}$), 128.98-127.12 ($C_{arom., C\text{-}H}$), 94.98 (C-1), 86.44 ($C_{quart., trityl}$), 82.52 (C-3), 80.22[1] and 80.2 (C-2 and C-4), 76.06 (Ph*C*H$_2$), 73.15 (Ph*C*H$_2$), 70.68 (C-5), 68.86 (Ph*C*H$_2$), 62.44 (C-6), 60.77 ($CH_3O$); ESI-TOFMS: *m/z* calcd for $[C_{47}H_{46}O_6+NH_4]^+$: 724.3633. Found: 724.3634.

*Benzyl-(benzyl 2,3-O-benzyl-4-O-methyl-α-D-glucopyranosid)uronate (**8**)*

2.52 g of **7** (3.56 mmol) was dissolved in 75 mL of acetone and a solution of $K_2Cr_2O_7$ (1.752 g, 5.95 mmol) in 19 mL of 6 N $H_2SO_4$ was added within 1 min. The reaction mixture was heated to 55 °C and stirred. TLC (1:1 *n*-hexane–EtOAc) showed complete conversion after 6 h. The reaction mixture was poured onto 600 mL $H_2O$ and subsequently extracted three times with 140 mL portions of $CH_2Cl_2$. The combined organic phases were washed once with 190 mL $H_2O$ and then dried over $MgSO_4$ and concentrated *in vacuo*. The crude product was dissolved in 80 mL of dry DMF, cooled with an ice bath and stirred. $Bu_4NI$ (3.798 g, 10.28 mmol) and $KHCO_3$ (2.619 g, 26.16 mmol) were added to the solution. BnBr (90 µL, 7.48 mmol)

[1] Assignments may be reversed.

was added, cooling was removed and stirring continued for 2.5 h. The reaction mixture was concentrated, poured into 300 mL $H_2O$ and extracted three times with 100 mL of $CH_2Cl_2$. The combined organic phases were extracted once with $H_2O$, dried over $MgSO_4$ and concentrated *in vacuo*. The residue was purified from a higher-running byproduct by HPLC (Lichrosorb Si60, 10 µm, 30 cm x 4 cm I.D., 10:1 *n*-hexane–EtOAc, flow rate 10 mL $min^{-1}$) to give **8** as a colorless syrup (1.42 g, 70 %); $[\alpha]_D^{20}$ +49 (*c* 1.3, $CHCl_3$); $R_f$ 0.51 (2:1 *n*-hexane–EtOAc); $^1$H NMR ($CDCl_3$): δ 7.41-7.19 (m, 20H, Ar), 5.23 (s, 2H, PhC$H_2$), 4.92 (d, 1H, $J_{gem}$ 10.8 Hz, PhC$H_2$), 4.83 (d, 1H, $J_{1,2}$ 3.6 Hz, H-1), 4.78 (d, 1H, $J_{gem}$ 10.9 Hz, PhC$H_2$), 4.72 (d, 1H, $J_{gem}$ 12.4 Hz, PhC$H_2$), 4.65 (d, 1H, $J_{gem}$ 12.1 Hz, PhC$H_2$), 4.54 (d, 1H, $J_{gem}$ 12.6 Hz, PhC$H_2$), 4.50 (d, 1H, $J_{gem}$ 12.2 Hz, PhC$H_2$), 4.19 (d, 1H, $J_{5,4}$ 9.9 Hz, H-5), 3.93 (dd, 1H, $J_{3,2}$ = $J_{3,4}$ 9.4 Hz, H-3), 3.51 (dd, 1H, H-2), 3.42 (dd, 1 H, H-4), 3.34 (s, 3 H, $CH_3O$); $^{13}$C NMR ($CDCl_3$): δ 169.73 (C-6), 138.81-135.41 ($C_{arom., quart.}$), 128.71-127.37 ($C_{arom., C-H}$), 96.10 (C-1), 81.65 (C-4), 81.50 (C-3), 79.22 (C-2), 75.88 (Ph*C*$H_2$), 73.33 (Ph*C*$H_2$), 70.64 (C-5), 69.61 (Ph*C*$H_2$), 67.28 (Ph*C*$H_2$), 60.78 ($CH_3O$); ESI-TOFMS: *m/z* calcd for $[C_{35}H_{36}O_7+NH_4]^+$: 586.2799. Found: 586.2795.

### *4-O-Methyl-D-glucopyranosyluronic acid (**9**)*

A solution of **8** (34.8 mg, 61 µmol) in 4.0 mL of neat acetic acid was stirred at rt in the presence of 10% Pd/C (19.0 mg ) for 16 h under hydrogen at atmospheric pressure. After TLC (5:5:1 MeOH–$CHCl_3$–water) showed complete conversion, the catalyst was removed by filtration through Celite and washed with dry HOAc. The solvent was concentrated *in vacuo* and 2 mL water was added. The residue obtained upon lyophilization of the filtrate was purified on a Bio-Gel P-2 column (water) to give 12.6 mg of **9** (61 µmol, 99 %); $[\alpha]_D^{20}$ +24 (*c* 0.3, $H_2O$); $^1$H NMR ($D_2O$): δ 5.06 (d, 1H, $J_{1\alpha,2\alpha}$ 3.8 Hz, H-1α), 4.45 (d, 1H, $J_{1\beta,2\beta}$ 3.8 Hz, H-1β), 3.92 (d, 1H, $J_{5\alpha,4\alpha}$ 10.0 Hz, H-5α), 3.59 (dd, 1H, $J_{3\alpha,2\alpha}$ 9.5, $J_{3\alpha,4\alpha}$ 9.5 Hz, H-3α), 3.56 (d, 1H, $J_{5\beta,4\beta}$ 9.8 Hz, H-5β), 3.44 (dd, 1H, $J_{2\alpha,1\alpha}$ 3.8, $J_{2\alpha,3\alpha}$ 9.8 Hz, H-2α), 3.38 (dd, 1H, $J_{3\beta,2\beta}$ 9.4, $J_{3\beta,4\beta}$ 9.4 Hz, H-3β), 3.33 (s, 6 H, $OCH_3$ (α+β), 3.15 (dd, 1H, $J_{2\beta,1\beta}$ 7.9, $J_{2\beta,3\beta}$ 9.6 Hz, H-2β), 3.13 (dd, 1H, $J_{4\beta,3\beta}$ 9.4, $J_{4\beta,5\beta}$ 9.7 Hz, H-4β), 3.10 (dd, 1H, $J_{4\alpha,3\alpha}$ 9.6, $J_{4\alpha,5\alpha}$ 9.6 Hz, H-4α); $^{13}$C NMR ($D_2O$): δ 176.65 (C-6α), 175.82 (C-6β), 95.79 (C-1β), 91.99 (C-1α), 82.36 (C-4α), 82.14 (C-4β), 76.29 (C-5β), 74.99 (C-3β), 73.97 (C-2β), 72.09 (C-3α), 71.75 (C-2α), 71.33 (C-5α), 59.89[2] and 59.80 ($CH_3$-O); ESI-TOFMS: *m/z* calcd for $[C_7H_{12}O_7$-$H]^+$: 207.0510. Found: 207.0514.

### *Allyl 4,6-O-benzylidene-D-glucopyranoside (**11**)*

Benzaldehyde was freshly distilled onto a stirred and solvent-free mixture of dry $ZnCl_2$ (3.34 g, 24.52 mmol) and **10** (4.50 g, 20.43 mmol). After addition of ~ 20 mL of benzaldehyde, the reaction mixture was stirred for 96 h at rt. The reaction mixture was poured into a stirred 1:1 mixture of ice-water and hexane (300 mL). The precipitate was filtered off, thoroughly washed with water and hexane and dried. The residue was applied to column chromatography (1:1 *n*-hexane - EtOAc) to yield 4.51 g (14.63 mmol, 72%) of **10** as colourless syrup; $R_f$ 0.12 (1:2 *n*-hexane-EtOAc); $^{13}$C NMR (α-anomer, 75.47 MHz, $CDCl_3$): δ 137.02 ($C_{arom., quart.}$), 133.29 (***C***H=$CH_2$), 129.20-126.29 ($C_{arom., C-H}$), 118.27 (CH=***C***$H_2$), 101.87 (Ph***C***H), 97.87 (C-1), 80.92 (C-4), 72.79 (C-2), 71.70 (C-3), 68.84 (O***C***$H_2$CH=$CH_2$), 68.83 (C-6) and 62.57 (C-5).

### *Allyl 2,3-di-O-benzyl-4,6-O-benzylidene-D-glucopyranoside (**12**)*

[2] Assignments may be reversed.

Compound **11** (3.12 g, 10.1 mmol) was dissolved in dry DMF (37.5 mL) and the solution was cooled to 0 °C. NaH (0.60 g of a 60% dispersion in oil, 1.22 mmol) was added. After 30 min BnCl (2.60 mL, 22.59 mmol) was added dropwise and the ice bath was removed. After 3 h the mixture was poured into ice-water (600 mL). Diethylether (150 mL) was added and the two phases were separated. The aqueous phase was extracted three times with diethylether (150 mL). The combined organic phases were dried over $Na_2SO_4$ and concentrated in vacuo. The residue was purified by column chromatography (10:1 *n*-hexane - EtOAc) to yield 4.14 g (8.48 mmol, 84%) of **12** as a white solid; $R_f$ 0.34 (3:1 n-hexane-EtOAc); $^{13}$C NMR (α-anomer, 75.47 MHz, $CDCl_3$): δ 138.77, 138.18, 137.39 ($C_{arom.,\ quart.}$), 133.60 (***C***H=$CH_2$), 128.86-126.00 ($C_{arom.,\ C\text{-}H}$), 118.27 (CH=***C***$H_2$), 101.22 (Ph***C***H), 96.77 (C-1), 82.18 (C-4), 79.23 (C-2), 78.59 (C-3), 75.32 (Ph***C***$H_2$), 73.57 (Ph***C***$H_2$), 69.00 (O***C***$H_2$CH=$CH_2$), 68.48 (C-6) and 62.52 (C-5).

*Allyl 2,3-di-O-benzyl-D-glucopyranoside **(13)***

To a solution of **12** (3.99 g, 8.17 mmol) in methanol (55 mL) was added water (25 mL) and then *p*-toluenesulfonic acid hydrate (1.84 g, 9.68 mmol). After 4 h at 80 °C the mixture was poured into ice-water. The aqueous phase was extracted three times with chloroform (100 mL). The combined organic phases were dried over $Na_2SO_4$, concentrated to a syrup and submitted to column chromatography (10:1 hexane - EtOAc) which yielded 3.08 g (7.70 mmol, 94%) of **13** as colourless syrup; $R_f$ 0.19 (1:1 *n*-hexane-EtOAc); $^{13}$C NMR (α-anomer, 75.47 MHz, $CDCl_3$): δ 138.75, 137.98 ($C_{arom.,\ quart.}$), 133.61 (***C***H=$CH_2$), 128.57-127.84 ($C_{arom.,\ C\text{-}H}$), 118.28 (CH=***C***$H_2$), 95.68 (C-1), 81.31 (C-3), 79.75 (C-2), 75.37 (Ph***C***$H_2$), 72.92 (Ph***C***$H_2$), 70.92 (C-5), 70.92 (C-4), 68.31 (O***C***$H_2$CH=$CH_2$), and 62.37 (C-6).

*Allyl 2,3-di-O-benzyl-6-O-trityl-D-gluco-pyranoside* **(14)**

Compound **13** (3.08 g, 7.70 mmol) was dissolved in anhydrous pyridine (15 mL) and trityl chloride (2.6 g, 9.33 mmol) was added. After 3 h at 100 °C the solution was allowed to cool to rt and toluene (30 mL) was added until no further precipitation of pyridinium hydrochloride was observed. The filtered solution was diluted with toluene (100 mL), extracted three times with 0.03 M aq $NaHCO_3$ solution (50 mL). The aqueous phase was re-extracted with toluene, the combined organic phases were dried over $Na_2SO_4$ and concentrated in vacuo. Column chromatography (7:1 *n*-hexane - EtOAc) afforded 4.04 g (6.28 mmol, 82 %) of **14** as colourless syrup; $R_f$ 0.35 (2:1 n-hexane-EtOAc); $^{13}$C NMR (α-anomer, 100 MHz, $CDCl_3$): δ 143.93 ($C_{arom.,\ quart.,\ trityl}$), 138.94, 138.30 ($C_{arom.,\ quart.,\ benzyl}$), 133.96 (***C***H=$CH_2$), 128.66-127.00 ($C_{arom.,\ C\text{-}H}$), 118.28 (CH=***C***$H_2$), 95.49 (C-1), 86.92 ($C_{quart.,\ trityl}$), 81.73 (C-3), 79.74 (C-2), 75.55 (Ph*C*$H_2$), 72.88 (Ph*C*$H_2$), 71.57 (C-4), 70.17 (C-5), 68.09 (O***C***$H_2$CH=$CH_2$) and 63.81 (C-6).

*Allyl 2,3-di-O-benzyl-4-O-methyl-6-O-trityl-D-glucopyranoside **(15)***

A solution of **14** (4.04 g, 6.28 mmol) in anhydrous DMF (40 mL) was cooled to 0 °C. NaH (0.44 g of a 60% suspension in oil, 18.23 mmol) was added in small portions. After 30 min MeI (0.71 mL, 11.35 mmol) was added, the ice bath was removed and stirring was continued for 1 h. Anhydrous MeOH (2 mL) was added at 0 °C. After 30 min the mixture was poured into ice-water (300 mL) and the aqueous phase was extracted two times with EtOAc (100 mL). The combined organic phases were washed with brine (100 mL) and dried over $Na_2SO_4$. Purification by column chromatography (5:1 *n*-hexane - EtOAc) gave 4.03 g (6.13 mmol, 98 %) of **15** as colourless syrup; $R_f$ 0.46 (1:1 n-hexane-EtOAc); $^{13}$C NMR (α-anomer, 100 MHz, $CDCl_3$): δ 144.15 ($C_{arom.,\ quart.,\ trityl}$), 138.96,

138.43 ($C_{arom., quart., benzyl}$), 133.94 (***C***H=$CH_2$),128.79-126.95 ($C_{arom., C-H}$), 118.20 (CH=***C***$H_2$), 95.35 (C-1), 86.32 ($C_{quart., trityl}$), 82.24 (C-3), 80.09 (C-2), 80.07 (C-4), 75.85 (Ph*C*$H_2$), 73.16 (Ph*C*$H_2$), 70.42 (C-5), 68.01 (O***C***$H_2$CH=$CH_2$), 62.38 (C-6) and 60.57 ($CH_3O$).

*Allyl 2,3-di-O-benzyl-4-O-methyl-D-gluco-pyranoside (**16**)*

To a solution of **15** (2.84g, 4.33 mmol) in chloroform (20 mL) was added *p*-toluene sulfonic acid hydrate (2.30 g, 12.09 mmol) dissolved in methanol (5 mL). After 4 h at rt the solution was diluted with chloroform (25 ml). The organic phase was consecutively extracted with saturated $NaHCO_3$ solution (10 mL) and water (10 mL), dried over $Na_2SO_4$ and concentrated in vacuo. Column chromatography of the residue (2:1 *n*-hexane - EtOAc) afforded 1.71 g (4.13 mmol, 95%) of **16** as colourless syrup; $R_f$ 0.31 (1:1 *n*-hexane-EtOAc); $^{13}$C NMR (α-anomer, 100 MHz, $CDCl_3$): δ 138.88, 138.25 ($C_{arom., quart.}$), 133.73 (***C***H=$CH_2$),128.41-127.56 ($C_{arom., C-H}$), 118.29 (CH=***C***$H_2$), 95.66 (C-1), 81.74 (C-3), 79.79 (C-2), 79.70 (C-4), 75.67 (Ph*C*$H_2$), 73.32 (Ph*C*$H_2$), 70.97 (C-5), 68.36 (O***C***$H_2$CH=$CH_2$), 61.94 (C-6), and 60.86 ($CH_3O$).

*Benzyl (allyl 2,3-di-O-benzyl-4-O-methyl-D-glucopyranosid)uronate (**17**)*

A solution of compound **16** (1.71 g, 4.13 mmol) in acetone (35 mL) was cooled to 0 °C. Then a solution of chromium trioxide (1.11 g, 11.14 mmol) in 6 N sulphuric acid (5.5 ml) was added dropwise. The reaction mixture was heated to 50 °C and stirred for 3 h and was then poured into ice-water (200 mL). The product was extracted with chloroform (3 times 100 mL). The combined organic phases were washed with water until neutral pH, dried over $Na_2SO_4$ and concentrated in vacuo. The crude product (1.75 g, 4.08 mmol) was dissolved in dry DMF (60 mL) and cooled to 0 °C, $KHCO_3$ (2.89 g, 26.24 mmol) was added and stirring was continued for 0.5 h. BnBr (1.0 mL, 8.41 mmol) was added and the solution was allowed to warm to rt. After 3 h, the reaction mixture was poured into ice-water (250 mL) and the aqueous phase was extracted 3 times with dichloromethane (100 mL). The combined organic phases were consecutively washed with saturated $NaHCO_3$ solution (100 mL) and water (100 mL), dried over $Na_2SO_4$ and concentrated in vacuo. Purification by column chromatography (6:1 *n*-hexane - EtOAc) gave 1.72 g (3.32 mmol, 80% over 2 steps) of **17** as colourless syrup; $R_f$ 0.60 (2:1 n-hexane-EtOAc); $^{13}$C NMR (α-anomer, 75.47 MHz, $CDCl_3$): δ 169.73 (C-6), 138.60, 137.95, 135.22 ($C_{arom., quart.}$), 133.28 (***C***H=$CH_2$), 128.52-127.58 ($C_{arom., C-H}$), 118.60 (CH=***C***$H_2$), 96.11 (C-1), 81.45 (C-3), 81.30 (C-4), 79.05 (C-2), 75.71 (Ph*C*$H_2$), 73.36 (Ph*C*$H_2$), 70.38 (C-5), 68.60 (O***C***$H_2$CH=$CH_2$), 67.09 (Ph*C*$H_2$-O-C=O) and 60.59 ($CH_3O$).

*Benzyl-(2,3-di-O-benzyl-4-O-methyl-D-glucopyranosyl)uronate (**18**)*

Compound **17** (341.2 mg, 0.66 mmol) was dissolved in 17 mL AcOH (+5% $H_2O$) and consecutively NaOAc (593.7 mg, 7.24 mmol) and $PdCl_2$ (431.1 mg, 2.43 mmol) was added. After 16 h of stirring at 40 °C, insoluble materials were collected on a Celite pad and the filtrate was diluted with 35 mL chloroform and 70 mL of hexane. The organic phase was extracted with ice-water (50 mL), saturated $NaHCO_3$ solution (50 mL) and ice-water (50 mL), dried over $Na_2SO_4$ and concentrated in vacuo. The residue was submitted to column chromatography (3:1 *n*-hexane - EtOAc) to yield 280.8 mg (0.59 mmol, 89%) of **18** as a white solid; $R_f$ 0.32 (2:1 *n*-hexane-EtOAc); $^1$H NMR (α-anomer, 300 MHz, $CDCl_3$): δ 7.37-7.25 (m, 15H, Ar), 5.23 – 5.20 (m, 3H, PhC*H*$_2$OC=O, H-1), 4.85 (d, 1H, $J_{gem}$ 11.2 Hz, PhC*H*$_2$), 4.78 (d, 1H, $J_{gem}$ 11.0 Hz, PhC*H*$_2$), 4.75 (d, 1H, $J_{gem}$ 11.8 Hz, PhC*H*$_2$), 4.64 (d, 1H,

$J_{gem}$ 11.8 Hz, PhC$H_2$), 4.41 (d, 1H, $J_{5,4}$ 9.6 Hz, H-5), 3.86 (dd, 1H, $J_{3,4}$ 8.9 Hz, H-3), 3.54 (dd, 1H, $J_{2,1}$ 3.6, $J_{2,3}$ 9.0 Hz, H-2), 3.44 (dd, 1H, H-4), 3.36 (s, 3H, $CH_3O$); $^{13}$C NMR (α-anomer, 75.47 MHz, $CDCl_3$): δ 169.45 (C-6), 138.57, 137.65, 135.27 ($C_{arom., quart.}$), 128.63-127.73 ($C_{arom., C-H}$), 91.84 (C-1), 81.22 (C-4), 80.57 (C-3), 78.93 (C-2), 75.60 (Ph$CH_2$), 73.53 (Ph$CH_2$), 70.58 (C-5), 67.25 (Ph$CH_2$-O-C=O) and 60.53 ($CH_3O$).

*4-O-Methyl-D-glucopyranosyluronic acid (**9**)*

A solution of **18** (240 mg, 0.5 mmol) in dry THF (2 mL) was hydrogenated in the presence of 10 % Pd/C at atmospheric pressure and rt for 2.5 h. The catalyst was collected on a Celite pad and washed with THF. Then the filtrate was concentrated in vacuo. The residue was purified by anion-exchange chromatography on DOWEX AG 1X8 ($HCO_3^-$ form) with a linear gradient of $NH_4HCO_3$ (0.05 → 0.3 M). The fractions containing **9** were combined and concentrated, and $NH_4HCO_3$ was removed by evaporating water from the residue several times. Lyophilization gave the $NH_4$-salt of **9 (**83.2 mg, 0.46 mmol, 92%) as a white solid (1.0:1.2 α/β according to the $^1$H-NMR spectrum).

*Methyl 4-O-Methyl-β-D-glucopyranosid uronate (**20**)*

To a solution of **19** (0.512 g, 2.46 mmol) in 0.05 M aq. KBr, a 8.4 M aq solution of TEMPO (3 mL) was added and the pH of the solution was adjusted to 10.5 by addition of 0.1 M NaOH. Within 30 min at rt, a 0.74 M aq solution of NaOCl (22.25 mL, ~16.5 mmol) was added dropwise and the pH was kept at 10.5 by adding additional portions of NaOH. The solution was stirred for 90 min and TLC (methanol-chloroform-water 10:10:3) indicated full conversion of the educt. MeOH (2 mL) was added and the solution was concentrated and the residue dried under vacuum. The residue was treated with dry methanol and filtered. The filtrate was concentrated and purified on silica gel using methanol-chloroform-water 10:10:3 as solvent. The product was obtained in 4 fractions A-D, still containing inorganic material (total weight 0.65 g).

*Deprotection of **20***

Fraction D (121 mg) was dissolved in 3 M aq. trifluoroacetic acid (5 mL) and stirred at 80 °C for 48 h. After cooling to rt, water (10 mL) was added to the solution and the solution was concentrated. This treatment was repeated 4 times and the residue was subjected to chromatography on silica gel (methanol-chloroform-water 10:10:3). Final desalting was achieved on a column of Sephadex G-10, which afforded 68.4 mg of **9** as a syrup.

## Results and discussion

*Synthesis from benzyl glucosides*

For the selective introduction of the 4-O-methyl group, glucose was first converted into an anomeric mixture of the benzyl glucopyranosides **1** using Fischer-type glycosylation of benzyl alcohol with acidic silica gel [13]. The anomeric mixture was separated following conversion into the 4,6-*O*-benzylidene derivatives **2** and **3** under standard conditions in 55% yield. The following transformations were then performed with the major α-anomer **3**.

Benzylation of **3** with benzyl bromide afforded the 2,3-di-*O*-benzyl derivative **4** in 94% yield, which was subsequently treated with HCl to remove the benzylidene acetal, giving **5** in 86% yield. Tritylation at position 6 was effected in near quantitative yield to afford compound **6** followed by methylation using methyl iodide / NaH in DMF to give the 4-*O*-methyl ether glucoside **7** in 97% yield. Conversion into the glucuronide was achieved via detritylation and oxidation with $K_2Cr_2O_7$/ $H_2SO_4$. In order to facilitate purification of the resulting acid,

the carboxylic group was esterfied under phase transfer catalysis to furnish the benzyl ester **8** in 70% yield (for three steps). The simultaneous cleavage of all benzyl groups was finally accomplished via hydrogenation on Pd-C in neat acetic acid to give the target compound **9** in 99% yield. Other solvents tested (THF, MeOH) led to substantial formation of lactone byproducts, which could not be reopened into the free acid under various conditions tested. Final purification of **9** was performed on a PD-10 Biogel column. The $^{1}H$ and $^{13}C$ NMR spectrum could be fully assigned and revealed the presence of a ~2:3 mixture of the α/β-forms (Figure 1).

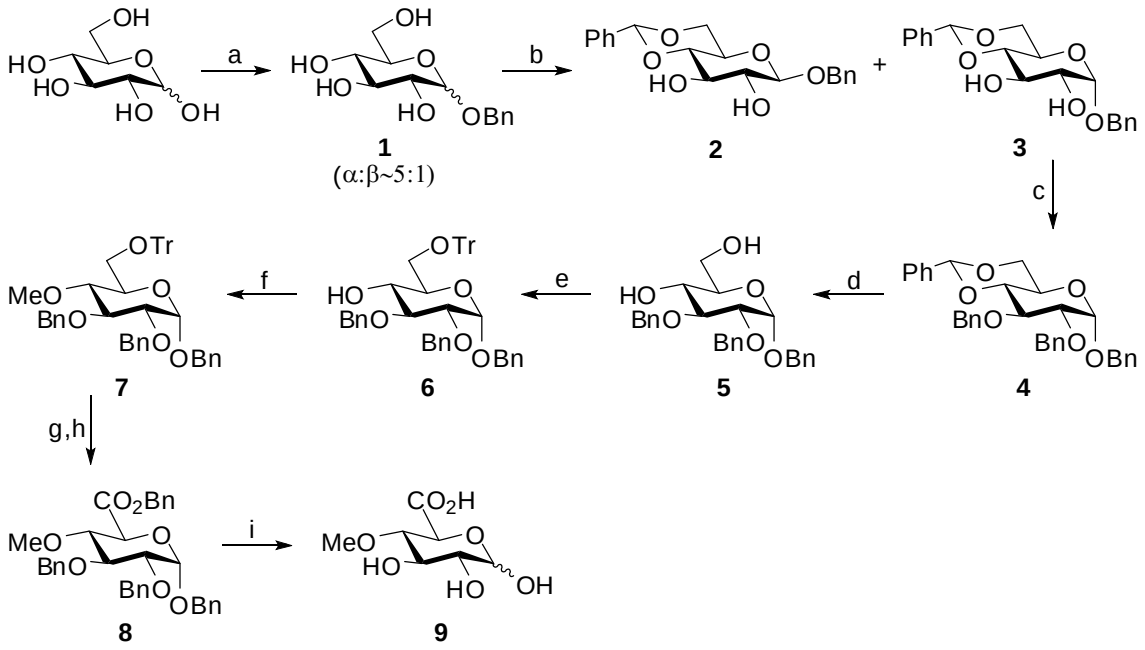


**Scheme 1**
**Reagents and conditions:** (a) BnOH, $H_2SO_4$-silica, 75 °C, 24 h, 49 %; (b) $PhCH(OMe)_2$, $NaHSO_4$-silica, MeCN, rt, 16 h, 55 %; (c) BnBr, NaH, DMF, rt, 3 h, 94 % (d) 0.5 M HCl, MeOH, reflux, 5 h, 86 %; (e) TrCl, Py, 100 °C, 4.5 h, 99 %; (f) MeI, NaH, DMF, rt, 2 h, 97 %, (g) $K_2Cr_2O_7$, 6 N $H_2SO_4$, acetone, 55°C, 6 h; (h) BnBr, $Bu_4NI$, $KHCO_3$, DMF, rt, 2.5 h, 70 % (g and h); (i) $H_2$, 10% Pd/C, HOAc, rt, 16 h, 99 %.

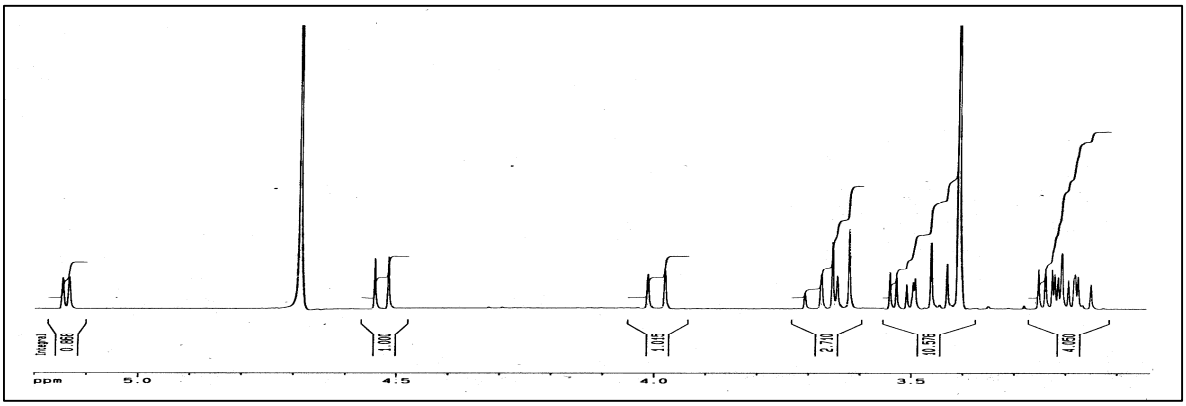


**Figure 1:** 300 MHz $^{1}H$ NMR spectrum of **9** recorded in $D_2O$.

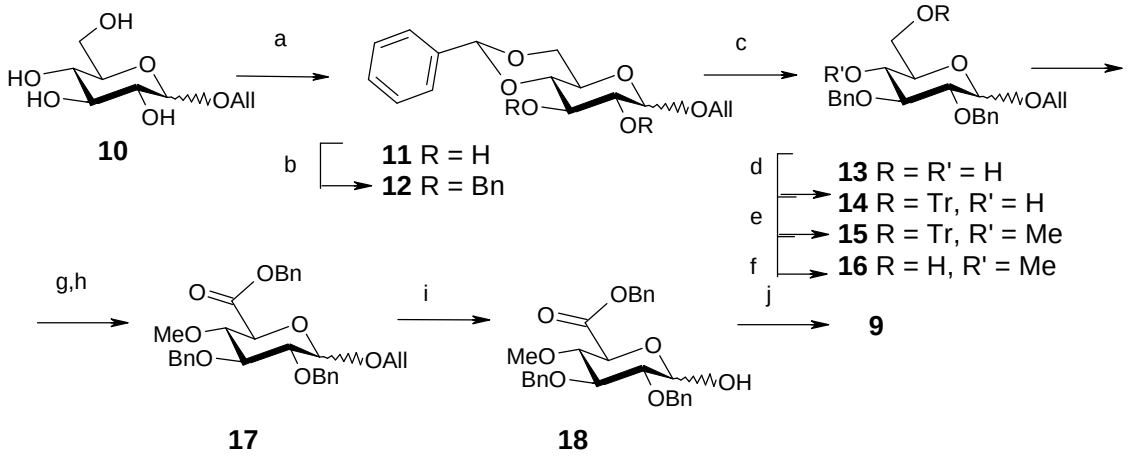


**Scheme 2**
**Reagents and conditions:** (a) PhCHO, $ZnCl_2$, rt, 24 h, 60%; (b) BnBr, NaH, DMF, rt, 3 h, 84 % (c) TosOH, aq MeOH, 80 °C, 3 h, 94 %; (d) TrCl, Py, 100 °C, 3 h, 81 %; (e) MeI, NaH, DMF, rt, 2 h, 98 %, (f) TosOH, $CHCl_3$, MeOH, rt, 4 h, 96%; (g) $CrO_3$, 6 N $H_2SO_4$, acetone, 55 °C, 2.5 h; h) BnBr, $Bu_4NI$, $KHCO_3$, DMF, rt, 14 h, 80 % (g and h); i) $PdCl_2$, NaOAc, rt, 16h, 81%; (j) $H_2$, 10% Pd/C, THF, rt, 2.5 h, 92 %.

*Synthesis from allyl glucosides*

In order to simplify the protocol and allow for selective liberation of the anomeric protecting group providing access to glycosyl donors of 4-*O*-methyl glucuronic acid, a related procedure was carried out starting from an anomeric mixture of allyl glucopyranoside **10** [14]. (Scheme 2). The ensuing transformations were performed along similar lines as described for the benzyl glucosides. Again, the yields of the individual steps were good to excellent and the synthesis can be performed on a multigram scale. The benzyl ester glucuronide **17** was eventually treated with $PdCl_2$ giving the reducing sugar **18** in 81% yield. Full deprotection was achieved by hydrogenolysis in THF to furnish the target compound **9** in 92% yield.

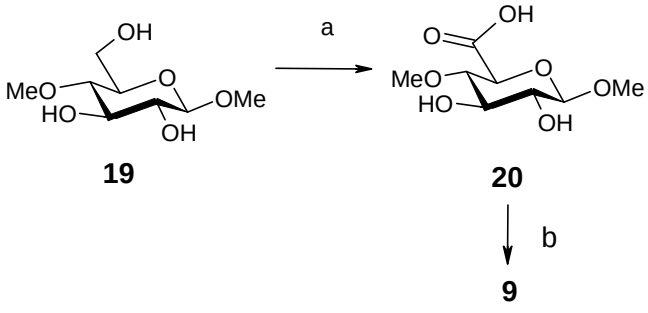


**Scheme 3**
**Reagents and conditions:** a), TEMPO, KBr, NaOCl, NaOH; b) 3 M TFA, 80 °C, 48 h.

*Synthesis from methyl 4-O-methyl β-D-glucopyranoside*

As a simple model compound for the anhydro glucose unit within cellulose, methyl 4-*O*-methyl β-D-glucopyranoside **19** has previously been synthesized [15]. TEMPO oxidation of **19** proceeded smoothly as observed by TLC, but isolation of the compound remained problematic due to the high amounts of salts in the reaction batch (Scheme 3) [16]. Extraction of the material with dry methanol removed part of the salt load, and silica gel chromatography of the residue using MeOH-$CHCl_3$-$H_2O$ as eluant resulted in several product fractions. Hydrolysis of the methyl glucuronide **20** was tested under various conditions. Treatment with trifluoroacetic acid at 80 °C for 48 h constituted a compromise between the onset of degradation reactions and incomplete hydrolysis of the methyl glycoside. Compound **9** was finally obtained upon hydrolysis of one fraction containing the glucuronide **20** and was finally desalted on a column of Sephadex G-10.

## Conclusions

The synthesis of 4-*O*-methyl glucuronic acid was preferably achieved via oxidation and subsequent benzyl ester formation of glucosides containing a temporary protecting group at the anomeric position such as benzyl or allyl groups. Whereas these groups were readily cleaved and allowed for a neat final hydrogenolytic deprotection, the acid-catalysed hydrolysis of methyl glucuronide proceeded sluggishly and led to incomplete conversion. The acid form of MeGlcA obtained upon hydrogenolysis may then be transformed into a defined salt form using anion-exchange chromatography.

## Acknowledgements

Financial support was provided by the Austrian government, the provinces of Lower Austria, Upper Austria and Carinthia as well as by the Lenzing AG. We also express our gratitude to the University of Natural Resources and Applied Life Sciences, Vienna, and the Lenzing AG for their in kind contributions as well as support of part of this work in the former CD-laboratory "Pulp reactivity" by Lenzing AG and the Christian Doppler Research Society.

## References

[1] T. Ebringerova and T. Heinze, Macromolecular Rapid Communications 21 (2000) 542–556.

[2] K. Shimizu, Wood and Cellulosic Chemistry; D.N.-S. Hon, N. Shiraishi (Eds.); Marcel Dekker: New York, (1991), pp 177-214.

[3] J. Li, G. Gellerstedt, Carbohydr. Res 302 (1997) 213-218.

[4] A. Granstrom, T. Eriksson, G. Gellerstedt, C. Roost, P. Larsson, Nord Pulp Pap Res 16 (2001) 18-23.

[5] J. Buchert, M. Tenkanen, L. Viikari, A. Teleman, V. Harjunpää, T. Vuorinen, Tappi J 78 (1995) 125-130.

[6] D. Barzyk, D.H. Page, A. Ragauskas, J Pulp Paper Sci 23 (1997) J59.

[7] J. Sjöberg, M. Kleen, O. Dahlman, R. Agnemo, H. Sundvall, Nordic Pulp Paper Res J 19 (2004) 392-.

[8] S. Danielson, K. Kisara, M.E. Lindström, Ind Eng Chem Res 45 (2006) 2174-2178.

[9] W.D.S. Bowering, T.E. Timell, Can J Chem 38 (1960) 311-312.

[10] A. Wacek, F. Leitinger, P. Hochbahn, Monatsh Chem 90 (1959) 562-567.

[11] N. Pravdic, D. Keglevic, Tetrahedron 21 (1965) 1897-1901.

[12] B. Abad-Romero, K. Mereiter, H. Sixta, A. Hofinger, P. Kosma, Carbohydr Res 344 (2009) 21-28.

[13] B. Roy, B. Mukhopadhyay, Tetrahedron Lett 48 (2007) 3783-3787.

[14] R.T. Lee, Y.C. Lee, Carbohydr Res 34 (1974) 151-160.

[15] J. Röhrling, A. Potthast, T. Lange, T. Rosenau, I. Adorjan, A. Hofinger, P. Kosma, Carbohydr Res 337 (2002) 691-700.

[16] A.E. De Nooy, A.C. Besemer, H. van Bekkum, Carbohydr Res 269 (1995) 89-98.

Lenzinger Berichte 87 (2009) 79-89

# PRE-HYDROLYSIS OF THE PHENYL GLYCOSIDIC BOND IN A MODEL COMPOUND

Martin Lawoko, Sagar Deshpande, and Adriaan R. P. van Heiningen

Department of Chemical and Biological Engineering, University of Maine, 117 Jenness Hall, Orono, ME, 04469-5737 USA

**A model compound, phenyl-β-D-glucopyranoside, was used to investigate if hydrolysis of the glycosidic bond occurred during different pretreatment methods of wood such as auto hydrolysis, green liquor pretreatment and acid hydrolysis. It was found that hydrolysis of the phenyl glycoside model compound at near neutral aqueous conditions (pH 6) was minimal (4 %) at 170 °C. On the other hand hydrolysis was nearly complete (95 %) at this temperature with the addition of acetic acid at a concentration expected to be generated from deacetylation of xylan in hardwoods (about 10 g/L). At acid conditions of pH 1.65 the temperature may be lowered to 105 or 121 °C while still obtaining a significant (80-90 %) hydrolysis yield.**

**Green liquor pre-treatment (at pH 12.5) produced phenol and levoglucosan while no glucose is formed, and at 155 °C, the hydrolysis was essentially complete with quantitative formation of levoglucosan and phenol.**

**Total Organic Carbon (TOC) measurements confirmed that no other degradation products than glucose, phenol and levoglucosan were formed at any of the experimental conditions studied.**

**Keywords:** *TOC, green liquor*

## Introduction

The heating value of wood carbohydrates is only half that of lignin. Therefore a more economical use of hemicelluloses is extraction as oligomers from wood chips prior to pulping followed by their conversion to high value-added products such as ethanol, polymers and other chemicals, as has been proposed by vanHeiningen (2006). However, when hemicellulose pre-extraction is performed at high temperature and acidity/alkalinity, the carbohydrates may degrade and lignin undergoes condensation reactions. These unwanted reactions must be minimized to obtain the hemicellulose sugars in un-degraded form and avoid problems during the subsequent delignification stage. Also it is known that the hemicelluloses in wood are covalently bonded to lignin (Lawoko et al, 2005). Three main types of native lignin carbohydrate bonds (LC-bonds) have been proposed in the literature, namely benzyl ether- and ester bonds (Freudenberg and Grion, 1959) and the phenyl glycoside types (Kosikova et al. 1972). Therefore it is important to know the reactivity and stability of these chemical bonds as a function of operating conditions used for hemicelluloses extraction.

Numerous studies on the acid hydrolysis of phenyl glycosides, e.g. (Heidt et al 1944, Overend, Rees and Sequiera, 1962, Bruyne and Wouters-Leysen 1970) are in consensus that the degradation of phenyl-

β-D-glucopyranoside proceeds by the unimolecular A-1 mechanism (Figure 1).

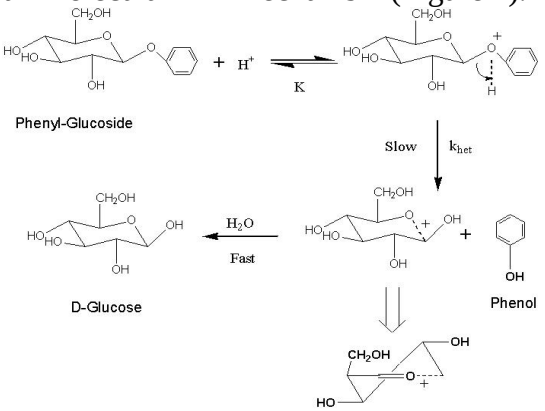


**Figure 1.** A-1 Mechanism of acid hydrolysis of phenyl-β-D-glucopyranoside.

Pre-extraction of hemicelluloses from hard woods to create more value from them is presently actively investigated as part of the biorefinery concept. Knowledge of the quantity and ease of cleavage of hemicellulose-lignin complexes is important for the design of subsequent separation and biological conversion processes of the extracted hemicelluloses. In the present work, the effect of pre-extraction conditions and that of a subsequent high temperature dilute acid treatment on the reactivity of the phenyl-glucosidic LCC bond was investigated using the simplest model compound, phenyl-β-D-glucopyranoside.

## Materials and Methods

### Chemicals

All chemicals used were of analytical grade. The model compound phenyl-β-D-glucopyranoside was purchased from TCI America (purity > 99 %). β-D-glucose and phenol were purchased from Fisher Scientific (both 99+ % purity).

Inositol was used as internal standard for the quantification of phenyl-glycoside, glucose and levoglucosan, while guaiacol was used as internal standard to quantify phenol. Both chemicals were obtained from Fisher Scientific. Reagents used for hydrolysis of model compound phenyl-β-D-glucopyranoside consisted of glacial acetic acid (HPLC grade), (12M) hydrochloric acid, sodium hydroxide, sodium carbonate; sodium sulfate and anhydrous sodium sulphate; all reagents obtained from Fisher Scientific.

Chemicals used for derivatization of the sample included dichloromethane, 25 % ammonium hydroxide, potassium borohydride solution, 1-methylimidazole, acetic anhydride, absolute ethanol and 7.5M potassium hydroxide; obtained from Fisher Scientific and Across Organic.

Hydrolyzed product were investigated using a gas chromatograph of SHIMADZU GC2010 with mass spectrum analysis QP2010S (GC-MS). Capillary column of type RTX 225 (length 30 m, internal diameter 0.25 mm, film thickness 0.25 µm). A gas chromatograph with flame ionization detector (GC-FID) of SHIMADZU GC2010 and capillary column of type RTX 225 and DB-225 (length 15 m, internal diameter 0.25 mm, film thickness 0.25 µm) was used for glucose analysis. A Dionex ASE-100 modified accelerated solvent extractor, autoclave (temperature range 105 °C to 121 °C), water bath (temperature range 40 °C to 90 °C) and rocking digester were also used for hydrolysis experiments.

### Reduction and acetylation of samples

The reduction of sugars to alditol and subsequent acetylation to alditol acetates was performed using a previously described method (Theander and Westerlund, 1986). The internal standard for the quantification of phenyl-glycoside, glucose and levoglucosan was prepared by dissolving 20 mg of Inositol in 20.0 mL solution obtained by combining 2 mL of 25% ammonium hydroxide solution with 18 ml of deionized water.

### Phenol extraction procedure

Phenol formed as a result of hydrolysis of the phenyl-glycoside was isolated using liquid-liquid extraction. To 1 ml of the neutralized solution after hydrolysis was 0.25 ml of 1 g/l of internal standard (guaiacol solution in dichloromethane) was

added followed by 2 ml of dichloromethane. The mixture was vortex mixed and kept at room temperature for phase separation. The dichloromethane phase was transferred into a GC vial (to 1.5 ml level) containing a pinch of anhydrous sodium sulphate added to absorb any small amount of water present in the transferred phase.

**Operating conditions of GC analysis**

For the GC-MS analysis of alditol acetates, injection temperature was maintained at 250 °C and the detector temperature at 260 °C. The oven temperature program was as follows; from 120 °C to 200 °C at a rate of 5 °C/min and held at 200 °C for 5 minutes, then from 200 °C to 280 °C at a rate of 4 °C/min and held at 280 °C for 10 minutes. The total flow was maintained at 25 ml/min. A split ratio of 1:20 was applied

For the GC-MS analysis of phenol, the injection temperature was maintained at 250 °C and the detector temperature at 260 °C. The oven temperature program was as follows: the oven was maintained at 40 °C for 1 minute, then from 40 °C to 120 °C at a rate of 5 °C/min and held for 5 minutes at 120 °C, from 120 °C to 280 °C at a rate of 4 °C/min and held at 280 °C for 10 minutes. The total flow was maintained at 27 ml/min. A split ratio of 1:20 was applied.

**ASE-100 extractor**

The ASE-100 equipment works at high pressure in the range of 11-15 MPa. When extracting wood with water, the pressure inside the extraction cell does not remain stable. If the pressure inside the extraction cell in the ASE-100 drops below a minimum set point of 11 MPa, the supply pump introduces fresh water into the extraction cell. If the pressure increases above the maximum set point of 15 MPa due to thermal expansion or generation of gases during extraction, the relief valve (relief valve-1, Figure 2) opens and releases liquid from the extraction cell.

In order to avoid release or addition of liquid during the extraction process, the Dionex ASE-100 was modified by connecting a pressurized expansion tank to the extraction cell.

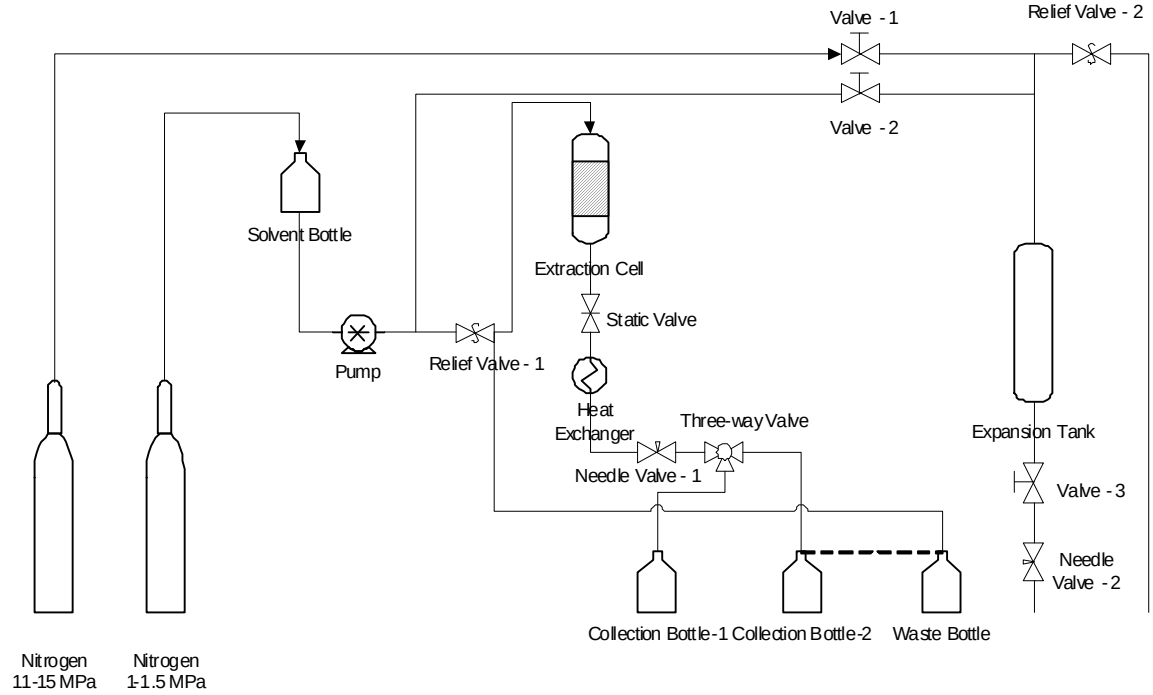


**Figure 2.** Modified Dionex ASE-100 extractor (Tunc and van Heiningen, 2008).

This allowed the ASE-100 to operate at constant volume extraction. Moreover, a heat exchanger was added to afford condensation of any volatile products (Tunc and vanHeiningen, 2008). The Modified ASE-100 extractor is represented schematically in Figure 2.

**Simulation of hot water extraction – Neutral Condition**

A known concentration of an aqueous phenyl-glycoside solution of pH 6 is pumped from the solvent bottle of the ASE 100 into the extraction cell. The pH of the solution was similar to the final pH of the extract when hardwood is contacted with a solution of "green liquor" as described in the so-called "near-neutral" extraction process (Mao et al., 2008). The present model compound experiments were performed at temperatures of 150, 160 and 170 °C for a constant time of 90 minutes. At the end of each experiment, a sample taken from the collection bottle was further analyzed using the earlier described alditol-acetylation and liquid extraction methods to quantify the amount of remaining phenyl-glycoside and formed glucose and phenol.

**Simulation of hot water extraction – Acidic Condition**

De-acetylation of xylan occurs during hydrothermal hemicelluloses extraction from hard woods. The release of acetic acid creates an acidic solution. The amount of acetic produced depends on the time and temperature of the wood extraction (Tunc and vanHeiningen, 2008). Based on these results, pre-determined amounts of acetic acid were added to the aqueous solution of the phenyl-glycoside in the ASE 100 experiments. Table 4.1 shows the amount of acetic acid added at the three different temperatures. At the end of each of the three models compound experiments the samples collected in the ASE 100 collection bottle were neutralized using 1M of sodium hydroxide solution. The neutralized samples were analyzed using the alditol-acetylation and liquid extraction methods for quantification of the remaining amount of phenyl-glycoside and formed glucose and phenol.

**Green liquor extraction – Alkaline Condition**

Pre-extraction of wood with green liquor to obtain hemicelluloses for value added products is presently being pursued at the University of Maine (Mao et al, 2008), hence the effect of green liquor on the cleavage of the phenyl-glycosidic bond was investigated in the present study.

Industrial green liquor is an alkaline solution containing 8.99 g/L sodium hydroxide, 29.14 g/L sodium sulfide and 69.98 g/L sodium carbonate (all concentrations expressed as sodium oxide, Na2O). For green liquor pretreatment of wood, 3% (as Na2O) of green liquor is charged based on dry wood at total liquor to wood ratio of 4:1 L/kg. For the present experiments, this composition was used to simulate the green liquor extraction process. The present green liquor pre-treatment experiments were performed in a rocking digester at temperatures of 137, 146, and 155 °C for 90 minutes. Each time a known amount of phenyl-glycoside was dissolved in a small quantity of water and then dissolved in the green liquor solution. The pH of the solution before and after high temperature treatment was 12.5. The rocking digester has a capacity of 20 L, but for hydrolysis of the phenyl-glycoside model compound 8 small bombs of 350 ml capacity were used simultaneously. Once the sealed bombs are properly placed inside the rocking digester, the digester was filled with water to 60 % of its capacity and then heated to the desire temperature. A heating period of 36 minutes to attain 160 °C temperature from room temperature (26.1 °C) was observed.

After every run, the cooled samples were neutralized using 1ml of 12M hydrochloric acid for 55 ml of green liquor solution. The neutralized samples were analyzed using alditol-acetylation to quantify the

remaining phenyl-glycoside and formed glucose and using liquid extraction method to quantify the amount of formed phenol.

Strong acidic treatment

Acid treatment of woody biomass and pulp fibers is commonly used to dissolve and hydrolyze the carbohydrate fraction to release and quantify the amount of lignin and mono sugars. Also dilute acid treatment of the sugars is an important pretreatment technique for biomass to overcome the "recalcitrance" of cellulose for production of biofuels. Thus it was important to establish the stability of the phenyl-glycoside at strong acidic conditions.

A strong acidity of pH 1.65 at room temperature was chosen using HCl as acid. Four temperatures were studied; 70 and 90 °C using a water bath, and 105 and 121 °C using an autoclave. At the lowest temperature of 70 °C the solutions in capped centrifuge tubes were taken out of the bath every hour for up to 5 hours (i.e. 1, 2, 3, 4, 5 hours) and after 12, 24, and 48 hours. At 90 °C the solutions in capped vials were taken out of the water-bath every hour for up to 4 hours, cooled and neutralized using known amount of 1M of sodium hydroxide solution. The neutralized samples were stored for further analysis using the alditol-acetylation and liquid extraction method.

**Preparation of calibration solutions**

Five standard flasks of 15.0 mL were used for series dilution. In the first flask 15.0 mg of phenol, glucose or phenyl glycoside was dissolved in 15ml with deionized water. From the first flask 5.0 mL, 4.0 mL, 3.0 mL and 2.0 mL and 1.0 mL was transferred respectively to the other flasks and diluted to the 15.0 mL mark with deionized water. As a result, each flask had a different phenol concentration. 1.0 ml was taken from each flask and was subjected to dichloromethane liquid extraction.

**Results and discussion**

The final mass of phenyl-glycoside and phenol after the hydrolysis treatment was determined by GC-MS, while GC-FID was used for glucose. The percentage of phenyl glycoside cleaved was calculated using the following three methods:

1) On the basis of phenyl-glycoside remaining:

$$= \frac{\text{(Initial mass of phenyl-glycoside – Final mass of phenyl-glycoside)} \times 100}{\text{(Initial mass of phenyl-glycoside)}}$$

2) On the basis of glucose formed

$$= \frac{(256 / 180) \times \text{(Final mass of glucose formed)} \times 100}{\text{(Initial mass of phenyl-glycoside)}}$$

where 256 g/mol is the molar mass of phenyl-glycoside and 180 g/mol is the molar mass of glucose.

3) On the basis of phenol formed

$$= \frac{(256 / 94) \times \text{(Final mass of phenol formed)} \times 100}{\text{(Initial mass of phenyl-glycoside)}}$$

where 94 g/mol is the molar mass of phenol.

**Investigating the effect of temperature on cleavage of the phenyl-glycosidic bond in pH 6 water**

The effect of pre-extraction temperature on the cleavage of the phenyl glycosidic bond at near neutral aqueous conditions (pH of 6) was studied. It was found that there was no significant cleavage of the phenyl-glycoside at 150 and 160 °C. At 170 °C only 4 % of the model compound was cleaved. These results show that pre-extraction at neutral aqueous conditions has a minimal effect on the phenyl-glycoside bond at the present selected temperatures**.**

**Simulation of hot water extraction – Effect of temperature and acidity**

Figure 3 shows the yield of phenyl-β-D-glucopyranoside reacted plotted versus hydrolysis temperature of 150, 160 and 170 °C at constant time of 90 minutes in the presence of acetic acid. The amount of acetic acid added is plotted on right y axis. As can be seen, the addition of acetic acid leads to a considerable increase in the cleavage of the phenyl-glycoside bond. At 170 °C the amount of phenyl-glucoside cleaved is in the range of 91 % to 96 % depending on the calculation basis; i.e. on the amount of phenyl-glycoside remaining, or amount of formed glucose or phenol. The amount of phenyl-glycoside reacted calculated using the three methods are in good agreement, implying that a good mass balance is achieved using the present experimental and analytical procedures.

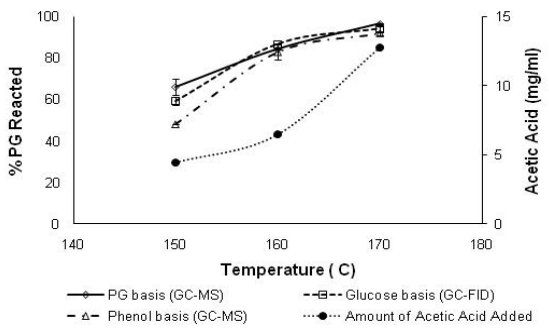


**Figure 3.** Phenyl-glycoside hydrolysis in hot water in the presence of acetic acid – treatment time 90 minutes.

The results show that during hot water hemicellulose pre-extraction of wood at 160 °C or higher for 90 minutes at a L/W ratio of about 4 a significant cleavage of phenyl-glycoside lignin-carbohydrate bond is obtained due to release of acetic acid from the hemicelluloses. The combined effect of temperature and acidity accomplishes the cleavage. By increasing the temperature from 150 to 160 °C the percentage of phenyl-glycoside bond cleavage increases considerably from about 55 % to about 85 %. No other products were seen in the chromatogram.

**Green liquor extraction – Alkaline Condition**

No glucose was detected at the simulated alkaline hydrolysis conditions, while phenol was measured. This indicates that glucose is further converted to other products. The GC-MS data revealed another significant peak that was determined by the NIST library data base to be levoglucosan. To confirm this, a commercial levoglucosan was derivatised using the alditol acetylation method and then analyzed using the GC-MS system. It gave an identical retention time and mass spectrum as the product identified in the green liquor hydrolysis experiments. Thus, it can be concluded that at the green liquor pre-extraction conditions, the phenyl-glycoside is cleaved to produce levoglucosan and phenol, no glucose was formed. The mechanism for the formation of levoglucosan from phenyl-glycoside has in fact been reported in the literature (William E., 1990). The percentage of phenyl glycoside cleaved on the basis of levoglucosan was calculated using the relationship:

$$\frac{(256 / 162) \times (\text{Final mass of levoglucosan formed}) \times 100}{(\text{Initial mass of phenyl-glycoside})}$$

Here 256 g/mol represent the molar mass of phenyl-glycoside, and 161 g/mol represent the molar mass of levoglucosan.

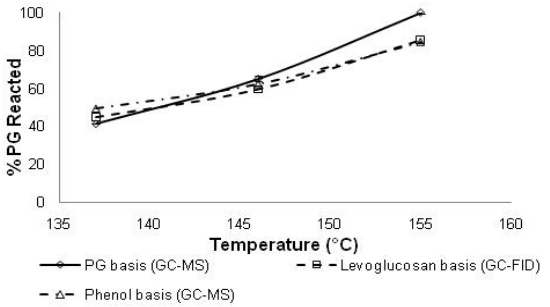


**Figure 4.** Phenyl-glycoside cleaved at simulated green liquor extraction conditions – extraction time 90 minutes.

Figure 4 shows the plot of phenyl-glycoside reacted as a function of hydrolysis temperature (137, 146 and 155 °C for 90 minutes). For the hydrolysis experiments at 137 and 146 oC, the percentage of phenyl-glycoside cleaved on the basis of levoglucosan formed were in very good agreement with those of phenol formed and phenyl-glycoside remaining. This indicates quantitative conversion of glucose to levoglucosan at these conditions At 155 °C however, there is no significant amount of phenyl-glucoside left (on remaining PG basis), while the calculation on the basis of phenol and levoglucosan formed show an 84 % cleavage. This indicates other degradation reaction of the phenyl-glucoside leading to products which are not analyzed by the GC system due to reduced volatility of these products.
Based on these results it may be concluded that during wood pre-extraction at alkaline conditions of pH 12.5 with green liquor for 90 minutes more than 50 % cleavage of the phenyl-glucoside lignin-carbohydrate bonds takes place at 145 °C, and increases to approximately 85 % at 155 °C.

**Strong acidic treatment**

The LC bond cleavage was also investigated at dilute acid pretreatment conditions. The pH of the aqueous hydrochloric acid solution used was 1.65 and the temperatures investigated were 70, 90, 105, and 121 °C with reaction time being another parameter. The hydrolysis of phenyl-β-D-glucopyranoside was studied on the three conversion bases [see equations (1), (2) and (3)]. Large mass balance discrepancies were observed when the percent cleavage calculated based on remaining phenyl-glycoside was compared with that based on formed phenol or glucose. The discussion below will concentrate mainly on the cleavage calculated based on the formation of glucose and phenol. The mass balance discrepancy will be addressed when discussing the carbon balance (TOC data).

*Strong acidic treatment at 70 °C*

At a low pH of 1.65 the temperature can be lowered while still achieving some cleavage of phenyl-glycoside. Figure 5.3.A shows phenyl-glycoside cleaved at 70 °C after 1, 2, 3, 4, 5, 24, 48, 72 hours on the basis of glucose and phenol formed.

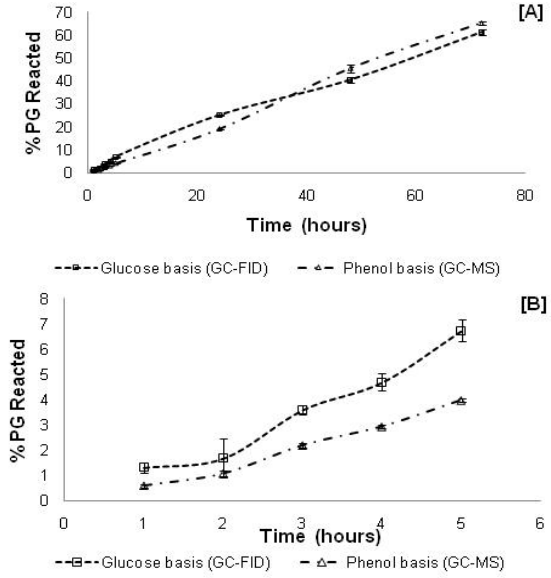


**Figure 5.** Phenyl-glycoside cleaved at pH 1.65 and 70 °C; [A] at 1 ,2, 3, 4, 5 , 24, 48 and 72 hours, [B] at 1 ,2 ,3, 4 and 5 hours.

The conversion yield calculated based on the two known products formed, i.e. phenol and glucose shows reasonable agreement with each other. The results show a nearly linear increase in conversion up to 63 % after 72 hours treatment.
The percentage yield of phenyl-glycoside hydrolysis on the basis of glucose formed was somewhat higher than that on the basis of phenol formed during the first 5 hours. This was further investigated by subjecting pure glucose and pure phenol to

the same conditions of pH 1.65 at 70 °C for 1, 5 and 24 hours, and the mass of the two components was unchanged by the hydrolysis, clearly showing that glucose and phenol were stable at these conditions and no other degradation products of glucose or phenol were formed.

*Strong acidic treatment at 90 °C*

The results in Figure 6 show the phenyl-glycoside hydrolysis yield at 90 °C after treatment for 1, 2, 3 and 4 hours.

The hydrolysis yield on the basis of phenol and glucose formed show good agreement with each other. During the first hour, 8 % cleavage occurs and this increases to 30% after 4 hours.

To determine whether any degradation product was formed from glucose or phenol, the pure compounds were subjected at 90 °C for 1 and 3 hours. Again, no significant conversion of either compound was detected by gas chromatographic analysis.

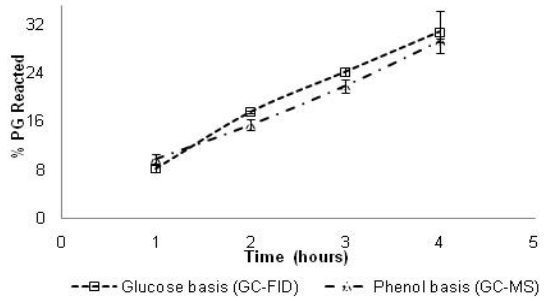


**Figure 6.** Phenyl-glycoside cleavage at pH 1.65 and 90 °C.

*Strong acidic treatment at 105°C*

Treatment at 105 °C was performed in the autoclave. For the analysis of the data it should be taken into account that it takes approximate 15 minutes for the reaction mixture to reach the desired final temperature. This explains why the hydrolysis of phenyl-glycoside at 105 °C begins after about 15 minutes as seen in Figure 7.

Only 3 % conversion is obtained at 15 minutes based on phenol and glucose formed due to heat-up to 105 °C in this period. Then the cleavage increases rapidly to 61 % after 1 hour. Subsequently the increase in cleavage rate slows down significantly giving a yield of 78 % after 2 hours, and 85% after 3 hours.

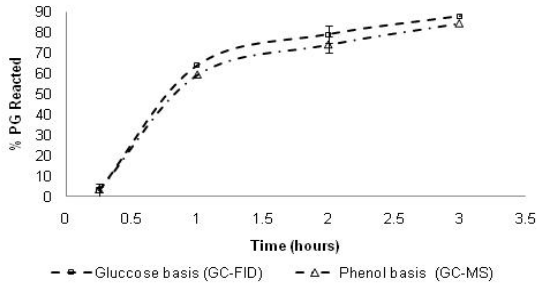


**Figure 7.** Phenyl-glycoside hydrolysis at pH 1.65 and 105 °C.

Since our data shows no formation of degradation products from pure phenol or glucose at 105oC, the observed reduced rate of formation of glucose and phenol may be due to depletion of the phenyl-β-D-glucopyranoside. However to verify this, further studies need to be performed whereby the concentration of the phenyl-β-D-glucopyranoside is changed to determine the reaction order of the phenyl-β-D-glucopyranoside hydrolysis kinetics.

*Strong acidic treatment at 121 °C*

As discussed before, it takes about 15 minutes to heat up the sample to the final autoclave temperature. This was again reflected in the initial delay time of about 15 minutes for phenyl-glycoside cleavage at 121 °C shown in Figure 8.

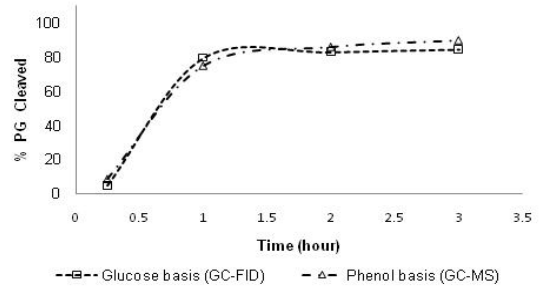


**Figure 8**. Phenyl-glycoside cleavage at pH 1.65 and 121 °C.

During the temperature rise to 121 °C about, 8% of the phenyl-glycoside was cleaved after 15 minutes. The data shows a rapid increase in yield up to 76 % after 1 hour and then only a small further increase

to around 82 % at 2 hour and 3 hours. No formation of degradation products from phenol or glucose was observed.

*Activation energy for strong acid treatment condition*

The activation energy is the amount of energy required to ensure that a reaction happens. It can be calculated by the Arrhenius equation which is given below

$$k = A * \exp^{(-E_a/R*T)}$$

The Arrhenius equation can be rearranged as follows;

$$\log(k) = \log A - \frac{E_a}{2.303 \times R} \times \frac{1}{T}$$

where k = rate percentage ($hour^{-1}$)

$E_a$ = activation energy ($kJ*mol^{-1}$)

R = gas constant; 0.008314472 ($kJ*°K^{-1}mol^{-1}$)

T = Temperature (°K)

A = proportionality constant

Figure 9 shows a straight line Arrhenius plot of the data in Table 1 in the form of log(rate) versus $1/T$.

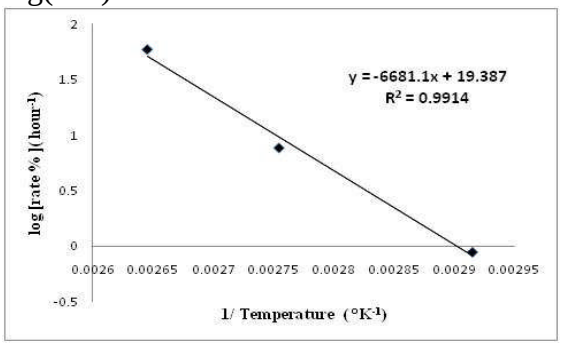


**Figure 9.** Arrhenius plot of degradation of phenyl-glucoside at pH 1.65.

**Table 1.** Rate constant at pH 1.65 at different temperatures.

| T (°C) | T (°K) | 1/T ($°K^{-1}$) | rate (k) ($\%.hr^{-1}$) | log k |
|---|---|---|---|---|
| 70 | 343 | 0.00292 | 0.8866 | -0.052 |
| 90 | 363 | 0.00275 | 7.6715 | 0.884 |
| 105 | 378 | 0.00265 | 58.843 | 1.769 |

The activation energy (Ea) was estimated from the slope of log(k) versus curve and found to be 128 kJ mol-1. This value is in good agreement with previous work, where the activation energy for the cleavage of the phenyl glycoside bond at acidic conditions was estimated to be between 125 kJ mol-1 and 135 kJ mol-1 (Overend, Rees and Sequiera, 1962).

**Total Organic Carbon (TOC) analysis**

In order to better understand the mass balance discrepancies obtained under acidic hydrolysis conditions, the total organic carbon content of the sample was determined using the TOC analyzer. The equations for the calculation of the theoretical amount of organic carbon based on the GC analyses are also given below:

($C_{PG}$) Carbon from phenyl-glycoside (PG)

$$= \frac{\text{Mass of carbon (12 x 12)}}{\text{Molar mass of PG}} \times \frac{(256 / 180) \times \text{(mass of glucose formed)}}{\text{(Initial mass of PG)}}$$

Please note that in the above formula the amount of PG remaining is calculated on basis of glucose formed because of problems with the analysis of PG as will be explained later.

($C_{Glu}$) Carbon from glucose

$$= \frac{\text{Mass of carbon (6 x 12) x Mass of glucose formed}}{\text{Molar mass of glucose}}$$

($C_{Phe}$) Carbon from phenol

$$= \frac{\text{Mass of carbon (6 x 12) x Mass of phenol formed}}{\text{Molar mass of phenol}}$$

Thus the total amount of carbon present in solution (mg/L):

$$(C_{total}) = \frac{(C_{PG} + C_{Glu} + C_{Phe})}{\text{Total volume (ml)} \times 1000}$$

At reaction time zero, i.e. when the phenyl-glycoside is dissolved in the acidic solution at room temperature and immediately neutralized, the TOC data from the analyzer is in excellent agreement with the calculated value of 0.35% difference (Table 2). When pure glucose and phenol were treated in the same way, the calculated carbon showed a difference of 3% with the TOC data, still within the margin of experimental error.

Also, when pure glucose and pure phenol were treated at different temperatures and pH 1.65, the TOC value measured and calculated from the GC analysis were in

agreement in the range of 94-97% (Table 3).
This clearly indicated that the formation of any degradation products from glucose or phenol is minimal at these conditions.
Based on the above results, the higher yield of phenyl glycoside cleaved during acid treatment calculated based on the amount of remaining phenyl-glycoside is likely to be the result of an analytical problem related to the acid treatment.

**Table 2.** Carbon calculations before reaction for the pure compounds at room temperature and pH 1.65.

| Compound | Phenyl-glucoside | Glucose | Phenol |
|---|---|---|---|
| Initial Carbon calculated (mg/Lit) | 8.5 | 13.05 | 33.53 |
| Carbon calculated from TOC analysis (mg/L) | 8.53 | 12.62 | 34.65 |
| % Difference | 0.35 | 3.29 | 3.23 |

**Table 3.** Carbon analysis for pure compounds at different temperature and pH 1.65.

| Compound | | Glucose (mg/L) | | | Phenol (mg/L) | | |
|---|---|---|---|---|---|---|---|
| Temp (°C) | Time ( hr ) | Carbon calculated before reaction | Carbon from TOC analysis after reaction | STD for TOC | Carbon calculated before reaction | Carbon from TOC analysis after reaction | STD for TOC |
| | 1 | 3.543 | 3.452 | 0.001 | 7.669 | 7.221 | 0.068 |
| | 2 | 3.543 | 3.491 | 0.087 | 7.669 | 7.32 | 0.072 |
| | 3 | 3.543 | 3.406 | 0.032 | 7.669 | 7.197 | 0.039 |
| 70 | 4 | 3.543 | 3.402 | 0.09 | 7.669 | 7.173 | 0.051 |
| | 1 | - | - | | 14.32 | 13.45 | 0.028 |
| | 2 | 10.47 | 9.837 | 0.01 | - | - | |
| 90 | 5 | - | - | | 14.32 | 13.46 | 0.084 |
| | 1 | 5.31 | 5.01 | 0.097 | 11.14 | 10.94 | 0.038 |
| 105 | 3 | 4.04 | 3.81 | 0.07 | 11.84 | 10.98 | 0.024 |
| 121 | 1 | 5.99 | 5.86 | 0.051 | 16.33 | 15.86 | 0.022 |

## Conclusions

The combined effect of temperature and acidity on the hydrolysis of phenyl-β-D-glucopyranoside was studied experimentally. The hydrolysis yield was quantified using GC/MS and GC/FID analysis after alditol acetylation derivatization of the products and starting material. The hydrolysis conditions were chosen to simulate different pretreatment methods such as auto hydrolysis, green liquor pretreatment and acid hydrolysis. It was found that hydrolysis of the phenyl glycoside model compound at near neutral aqueous conditions (pH 6) was minimal (4 %) at 170 °C. On the other hand hydrolysis was nearly complete (95 %) at this temperature with the addition of acetic acid at a concentration expected to be generated from deacetylation of xylan in hardwoods (about 10 g/L). At acid conditions of pH 1.65 the temperature may be lowered to 105 or 121 °C while still obtaining a significant (80-90 %) hydrolysis yield.
The hydrolysis experiments performed simulating green liquor extraction showed as previously reported that the hydrolysis of phenyl-glucoside produces phenol and levoglucosan while no glucose is formed. The result showed that hydrolysis of the phenyl glucoside at 155 °C was essentially complete with quantitative formation of levoglucosan and phenol rather than glucose and phenol. No other degradation

products than glucose, phenol and levoglucosan were observed at any of the experimental conditions studied.

At pH 1.65, and for all temperatures studied (70, 90, 105 and 121 °C), it is recommended that the products (phenol and glucose) rather than the amount of substrate left (phenylglycoside) be used to quantify the bond cleavage, based on the inconsistent data obtained when the amount of substrate left was used.

**References**


- Adriaan R.P van Heiningen. **Converting a kraft pulp mill into an integrated forest biorefinery.** Pulp and Paper Canada. (2006). 107(6), 38-43.
- Bruyne and Wouters-Leysen. **The influence of acids on the hydrolysis of glucopyranoside.** Carbohydrate Research. (1970). 17, 45-56.
- Freudenberg, K. and Grion, G. **Contribution to the mechanism of formation of lignin and of the lignin-carbohydrate bond.** Chem Ber. (1959). 92, 1355-1363.
- Heidt, Lawrence J.; Purves, Clifford B. **Thermal rates and activation energies for the aqueous acid hydrolysis of α- and β- methyl, phenyl and benzyl D-glucopyranosides, α- and β- methyl and β- benzyl D-fructopyranosides and α-methyl D-fructofuranoside.** Journal of the American Chemical Society. (1944). 66, 1385-9.
- Kosikova B; Joniak D. and Skamla J. **Lignin-Carbohydrate bond in beech wood.** Cellulose chemistry abd technology. (1972). 6(5), 579-588
- Lawoko. M, Henriksson G. and Gellerstedt G., **Structural differences between lignin carbohydrate complexes present in wood and in chemical pulps**. Biomacromolecules. (2005). 6, 3467-3473.
- Mao H, Genco J.M, Yoon S.H, A. van Heiningen and Pendse H, **Technical Economic Evaluation of a Hardwood Biorefinery Using the "Near-Neutral" Hemicellulose Pre-Extraction Process**. Journal of Biobased Materials and Bioenergy. (2008). 2, 177-185.
- Overend, W.G., Rees, C.W and Sequiera, J.S. **Reaction at position 1 of carbohydrates. Part III. The acid catalysed hydrolysis of glucosodes**. J. Chem. Soc. (1962). 3429-3440.
- Theander, O and Westerlund, E, A. **Studies on dietary fiber.3. Improved procedures for analysis of dietary fiber,** Journal Agriculture Food Chem. (1986). 34, 330-336.
- Traynard, P., Ayroud, A.M. and Eymery, A. **The existence of a lignin-carbohydrate union in wood.** Assoc Tech Ind Papetiere Bull. (1953). 2, 45-52.
- Tunc, M.S and van Heiningen A.R.P. **Hydrothermal dissolution of mixed southern hardwoods**. Holzforschung. (2008). 62(5), 539-545.
- William E.M **High Temperature Alkaline Degradation of Phenyl-β-D-Glucopyranoside,** Journal of Wood Chemistry and Technology. (1990). 10(2), 209-215.

Lenzinger Berichte 87 (2009) 90-98

# COUPLING OF FUNCTIONAL MOLECULES ONTO LIGNIN MODEL COMPOUND DIBENZODIOXOCIN

Tukayi Kudanga[a], Endry Nugroho Prasetyo[a], Jussi Sipilä[b], Gibson S. Nyanhongo[a], Georg M. Guebitz

[a]Graz University of Technology, Institute of Environmental Biotechnology, Petersgasse 12/1, A-8010, Graz, Austria
[b]University of Helsinki, Department of Chemistry, P. O. Box 55 (A. I. Virtasen aukio 1), 00140, Helsinki, Finland

Phone: +43316 873 8404; Fax: +433168738819; E-mail: g.nyanhongo@tugraz.at

**Laccase-mediated grafting of functional molecules presents an eco-friendly approach to functionalise lignocellulose materials. In this study functional molecules in the form of reactive phenolic amines, hydrophobicity enhancing fluorophenols and selected wood preservatives were successfully coupled onto lignin model compound dibenzodioxocin as demonstrated by HPLC analysis. This work therefore presents for the first time a model for functionalizing lignocellulose using the lignin model dibenzodioxocin.**

**Keywords:** *Coupling, laccase, Dibenzodioxocin*

## Introduction

Lignin is the most abundant form of aromatic carbon in the biosphere and one of the three major components of wood which include cellulose and hemicellulose. In nature, it provides mechanical strength to wood by binding fibres together; is involved in water transport in plants and forms a barrier against microbial destruction by protecting the readily hydrolysable polysaccharides (Hofrichter, 2002). It is a three dimensional optically inactive polymer formed by the dehydrogenative polymerization of three *p*-hydroxycinnamyl alcohol precursor molecules coumaryl alcohol, coniferyl alcohol and sinapyl alcohol linked together in an irregular manner (Sjöström, 1993; Boudet, 2000; Martínez et al., 2008). Polymerisation of the precursor molecules is initiated by laccase and/or peroxidase oxidation of the phenylpropanoid units to form radicals. These radicals undergo resonance stabilisation forming different mesomeric forms that can couple in many possibilities forming inter-unit linkages which include *β*-O-4, *β*-5, 5-5, *β*-*β*, 5-O-4 and the more recently discovered dibenzodioxocin 5-5-O-4 (Karhunen et al. 1995a;b). These inter-unit linkages are globally classified as non-condensed (mainly aryl-alkyl-*β*-O-4 ether bonds) and condensed lignin (mainly C-C bonds) (Kukkola et al. 2003). The dibenzodioxocin linkage involves the formation of α, β ethers on the same 5-5' biphenyl structures (Argyropoulos et al. 2002; Brunow et al. 1998). Recently, there has been an increase in the number of studies aimed at improving properties of wood using enzymes. Lignin has been the target polymeric unit as it can be modified with minimal effect on the structural integrity of the wood. The process usually involves targeted modification of wood fibre surfaces using oxidative enzymes to create a reactive surface which can be used to functionalise the wood. The main oxidative enzymes which are able to modify lignin are laccases and peroxidases. However, laccase is usually

preferred as peroxidases require hydrogen peroxide as cofactor which would make the process expensive.

Laccases (EC 1.10.3.2, p-diphenol:dioxygen oxidoreductase) are glycoproteins which catalyse the monoelectronic oxidation of a suitable substrate molecule such as phenols and aromatic or aliphatic amines to the corresponding reactive radical coupled with reduction of molecular oxygen to water (Nyanhongo et al., 2005, Riva, 2006). Although laccases have found application potential in many areas (Couto and Herrera, 2006), there is now a new wave of interest in laccase mediated surface activation with a view to grafting molecules of interest. In wood functionalisation, the process usually involves oxidation of lignin moieties on the wood surface to create a radical-rich reactive surface to which molecules of interest can be grafted (Kudanga et al., 2008). A recent review summarised several studies that demonstrated the possibility of laccase-catalysed bonding of low molecular weight compounds such as syringic acid, vanillic acid, gallic acid, hydroxytyramine and 4-hydroxybenzoic acid onto lignin (Widsten and Kandelbauer, 2008). We recently reported coupling of phenolic amines (Kudanga et al., 2008; 2009a) onto lignocellulose material. The *in vitro* coupling reactions were demonstrated using the lignin models syringylglycerol β-guaiacylether (G-S-β-ether) and guaiacylglycerol β-guaiacyl (erol). However, as dibenzodioxocin is an important substructure constituting up to 11 % in softwood lignin (Kukkola et al., 2003; Argyropoulos et al., 2002), *in vitro* experiments using this molecule have important implications on wood functionlisation. Indeed, it has been discovered that the majority of the *5,5*-dihydroxybiphenyl structures are etherified with phenylpropanoid units to form dibenzodioxocin structures (Karhunen et al. 1996; Brunow et al. 1998) and together with 5,5 linkages dibenzodioxocin constitute 18-25 % of linkages in softwood lignin (Argyropoulos et al., 2002; Froass et al., 1996). This study therefore demonstrates the coupling of functional molecules (amines, fluorophenols, wood preservatives) onto the lignin model compound dibenzodioxocin which provides an alternative model for functionalising lignocellulose materials.

## Materials and methods

*Chemicals*

The lignin model compound dehydrodivanillyl alcohol type dibenzodioxocin (Figure 1a) was synthesized as described in Karhunen et al. (1995). The functional molecules tyramine, hydroxytyramine, 3-O-methyldopamine, 4-Fluoro-2-methyl-phenol, 4-[4-(Trifluoromethyl)phenoxy]-phenol, triphenylphosphate and 2 phenylphenol (Figure 1b-h) were purchased from Sigma-Aldrich.

Beech (*Fagus sylvatica*) wood samples were provided by Mitteramskogler GmbH, Austria.

*Laccases*

Three laccase enzymes were used namely; *Bacillus* SF laccase produced as reported by Held et al. (2005), *Trametes hirsuta* laccase produced and purified as previously reported by Almansa et al. (2004), and *Trametes villosa* laccase, a kind donation from Novo Nordisk. The activity of laccases was measured by monitoring the rate of oxidation of ABTS according to Niku-Paavola et al. (1988) with some modifications. Briefly, the reaction mixture contained 30 µL laccase, 350 µL ABTS (1 mM) and 50 mM succinate buffer pH 4.5 to make a final volume of 1.5 mL. A blank was set in the same way as the sample experiment except that the laccase was initially heat denatured at 100 °C for 10 minutes.

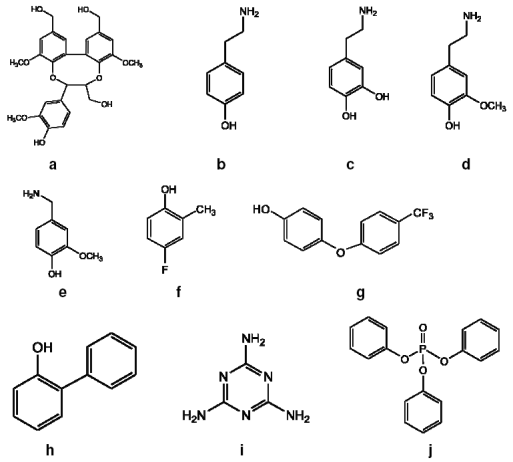


**Figure. 1.** Chemical structures of lignin models and functional molecules used in the coupling reactions: (**a**) dibenzodioxocin (**b**) tyramine (**c**) 3-hydroxytyramine (**d**) 3-O-Methyldopamine (**e**) 4-Fluoro-2-methylphenol (**f**) 4-[4-(Trifluoromethyl)phenoxy]phenol (**g**) 2-Phenylphenol (**h**) Triphenylphosphate.

The spectrometric measurements were done by recording the absorbance in the time scan mode for 2 minutes.

*Oxidation of functional molecules and dibenzodioxocin*

The ability of the three laccases to oxidize the functional molecules was monitored by UV/Vis- spectrophotometry and confirmed by HPLC analysis. To start the reaction, laccase with a final activity of 2.0 nkat $mL^{-1}$ was added to a reaction mixture containing 0.1 mM functional molecule in 50 mM succinate buffer pH 4.5 (0.1 M phosphate buffer pH 7.0 for *Bacillus* SF laccase). The reactions were monitored by UV/Vis-spectrophotometry in the wavelength scan mode from 900 nm – 200 nm at 3 min per cycle for a total of 18 min to identify oxidation products.

*Coupling of functional molecules onto dibenzodioxocin*

The reaction mixture contained 1.0 mM functional molecule, 2.3 mM dibenzodioxocin and 2.0 nkat $mL^{-1}$ laccase in 50 mM ammonium acetate buffer pH 4.7 (pH 7.0 for *Bacillus* SF laccase). Reactions were carried out at 37 ºC while shaking at 650 rpm using a thermomixer (Thermomixer Comfort Eppendorf AG, Hamburg Germany). The reactions were incubated for 1 hour when 2 phenylphenol was used as functional molecule, 2 hours when 3-hydroxytyramine was used and 3 h for the rest of the molecules. The coupling products were analyzed by HPLC.

*HPLC analysis of reaction products*

To the incubation mixtures an equal volume of ice cold methanol was added to precipitate protein. The mixture was centrifuged at 0 ºC for 15 minutes at 14000 g and 650 µL aliquots were transferred into clean vials. HPLC analysis was performed using a system from Dionex equipped with a P580 pump, an ASI-100 autosampler and a PDA-100 photodiode array detector while monitoring elution at 254 nm. Separation of coupling products was achieved by reversed phase HPLC RP-C18 column (Eurospher 100-5, C18, 150 x 4.6 mm with precolumn, Knauer GmbH, Berlin, Germany) using a linear gradient of acetonitrile (solvent B) and 0.1% $H_3PO_4$ (solvent A) as solvent at a flow rate of 1 ml $min^{-1}$, an injection volume of 10 µl and an oven temperature of 30 °C. The gradient was set as shown in Table 1. Alternatively 0.1% formic acid was used instead of 0.1% $H_3PO_4$ although this led to a slight shift in retention time.

**Table 1**. Gradient set up for HPLC analysis.

| Time (min.) | Initial | 5 | 20 | 21 | 35 | 35.1 | 45(end) |
|---|---|---|---|---|---|---|---|
| Solvent A% | 80 | 80 | 25 | 10 | 10 | 80 | 80 |
| Solvent B % | 20 | 20 | 75 | 90 | 90 | 20 | 20 |

The coupling product of the phenolic amine 3-hydroxytaramine was observed under isocratic conditions using acetonitrile, 10 mM sulphuric acid and deionized water (4: 3:13) as solvent at a flow rate of 1 mL $min^{-1}$ and an oven temperature of 25 °C. Identification and quantitative determination of amine substrates (after coupling) was done by reversed phase HPLC on a Discovery HS C18 column (5 µm; 15 cm x 4.6 mm, Supelco, Bellefonte, USA) using acetonitrile and 50 mM potassium phosphate buffer, pH 4.6 (1:49 v/v) as solvent at a flow rate of 1 mL $min^{-1}$ and an oven temperature of 25 °C.

## Results and Discussion

### Oxidation of functional molecules and lignin model compound dibenzodioxocin

The retention time of dibenzodioxocin was $t_R$=9.4 min. Upon laccase oxidation, 3 oxidation products ($t_R$=12.2 min $t_R$=13.0 min $t_R$=13.6 min) were observed. Similarly, laccase oxidation products were observed with the molecules 3-hydroxytyramine ($t_R$=37.8), 3-O-methyldopamine hydrochloride ($t_R$=37.9), 4-Fluoro-2-methylphenol ($t_R$=5.4), 2 phenylphenol ($t_R$=23.9) and triphenylphosphate ($t_R$=5.4). More products were observed upon dibenzodioxocin oxidation probably due to enzymatic cleavage (Guerra et al., 2004) or oligomerisation (Thurston, 1994; Buchert et al., 2002). However, tyramine was not readily oxidized by all laccases used probably because it lacks an electron donating substituent *ortho* to a hydroxyl group which is usually a pre-requisite for non-mediated laccase oxidation (Paice et al., 1995). However, some fungal laccases can oxidize simple monophenolic molecules (Takahama, 1995). Triphenylphosphate is the only molecule which lacks a phenolic hydroxyl group and was oxidised probably because of high electron density as a result of the 3 benzene rings which makes electron abstraction easier.

### HPLC analysis of coupling of functional molecules to lignin model compound

#### *Coupling of phenolic amines onto Dibenzodioxocin*

Coupling or grafting reactions are negatively affected by quenching of radicals and one study has reported that up to 90 % of radicals were quenched within a few hours in laccase-treated thermo-mechanical pulp (Grönqvist et al. 2006). In our earlier study we reported an increase in coupling of fungicides onto amine functionalized wood using *Trametes hirsuta* laccase (Kudanga et al., 2008). It was proposed that phenolic amines act as anchor groups creating a stable reactive surface which counteract negative effects of radical quenching during the coupling/grafting reactions. In a follow up mechanistic study using *Bacillus* SF laccase, tyramine was successfully covalently coupled onto syringylglycerol β–guaiacylether via a 4-O-5 bond, leaving the -$NH_2$ group free for further attachment of functional molecules (Kudanga et al., 2009). Here coupling of phenolic amines was demonstrated using the most recently discovered lignin subunit dibenzodioxocin. As dibenzodioxocin is a laccase substrate (Kudanga et al., 2008), it was possible to couple the laccase substrates 3-hydroxytyramine and 3-O-methyldopamine and the non laccase substrate tyramine. According to HPLC analysis, peaks observed in coupling reactions and not in the control reactions indicate coupling products between the model and amine (Figure 2).

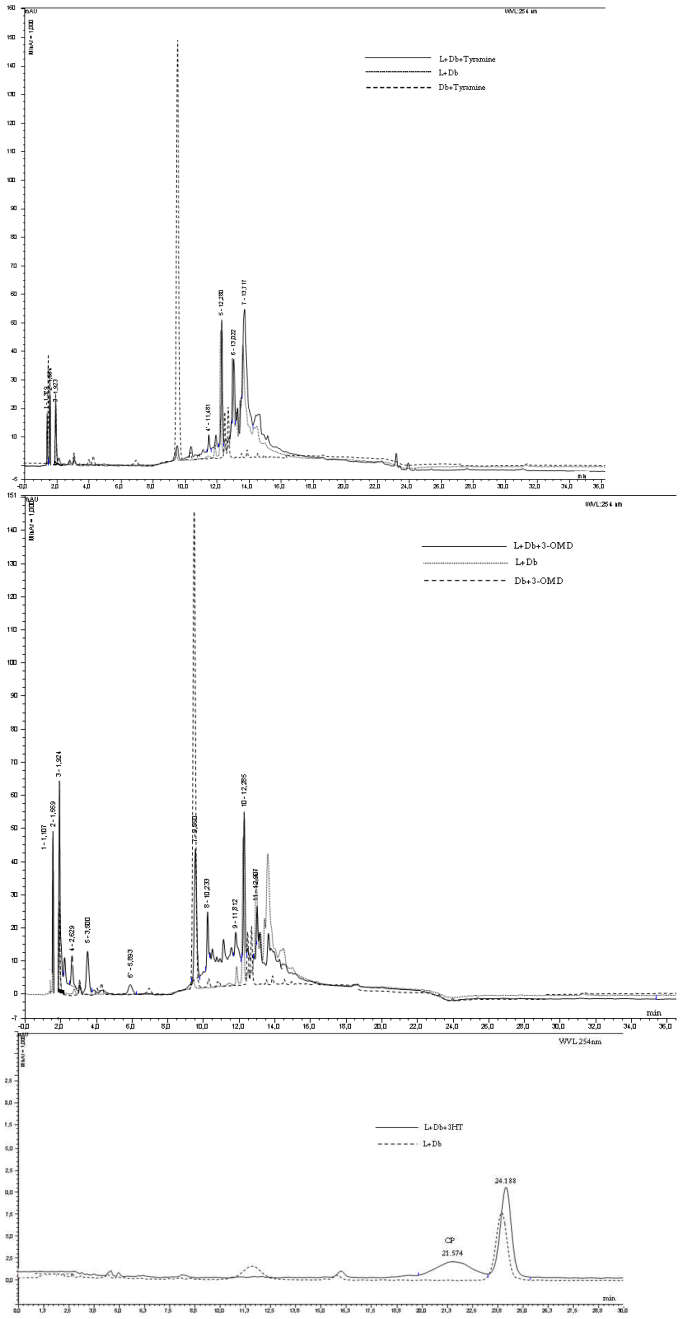


**Figure 2.** Laccase-mediated coupling of phenolic amines tyramine, 3-O-methyldopamine (3-OMD) and 3-hydroxytyramine (3HT) onto lignin model compound dibenzodioxocin (Db).

A new peak was observed in tyramine coupling reaction with retention time ($t_R$=11.4 min) while coupling products were observed at retention times $t_R$=3.5 min and $t_R$=5.9 min when 3-O-methyldopamine was used. Using isocratic conditions a 3-hydroxytyramine coupling product ($t_R$=21.6) was observed. Since tyramine was observed to be a non-laccase substrate, it was possible to quantify enzymatic coupling to lignin model compound and wood using HPLC based on the consumption of tyramine (Table 2). The percentage tyramine transformation appeared to be directly related to the redox potential of the enzyme. Bacterial laccases have been reported to exhibit a lower redox potential of about 0.5 V (Melo et al 2007) compared to 0.5 - 0.8 V for fungal laccases (Kumar et al., 2003; Kersten et al., 1990).

**Table 2.** Coupling of tyramine (initial concentration 1 mM) to laccase-oxidized dibenzodioxocin and beech (*Fagus sylvatica*) wood.

| Enzyme | Tyramine transformation (%)* | |
|---|---|---|
| | Model | Beech wood |
| *Trametes hirsuta* laccase | 13.6 ± 1.7 | 18.0 ± 2.1 |
| *Trametes villosa* laccase | 16.0 ± 2.0 | 20.9 ± 3.4 |
| *Bacillus* SF laccase | 6.8 ± 0.6 | 7.3 ± 2.5 |

*All values are means of three replicates ± standard deviation

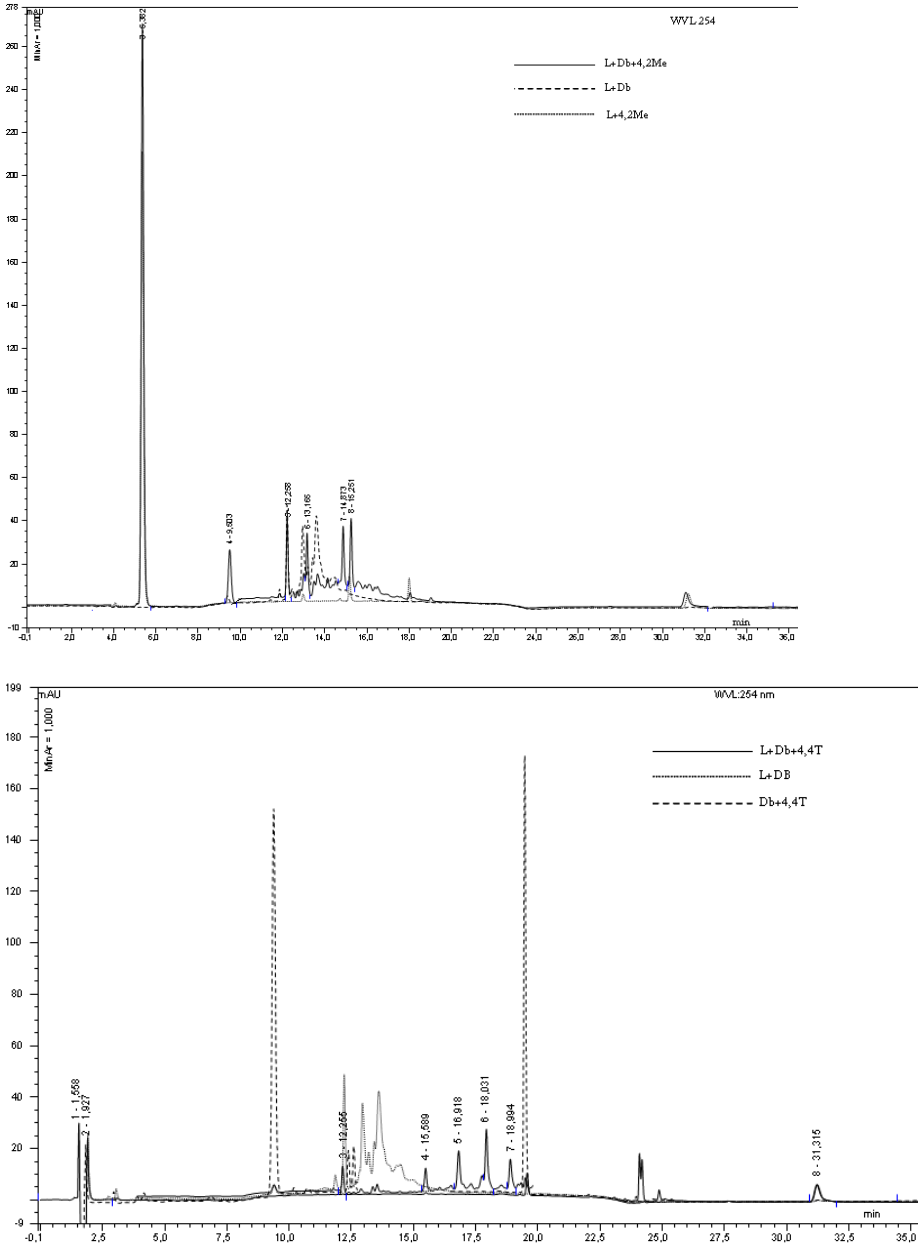


**Figure 3.** Laccase-mediated coupling of 4-fluoro-2-methylphenol (4,2 Me) and 4-[4-(Trifluoromethyl)phenoxy]phenol (4,4T) onto lignin model compound dibenzodioxocin.

***Coupling fluorophenols onto dibenzodioxocin***

Previously fluorophenols have been chemically applied to materials as a way of increasing hydrophobicity (Zhang and Huang, 2000; Tsukada et al., 2006). In this study the fluorophenols 4-Fluoro-2-methylphenol and 4-[4-(Trifluoromethyl)phenoxy]phenol were readily coupled enzymaticaly onto dibenzodioxocin. A new coupling product peak ($t_R$=14.9) was observed when 4-Fluoro-2-methylphenol was used while in the presence of 4-[4-(Trifluoromethyl)phenoxy]phenol, four coupling products were observed at retention times $t_R$=15.6, $t_R$=16.9 $t_R$=18.0 and $t_R$=19.0 (Figure 3). Enzymatic coupling of fluorophenols has practical significance since chemicals physically adsorbed are bonded by relatively weak Van der Waal forces and leach out over a long time due to continuous exposure to water. (Razzaque et al., 1982). This does not only leave the material hydrophilic and therefore prone to biodeterioration, but also exposes the environment to hazardous chemicals.

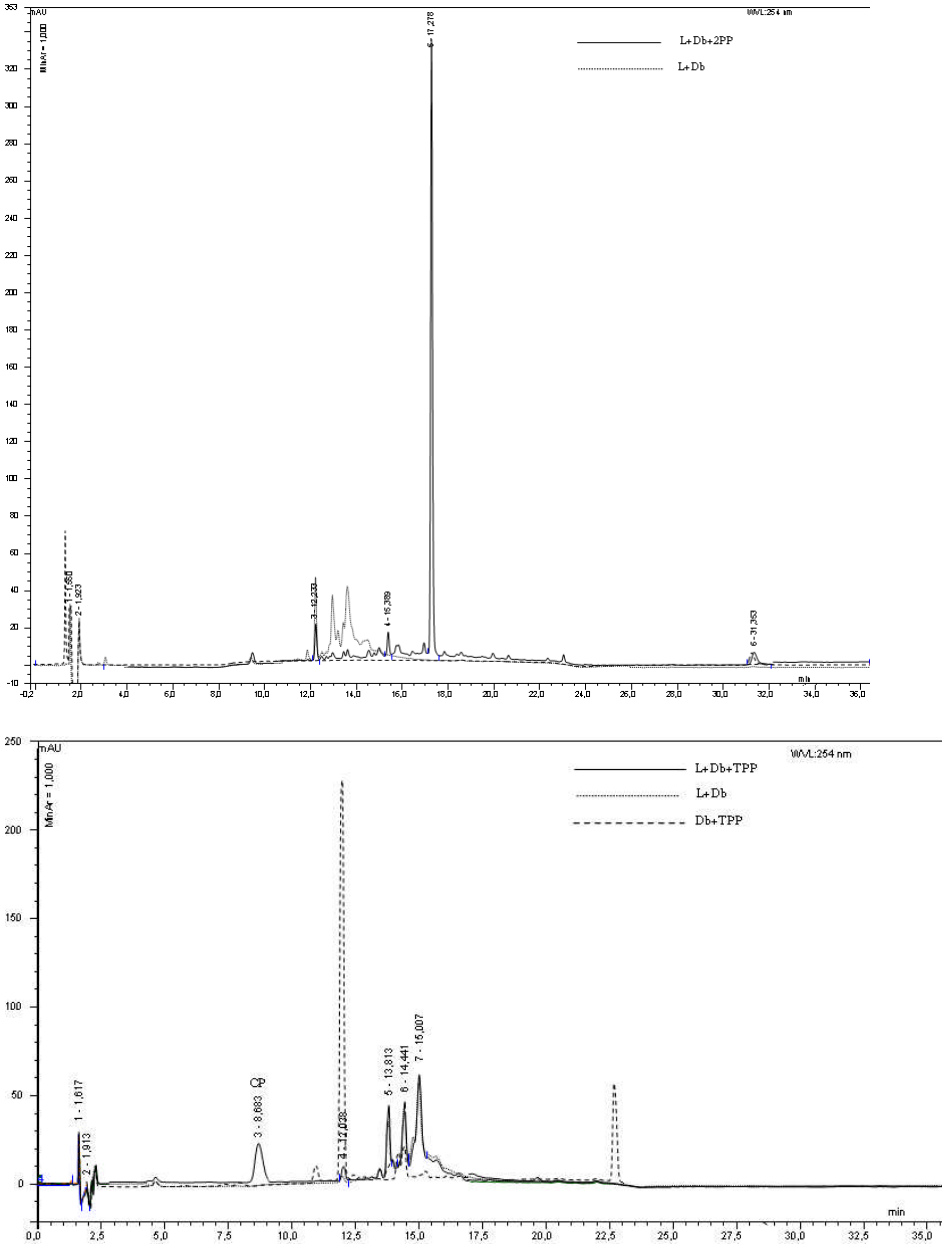


**Figure 4.** Laccase-mediated coupling of 2-phenylphenol (2PP) and triphenylphosphate (TPP) onto dibenzodioxocin.

***Coupling of wood preservatives 2 phenylphenol and triphenylphosphate onto dibenzodioxocin***

2-Phenylphenol is a fungicide used in agriculture, on fibers and other materials and is a general disinfectant while triphenylphosphate is used as a fire retardant in many materials including lignocellulosics. A coupling product between 2-phenylphenol and dibenzodioxocin was observed with retention time $t_R$=15.4 min while a coupling product ($t_R$=8.7) was observed with triphenylphosphate (Fig 4). Although a recent European Food Safety Authority (EFSA) Scientific Report list 2-phenylphenol as biodegradable, the same report also considered the chemical as toxic to aquatic organisms and proposed its classification as R50 ("very toxic to aquatic organisms") (EFSA Scientific Report, 2008). Although solubility of 2-phenylphenol is less than 0.1 g/litre at 20 °C, its sodium salt is very soluble (122 g dissolve in 100 ml water) and is therefore easily leached into the environment. Triphenyl triphenylphosphate is also generally regarded as biodegradable (Saeger et al., 1979). However, it easily enters aquatic systems via hydraulic fluid leakage as well as leaching and is known to be toxic to some aquatic organisms like fish and algae. Laccase-mediated grafting covalently binds the molecules onto lignocellulose material thereby preventing leaching and release into the environment.

## Conclusions

This study demonstrated for the first time coupling of functional molecules (phenolic amines, fluorophenols and selected wood preservatives) onto the lignin model dibenzodioxocin. Phenolic amines can act as anchor groups onto which other molecules of interest can be grafted. Coupling of hydrophobicity enhancing fluorophenols and the preservatives (2-phenylphenol and triphenylphosphate) covalently binds them to lignocellulose material so that they are not readily displaced into the environment. Since laccase work at ambient temperature using oxygen as electron acceptor and releasing water as the only by-product, this study therefore presents an eco-friendly model for functionalising lignocellulose material.

## Acknowledgements

This work was kindly funded by the Austrian Academic Exchange Service (OEAD) and European Union Biorenew Project [Sixth Framework Programme (FP6-2004-NMP-NI-4)].

## References

[1] Á.T. Martínez, J. Rencoret, G. Marques, A. Gutiérrez, D. Ibarra, J. Jiménez-Barbero and J.C. del Río. Phytochemistry 69 (16), (2008) 2831-2843

[2] S. Riva, Trends in Biotechnology 24(2006), 219-225.

[3] S.Grönqvist, K. Rantanen, A. Raimo, M. Mattinen, J. Buchert and L.Viikari, Holzforschung 60 (2006) 503–508

[4] M. Hofrichter, Enzyme and Microbial Technology 30 (2002) 454–466

[5] E. Sjöström Academic Press. Orlando. (1993) 293pp.

[6] S. Rodriguez Couto and J.L.T. Herrero, Biotechnol. Adv. 24 (2006) 500–513.

[7] P.Widsten, A. Kandelbauer . Enzy. Microb. Technol. 42 (2008) 293-307.

[8] T. Kudanga, E. Nugroho Prasetyo, J. Sipilä, A. Eberl, G.S. Nyanhongo, G. Gübitz, Journal of Molecular Catalysis B: Enzymatic doi:10.1016/j.molcatb.2009.06.001

[9] T. Kudanga, E. Nugrohojo Prasetyo, J. Sipilä, P. Nousiainen, P. Widsten, A. Kandelbauer, G.S. Nyanhongo, G.M. Guebitz, Eng. Life Sci. 8 (2008) 297-302.

[10] E.M.Kukkola, S. Koutaniemi, M. Gustafsson, P. Karhunen, K. Ruel, T.K. Lundell, P. Saranpää, G. Brunow, T.H. Teeri, K.V. Fagerstedt Planta. 217 (2003) 229-37.

[11] P. Karhunen, P. Rummakko, J. Sipila, G. Brunow and I. Kilpeläinen, Tetrahedron *Lett.* 36 (1995a)169-170.

[12] P. Karhunen, P. Rummakko, J. Sipila , G. Brunow and I. Kilpeläinen. Tetrahedron Lett. 36(1995b)4501-4504.

[13] G. Brunow, I. Kilpeläinen, J Sipilä, K. Syrjänen, P. Karhunen, H. Setälä, P. Rummakko ACS Symp Ser vol 697. American Chemical Society, Washington, DC, (1998) pp 131–147

[14] A.M. Boudet, Plant Physiol. Biochem. 38( 2000) 81-96.

[15] E. Almansa, A. Kandelbauer, L. Pereira, A. Cavaco-Paulo, G.M. Guebitz, Biocat. Biotrans. 22 (2004) 315-324.

[16] C. Held, A. Kandelbauer, M. Schroeder, A. Cavaco-Paulo, G.M. Guebitz. Environ Chem Lett.3(2005):74-77.

[17] M. L. E. Niku-Paavola,. P.Karhunen, V. Raunio, Biochem. J. 254 (1988) 877–884.

[18] E.P. Melo, A.T. Fernandes, P.Dura, L.O. Martins, Biochem. Soc. Trans. 35 (2007) 1579-1582.

[19] S. Kumar, P. Phale, S. Durani, and P. Wangikar. Biotechnol. Bioeng. 83 (2003)386-394.

[20] P. J. Kersten, B. Kalyanaraman, K. E. Hammel, B. Reinhammar and T. K. Kirk. Biochem. J. 268(1990) 475–480.

[21] L. Zhang, W.Y. Huang, Journal of Fluorine Chemistry 102 (2000) 55-59.

[22] Y. Tsukada, K. Iwamoto, H. Furutani, Y. Matsushita, Y. Abe, K. Matsumoto, K. Monda, S. Hayase, M. Kawatsura and T. Itoh. Tetrahedron Lett. 47 (2006) 1801–1804.

[23] *EFSA Scientific,* Conclusion on pesticide peer review regarding the risk assessment of the active substance 2-phenylphenol. *Report* (2008) 217, 1-67.

[24] M.A. Razzaque, University of Wales, Ph.D. Thesis (1982)

[25] M.G. Paice, R.Bourbonnais, I.D. Reid. Tappi J.78(1995)161–169.

[26] U. Takahama Physiol Platanum 93 (1995) 61- 68.

[27] P. Karhunen, P. Rummakko, A. Pajunen, G. Brunow, J. Chem. Soc., Perkin Trans. 1, (1996) 2303-2308.

[28] D. Argyropoulos, L. Jurassic, L. Krištofová, Z. Xia, Y. Sun, and E. Paluš. J. Agric. Food Chem. 50 (42002) 658–666.

[29] P.M. Froass, A.J. Ragauskas, J. Jiang, *J. Wood Chem. Technol.* 16 (1996)347-365.

[30] A. Guerra, R. Mendonça, A. Ferraz, F. Lu, and J. Ralph. Appl. Environ. Microbiol. 70 (2004) 4073–4078.

[31] C.F. Thurston, Microbiology 140 (1994), 19–26.

[32] J. Buchert, A. Mustranta, T. Tamminen, P. Spetz, B. Holmbom. Holzforschung 56 (2002) 579–584.

Lenzinger Berichte 87 (2009) 99-106

# COMPARATIVE CHARACTERISATION OF MAN-MADE REGENERATED CELLULOSE FIBRES

**Thomas Röder[1], Johann Moosbauer[1], Gerhard Kliba[1], Sandra Schlader[2], Gerhard Zuckerstätter[2], and Herbert Sixta[3]**

[1]Lenzing AG, Department FE, A-4860-Lenzing, Austria
[2]Kompetenzzentrum Holz GmbH, A-4021 Linz, Austria
[3]Helsinki University of Technology, 02150 Espoo, Finland

Phone: (+43) 07672-701-3082; Fax: (+43) 07672-918-3082; E-mail: t.roeder@lenzing.com

Presented during the 8th International Symposium Alternative Cellulose Manufacturing, Forming, Properties 03-04th September 2008 Rudolstadt/Germany

**Man made cellulose fibres show a large bandwidth of properties depending on their manufacturing process. Despite the differences in structure and morphology, molecular weight and its distribution, fibre properties and cross section, crystallinity and orientation, the chemical substrate is always cellulose in the modification II. The great variability of their properties is the basis for the manifold use of these fibres all over the world.**

**Commercial man made cellulose fibres of different types (viscose, cuam and high modulus rayon, tire cord, lyocell) are compared against experimental regenerated cellulose fibres (e.g. fortisan, fibre B "bocell", lyocell). Numerous characterisation methods (e.g.: REM, Raman/WAXS, SEC, NMR, fibre properties) are used to highlight similarities, differences, and characteristics of cellulose fibres. Structure – property – relationships will be presented and discussed.**

**Keywords:** *man made cellulose fibres, fibre properties, viscose, lyocell, modal, fortisan, bocell, cuam, celsol*

## Introduction

In contrast to cotton the use of cellulose pulp made from wood to produce textiles needs a forming procedure based on cellulose dissolution followed by a forming (and a regeneration) step.

The history of man-made cellulose fibres started in 1846 with the discovery of cellulose nitrate by Karl-Friedrich Schönbein. In 1892 the first factory was built in Besançon (France) by Comte Hilaire de Chardonnet producing "Chardonnet silk". Cuprammonium rayon was discovered in 1857 by Eduard Schweizer, the first factory was built in 1899. Viscose (cellulose xanthate) was discovered in 1891 by Cross, Bevan, and Beadle.

Nowadays a great variety of man-made cellulose fibres is known. But only a few are produced in industrial scale: viscose (CV, staple and filament), modal (CMD), lyocell (CLY), cupro (CUP), acetate (AC), and triacetate (CTA).

The fibres are divided into two categories: cellulose fibres (e.g. CV, CMD, CLY, CUP) and cellulose derivative fibres (e.g. AC, CTA). We will focus on the cellulose fibres only.

Cellulose fibres can be produced via cellulose derivatisation followed by regeneration (involving the destruction of the derivative, e.g. viscose) or via dissolution in a non-derivatising solvent (e.g. NMMO, Cuoxam, ionic liquids) and consequent regeneration.

**Fibre samples**

In this study various commercial fibres are compared with a great variety of experimental fibres. Commercial fibres are viscose fibres (viscose, tire cord viscose, polynosic fibres), modal fibres, cupo fibres (Asahi Kasai), and lyocell fibres (Tencel®).

Fibres based on cellulose derivatives are
*Fortisan® fibres:*
A saponified cellulose acetate prepared by dry spinning a solution of cellulose acetate in acetone (Celanese Corp., sample kindly provided by Prof. H. Chanzy, Grenoble, France). Fibres are highly oriented. The yarn is no longer produced.
*"Fibre B" (Bocell):*
Anisotropic solutions of cellulose in superphosphoric acid spun via air-gap into acetone and saponification in water/soda. Fibres have high tenacities and are highly oriented (developed by H. Boerstoel (Akzo Nobel), sample kindly provided by Dr. S. Eichhorn, Manchester, UK).
*Viscose fibres:*
Cellulose xathogenate dissolved in sodium hydroxide and spun via wet spinning process into sulphuric acid/ sodium sulphate/ zinc sulphate. Modal fibres are produced by a modified viscose process.
*Celsol fibres:*
Cellulose is dissolved in sodium hydroxide and regenerated in water (Institute of Chemical Fibres, Lodz, Poland).

Fibres based on direct dissolved cellulose are
*Cupro fibres:*
Cellulose dissolved in tetraaminecopper dihydroxide (complexation) and regenerated in water (Asahi Kasai).
*Lyocell fibres:*
Cellulose is directly dissolved in NMMO/water (Tencel®) or ionic liquids and spun through an air gap and precipitated in water.

**Cellulose solvents, resulting fibre types and their characterisation**

The cross section is a structural parameter of the fibre which is accessible via microscopy. Fibre diameters around 10 microns allow the use of light microscopy as well as scanning electron microscopy. Independent of the used solvent system for cellulose similar cross sections can be made (Figure 1) assuming the use of similar spinnerets. However, the same solvent system but a modified spinning bath leads to different cross sections (Figure 2). For viscose the acid concentration (same dope, same machine, all the other parameters are the same) influence the regeneration of the cellulose xanthate. A lower acid content leads to a "softer" regeneration. However, high acid content results in a massive loss of degree of polymerization (DP).
The commercially available viscose type fibres CV, CV tire cord, CMD, and polynosic (Figure 3) differ in DP of cellulose (source), spinning process, and after treatment. Their fibre properties vary over a wide range. Nevertheless, further diversification needs the use of other solvent systems. Higher tenacity, e.g., is available by using the lyocell process. Crystallinity increases, too. The solvent for the commercial Lyocell process is NMMNO (Tencel®). Similar to Lyocell, BISFA defines a cellulose fibre obtained by a spinning process from an organic solvent mixed with water."Solvent-spinning"
means dissolution and spinning without derivatization. Therefore, every spinning process using ionic liquids to dissolve and to spin cellulose is a Lyocell process.

Examples for these are given in Figures 1 and 4. The shape and the overall properties of these fibres are comparable to Tencel® fibres.

The use of special pulp sources (e.g. cotton linters pulp) and special spinning conditions allows the manufacturing of fibres with higher tenacity and higher modulus. However, the fibre properties are in the same range as for NMMO fibres, which could be improved by the named changes in pulp source and spinning conditions, too.

NMMO and ionic liquids are the most recent cellulose solvents used and lie in the focus of actual research. Other solvents for cellulose like hydrates of inorganic salts, e.g., zinc chloride and lithium perchlorate; lithium chloride and dimethylacetamide (DMAc); and metal complex solvents, e.g., copper ethylendiamine (Cu-en), are known and some are used for analytical purpose (LiCl-DMAc for SEC; Cu-en for intrinsic viscosity measurement), but they are not used to make fibres.

Another interesting approach is the CELSOL concept: Cellulose is dissolved in sodium hydroxide. Known from the viscose process, where cellulose reacts with sodium hydroxide to sodium cellulose, sodium hydroxide is able to dissolve hemicellulose and shorter cellulose molecules. The idea is to use sodium hydroxide directly without cellulose xanthate as for viscose to produce man made fibres. The disadvantage is in the limited solubility of longer cellulose chains. Therefore, presumably only fibres lower than viscose quality will be possible.

During World War 2 a process for manufacturing of cellulose silk for parachutes was developed: Fortisan® (Figure 4). These fibres have a high crystallinity, high orientation, and high modulus. Therefore they are very lean and thin. Fortisan® was produced via a dry spinning process.

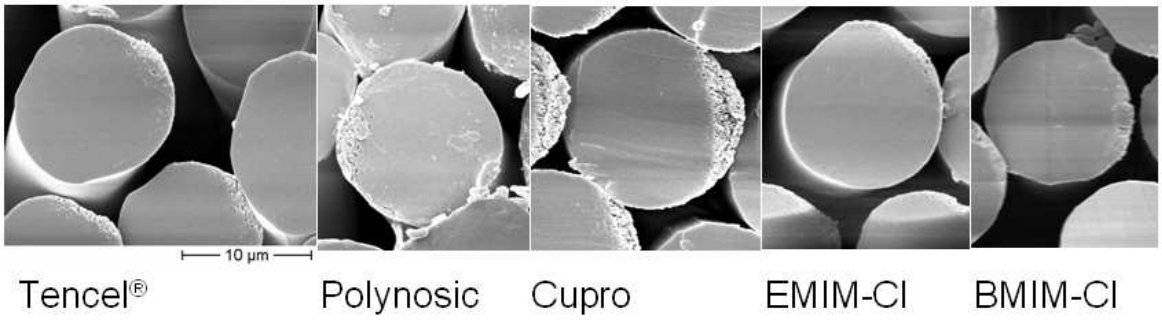


**Figure 1.** SEM figures of regenerated cellulose fibres with round shape.

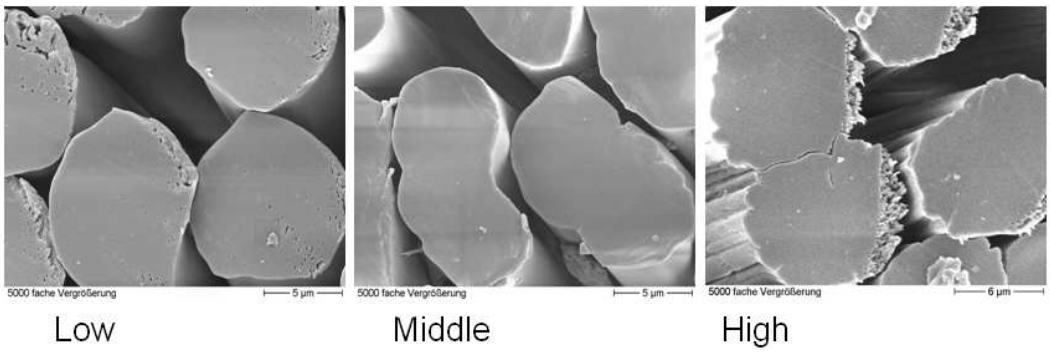


**Figure 2.** Influence of acid content in spinbath for viscose types of fibres.

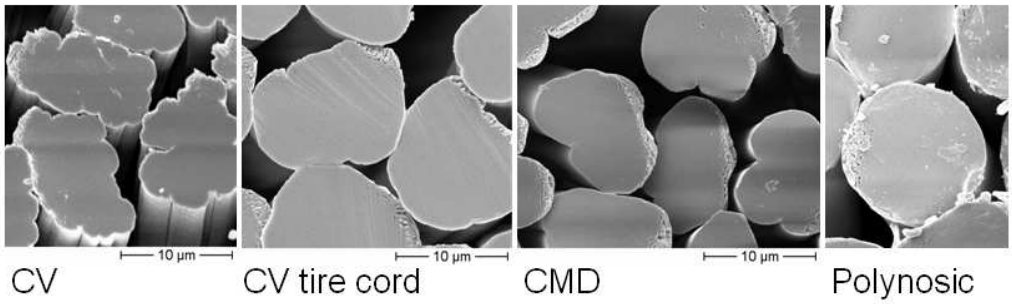


**Figure 3.** SEM figures of different viscose types of fibres.

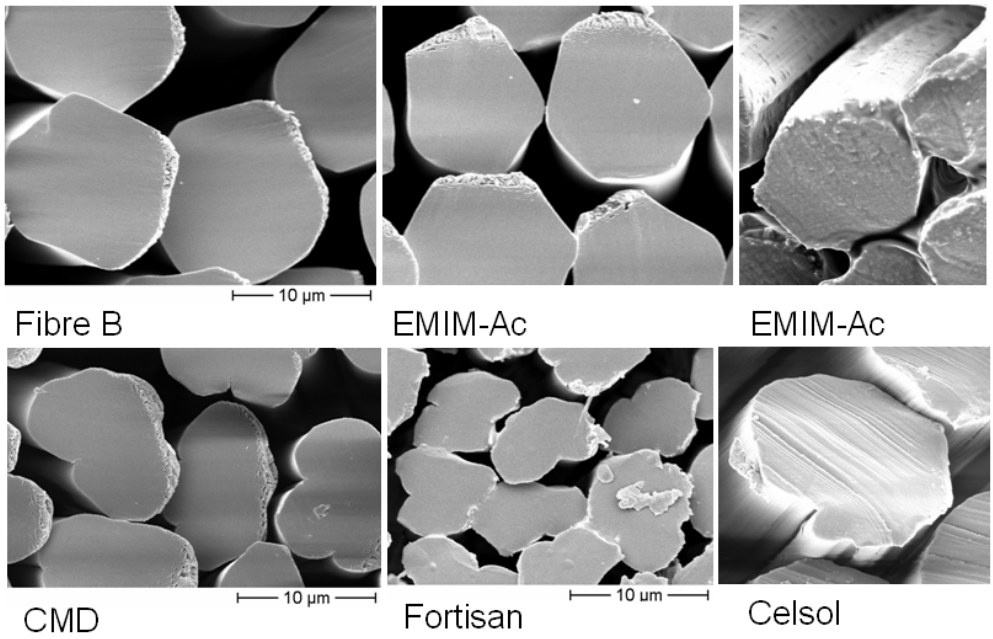


**Figure 4.** SEM figures of regenerated cellulose fibres with different cross sections.

**Table 1.** Fibre data.

| | titre | Tenacity cond. | Elongation cond. | Tenacity wet | Elongation wet | BISFA modulus | modulus cond. | Commercial/ experimental |
|---|---|---|---|---|---|---|---|---|
| | [dtex] | [cN/dtex] | [%] | [cN/dtex] | [%] | [cN/tex/5%] | [cN/tex/%] | fibre |
| Tencel® | 1,3 | 40,2 | 13,0 | 37,5 | 18,4 | 10,8 | 8,8 | com. |
| polynosic | 1,8 | 38,2 | 9,7 | 26,0 | 11,0 | 12,1 | n.a. | com. |
| cupro | 2,5 | 22,3 | 24,3 | 17,6 | 51,3 | 5,0 | 9,9 | com. |
| EMIM-Cl | 1,7 | 43,0 | 9,6 | 35,9 | 11,6 | 14,0 | 8,1 | exp. |
| BMIM-Cl | 1,5 | 50,1 | 9,3 | 39,4 | 10,4 | 17,8 | n.a. | exp. |
| CV | 1,4 | 23,9 | 20,1 | 12,5 | 22,0 | 2,4 | 5,3 | com. |
| CV tire cord | 1,9 | 52,3 | 15,1 | 38,4 | 22,9 | 3,1 | 11,1 | com. |
| CMD | 1,3 | 33,1 | 13,5 | 18,4 | 14,1 | 5,2 | 6,3 | com. |
| fibre B | 1,6 | 89,4 | 6,8 | 75,8 | 7,9 | 39,0 | 23,5 | exp. |
| EMIM-Ac | 1,8 | 44,7 | 10,4 | 38,1 | 11,9 | 13,2 | 10,0 | exp. |
| Fortisan® | 0,7 | 23,9 | 3,2 | 27,7 | 5,1 | 27,0 | n. a. | exp. |
| Celsol | 3,32 | 16,96 | 7,8 | 7,2 | 11,2 | 4 | n. a. | exp. |

Up to now the highest crystallinity, orientation, and tenacity is known from the so-called “fibre B”. This experimental fibre is produced from liquid crystalline solution of cellulose in superphosphoric acid and spun into acetone followed by saponification. This has similarities to the old Fortisan® process where cellulose acetate is spun into acetone, too.

In contrast to viscose type fibres (wet spinning) all these fibres are produced via air-gap in a dry-wet (Lyocell) or in a dry spinning process (followed by saponification: Fortisan®, fibre B).

Characteristic fibre data are given in Table 1.

## Structural parameters and fibre properties

Fibre properties can be varied within a wide range by using the same dope and the same spinning process. The level of stretching determines the tenacity and elongation level. A high degree of stretching results in a relatively tear-resistant and low-strain fibre.

The product of tenacity and elongation is called “working capacity”. This “working capacity” is mainly determined by the process and the solvent used. The molecular weight of the cellulose should be in an optimum range for the used solvent. The length of cellulose chains should be high enough to be able to form fibres. Cellulose chains should, however, not be too long, since this would increase the viscosity of the dope too much. For every manufacturing process there exists a different optimum range. Structural parameters like orientation are mainly influenced by the stretching during fibre making. The liquid crystalline structure of the dope for “fibre B” is one reason for the high crystallinity of the fibres. The structure of the cellulose inside the dope, the width of cellulose molecular weight distribution, and the velocity of regeneration process mainly determine the crystallinity of the fibres. WAXS (wide angle X-ray scattering) is the standard method for the determination of crystallinity of man-made cellulose fibres (Hermans and Weidinger 1949) [1].

The information concerning crystallinity of cellulose II can be obtained by other methods as well, e.g. Fourier Transform (FT) Raman, FT-infrared (IR), or solid state $^{13}C$ NMR (nuclear magnetic resonance) spectroscopy. Raman and IR based methods normally use a calibration with WAXS data [2] [3]. Therefore these methods can only be as good as the reference method itself.

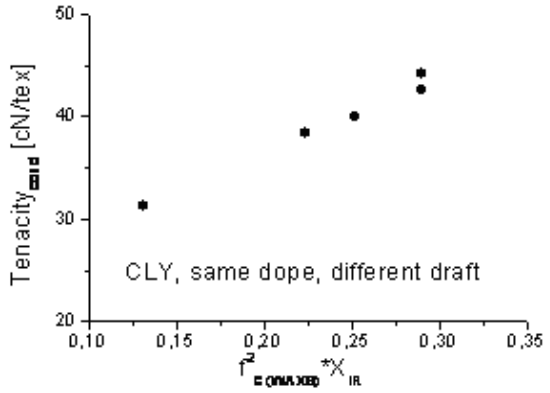


**Figure 5.** CLY fibre manufacturing with the same dope at various draft levels – correlation of tenacity and structural parameters orientation and crystallinity.

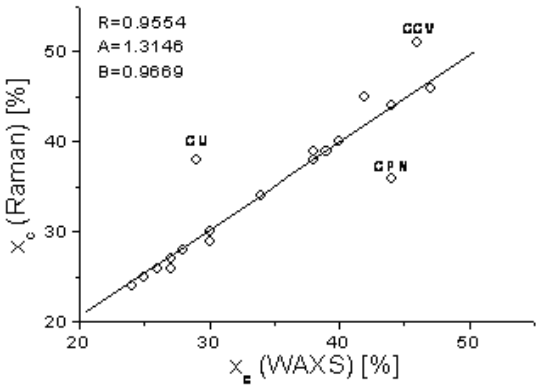


**Figure 6.** WAXS versus FT-Raman crystallinity. [2]

One of the factors determining the properties of cellulose fibres is the alignment of the fibrillar elements relative to the fibre axis. A relationship between the degree of orientation and the tensile strength of viscose fibres was put forth by Krässig and Kitchen [4]:

Strength or tenacity in the conditioned state

$$FFc \sim f^2_c$$

and strength or tenacity in the wet state.

$$FFn \sim f^{2,5}_{tot}$$

The classical method to quantify orientation of polymer fibres is wide angle X-ray scattering (WAXS). The WAXS results were compared with Raman results to obtain a Raman-based method to determine the degree of orientation of cellulose II (Figure 7 and 8).

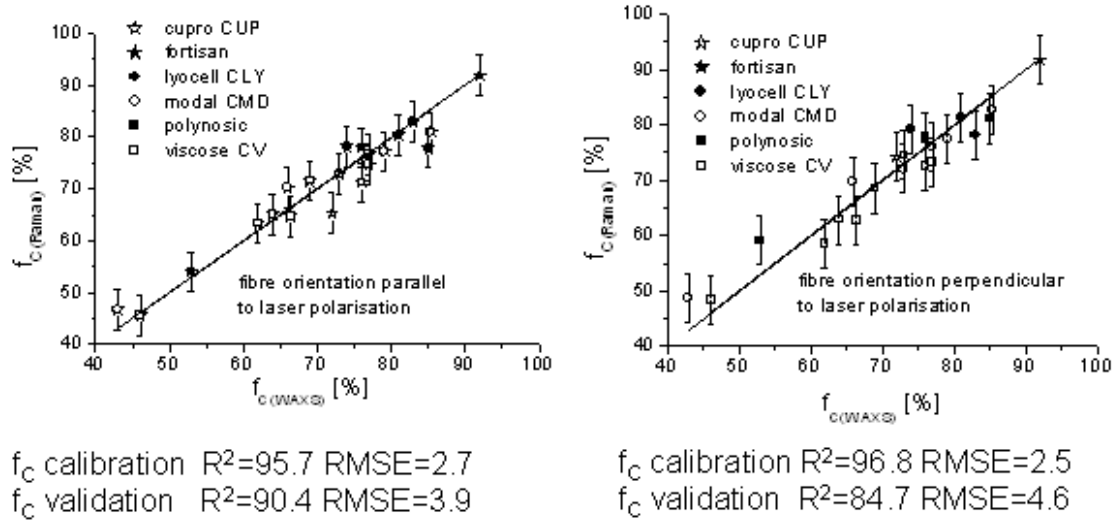


**Figure 7.** Calibration of crystalline fibre orientation - WAXS versus Raman.

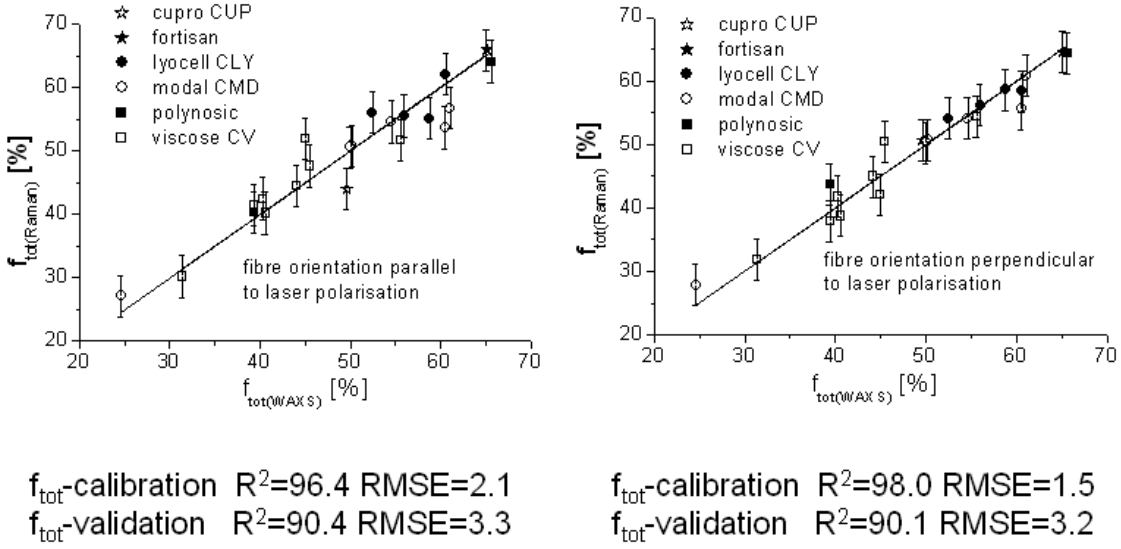


**Figure 8.** Calibration of total fibre orientation – WAXS versus Raman.

The higher resolution of Raman spectroscopy can be used as a tool for determining the local fibres orientation.

Another common method to measure the fibre orientation is the birefringence. A microscope equipped with polarisers and a compensator is used. The birefringence $\Delta n$ is obtained by dividing the measured retardation of polarised light by the respective fibre thickness. By relating $\Delta n$ to the maximum birefringence of cellulose $\Delta n_{max}$, the orientation factor $f$ (Hermans' orientation factor) can be calculated according to $f = \Delta n / \Delta n_{max}$.

Factor $f$ = 1 means perfect orientation parallel to the fibre direction, $f$ = 0 for random orientation, and -1 for perfect transverse orientation. This method is very useful for fibres with a round cross section, e.g. lyocell, and no crimp and distortion. Unfortunately, most of commercial fibres have no round cross section, are crimped, or both. This results in large differences of orientation values.

According to Krässig and Kitchen [4] a linear correlation between the degree of orientation and the fibre tenacity in conditioned as well as in wet state was found. Especially a series of CLY made from the same dope spun under different drafts showed a very good correlation

(Figure 5). The comparison of different man-made cellulose fibres used for analytical method development is given in Figures 9 and 10. Despite the CV tire cord the fibres showed more or less a linear correlation between tenacity and fibre orientation.

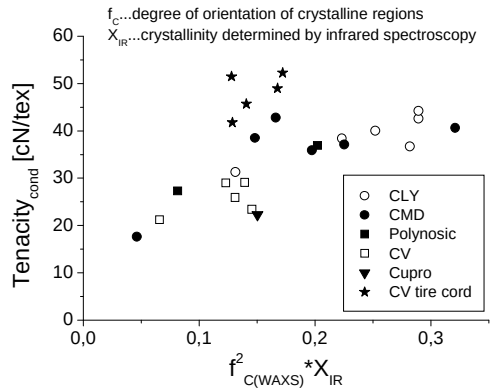


**Figure 9.** Correlation between tenacity (conditioned state) and structural parameters – crystalline fibre orientation and crystallinity.

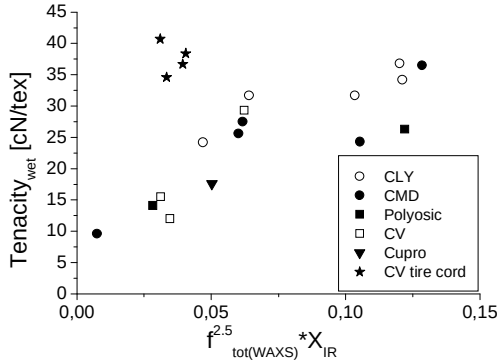


**Figure 10.** Correlation between tenacity (wet state) and structural parameters – total fibre orientation and crystallinity.

As mentioned above, the molecular weight distribution is another important parameter. State of the art is the determination of the molecular weight distribution by size exclusion chromatography (SEC). Essential is the choice of a suitable solvent system, e.g. LiCl-DMAc. Another possibility is the use of cellulose derivatives, e.g. cellulose nitrate. In this study SEC based on LiCl-DMAc was used (Figure 11).

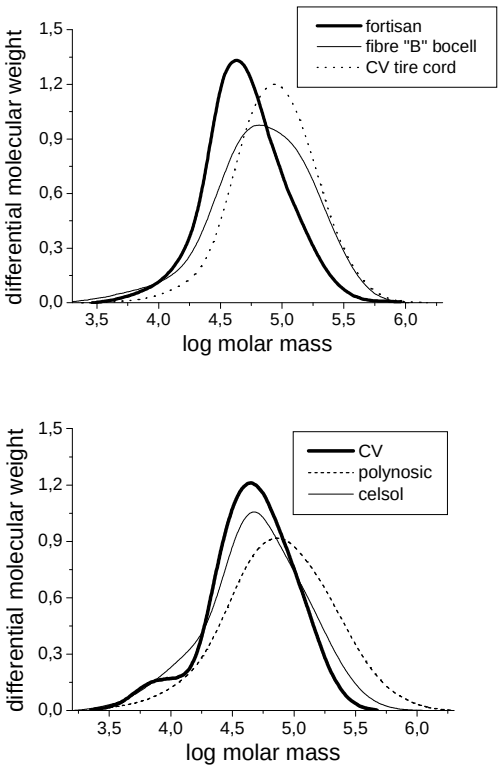


**Figure 11.** Comparison of molecular weight distribution of man-made cellulose fibres.

Lyocell fibres (Tencel® and ionic liquid fibres) have a higher molecular weight than viscose fibres. The spectrum depends on the used pulp. While the cellulose is degraded in the ripening step in the viscose process, the degradation during the lyocell process is prevented by added stabilizers. Therefore, the molecular weight of lyocell fibres is mainly determined by the used pulp. Normally, the degradation during the lyocell process should be less than 10%.

The elastic modulus (Young's modulus) is the linear slope of stress (tenacity) versus strain (elongation). It is a measure of the stiffness of a material. A higher elastic modulus means a higher resistance of the fibre against deformation. A comparison of typical stress-strain-curves is given in Figures 12 and 13. The highest value for the elastic modulus and tenacity as well was reached by fibre "B" (bocell). The lowest value was determined for viscose fibres. To get fibres in between these two values, the solvent and/or the

manufacturing process has to be chosen carefully.

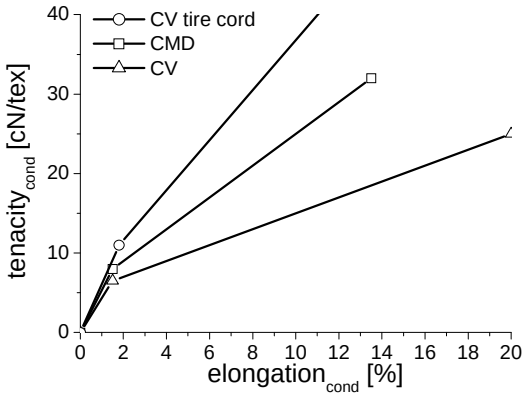


**Figure 12.** Stress-strain curve of viscose type man made fibres.

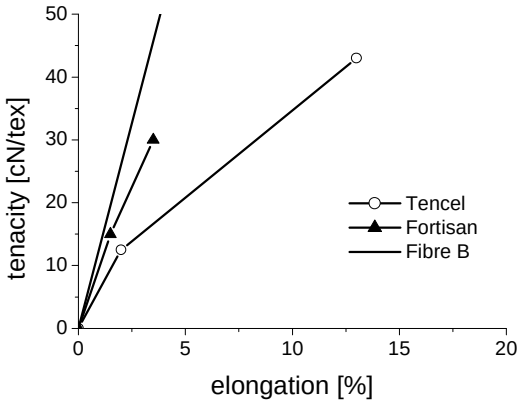


**Figure 13.** Stress-strain curve of high modulus fibres compared with Tencel®.

## Conclusions

Man-made cellulose fibres are manifold and open a fascinating field of research and application. The further development of these fibres will surely direct to some surprising properties and facts. After more than 100 years of viscose fibres, even there the development is not completed.

## Acknowledgements

The authors thank Dr. Hans-Peter Fink and Dr. Andreas Bohn (IAP Golm, Germany) for the WAXS measurements concerning crystallinity, Prof. Dr. Peter Zipper and Dr. Boril Cernev (University of Graz, Austria) for the WAXS measurements concerning orientation, and Anneliese Flachberger (Lenzing AG, Austria) for the textile measurements.
We would like to thank Prof. Dr. Henry Chancy (Grenoble, France) for the kind donation of the Fortisan fibre, Dr. Frank Dürsen (Obernburg, Germany) for the viscose tire cord fibres, Dr. Birgit Kosan (TITK Rudolstadt, Germany) for the ionic liquid fibres, and Dr. Stephen J. Eichhorn (University of Manchester, UK) for the fibre “B” (bocell).

## References

[1] P.H. Hermans and A. Weidinger. X-ray studies on the crystallinity of cellulose, *J. Polymer Sci.* 4 (1949) 135-144.
[2] T. Röder, J. Moosbauer, M. Fasching, A. Bohn, H.-P. Fink, T. Baldinger, and H. Sixta. Crystallinity determination of native cellulose -comparison of analytical methods, *Lenzinger Berichte* 86 (2006), 85-89.
[3] T. Baldinger, J. Moosbauer, and H. Sixta. Supermolecular structure of cellulosic materials by Fourier Transform Infrared Spectroscopy (FT-IR) calibrated by WAXS and $^{13}C$ NMR, Lenzing Berichte, 79 (2000) 15 - 17.
[4] H. Krässig and W. Kitchen. Factors influencing tensile properties of cellulose fibres, *J. Polymer Sci.* **51** (1961) 123-172.

Lenzinger Berichte 87 (2009) 107-117

# CELLULOSIC SHAPES FROM IONIC LIQUIDS MODIFIED BY ACTIVATED CHARCOALS AND NANOSILVER PARTICLES

**Frank Wendler, Birgit Kosan, Marcus Krieg, and Frank Meister**

Centre of Excellence for Polysaccharide Research, Thuringian Institute for Textile and Plastics Research, D-07407 Rudolstadt, Germany; Member of the European Polysaccharide Network of Excellence (EPNOE), www.epnoe.eu

Phone: (+49) 03672 379-253; Fax: (+49) 03672 379-255; E-mail: wendler@titk.de

**Functional cellulose shapes offer valuable properties for innovative application potentials in textile and medical products. Thereby excellent textile physiological properties of cellulose are allowed to be connected with novel application characteristics like bioactivity, electrical conductivity, heat storage or ability to adsorb liquids or gases. A very advantageous way to modify the properties of fibers, films or textile structures is to introduce particular additives via the Lyocell process.**

**Regard to technical applications, the incorporation of functional additives in the case of using *N*-methylmorpholine-*N*-oxide monohydrate (NMMO) as solvent, implicate massive technological difficulties and deterioration of properties of the spinning dope. Beside a couple of limiting moments, ionic liquids (ILs) offer as direct solvents an excellent chance for physical modification of cellulose shapes. In contrast to NMMO, they exhibit a significantly higher thermal stability as well as a higher chemical resistance. ILs exhibit most widely a better dissolving capability for a number of different polymers. First results of the development of adsorber materials as well as novel bioactive fibers will be discussed and fiber characteristics will be given.**

**Keywords:** *antibacterial activity; cellulose; activated charcoal; Lyocell process; ionic liquids, thermostability*

## Introduction

Direct dissolution of cellulose without derivatization applied for dry-wet/wet spinning of polymer solutions has been emerged to an efficient tool for the design of textile functional materials [1-3]. With the advancement of essential technological know-how for the manufacturing of cellulosic staple and endless fibers in a technical range (Lyocell process) in the foreground, the development tends to innovative functional fibers from the late `90s of last century. The ongoing progress yields on one side textile processible fibers with novel cross-sections and innovative dry-wet shaping techniques, e. g. blow casting and melt blowing, and on the other hand a series of completely new cellulosic functional fibers [4,5].

*N*-Methylmorpholine-*N*-oxide mono-hydrate (NMMO) – up to now the exclusively used solvent in technical scale, possesses by reason of its chemical structure a number of properties which could have a drastically impact on process

safety and efficient process conducting. By presence of oxydizable or reducible compounds and temperatures clearly above 100°C an intensified degradation of the solvent is expected, in worst cases with severe effects. These side reactions investigated already in the beginning of dry-wet spinning development [6, 7], may be triggered by a variety of impurities of the raw materials as well as typical reactants in the manner of air oxygen or free protons to be found in process environment [8]. Consequently, a serious deterioration of the economic viability of the process has to be taken into account connected with yield losses of recycled solvent and regenerated fiber with diminished features or in case of autocatalytic solvent decomposition with highly charged runaway reactions. Especially the latter gave rise to accidents not only during development but also by conducting of technical shaping plants. Moreover, in the case of modified solutions by the admixture of functional additives the start of thermal irregularities is shifted to lower temperatures. Furthermore, higher amounts of additives have to be incorporated to reach an efficient effect. Thus, reactivity and concentration of the additives enhance the complexity of reactions in cellulose/NMMO solutions [9]. Precise evaluation of additive properties such as surface topology and metal content is therefore a must for the choice of the proper materials.

In addition, it has to be mentioned that the preferably used solvent NMMO exhibits a very specific dissolution behavior most widely limited to cellulose and only a few other polysaccharides. Not least these disadvantages promoted the search for alternative direct solvents as a continuously task.

Thus, of actual importance are the activities concerning the direct dissolution of polymers in ionic liquids (ILs). In particular the 1-alkyl-3-methylimidazolium salts proved to be suitable solvents for cellulose [10, 11]. Beside efficient dissolution efficiency special features such as the workability of polymer solutions at moderate and room temperatures, negligible vapor pressures under typical processing conditions as well as comparable chemical and thermal consistency, distinguish the ILs from other polymer solvents [12-14].

The present report describes the solution behavior of cellulose in ILs in the presence of functional additives, textile properties of the shaped bodies and further examinations regard to the thermal stability of ILs.

## Experimental

*Reagents*

*N*-Methylmorpholine-*N*-oxide (NMMO) was purchased from BASF (Ludwigshafen, Germany) and used as 50 % (v/v) aqueous solution. The ionic liquids (ILs, Scheme 1) 1-ethyl-3-methylimidazolium acetate (EMIMac), mp. -45°C and 1-butyl-3-methylimidazolium chloride (BMIMCl), mp. 73°C were purchased from BASF (Ludwigshafen, Germany) and Solvent Innovation (Köln, Germany) without further purification. An eucalyptus pulp with a degree of polymerization (DP) of 569 and a bleached beech sulfite pulp characterized by the following data: α - cellulose 90.6%, (DP) 495, carboxyl groups 6.9 µmol/g, carbonyl groups 48.3 µmol/g, moisture 7.5% were used. Modification was provided with the following additives: activated charcoal, strong reactive (Grain size < 10 µm; Pica (Levallois, France); activated charcoal, medium reactive (Grain size < 10 µm; Blücher, Erkrath, Germany); nano-scaled silver particles (porous MicroSilver BG™, 80-140 nm and colloidal NanoSilver BG™, 5-20 nm).

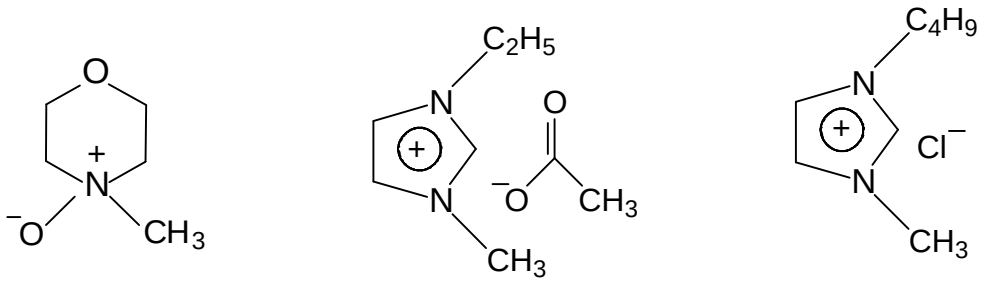

**Scheme 1.** *N*-methylmorpholine-*N*-oxide (NMMO) and ionic liquids used in this study: 1-ethyl-3-methylimidazolium acetate (EMIMac) and 1-butyl-3-methylimidazolium chloride (BMIMCl).

*Preparation of cellulose solutions*

The preparation of cellulose solutions was carried out in a special vertical kneader system, linked with a RHEOCORD 9000 (HAAKE). Temperature, torque moment and revolutions per minute (rpm) vs. reaction time were determined on-line. For the dissolution process the cellulose was disintegrated by means of an ultra-turrax shearing step in water, was separated from excessive water and was transferred in the aqueous *N*-methylmorpholine-*N*-oxide or ionic liquid. The obtained stable suspension was poured in the vertical kneader system. Afterwards the water was removed at temperatures between 90 and 130°C, a reduced pressure between 700 and 5 mbar and a shearing rate of 10 to 80 rpm. The resulting cellulose solution was analytically characterized and used for a further dry-wet shaping process. The details of the solution preparation were described in former publications [15].

*Spinning trials*

A self-made piston spinning equipment, which is consisting of a heatable cylinder, a spin package, an air-conditioned air gap, a spinning bath, a turning round godet and a take-off godet, was used for the shaping trials. The spinning dope is fed definitely to the spin package by a precise drive of the piston. Spin package contains the filter package, a heat exchanger and the spinneret. The heat exchanger permits beside a homogenization of the mass temperature also a continuous increasing of the spinning dope temperature from 80 to 120°C at short dwell periods directly before the entrance into the spinneret. The air gap arranged between spinneret and coagulation is continuously movable between 10 and 150 mm through a vertical height adjustment. It is conditioned by means of a gas flow with definite temperature and moisture. The coagulation bath passes the spinning box, circulates by means of a pump and is adjustable in the height between 10 and 150 mm. A turning round godet collects the capillary skein and transports it over a traverse to the take-off godet. Finishing is carried out discontinuously after cutting the initial wet fibres into staples of uniform length.

*Differential scanning calorimetry (DSC)*

Measurements were performed on a Mettler Toledo DSC 822e device with a heating rate of 10 K/min from room temperature up to 160°C. The value of the first visually detectable deviation from the base line corresponds to the onset temperature, which indicates the initial thermal degradation.

*Reaction calorimetry*

Thermal investigations were realized with the Systag reaction calorimeter RADEX (mini-autoclave) [16]. Approximately 2 g of the cellulose/NMMO solution were used in the steel vessel (design pressure: 100 bar) equipped with bursting disk and an internal sensor device for temperature determination. In the case of cellulose/IL

solutions 1 g was weighed in a glass container which was inserted into the steel vessel. The vessel is kept by a temperature controlled steel/aluminium jacket. Ensuring a defined thermal resistance of the airspace between jacket and vessel, the temperatures of sample and jacket are measured continuously. For dynamic measurements (screening), the vessel was heated with a heating rate of 0.75 K/min from room temperature up to 300°C followed by holding this temperature for 1 h dwell time. The onset temperature ($T_{on}$) was determined by plotting the deviation of pressure with respect to time (dp/dt) against the temperature and registering the temperature at the threshold value of 0.0002 bar/s.

*Determination of fiber properties*
For fiber characterization the fiber fineness (DIN EN ISO 1973), wet and conditioned tenacity as well as elongation at break (DIN EN ISO 5079), loop tenacity (DIN 53843, Part 2) have been measured.

*Antibacterial activity*
The permanence of the antibacterial activity before and after defined washing was carried out according to JIS Japanese Industrial Standard (JIS L 1902: 2002) with the test strains *staphylococcus aureus* ATCC 6588 and *klebsiella pneumoniae* ATCC 4352. The total antibacterial activity was estimated with the calculation *log cfu (igc)18h – log cfu (sample)18h = total antibacterial activity* where *cfu* is colony forming units and *igc* is internal growth control. Criteria of evaluation for antibacterial activity are declared by the standard method: slight 0.5 – 1; significant > 1 - < 3; strong ≥ 3.

*Nephelometry*
Nephelometric measurements were provided for the solvents *N*-methylmorpholine-*N*-oxide monohydrate and 1-ethyl-3-methylimidazolium acetate. After dilution with a CASO bouillon (0,001% - 1%) the growth of the test strain *staphylococcus aureus* was conducted with a microplate nephelometer (NEPHELOstar Galaxy, BMG, Offenburg, Germany). Measurements (%NTU: nephelometric turbidity unit) were done every hour and put into growth curves with a total incubation time of 24 h.

*Intake capacity*
A desiccator was equipped with a beaker filled with 25 mL toluene or carbon tetrachloride, respectively, for one hour to maintain an saturated atmosphere. Then a second beaker with 1 g of the fiber was exposed into the desiccator for 24 hours. The weight gain of the fiber was measured.

## Results and discussion

*Thermal properties of Ionic Liquids (ILs) and cellulose/IL solutions*

Direct dissolution of cellulose requires temperatures above 85°C to produce homogeneous solutions within economically acceptable time. Under industrial conditions cellulose solutions are expired to mechanical shearing and enhanced temperatures over longer time periods. The physical dissolution process is attended by degradation reactions due to interactions of the solvent with cellulose and impurities of by-products or heavy metals. Autocatalytic reactions can initiate exothermicities, so-called thermal runaway reactions, which may end up in deflagrations [8]. Thus, besides the demands for efficient solubilization and non-derivatization the solvents has to be stable up to temperatures quite far above the process temperature.

The beginning of an exothermicity can be detected by the onset temperature ($T_{on}$) using dynamic calorimetric measurements (DSC). Figure 1 displays the DSC curves of cellulose solutions in BMIMCl and NMMO as well as of pure NMMO. Whereas the cellulose/BMIMCl solution

shows neither an endothermic melt peak nor an exothermic degradation peak, both NMMO and the cellulose/NMMO offers the typical start of melting near 70°C and the pronounced exothermicity beginning at about 160°C. By using of DSC, BMIMCl and further 1-alkyl-3-methylimidazolium salts used as cellulose solvents do not exhibit any thermal degradations up to temperatures of 220°C and higher. However, investigations of cellulose/IL solutions showed similar to cellulose/NMMO solutions decreasing DP`s of the dissolved cellulose.

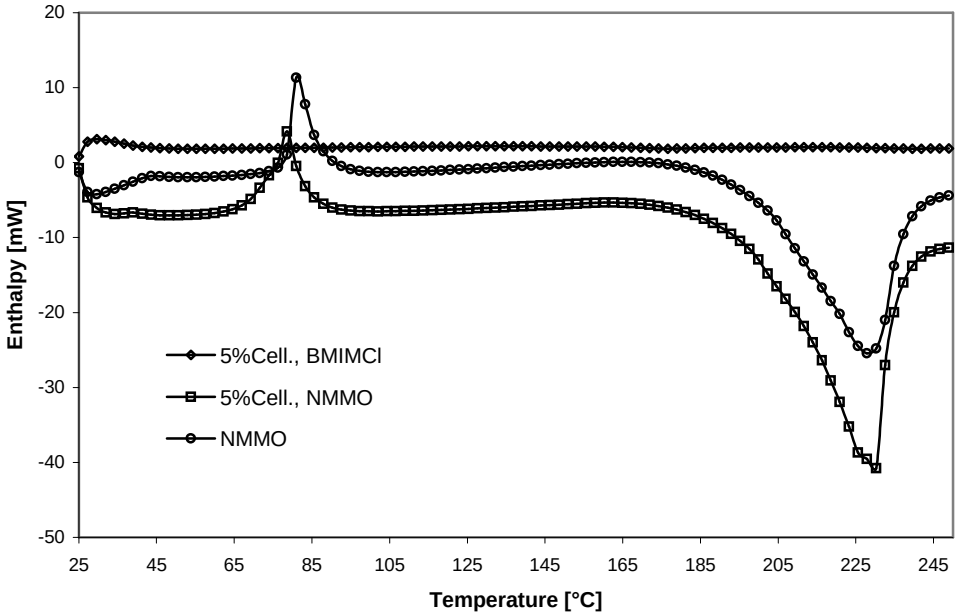


**Figure 1.** DSC measurements: Relationship between temperature and enthalpy of cellulose solutions in 1-*N*-butyl-3-methylimidazolium chloride (BMIMCl) and *N*-methylmorpholine-*N*-oxide (NMMO) as well as pure NMMO.

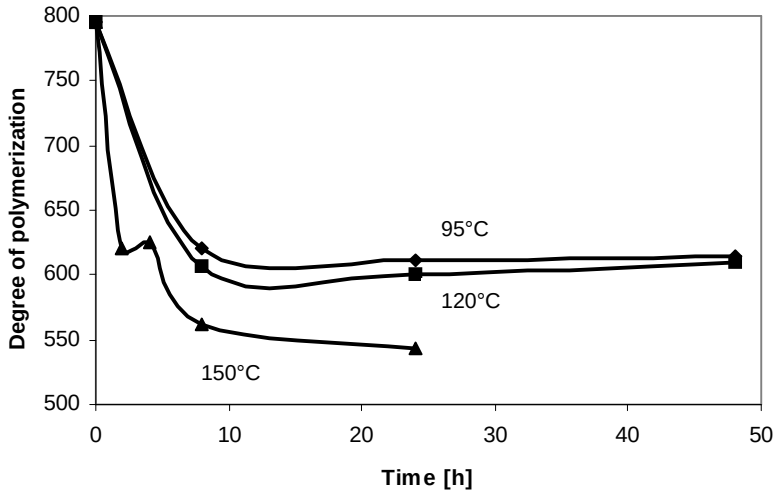


**Figure 2.** Stability of spinning dopes in EMIMac: Relationship between degree of polymerization and time for different temperatures (12 wt.-% Linters, DP795) adapted from Hermanutz et al.[18].

To quantify the stability of the cellulose/IL solutions the degree of polymerization (DP) as a function of temperature and storage time was investigated [17]. The results are displayed in Figure 2.

A slight decrease of molecular weight can be determined after spinning dope preparation which is caused by the mechanical shearing. The dopes are stable up to storage temperatures of 120°C which is above the processing temperature. When exposed to 150°C DP is decreased up to 29% after 8 h. Therefore, a stabilization of the system is necessary. Consequently, a combination of several chemical inhibitors against cellulose degradation as well as pH buffering of the anion has to be applied and is a topic of further research. Especially in the case of modified solutions by the admixture of functional additives, degradation reactions of both cellulose and solvent could be a sensitive problem.

In Table 1 $T_{on}$ for cellulose dissolved in NMMO and different ILs are summarized. Compared to NMMO the ILs tested possesses $T_{on}$ of 202°C for BMIMCl and 183°C for EMIMac. By increasing the cellulose concentration in EMIMac, a slight reduction of $T_{on}$ to 176°C was observed. This reduction can be eliminated and a value of 181°C appears after addition of the stabilizer system NaOH/propyl gallate that is commercially applied to stabilize cellulose/NMMO solutions [18, 19]. $T_{on}$ of EMIMac is minor compared to BMIMCl. Influences of type of anion were also described in the above mentioned references, however, data about acetate containing imidazolium salts are missing. By that reason and the fact that acetates are promising alternatives to chloride ILs, further studies are ongoing [20]. Even EMIMac possesses extraordinary features compared to BMIMCl, because it is non-corrosive, non-toxic and higher concentrated cellulose solutions (> 20 wt.-%) can be realized [17].

Further advantage is the efficient functionalization of cellulosic matrices in solutions of ILs by physical incorporation of additives, e.g. metallic nano-scaled particles or adsorption materials. While the low thermal stability of NMMO against catalytic degradation restricts the incorporation of this type of substances at a technical scale, in ILs it succeeded most widely without problems.

Cellulose solutions produced by this route and added with relatively high amounts of nano-scaled silver particles do not suffer from a setback of onset temperatures compared to cellulose/NMMO solutions as depicted in Table 2. A cellulose solution in BMIMCl mixed with 0.1% of silver starts at approx. 200°C to decompose whereas the cellulose/NMMO solutions shows first thermal activity at 145°C. By addition of medium or strong reactive activated charcoal only a slight decrease is to be registered compared to the pure solvent and an unmodified cellulose/IL solution.

**Table 1.** Comparison of onset temperatures ($T_{on}$) of cellulose (bleached beech sulfite pulp) solutions in NMMO and different ionic liquids. *Stabilizer: 0.04% NaOH, 0.06% propyl gallate.

| Solvent | Concentration of cellulose | Molar ratio cellulose : solvent | $T_{on}$ [°C] |
|---|---|---|---|
| NMMO | 12 | 8.8 | 146 |
| BMIMCl | 12 | 6.8 | 202 |
| EMIMac | 9 | 9.6 | 183 |
| EMIMac | 23.5 | 3.1 | 176 |
| EMIMac* | 23.5 | 3.1 | 181 |

**Table 2.** Comparison of onset temperatures ($T_{on}$) of cellulose (bleached beech sulfite pulp) solutions in NMMO and ionic liquids with different additives.

| Concentration of cellulose [%] | Ionic liquid | Additive | Concentration of additive [%] | $T_{on}$ [°C] |
|---|---|---|---|---|
| 12 | NMMO | MicroSilver | 0.1 | 145 |
| 12 | BMIMCl | MicroSilver | 0.1 | 200 |
| 12 | NMMO | Activated charcoal, strong reactive | 6 | 137 |
| 12 | BMIMCl | Activated charcoal, strong reactive | 6 | 197 |
| 18 | EMIMac | Activated charcoal, medium reactive | 9 | 177 |
| 23.5 | EMIMac | Activated charcoal, medium reactive | 11.75 | 176 |

**Table 3.** Textile-physical properties of fibers modified with nano-scaled silver particles spun from different ionic liquids. Cellulose: bleached beech sulfite pulp.

| | | Fiber 1 | Fiber 2 | Fiber 3 |
|---|---|---|---|---|
| Concentration of cellulose | % | 12 | 23.5 | 23.5 |
| Ionic liquid | | BMIMCl | EMIMac | EMIMac |
| Type of additive | | MicroSilver | MicroSilver | NanoSilver |
| Concentration of additive | % | 0.1 | 0.1 | 0.05 |
| Fineness | dtex | 1.80 | 1.62 | 1.56 |
| Tenacity, cond. | cN/tex | 42.3 | 55.9 | 50.8 |
| Elongation, cond. | % | 10.6 | 9.1 | 10.0 |
| Loop tenacity | cN/tex | 22.3 | 9.6 | 22.9 |

Noteworthy, using NMMO as solvent the $T_{on}$ is not exceeding an amount of 137°C, which is only 37°C above the operating temperature. Therefore, an effective stabilization is necessary as well as the precise evaluation of properties such as metal content is a must for choice of modifiers for the Lyocell process [21].

*Modification of cellulosic shapes in IonicLiquids*The spinning process with the application of nano-scaled silver particles proceeds up to 0.1% without any impact on textile physical parameters (Table 3) compared to unmodified fibers. A crucial issue concerning the functional effect of the fiber is the homogeneity of silver particles in the spinning solution. The addition of silver as a suspension in NMMO assures sufficient distribution in the fiber. Desired silver content is adjustable with a recovery rate of approx. 70%. What is noteworthy in the application of colloidal silver in those concentration ranges is that it results in fibers of very high whiteness [22].

Table 4 summarizes the antimicrobial activity of fibers modified with nano-scaled silver particles. Fibers with porous MicroSilver show antimicrobial effects only for higher concentrations (from 0.1%). Because of the formation of aggregates, the antimicrobial performance of nano-scaled particles is achievable only by increasing the concentration. On the other hand, fibers with colloidal NanoSilver exhibit a higher performance (from 0.05%) as reported earlier in detail [22]. Further it can be drawn from the table, using chloride containing ILs as solvent no antimicrobial effect is detectable. Even the application of acetate gives a strong antimicrobial effect for both test strains. After defined washing (40 times, 60°C) a strong effect is measured for *klebsiella pneumoniae* and a significant

one for *staphylococcus aureus* in the case of 0.1% MicroSilver.

In addition, the antibacterial activity of the solvent EMIMac solely were investigated in more detail. Although the produced fibers are washed after spinning intensively, it has to be taken into account that there are residues of solvent in the fiber, which might be responsible for slight irregularities. Consequently, the effect of EMIMac on the growth of *staphylococcus aureus* was measured by nephelometry. Compared to NMMO which did not show any antibacterial activity, the ionic liquid exhibits after 12 h at a concentration of 0.5% a clear bacteriostatic effect (Figure 3). On condition that the residue concentrations of solvent lie in the ppm – range (< 0.01%) only less influences are to be assumed. Further investigations are in progress, in particular regard to purity monitoring of the shaped fibers. However, the strong difference between NMMO and EMIMac is remarkable, which confirms the harmless effect of NMMO as well as possibly new application routes for ionic liquids.

A composition of 50% cellulose and 50% adsorption materials, e.g. activated charcoal, result in fibers, which can be processed by conventional techniques to form non-wovens with sufficient mechanical stability and uniform charcoal loading (Table 5). The charcoal particles are evenly distributed in the whole fiber. Additionally, the cellulose acts as a three-dimensional carrier that is responsible for the mechanical stability [23].

Non-wovens made there from have been investigated concerning its adsorption ability of organic compounds from the vapors as displayed in Figure 4. In general, it should be noticed that carbon tetrachloride has a higher ability to adsorption on activated charcoal than toluene. The differences between carbon tetrachloride and toluene in its adsorption behavior can be explained by specific properties of the compounds.

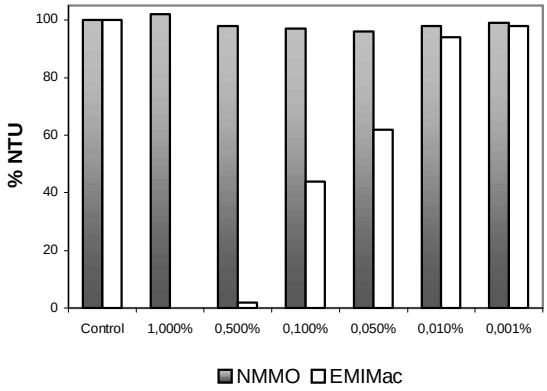


**Figure 3.** Nephelometric measurements of the effect of EMIMac compared to NMMO (Control CASO bouillon) on growth of *staphylococcus aureus* after 12 h for different concentrations.

**Table 4**. Test results of antimicrobial activity of solvents fibers modified with MicroSilver and NanoSilver spun from NMMO and ionic liquids. *after washing.

| Fiber | Type of additive | Solvent | Antimicrobial activity | |
|---|---|---|---|---|
| | | | *staphylococcus aureus* | *klebsiella pneumoniae* |
| 1 | 0.1% MicroSilver | BMIMCl | non antibacterial | non antibacterial |
| 2 | 0.1% MicroSilver | EMIMac | strong antibacterial | strong antibacterial |
| 2* | 0.1% MicroSilver | EMIMac | significant antibacterial | strong antibacterial |
| 3 | 0.05% NanoSilver | EMIMac | strong antibacterial | strong antibacterial |
| 3* | 0.05% NanoSilver | EMIMac | slight antibacterial | strong antibacterial |
| 4 | - | EMIMac | slight antibacterial | non antibacterial |
| 5 | - | NMMO | significant antibacterial | non antibacterial |
| Solvent | - | NMMO | non antibacterial | non antibacterial |
| Solvent | - | EMIMac | slight antibacterial | non antibacterial |

**Table 5.** Textile-physical properties of fibers modified with activated charcoals (50% with respect to cellulose) and spun from ionic liquids. Cellulose: bleached beech sulfite pulp.

| | | Fiber 6 | Fiber 7 | Fiber 8 |
|---|---|---|---|---|
| Concentration of cellulose | % | 12 | 18 | 18 |
| Ionic liquid | | BMIMCl | EMIMac | EMIMac |
| Activated charcoal | | strong reactive | strong reactive | medium reactive |
| Fineness | dtex | 2.18 | 3.07 | 2.86 |
| Tenacity, cond. | cN/tex | 12.9 | 12.2 | 11.7 |
| Elongation, cond. | % | 9.9 | 12.8 | 12.4 |
| Loop tenacity | cN/tex | 3.6 | 5.95 | 3.06 |

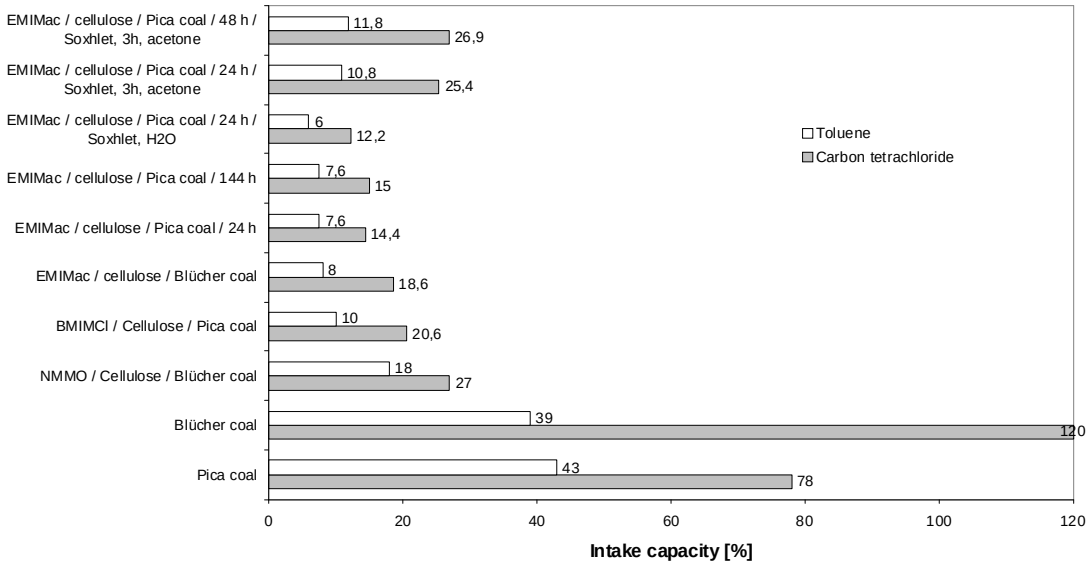


**Figure 4**. Intake capacity of different activated charcoals (1 – medium reactive, 2 – strong reactive) and fibers spun from NMMO and ionic liquids. The adsorption time is 24 h except where denoted.

An equilibrium state has been reached and stabilized after one day, however, the equilibration loading level is already reached after 8 h. The fibers have a lower affinity towards carbon tetrachloride and toluene than the pure active charcoal. Thus, a certain amount of the adsorbent must be inactive. First investigations of the produced fibers from ILs revealed that the adsorption effect do not reach the efficiency of the NMMO spun fibers. Reason might be aroused from the insufficient solvent extraction during fiber after-treatment. Even an additional reaction time in the desiccator as well as *Soxhlet* extraction using acetone brought an improvement of the intake capacity, comparable to those from NMMO.

## Conclusions

Direct dissolution of cellulose and dry-wet shaping in ionic liquids provide regenerated fibers of high tenacity with versatile applications in the textile-technical sector. Main inconveniences of the so far used solvent *N*-methylmorpholine-*N*-oxide monohydrate

(NMMO) were the incorporation of metallic nano-scaled particles and adsorber materials, thermal and chemical instability as well as high selectivity for almost exclusive dissolution of cellulose. In opposite to NMMO ionic liquids (ILs) exhibit a distinctively thermal resistance. The relative high decomposition temperatures of ILs are reflected in the onset temperatures ($T_{on}$) of cellulose/IL solutions ensuring higher process temperatures with lower risk of exothermic reactions and therefore, enhanced process safety. A slight decrease of $T_{on}$ with higher cellulose concentrations was ascertained, which can be compensated by an effective stabilization. Activated charcoal and nano-scaled materials also minimize $T_{on}$. However, this decline is low compared to modified cellulose/NMMO solutions and can be attenuated by stabilizers, too. Structure/property relations with regard to the alkyl chain length and the anion/cation as well as recycling procedures will be a matter of further research.

First efforts regard to the functional cellulose fibers containing nano-scaled silver particles and activated charcoal revealed reduced effects compared to cellulose fibers from NMMO. However, regard to the charcoal fiber further optimisation of the cleaning procedure resulted in an adsorption capacity that reach the efficiency of fibers produced from NMMO. Here and on the development of simply technological capabilities towards recycling of ILs the focal points of actual research activities are to be laid.

## Acknowledgements

Financial support by the Deutsche Bundesstiftung Umwelt (DBU) under registration no. 24762-31 is gratefully acknowledged. The assistance of Dr. U.-C. Hipler, Friedrich Schiller University Hospital Jena, Department of Dermatology and Dermatological Allergology, with the examination of the antibacterial activity is highly appreciated.

## References

[1] H. Chanzy, S. Nawrot, A. Peguy, P. Smith and J. Chevalier, J. Polym. Sci. 20 (1982) 1909-1924.

[2] C. Michels, R. Maron and E. Taeger, Lenz. Ber. 9 (1994) 57-60.

[3] K. Bredereck and F. Hermanutz, Rev. Prog. Color. 35 (2005) 59-74.

[4] P. White, in Regenerated Cellulose fibres, (Woodings, C., Ed.) Woodhard Publishing, Cambridge, 2000, p. 62 ff.

[5] F. Meister, D. Vorbach, F. Niemz, T. Schulze and E. Taeger, Mat.-wiss. u. Werkstofftech. 34 (2003) 262-266.

[6] E. Taeger, H. Franz, H. Mertel, H. Schleicher, H. Lang and B. Lukanoff, Formeln, Faserstoffe, Fertigwaren 4 (1985) 14-22.

[7] F. A. Buijtenhuijs, M. Abbas and A. J. Witteveen, Papier 40 (1986) 615-619.

[8] T. Rosenau, A. Potthast, H. Sixta and P. Kosma, Prog. Polym. Sci. 26 (2001) 1763-1837.

[9] F. Wendler, A. Konkin and T. Heinze, Macromol. Symp. 2008, 262, 72-84.

[10] R. P. Swatloski, R. D. Rogers and J. D. Holbrey, PCT Patent 2003, WO 03/029329.

[11] T. Liebert and T. Heinze, Bioressources 3 (2008) 576-601.

[12] S. Zhu, Y. Wu, Q. Chen, Z. Yu, C. Wang, S. Jin, Y. Ding and G. Wu, Green Chem. 8 (2005) 325-327.

[13] H. Weingärtner, Angew. Chem. 120 (2008) 664-682.

[14] P. Wasserscheid and T. Welton, Ionic Liquids in Synthesis. 2nd edition, WILEY-VCH, Weinheim, 2008.

[15] C. Michels and B. Kosan, Lenz. Ber. 84 (2005) 62-70.

[16] F. Wendler, G. Graneß and T. Heinze, Cellulose 12 (2005) 411-422.
[17] F. Hermanutz, F. Gähr, E. Uerdingen, F. Meister and B. Kosan, Macromol. Symp. 262 (2008) 23-27.
[18] W. Kalt, J. Männer and H. Firgo, Patent 1993, EP 0670917.
[19] T. Rosenau, A. Potthast, I. A. Hofinger, H. Sixta, H. Firgo and P. Kosma, Cellulose 9 (2002) 283-291.
[20] S. Dorn, F. Wendler, F. Meister and T. Heinze, Macromol. Mat. Eng. 293 (2008) 907-913.
[21] F. Wendler, F.G. Lepri, D.L.G. Borges, R.G.O. Araujo, B. Welz and F. Meister, J. Appl. Polym. Sci., submitted.
[22] F. Wendler, F. Meister, R. Montigny and M. Wagener, Fibres & Textiles in Eastern Europe 64-65 (2007) 41-45.
[23] R. Büttner and A. Kolbe, Technische Textilien 46 (2003) 270-272.

Lenzinger Berichte 87 (2009) 118-124

# IDENTIFICATION OF PLANT COMPOUNDS IN LENZING FIBERS

**Heidrun Fuchs[1], Christian Hager[1], Heinrich Firgo[1], Aline Lamien-Meda[2], Karin Zitterl[2], and Chlodwig Franz[2]**

[1]Lenzing AG, Business Development & Innovation Textile Fibers A-4860 Lenzing, Austria
[2]Institut für Angewandte Botanik und Pharmakognosie, Veterinärmedizinische Universität Wien, Veterinärplatz 1,
A-1210 Wien, Austria

*Presented at the 4th INTERNATIONAL TEXTILE, CLOTHING & DESIGN CONFERENCE – Magic World of Textiles, October 05th to 08th 2008, DUBROVNIK, CROATIA*

**Due to their natural provenance it was assumed that Lenzing's man-made cellulose fibers might still contain secondary constituents from their plant origin with some biological potential.**
**TENCEL® and Lenzing Modal® fibers as well as the basic eucalyptus and beech wood pulps were extracted in ethanol, methanol-HCl, dichloro-methane and supercritical $CO_2$. Extracts underwent GC-MS, GC-FID and HPLC analysis. Extracts were further assessed for total phenolics and antioxidant activity by the Folin and the DPPH assay.**
**Both pulps and fibers still contain phytophenols as well as substantial amounts of squalene and phytosterols from the original plant source. All exctracts showed anti-oxidant activity.**
**The finding that valuable constituents from the original plant are carried through all over the pulping as well as fiber formation steps suggests that Lenzing's processes are not that detrimental to wood material. This supports the view that man-made cellulose fibers can be regarded as natural 'botanic' fibers.**

***Keywords:*** *TENCEL®, Lenzing Modal®, extraction, antioxidant activity, phenols, squalene*

## Introduction

Consumers have been used to regard Lenzing's man-made cellulosic fibers viscose, Lenzing Modal® as well as the solvent spun cellulosic fiber TENCEL® (generic name Lyocell) as being 'synthetic' or 'chemical' fibers since, contrary to cotton or linen, they are not directly 'harvested' or extracted from the plant source but are produced from dissolving pulp by precipitation from a physical or regeneration from a chemical solution.
In fact, Lenzing's man-made cellulosic fibers are 'botanic' fibers, since they are derived from sustainably grown plant material, the sources being beech wood for Lenzing Modal® and eucalyptus wood for TENCEL®. The fibers are produced in closed cycles and it has been shown in extensive studies [1] that the impact on the environment is much lower than for standard cotton production. To give further evidence of the natural provenance of Lenzing fibers, this work was aimed to study what had been anticipated from their wood provenance: that fibers still contain, beside cellulose, secondary constituents from their plant origin with biological potential which survive the pulping and fiber formation process.
So, the aim of this study was to investigate a) if secondary plant products are still detectable in Lenzing fibers and the respective originating pulps b) to determine the classes of compounds they belong to and identify the main substances

c) to determine potential biological functionality such as antioxidant activity.
The works of Huber [2], Cruz et al [3] and Zule&Moze [4] were taken as a basis to choose an appropriate methodology. They reported the extraction and identification of a variety of phenolic compounds, saturated and unsaturated fatty acids and phytosterols in the wood of *Eucalyptus urophylla*, *Eucalyptus globulus* and *Fagus sylvatica* respectively.
In order to get a full picture of extractable compounds, different lots of TENCEL® and Lenzing Modal® fibers, all without spin finish, as well as samples from the originating beechwood and eucalyptus pulps were extracted in the solvents ethanol, dichloromethane as well as methanol-HCl 1:1 mixture. The latter solvent system is appropriate to hydrolyse glycosidic bonds. Finally, extraction of TENCEL® and eucalyptus pulp was performed also using supercritical $CO_2$. Accelerated solvent extraction was compared to soxleth extraction. To study the influence of fiber preparation, especially the conditions of fiber drying on the extraction yield, TENCEL® fibers from one lot were extracted after freeze drying, air drying, drying in a lab dryer at 60°C as well as in a never dried state. All extracts underwent GC/-MS, GC/-FID and HPLC analysis for identification and quantification of compounds. Extracts were further assessed for total phenolics by the Folin assay and for antioxidant activity by DPPH assay.

## Materials and Methods

### Samples

*Pulp:* 6 bleached Eucalyptus pulp samples produced in craft and sulphite pulping processes which are the basic material for the production of TENCEL® and 4 different lots of beech wood pulp samples from the Lenzing Mg-sulphite pulping process which are the basis of Lenzing Modal® were obtained from Lenzing AG. Pulp samples were either milled (eucalyptus pulp) or cut with a paper cutter to obtain a small particle size for extraction.

*Fibers:* Different lots of TENCEL® and Lenzing Modal® were taken prior to spin finish from the Lenzing production process. If not otherwise stated, fibers were either freeze-dried or air-dried.

### Extraction Methods

*Dichloromethane (DCM) Extracts*
10 g of sample were extracted using 170 mL of solvent. The extraction was performed using a cooled ultrasonic, for 1 hour, and filtrated with filter paper. The extract was concentrated at the rotavapor at 40°C. The dried extract was dissolved in 1.5 mL of Methanol HPLC (in the ultrasonic) and used for the different analysis.
For the squalene quantification, the dried extract was dissolved in 1.5 mL of dichloromethane.
Blank extracts without sample (only 170 mL of solvent) were done following the same process, to make the solvent correction from the results.

*Ethanol (EtOH) Extracts*
10 g of sample were extracted with 170 mL of solvent (ethanol absolute) at 80 ºC, during 6 hours under reflux. The extract was filtrated and concentrated to dryness using a rotavapor at 40°C. The dried extract was dissolved in 1.5 mL of Methanol HPLC (in the ultrasonic) and used for the different analysis.
A blank extract without sample (only 170 mL of solvent) was done following the same process, to make the solvent correction from the results.

*Methanol-HCl 2N (1:1) Extracts*
10 g of sample were extracted with 170 mL of solvent (80 ºC, 90 min hydrolysation). The extract was filtrated and concentrated at the rotavapor at 40°C to remove the methanol. The water-HCl phase was neutralized with 10g of $CaCO_3$,

and a liquid extraction with ethyl acetate (3 x 30 ml) was done to take the phenolic compounds. After that, the ethyl acetate phase was concentrated at 40°C, and the dried extract was dissolved in 1.5 mL of Methanol HPLC (in the ultrasonic) and used for the different analyses.
A blank extract without sample (only 170 mL of solvent) was done following the same extract process, to make the solvent correction in the results.

*Accelerated Solvent Extraction in Ethanol / Dichloromethane*
8 g of sample was extracted with 35 mL solvent (dichloromethane or ethanol absolute) for 1 hour under the following conditions:
dichloromethane: 100°C; 1500 psi; ethanol: 140°C; 2200 psi
The solvent was evacuated to dryness using a rotavapor at 40°C. The dried extract was dissolved in 1.5 mL of methanol.

*Supercritical Fluid Extraction with $CO_2$*
1 kg of air-dried sample was extracted at 450 bar 65°C over 2.5 hours and a flow rate of 25kg/h $CO_2$ in a small scale $CO_2$ extractor at Natex Prozesstechnologie, Ternitz, Austria. Ca. 50 g aqueous extract was collected from the 1st separator which was kept at 50 bar 40°C. Non water-soluble extract material was dissolved in 30 mL 99% ethanol.

**Analytical Methods**
*GC Analysis of Extracts*
Extract analysis was performed a) via GC-MS after the silylation method according to Cruz et al.[3].
Methanol extracts were evaporated to dryness + 40 µL THF + 200 µL BSA + 10 µL TMCS (60°C for 20 min).

*GC-MS Method*
Gas Chromatography HP 6890 series equipped with a MSD detector and a DB-5MS capillary column (30 m x 0.25 mm; 0.25 µm film thickness) was used. Helium was the carrier gas (42cm/s) and the oven program was as follows (Fukushima & Hatfield, 2001): initial temperature 160°C (held for 5 min), ramp at 4°C/min to 200°C, ramp at 10°C to 200°C (held for 5 min), followed by a ramp of 15°C to 300°C (held for 5 min). The injection volume was 1µL, and syringic acid, vanillic acid, palmitic acid, linoleic acid, oleic acid, and stearic acid were used as standards.

*GC-FID Method*
column: Phenomenex Zebron ZB-5HT Inferno, 15 m length, 0.25mm I.D., 0.10 film thickness (µm)
Oven: 60°C; 12°C/min 340°C; 5 min
Inj: split/splitless 340°C, split flow 15 mL, Injection 1 µL
Pressure: 70 kPa constant flow; 40°C
Det: FID 350°C

*HPLC Analysis of Extracts*
Waters Instruments: PDA996 detector; a 626 pump; 717 plus autosampler; Symmetry C18 column (5.0µm, 4.6 x 150 mm) with a column oven operating at 25°C. Gradient elution was carried out at a flow rate of 1.5 mL/min using 1% acetic acid : acetonitril 85:15 (solvent A) and methanol (solvent B). The following gradient was used: 0 min (90% A : 10% B), 0 – 30 min (0% A : 100% B), 30 – 40 min (0% A : 100% B); detection was done at 250 nm.

*Analysis of Total Phenolics with Folin-Ciocalteu Assay*
The colorimetric method with Folin Ciocalteu reagent (FCR) was used.
Reaction: 40 µL of extract + 2 mL $H_2O$ + 100 µl FCR (2N); After 3 min, + 200 µL $Na_2CO_3$ (35 g in 100 mL $H_2O$) + 2660 µL $H_2O$. The absorbance was read after 1 hour at 725 nm against a blank prepared with 40 µL $H_2O$. Caffeic acid (0 – 40 µg) was used as standard for calibration curve. The results were expressed in µg CAE/g of sample.

*DPPH Assay for Antioxidant Activity*
DPPH (1,1-diphenyl-2-picrylhydrazyl) reagent (0.015% in methanol) was used.
Reaction: 10 µl of extract + 90 µL $H_2O$ + 100 µl DPPH solution (0.015%). After incubation at room temperature in the dark for 30 min, the absorbance of the reaction mixture was measured at 490 nm using a plate reader. A blank consisting of high concentration of trolox (31.3 µg) was used to correct all readings. Trolox (0 – 5.06 µg) was used as standard for the calibration curve. The results were expressed as µg TE/g of sample.

## Results

*Selection of appropriate solvent*
Overall, 4 types of phytochemicals could be detected in the extracts: phenolic substances, aliphatic acids, sugars and phytosterols. For the extraction of bigger non-polar substances dichloromethane turned out to be the more appropriate solvent, giving slightly higher yields with steroids and steroid ketones than the ethanol extracts. Ethanol turned out to be more suitable for the phenolic compounds extraction. The results with methanol:HCl however did not differ much from the results obtained with ethanol, suggesting that most of the compounds in question don't require liberation by hydrolysis of glycosidic bonds. Supercritical fluid extraction with $CO_2$ gave a similar pattern of components as ASE-extraction, yet lower yields

*Influence of Sample Preparation / Drying*
To remove water gently from the cellulosic matrix, the standard sample preparation was freeze drying. However to evaluate the influence of drying conditions, two trials were performed where TENCEL® fibers were freeze dried, air dried, dried in a lab oven at 60°C respectively used in the never dried state. The latter underwent a 2-fold solvent exchange with ethanol prior to dichloromethane extraction.

It could be shown that freeze-dried and never-dried samples yielded highest and oven-dried samples lowest concentrations of steroids and total phenols in ethanol extracts.

*Results from GC-FID Analysis of Extracts*
One of the main compounds with reported anti-oxidant activity detected in pulp as well as fiber extracts (dichloromethane, but also ethanol extracts) is the tri-terpenic hydrocarbon squalene wich was quantified by GC-FID with the respective reference substance. Other phytosterols detected are beta-sitosterol, stigmastanol and steroid ketons such as sigmast-4-en-3-one. The beech pulp has lower squalene concentrations, whereas the concentration of the other steroids was found to be higher than in eucalyptus pulp. Modal and viscose fibers show significantly lower phytosterol contents than TENCEL®. On an average, the squalene content was slightly higher in fiber extracts as compared to the originating pulps which might be a question of accessibility to the solvent.

*Results from GC-MS analysis of ethanolic extracts*
In the non-silylated extracts of TENCEL® fiber 2,4-di-tert-butyl phenol, a compound identified in *Eucalyptus urophylla* wood by Huber [2] could be detected. 2,4 dit-tert-butyl phenol is also a well known antioxidant.

Ethanolic extracts from eucalyptus and beech pulp samples as well as a TENCEL® fiber sample were analysed via GC-MS after silylation. Around 40 different compounds, predominantly fatty acids, phenolic compounds, sugars but also steroid derivatives have been identified, see Table 2.

**Table 1**. squalene and phytosterols beta-sitosterol and stigmastanol in Lenzing pulp and fiber extracts.

| sample | solvent | squalene mg/kg fiber | beta- sitosterol mg/kg fiber | stigmastanol mg/kg fiber |
|---|---|---|---|---|
| Eucalyptus sulphite pulp | EtOH / DCM | 18 | n.d. | n.d. |
| Eucalyptus sulphite pulp | DCM | 10 | 1 | 1 |
| Eucalyptus craft pulp | DCM | 22 | n.d. | n.d. |
| Beech pulp Lenzing lot 1 | DCM | 3 | 7 | 4 |
| Beech pulp Lenzing lot 2 | DCM | 3 | 8 | 6 |
| Beech pulp Lenzing lot 3 | DCM | 21 | 17 | 10 |
| Beech pulp Lenzing lot 4 | DCM | 9 | 3 | 4 |
| Beech pulp Lenzing lot 5 | DCM | 11 | 3 | 4 |
| TENCEL® (eucalyptus) lot 1 | EtOH / DCM | 40 | n.d. | n.d. |
| TENCEL® (eucalyptus) lot 2 | DCM | 27 | 10 | 13 |
| Lenzing Modal ® (beech) | DCM | 6 | < 1 | <1 |
| Viscose eucalypt. based | DCM | 7 | < 1 | < 1 |

n.d. not detected

**Table 2.** qualitative results from GC-MS analysis of Ethanol extract of Eucalyptus derived TENCEL® fiber (T®), eucalyptus sulphite pulp (ESP) eucalyptus craft pulp (EKP) and Lenzing beech pulp (LBP).

| RT | Compounds | ESP | T® | EKP | LBP |
|---|---|---|---|---|---|
| **4.257** | 2-Deoxy-pentofuranose | - | + | - | - |
| **4.498** | Gluconic acid-derived | - | + | - | - |
| **4.568** | n-Hexadecanol | + | + | - | - |
| **4.675** | Butanoic acid derived | - | + | - | - |
| **5.063** | Heptanedioic acid | - | - | - | + |
| **5.214** | Octadecatrienoic acid derived | + | + | - | - |
| **5.381** | Arabinose | - | - | - | - |
| **5.816** | Tartaric acid | - | - | - | - |
| **6.043** | Arabinose derived | - | - | - | - |
| **6.709** | Octanedioic acid | + | - | - | + |
| **7.335** | D-Xylose | + | - | + | + |
| **8.254** | Vanillic acid | + | - | + | + |
| **8.648** | 1-Heptadecanol | - | + | - | - |
| **8.935** | Azelaic acid | - | - | - | + |
| **9.086** | Malic acid | + | - | - | - |
| **10.006** | Tetradecanoic acid | + | + | + | + |
| **10.213** | Acrylic acid | - | - | - | + |
| **11.443** | Syringic acid | - | - | - | + |
| **12.326** | n-Pentanoic acid | - | - | + | + |
| **12.329** | n-Pentadecanoic acid | + | + | + | - |
| **14.635** | Palmitic acid | + | + | + | + |
| **16.592** | Heptadecanoic acid | + | - | + | + |
| **16.653** | Undecanoic acid | + | + | - | - |
| **16.794** | 1-oxyoctadecane | - | - | + | + |
| **16.799** | Octadecane | - | + | - | - |
| **17.302** | Octadecatrienoic acid derivative | + | - | - | - |
| **17.604** | Linoleic acid | + | + | + | + |
| **17.677** | trans-9-Octadecenoic acid | + | - | - | - |
| **17.680** | Oleic acid | - | + | + | - |
| **17.791** | 9-octadecenoate | - | - | - | + |
| **18.063** | Stearic acid | + | + | + | + |
| **24.107** | Palmitic acid | + | + | + | + |
| **25.659** | derivative aliphatic acid | - | + | + | + |
| **26.293** | derivative aliphatic acid | - | + | + | + |
| **26.727** | Stearic acid derived | + | + | + | + |
| **30.200** | cholesterol derivative | - | + | + | + |
| **31.125** | Cholesterol | + | + | - | + |
| **31.243** | 3-[oxy]cholestane | + | + | + | + |
| **31.333** | Cholestane, 2,3-epoxy | + | - | + | + |
| **31.841** | Cholesta-3,5-dien-7-one | + | + | + | + |
| | second main compound | | | | |
| | first main compound | | | | |

**Table 3.** HPLC quantitative results of the Eucalyptus pulps (ESP 1-5, EKP) and Lenzing Beech pulps (LBP1-4) extracts.

| **Sample** | **Vanillin (µg/10g)** | | | **Vanillic acid (µg/10g)** | | | **Syringic acid (µg/10g)** | | | **Cinnamic acid (µg/10g)** | | |
|---|---|---|---|---|---|---|---|---|---|---|---|---|
| *solvent* | *DCM* | *ETOH* | *MeOH/ HCl* | *DCM* | *ETOH* | *MeOH/ HCl* | *DCM* | *ETOH* | *MeOH/ HCl* | *DCM* | *ETOH* | *MeOH/ HCl* |
| ESP1 | 0 | 0 | 0 | 0 | 1,4 | 0 | 0 | 0,5 | 2,7 | 0 | 0 | 0 |
| ESP2 | 0 | 0 | 0 | 0 | 1,1 | 0 | 0 | 0,5 | 1,9 | 0 | 0 | 0 |
| ESP3 | 0 | 0 | 0 | 0 | 1,9 | 0 | 0 | 0,5 | 8,0 | 0 | 0 | 0 |
| ESP4 | 0 | 0 | 0 | 0 | 2,4 | 0 | 0 | 0,4 | 8,6 | 0 | 0 | 0 |
| ESP5 | 0 | 0 | 0 | 0 | 4,1 | 0 | 0 | 1,2 | 14,2 | 1,1 | 0 | 0 |
| EKP | 0,1 | 0,9 | 4,0 | 0 | 56,0 | 2,2 | 4,31 | 0,9 | 8,0 | 0,8 | 0 | 0 |
| LBP1 | 0 | 0 | 0,5 | 0 | 0,4 | 1,0 | 0 | 0,2 | 41,3 | 0 | 0 | 0 |
| LBP2 | 0 | 0 | 0,9 | 0 | 0,3 | 1,9 | 0 | 0,2 | 24,3 | 0 | 0 | 0 |
| LBP3 | 0 | 0 | 0,6 | 0 | 2,2 | 0,8 | 0 | 0,2 | 28,7 | 0 | 0 | 0 |
| LBP4 | 0,1 | 0,6 | 1,5 | 0,3 | 5,2 | 3,8 | 0 | 1,2 | 10,6 | 0,3 | 0 | 0 |

**Table 4**. HPLC quantitative results of two lots of TENCEL® fibers (T®) as well as Lenzing Modal® fibers (LM®).

| **Samples** | **Vanillin (µg/10g)** | | | **Vanillic acid (µg/10g)** | | | **Syringic acid (µg/10g)** | | | **Cinnamic acid (µg/10g)** | | |
|---|---|---|---|---|---|---|---|---|---|---|---|---|
| *solvent* | *DCM* | *ETOH* | *MeOH/ HCl* | *DCM* | *ETOH* | *MeOH/ HCl* | *DCM* | *ETOH* | *MeOH/ HCl* | *DCM* | *ETOH* | *MeOH/ HCl* |
| T® 1 | 0 | 0,1 | 0,2 | 0 | 0 | 1,3 | 0 | 1,6 | 52,7 | 0,8 | 0 | 0 |
| T® 2 | 0 | 0 | 0 | 0 | 0 | 1,7 | 0 | 0 | 43,3 | 0 | 0 | 0 |
| LM® | 0 | 0 | 0 | 0 | 0 | 2,3 | 0 | 0 | 25,0 | 0 | 0 | 0 |

*Analysis of Phenolic Compounds by HPLC*
DCM, ethanol as well as methanol/HCl extracts were taken for analysis via HPLC. Vanillin, vanillic acid, cinnamic acid, and syringig acid, all having antioxidant activity, were detected in different amounts in all pulp samples from eucalyptus as well as beech, and in TENCEL® fibers.
In Lenzing Modal® vanillic and syringic acid were identified.

**Table 5.** Total phenolic substances as caffeic acid equivalents (CAE) and antioxidant activity of ethanol extracts from pulps and Lenzing Fibers.

| **sample** | **Total phenolic substances mg CAE/kg dry fiber** | **Antioxidant activity mg TE/kg dry fiber** |
|---|---|---|
| Eucalyptus pulp | 15 - 20 | 8 - 10 |
| Beech pulp | 8 - 15 | 3 - 5 |
| TENCEL ® (Eucalypt.) | 5 - 10 | 2 - 8 |
| Lenzing Modal ® | 10 | 6 |

*Total Phenolics and Antioxidant Activity*
Total phenolics and antioxidant activity of pulp and fiber samples were determined in dichloromethane, ethanol as well as methanol/HCl-extracts. Since extraction yields were highest in the alcoholic extracts, only respective results are listed in the table below. The data demonstrate that even after the fiber formation process both man-made cellulose fiber types TENCEL® as well as Lenzing Modal® still retain some phenolic substances as well as antioxidant activity.

## Conclusions

The present study demonstrates that dissolving pulps which are the raw material for man-made cellulose fiber production, but also the cellulose fibers Lenzing Modal® and TENCEL® themselves still contain secondary plant compounds from the originating wood source.
HPLC analysis revealed the presence of vanillin, vanillic and syringic acid in both types of pulps, and in TENCEL® fibers from eucalyptus wood the component 2,4 di-tert-butyl-phenol could be identified. Total phenolic substances (Folin-Ciocalteau assay) gave up to 20 mg/kg in pulps and around 10 mg/kg caffeic acid equivalents in both Lenzing Modal® and TENCEL® fibers.
By GC-MS a series of phytosterols were found in both pulp types with individually different patterns depending on wood

source. In all cases the main compound was beta-sitosterol, substantial amounts of which were detected in TENCEL® fibers and some also in Lenzing Modal® fibres. Pulps and Lenzing Modal® as well as TENCEL® fibers contain significant amounts of the isoprenoid squalene, a substance with reported antioxidant and radical scavenging activity. Antioxidant activity was proved in all types of extracts by the DPPH assay.

The results suggest that there should be a principle possibility – which of course would require further detailed investigation - to identify the pulp resp. wood source the fiber is made from by a fingerprint of secondary plant constituents. In any case, the results give evidence that pulp as well as fiber production to generate Lenzing Modal® and especially TENCEL® fibers are not such severe destructive processes, preserving beside cellulose other valuable constituents from the plant origin within the fiber.

These findings may support the view that man-made cellulose fibers, spuriously perceived as being synthetic, are rather to be classified as 'botanic' fibers derived from natural plant material.

## References

[1] Shen, L.; Patel, M.: Life Cycle Assessment of Man-Made Cellulose Fibres: Tencel and Modal, *Lecture at the Lenzing Botanic Symposium* Paris, 21th Feb 2008, Universtiy Utrecht (NL)

[2] Huber, S.: Charakterisierung der Extraktstoffe von *Eucalyptus urophylla*, *Doctoral thesis* (2004), Johannes Kepler Univ. Linz

[3] Cruz, J.M.; Dominguez, H.; Parajo, J.C.: Anti-oxidant activity of isolates from acid hydrolysates of *Eucalyptus globulus* wood, *Food Chemistry* **90** (2005) , pp. 503 – 511

[4] Zule, J.; Moze, A.: GC analysis of extractive compounds in beech wood. *Journal of Separation Science* **26** (2003) pp.1292 - 1294.

Lenzinger Berichte 87 (2009) 125-135

# DISTRIBUTION OF WATER IN FILLING FIBRES VISUALISED BY NEUTRON RADIOGRAPHY

Ksenija Varga[1*], Fareeha Hameed[2], Michael Zawisky[2], and K. Christian Schuster[3]

[1]Christian–Doppler–Laboratory for Chemistry of Cellulosic Fibres & Textiles, Leopold–Franzens University Innsbruck; Present Address: Lenzing AG, Business Development & Innovation Textiles, Fiber Science Group, A–4860 Lenzing; Tel. +43 7672 701 2757; Fax. +43 7672 918 2757; E–Mail: k.varga@lenzing.com
[2]Atomic Institute of Austrian Universities, Vienna University of Technology
[3]Lenzing AG, Business Developement & Innovation Textiles, Process Technology Group

**Neutron imaging (neutron radiography) provides a method to visualise the moisture distribution in textiles, due to sensitivity of neutrons for hydrogen. The method was used to investigate the moisture distribution in filling fibres under practically relevant conditions in duvet. Real time neutron radiography made it possible to follow the dynamics of the moisture transport without disturbing the ensemble during measurement. The distribution of water was rather even over the lyocell fleece, with somewhat higher moisture content on a bottom side (simulating skin face). In polyester filling, water was localised in two distinct zones, near the "skin face" of the duvet model, and near the upper surface exposed to the environment. Comparing the mass increase of fleeces with known moisture sorption data, it was concluded that in lyocell fillings, most of the water was absorbed by the fibres, whereas in polyester filings, condensation on fibre surface took place.**

**Keywords:** *lyocell, sorption, neutron radiography, imaging, non–destructive testing, visualisation*

## Introduction

Comfort during sleep is influenced by fibre breathability, that is, the transport of heat and moisture through duvets and bedding textiles (Bartels and Umbach, 2003; Libert et al., 1988). Breathability can be measured by the sweating guarded hot plate instrument (Umbach 1987; ISO 11092). In addition, the ability of textile materials to absorb moisture plays an important role, as this influences heat buffering capacity of textiles (Schuster et al., 2006). Thermoregulation is connected to heat capacity and heat of sorption of moist textiles (Varga et al., 2007).

Measurements with test persons of the climate in bed by Helbig (2006) showed favourable conditions when cellulosic filling fibres were used, as compared to synthetic fibres. An assessment of the effects of bedding materials on sleep comfort by a combined physiological and psychological approach showed improved sleep quality with cellulosic fibres (Moser et al., 2007). Based on Helbig's (2006) temperature and moisture data, the gradient of heat and moisture in duvet was calculated (Suchomel et al., 2008), and the occurrence of a dew point within a duvet was identified in the polyester fillings.

An important point in the context of moisture transport is the water distribution. On the microscopic level, the question arises whether water is present in free water films or droplets on the fibre surface, or absorbed in the fibre structure. Cellulosic fibres absorb water into their structure, whereas on synthetic fibres, water films or droplets are formed on the fibre surfaces. This can be visualised on the level of individual fibres (Schuster et

al., 2006) and of yarns (Varga, 2009) by environmental scanning electron microscopy. The distribution of water on a larger scale, e.g. over the cross–section of a duvet, is more difficult to assess by non-destructive methods.

Neutron radiography (NR) provides an efficient tool for investigation into non–destructive testing as well as for many applications in fundamental research. Neutrons, due to their specific properties, offer a unique probe for materials research and characterisation (Zawisky et al., 2008). When a neutron beam passes through a material, the neutrons will interact with the nuclei of the material (Pel et al., 1993). A neutron beam penetrating the specimen is attenuated by the sample according to the basic law of radiation attenuation. Neutrons are attenuated by some light materials, e.g. hydrogen, boron and lithium, but also penetrate many heavy materials. The attenuation of the neutron beam is determined by the cross–section for scattering and absorption of the nuclei present in the sample. Because of the relatively large scattering cross–section of hydrogen, this method is very sensitive for water. The moisture content can be determined by measuring the transmission $I$ through a sample of a given thickness $d$ (Pel et al., 1993).

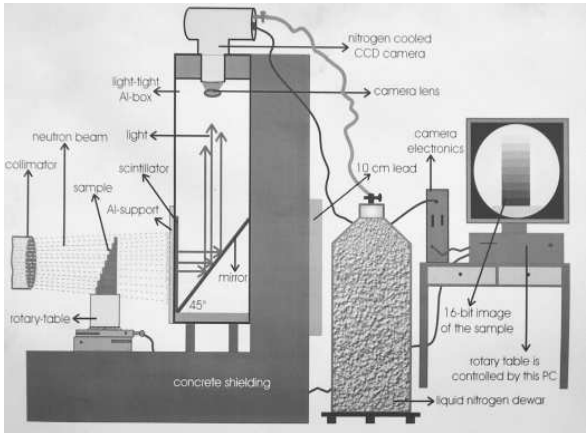


**Figure 1.** NR assembly at Atomic Institute in Vienna.

At the Atomic Institute Vienna, with a 250 kW TRIGA MARK II reactor, neutron imaging has a long tradition (Zawisky et al., 2008). This low–power reactor possesses a collimated thermal beam with neutron flux of 1.3 x $10^5$ n $cm^{-2}s^{-1}$. The basic experimental layout of NR consists of a neutron source, a collimator functioning as a beam formatting assembly, a detector and the sample, which is placed between the exit of the collimator and the detector (Figure 1).

For the experiments in this work, two types of detector were used: *scintillator* (with camera) and *neutron imaging plate systems (NIP)*. Scintillator / camera system – this type of detector has a neutron-sensitive scintillator screen (which converts the neutrons to photons) and a camera (which can take a picture of the light emitted by the scintillator). Typical scintillator materials are ZnS(Ag)–$^6$LiF or ZnS(Cu)–$^6$LiF. $^6$Li is a good choice as neutron absorber because it offers the best gamma discrimination ($\gamma$-rays represent a noise in the NR).

In the LiF:ZnS scintillator screen the neutrons are converted to green light with an absorption maximum at 520 nm:

$$^6_3Li + n \rightarrow {}^3_1H + {}^4_2He + 4.78MeV$$

The light emitted by the scintillator is reflected to the CCD–camera by the mirror. The performance of camera can be enhanced by cooling it with $LN_2$ to –120 °C (Atomic Institute, Internet Page). Using this detector, 200 µm resolution can be achieved.

The *neutron imaging plate* (NIP) works on a different principle: information is stored in an imaging plate (IP), read with a scanner and afterwards erased by light (Zawisky et al., 2008).

Neutrons are absorbed in $Gd_2O_3$ (plate) which is uniformly dispersed in the photoactive phosphorus (BaFBr:Eu) layer and an organic binder:

$n + {}^{157}Gd \rightarrow {}^{158}Gd + \gamma + e^-$ (30–200 keV conversion)

$n + {}^{155}Gd \rightarrow {}^{156}Gd + \gamma + e^-$ (30–200 keV conversion)

The secondary particles excite the BaFBr:Eu to a metastable state, where electrons are trapped. The information is

stored in locally trapped electron–hole pairs in the phosphor as a latent image. This information is registered by optical simulation with a focused He–Ne laser. During the readout process in the scanner, the trapped electrons are further excited by the red light from a He–Ne laser which causes luminescence of blue light which is finally detected by a photomultiplier tube. Layer thickness (135 µm) and composition have been optimised in spatial resolution and photo-stimulated luminescence. After readout the NIP is erased with bright white light and can be reused many times as long as no mechanical damage occurs. The resolution of IP is 50 µm. Every detector has certain advantages and disadvantages, and hence has specific application (Zawisky et al., 2008).

In **fibre science**, neutron radiography was applied for the first time by Weder et al. (2004). A selection of clothing systems composed of layers with differing water transport properties was studied to demonstrate the feasibility of this technique. The results are compared to the weights of the individual layers obtained during separate sets of measurements in the same horizontal configuration, as well as in vertical configuration on a heated cylinder. The results of the three measurement approaches agree with respect to layerwise moisture distribution in the different textile combinations, and the radiographic data provide a lateral visualisation of the distribution. A decisive role in fluid water transport is revealed for the innermost two layers (Weder et al., 2004).

Reifler et al. (2006) used neutron radiography to determine the exact water content in aramid-based soft body armour panels. While investigating the ballistic resistance of aramid–based body armour panels under wet conditions, it is important to precisely determine their water content and its chronological development. Using the neutron radiography method, the influence of water amount and location on impact testing as well as its time dependence was shown. In the ballistic panels used, spreading of water strongly depended on the kind of quilting. Very fast water migration could be observed when the panels were held vertically. Some first results regarding the water distribution in wet panels immediately after the impact are presented. On the basis of the presented results, requirements for a standard for testing the performance of ballistic panels in the wet state were deduced (Reifler et al., 2006).

The aim of our work was to visualise the moisture in lyocell filling fibres (fleece) by radiographic observations. Static and dynamic experiments were done on lyocell and polyester filling fibres. In the static experiments, fibres with defined moisture content were enclosed in the bags. The dynamic experiments were performed by using a humidifier which enabled continuous moisture evaporation with increasing temperature. The transmission data of both, lyocell and polyester fleeces were calculated from the grey–values obtained from NR images. Additional gravimetrical measurements of the total mass increase were performed to support the NR data.

## Materials and Methods

### Materials

For examination with NR, lyocell, and polyester fleeces were prepared on the carding machine having a fleece weight of about 200 $gm^{-2}$. Polyester fleeces were thicker (6 cm) than lyocell (4 cm) due to the higher stiffness of polyester fibres. The Table 1 shows the data of the samples used for neutron radiographic examinations.

### Static and dynamic experiments

Two kinds of experiment were performed: static and dynamic. In the static experiment, fibres were enclosed in sealed plastic bags containing 10 and 30 wt% water (Figure 2). The images were taken using the IP detector with exposure time 50 min to obtain high–quality images.

**Table 1.** Fleeces used for neutron radiography.

| Type | Characteristics<br>Fabric weight [$gm^{-2}$] | Supplier | Additional information |
|---|---|---|---|
| Lyocell fill | Fleece, 200; thickness 4 cm | LENZING AG, AT | Fibres 6.7 dtex; 60 mm, unfinished |
| Polyester fill | Fleece, 200; thickness 6 cm | ADVANSA, TR | Fibres 6.7 dtex, 60 mm |

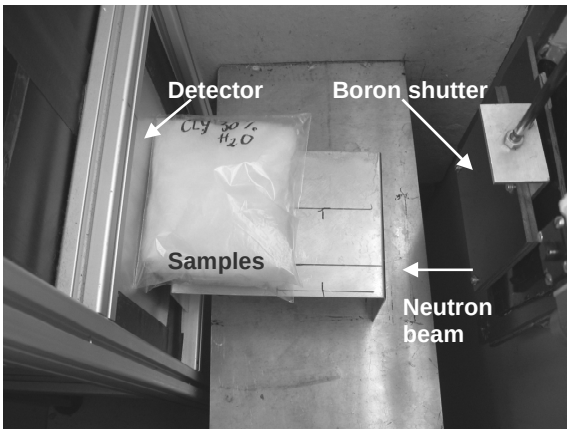


**Figure 2.** Sample area of the NR instrument with samples.

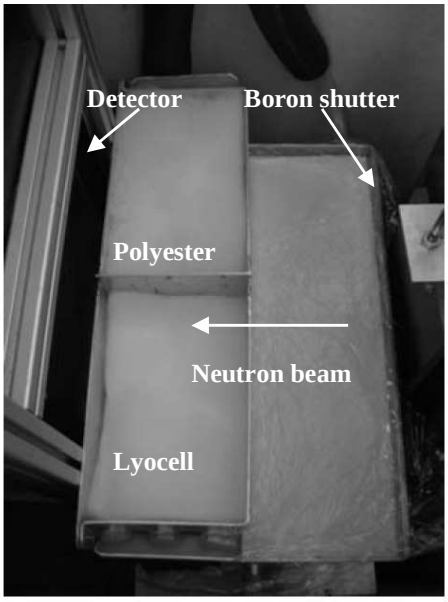


**Figure 3.** Construction for first dynamic experiments using Al–box to separate samples.

Dynamic neutron radiography or *real time neutron radiography* means that images can be made continuously after a fixed time interval depending on the exposure time chosen. The process (water sorption) can be followed in real time without any disturbance to the experimental arrangement. Using the scintillator detector, a time between two images can be decreased to 53 seconds while the use of the imaging plate consumes time for reading and erasing information.

For the dynamic experiments with textile fibres, a humidifier was placed between the neutron source and the detector. This was a steel tray with a layer of wetted viscose fleece. The experimental setup was adjusted a lot until the optimal experimental conditions were found. First, the aluminium box was on the humidifier between fleeces, then the fleeces were packed into pillows. To avoid liquid water being transported from the humidifier to the test fleece by direct contact of the fleece with the humidifier, aluminium wires were put below the pillows as a support. Finally, the best results came when a polypropylene fly–screen was put below the fleeces.

## Dynamic Experiments on Fleeces in an Aluminium Box with Humidifier

The first experiments were done by putting the lyocell and polyester fleeces in the aluminium box, and taking the images with the scintillator. Unfortunately, this experiment was not successful due to the thick aluminium plate. In general, aluminium is transparent for neutrons if the plate is thin enough. In our case, the plate was too thick to be transparent for neutrons (Figure 3).

## Dynamic Experiments on Pillows with Humidifier

Fleeces were enclosed in stitched pillow–cases to simulate real conditions in a duvet. Pillow-cases in a size 20 by 20 cm and a thickness 4 cm for lyocell filling and

6 cm for polyester filling were made with a cover from a satin weave of lyocell micro fibres (0.9 dtex). Aluminium wires were placed on the humidifier walls at a height about 1.5 cm in order to see the bottom of the pillows. The purpose was to raise the samples so that the lower part of the pillow wasn't hidden behind the walls. The fibres were then placed on the top of the wires.
A series of 90 images was started at room temp using the scintillator detector interval 53 s (40 s exposure time and 13 s grabbing time). The temperature increased to 35 °C and afterwards to 50 °C. Additional images with the imaging plate detector were taken at temperature 50 °C to compare the quality of the images taken with scintillator / imaging plate detector with an exposure time 10 min (Figure 4).

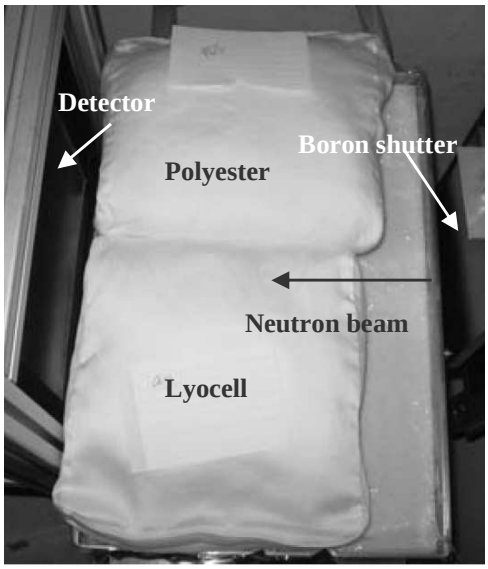


**Figure 4.** Fleeces enclosed in pillows.

## Final Dynamic Experiments with Humidifier and Imaging Plate Detector

The experiments were started with the humidifier at ambient temperature and then increasing its temperature to 35, 50 and 60 °C. The stable temperature of 35 °C was achieved after 40 min, 50 °C after 60 min and 60 °C after 90 min. Only the imaging plate detector was used. Exposure time was 10 min (Figure 5). The grey–value calculations were made from these images.

## Analysis of NR images

The analysis was done by measuring the grey–values. The lower the value, the higher is the quantity of absorbed water per sample. In the case of small absorption and low scattering, the neutron attenuation can be approximated by the exponential law:

$$I \cong I_0 e^{-\sum t} \qquad \textit{(Eq. 1)}$$

where $I$ is the intensity of the transmitted neutrons after penetrating a distance $t$ into the target. In our case, $t$ is the thickness of the sample. $I_0$ is the intensity of the beam incident on the sample. $\sum$ is the macroscopic cross–section.

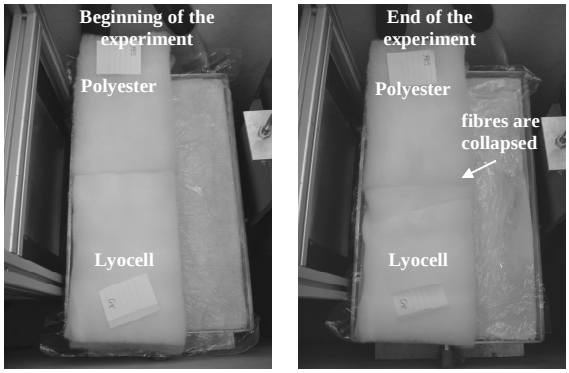


**Figure 5.** Lyocell and polyester fleeces taken with IP detector at the beginning and end of the experiment.

The measurement of neutron transmission through the sample allows in principle an absolute determination of the sum of cross–sections and densities of the sample:

$$T = \frac{I}{I_0} = e^{-\Sigma t} \qquad \textit{(Eq. 2)}$$

Where,

$$\Sigma = \sum_i \Sigma_i$$

and

$$\Sigma_i = \frac{N_A \sigma}{A} \rho_i \qquad \textit{(Eq. 3)}$$

From the neutron images, the macroscopic cross–section can be calculated. From the macroscopic cross–section, the density of the material may be determined. $\rho$ is the density of the material in gcm$^{-3}$, A is the atomic weight, $N_A$ Avogadro's number

and $\sigma$ the microscopic cross–section in $cm^2$.
This investigation was mainly concerned with the water content, therefore the intensities behind the wet sample to the dry sample were normalised in order to determine

$$T_{water} = \frac{I_{wet}}{I_{dry}} = \exp(-\sum_{water} t) \quad (Eq.\ 4)$$

From $\sum_{water}$ the absolute density $\rho_{water}$ could be evaluated.

## Results and Discussion

### Static Experiments

Carded lyocell and polyester fibres were sprayed with water before enclosing into plastic bags. The fibres contained 10 and 30 wt % water. Then neutron imaging was done under stable conditions, where the exposure time was increased to 50 min – this giving maximum hydrogen sensitivity and 16 bit image gradation.

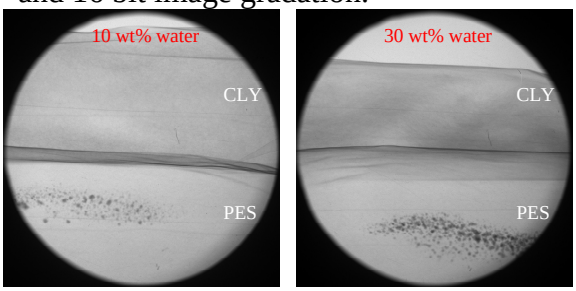


**Figure 6.** Neutron radiographies made with an imaging plate with an exposure time of 50 minutes: left–with 10 wt% water content; right–with 30 wt% water content.

The water is very homogenously distributed within the lyocell fibre. The lyocell samples with 30 wt% water look greyer in comparison with samples containing 10% water. On polyester fibres the condensation in the centre of the fleece occurs. In the polyester sample with 30 wt% water, water is condensed in the bottom part of the sample. With the static experiments, the distribution of water in equilibrium conditions can be visualised enabling high–resolution images due to the high exposure time and imaging plate detector.

### Dynamic Experiments on Fleeces in Aluminium Box with Humidifier

For the dynamic experiments, the humidifier filled with a few wet viscose non–woven layers was placed in the NR–assembly between the neutron source and the detector. In the images, this is hidden behind the wall of the humidifier. An additional lyocell film (8 µm thickness) was put between wet non–woven in the humidifier and the examined fleeces to ensure slow and homogenous moisture evaporation. The fleeces (lyocell and polyester) were put on the humidifier, which simulates the humid skin of a sleeping person. To simulate the temperature differences between the skin and a cool sleeping room or outdoor environment, it was not possible in the reactor room to cool the environment. So, the humidifier temperature was raised to achieve temperature differences. The temperature was increased from 24 (room temperature) to 35, 50 °C, and 60 °C. The trials were therefore operating at a higher level of temperatures and absolute humidity; however, the principle conditions are realistic as a model. Figure 7 (A) shows the experimental arrangement showing the aluminium box (Al–box) placed close to the scintillator, (B) NR of the fleeces inside the Al–box and (C) NR of the fleeces without the Al–box. On the lower side the dark region shows the walls of the humidifier. In the middle of the Al–box, there was a double wall of 6 mm thickness. This Al–layer is visible to neutrons and the area covered in the image is quite large. So the experiment was then performed without Al–box.

### Dynamic Experiments on Pillows with Humidifier

In order to set the experiment in conditions close to practical use of substrates, the lyocell and polyester fleeces were enclosed into pillows (made from lyocell fibres 0.9 dtex in sateen weave) and placed on the humidifier (Figure 4).

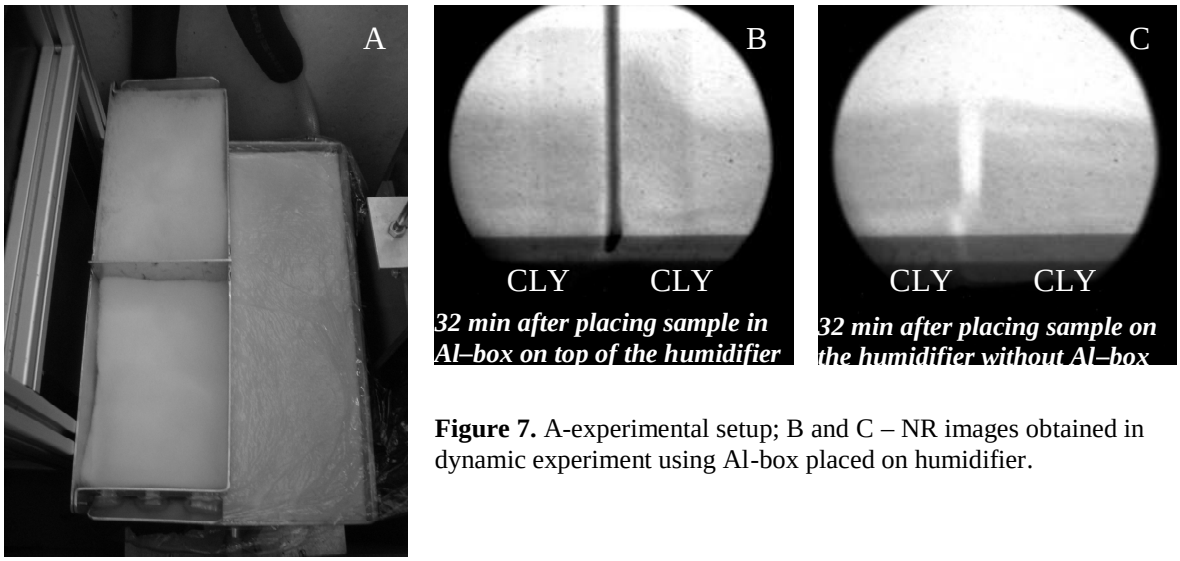


**Figure 7.** A-experimental setup; B and C – NR images obtained in dynamic experiment using Al-box placed on humidifier.

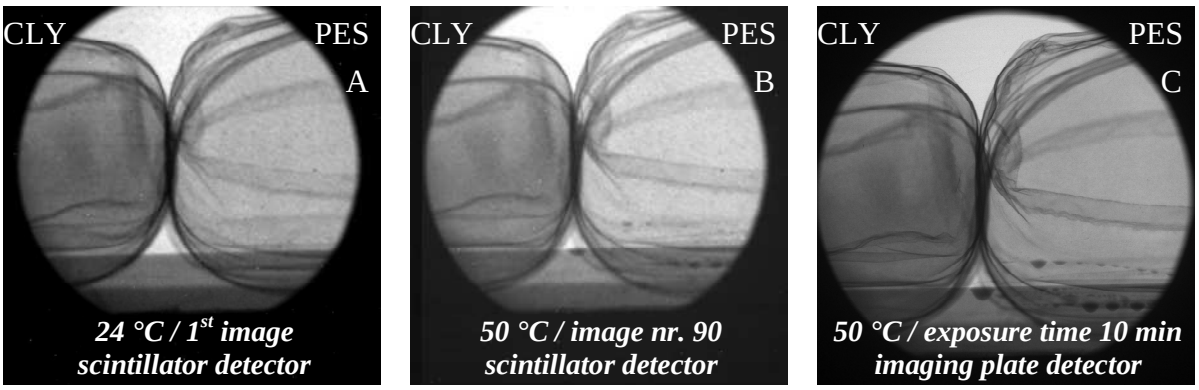


**Figure 8.** NR images obtained in dynamic experiment after inclosing fleeces in the pillows after 0, 80 minutes, 270 minutes.

The wires were placed on the humidifier (below the pillows) in order to be able to see the bottom of the pillow on the NR images.

The experiment started at room temperature 24 °C. A few images were made in these conditions. Then the thermostat was switched to a temperature of 35 °C. A series of 90 images was started at room temperature. The temperature became stable at 35 °C in about 15 minutes and was maintained for half an hour. After that the temperature was increased to 50 °C (which took about 15 min). Again this temperature was maintained for half an hour. During all this time, images were taken at an interval of 53 seconds (the exposure time being 40 s with a grabbing time of about 13 s). Figure 8 shows images of fleeces enclosed in pillows: A–taken at room temperature after 53 s (beginning of the experiment); first image of the time series, B–at 50 °C after 80 min; image number 90 of the time series and C–at 50 °C taken with imaging plate detector after 270 min exposed for 10 min.

It can be seen from the images that no considerable difference in the water content in the lyocell fibres at the beginning and at the experiment and 90 min later could be observed. The moisture is absorbed in lyocell pillow–cases. The condensation of water is visible on the bottom of polyester filled pillow. It is unclear if the condensation occurs within the pillow or on the wires placed on the humidifier below the pillow.

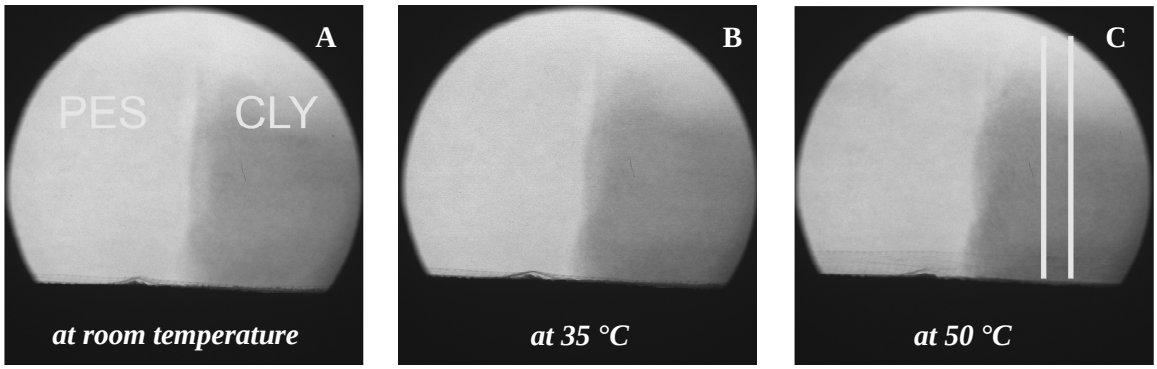


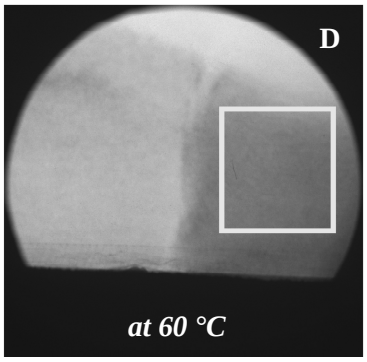


**Figure 9.** NR images taken with imaging plate detector: Humidifier temperature: starting at room temperature (A), at 35 °C (B), 50 °C (C) and 60 °C (D).

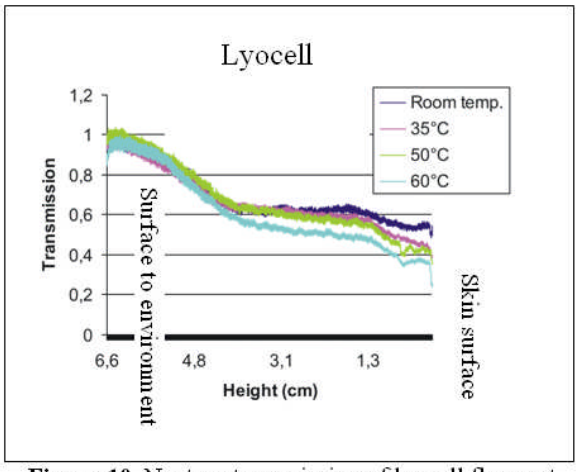


**Figure 10.** Neutron transmission of lyocell fleece at various humidifier temperatures.

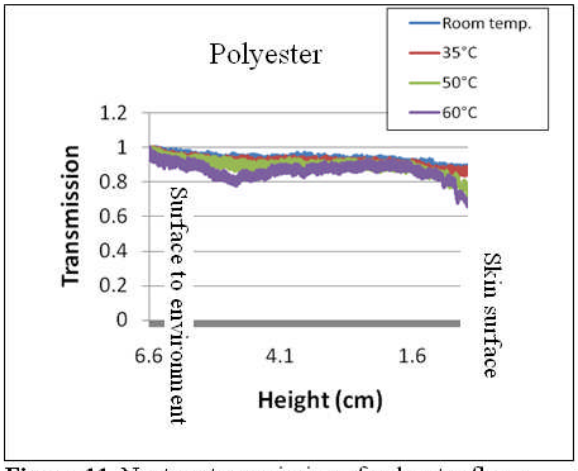


**Figure 11.** Neutron transmission of polyester fleece at various humidifier temperatures.

It is assumed that water is absorbed by the lyocell covers therefore most probably moisture condenses on the Al–wires. It was then decided to perform further experiments without pillows. Images obtained using the imaging plate detector have a much better quality. After exposure, time is required for scanning and erasing the plate before it can be reused. So the repetition interval between two such images would be about one hour.

## Final Dynamic Experiments with Humidifier and Imaging Plate Detector

The experiment setup was the same as for preliminary experiments as shown in Figure 5. Lyocell and polyester fleeces were placed next to each other on the humidifier and the experiment started at room conditions (25 °C, 40 % RH). The temperature of the humidifier was raised to 35, 50, and 60 °C, respectively. The imaging plate detector was used with exposure time 10 min.

From Figure 9 it can be seen that the temperature has a detectable influence on the water content. The higher the temperature of humidifier, the higher is the water content and the lower is the overall neutron transmission. Time of the sample at a certain temperature is not a considerable influencing factor because the grey–values do not differ a lot when exposing the sample at 35 ºC for a longer time period. In Figure 10, a line profile was taken vertically along the height of the sample starting from the bottom to about 2 cm above the lyocell sample. The height of the lyocell sample was 4 cm and that of the polyester sample was 6 cm. The transmission was calculated and plotted relative to the height. Lower transmission corresponds to higher value of moisture content. So we see that there is higher moisture content on the lower part of the sample which is close to the humidifier with both fibre types. As the temperature increases, the transmission decreases and hence the moisture content increases. There is a non linear relationship between the transmission and the water content. With lyocell fibres, the decrease in transmission is quite even over the cross–section of the fleece, with somewhat higher decrease in the bottom part. With polyester, the decrease in transmission is concentrated on the region near the skin surface, and the height of approximately 5 cm, near the surface exposed to the environment. The lyocell sample changed its shape a little bit during the experiment. In this Lyocell fibres become soft after moisture has been absorbed and therefore fleece will change shape (collapse in the centre).

The neutron images support the study of swelling/condensation on hygroscopic/ hydrophobic fibres by environmental scanning electron microscopy (ESEM). In those experiments, the water vapour pressure was increased in the ESEM chamber from 3 to 7 Torr at 5 °C, which corresponds to 40 to 100 % RH. From the starting point, pressure raised in 0.2 Torr steps. Strong swelling of lyocell fibres started at 5 Torr (75 % RH) and the condensation on polyester at saturated atmosphere 7 Torr (100 % RH). (K. Varga, *Doctoral Thesis*, 2009).

**Gravimetric Analysis**

In order to compare the transmission calculations from neutron images, the gravimetric analysis on the fleeces was performed in Lenzing AG lab by the same procedure like at Atomic Institute. Lyocell and polyester fleeces were placed on the humidifier filled with wet viscose fleece. To ensure slow and continued moisture evaporation, Lyocell foil (8 µm thickness) and fly–screen (polypropylene) were putted on the wet fleece.

After placing the CLY/PES fibres on humidifier, the thermostat was switch on to 35, 50, and 60 °C, respectively. For every experiment new CLY/PES fibres were used.

The time needed to achieve stable temperature exceeded 40 min for 35 °C, 60 min for 50 °C and 90 min for achieving 60 °C. After wetting, fleeces were dried at 80 °C for 60 min in order to calculate the water content in the materials. The water content in the fleeces at various temperatures is shown in Figure 12.

The gravimetric data obtained by the same procedure like neutron images support the radiographic results. As the temperature increases, fleece samples take up more water. Therefore, the transmission of neutrons through the sample decreases with increasing water content.

Sorption isotherms (Figure 13) and water retention (Table 2) show that polyester fibres do not take up a substantial amount of water vapour or liquid water, whereas lyocell can absorb water vapour and liquid water. Comparing these numbers with the measured uptake in Figure 12, it can be concluded that in case of polyester fillings, the water in the fleece must be present mostly as free water in films of droplets on the fibre surface, whereas in the Lyocell

fillings the water is mostly absorbed into the fibre structure.

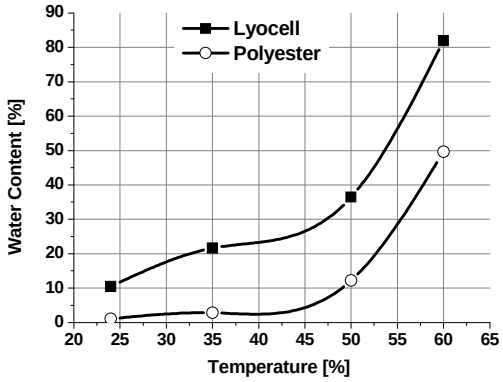


**Figure 12.** Total water content in fleeces after dynamic experiments.

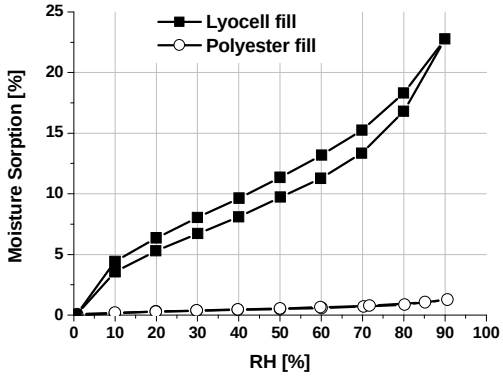


**Figure 13.** Water vapour sorption isotherms of lyocell fill and polyester fill fibres at 25 °C.

**Table 2.** Moisture regain and liquid water retention of the fibres used (in percent based on dry matter, indicative values).

| Fibre | Water retention value | Moisture regain at 90 % RH | Moisture regain at 100 % RH |
|---|---|---|---|
| Lyocell fill | 70 | 22.8 | 33 |
| Polyester fill | 3 | 1.3 | 2 |

## Conclusions

In this study, the water distribution in lyocell and polyester filling fibres under simulated practical conditions was visualised by the non–destructive method of neutron imaging (neutron radiography). Raising the temperature difference between a humidifier simulating the human skin, and the cooler environment, it was shown that an increasing amount of water was taken up by the lyocell fibres, visualised by lower neutron transmission and confirmed by the weight of the fleece. From the comparison of moisture uptake measured by fleece weight and the known data of moisture and liquid water absorption in fibres, it can be concluded that in polyester fleece condensation on surfaces occurred under applied conditions.

The distribution of water is rather even over the cross–section of lyocell feeling, with somewhat higher moisture content near the “skin face” of the duvet model. In polyester filling, water is localised mostly in two distinct zones, near the “skin face” of the duvet model, and near the upper surface. The neutron radiography method presented in this study supported the known images from environmental scanning electron microscopy where swelling of hygroscopic and water condensation on hydrophobic fibres was visualised on the fibre cross–sections.

To get more insight into water content in the fleeces during the neutron imaging, additional calculations are necessary based on the grey–values of neutron images

## Acknowledgements

Authors gratefully acknowledge the Christian–Doppler Society Vienna and Lenzing AG for financial support of this work, to Mr. Johann Gruber and Dr. Clemens Bisjak for build–up of the apparatus and to Mr. Johann Männer for discussions on filling fibres topics. Thanks to Mag. Michael F. Noisternig and Prof. Ulrich J. Griesser, University of Innsbruck, for the sorption isotherms.

## References

Bartels V.T. & Umbach K.-H., Messverfahren zur Beurteilung der Atmungsaktivität von Textilien für Bekleidung und Bettsysteme. *Melliand Textilberichte* **3** (2003), pp. 208–210.

Helbig K: Comparative Research: Microclimate of Bedding Components, *Lenzinger Berichte* **85** (2006), pp. 51–53.

http://www.ati.ac.at/~neutropt/experiments/Radiography/radiography.html (06.10.2009).

Libert J. P., Di Nisi J., Fukuda H., Muzet A., Ehrhart J., and Amoros C.: Effect of continuous heat exposure on sleep stages in humans, *Sleep* **11** (1988), pp. 195–209.

Moser M., Frühwirth M., Avian A., Kelz C., and Köhldorfer P.: Influence of textile materials on a restful sleep. *Proceedings of the 46th Dornbirn Man-Made Fibres Conference*, 19–21 September 2007.

Pel L., Ketelaars A. A. J., Adan O. C. G., and van Well A. A.: Determination of the Moisture Diffusivity in Porous Media Using Scanning Neutron Radiography, *International Journal of Heat and Mass Transfer* **36** (1993), pp. 1261–1267.

Reifler F. A., Lehmann E. H., Frei G., May H., and Rossi R.: The method of neutron imaging as a tool for the study of the dynamics of water movement in wet aramid-based ballistic body armour panels, *Measurement Science & Technology* **17** (2006), pp. 1925–1934.

Schuster K. C., Suchomel F., Männer J., Abu–Rous M., and Firgo H.: Functional and Comfort Properties of Textiles from TENCEL® Fibres Resulting from the Fibres' Water-Absorbing Nanostructure: A Review, *Macromolecular Symposia* **244** (2006), pp. 149–165.

Suchomel F., Männer J., and Firgo H.: PCT International Patent Application WO2008/049142.

Umbach K.-H.: Messmethoden zur Prüfung physiologischer Anforderungsprofile an Zivil-Arbeits- und Schutzbekleidung sowie Uniformen, *Melliand Textilberichte* **68** (1987), pp. 857–865.

Varga K, Schädel, U., Nilsson, H., Persson, O., and Schuster, K. C. Measuring the Heat of Wetting of Textile Fibres by Reaction Calorimetry. *Fibres & Textiles in Eastern Europe* **15** (2007), pp. 59–63.

Varga K: Man–Made Cellulosics: Thermodynamic of Water Sorption, Structure Visualisation and Modification by Conductive Polymers, *Doctoral Dissertation*, Leopold–Franzens University Innsbruck, Austria, 2009.

Weder M., Brühwiler P. A., Herzig U., Huber R., Frei G., and Lehmann E.: Neutron Radiography Measurements of Moisture Distribution in Multilayer Clothing System, *Textile Research Journal* **74** (2004), pp. 695–700.

Zawisky M., Hameed F., Dyrnjaja E., and Springer J.: Digitized Neutron Imaging with High Spatial Resolution at a Low Power Research Reactor: I. Analysis of Detector Performance *Nuclear Instruments and Methods in Physic Research A* **587** (2008), pp. 342–349.

Lenzinger Berichte 87 (2009) 136-142

# PHYSIOLOGICAL INVESTIGATION OF RESIN-TREATED FABRICS FROM TENCEL® AND OTHER CELLULOSIC FIBERS

**Ksenija Varga[1], Alenka Kljun[2], Michael F. Noisternig[3], Roger N. Ibbett[4], Johann Gruber[5], Jörg Schlangen[5], Ulrich J. Griesser[5], and K. Christian Schuster[5]**

[1]Christian–Doppler Laboratory for Chemistry of Cellulosic Fibres and Textiles, Institute of Textile Chemistry and Textile Physics, Leopold–Franzens University Innsbruck, Höchsterstrasse 73, A–6850 Dornbirn, Austria
[2]University of Ljubljana, Faculty of Natural Sciences and Engineering, Department of Textiles, Snezniska 5, SI–1000 Ljubljana, Slovenia
[3]Institute of Pharmacy, Leopold–Franzens University Innsbruck, Innrain 52c, A–6020 Innsbruck, Austria
[4]Christian–Doppler Laboratory for Textile and Fibre Chemistry in Cellulosics, School of Materials, Department of Textiles, University of Manchester, Sackville Street Building, M601 QD, Manchester, UK
[5]Lenzing AG, Innovation & Business Development Textiles, Werkstrasse 2, A–4860 Lenzing, Austria

*Presented at the 4th INTERNATIONAL TEXTILE, CLOTHING & DESIGN CONFERENCE – Magic World of Textiles, October 05th to 08th 2008, DUBROVNIK, CROATIA*

**Resin–treatment is widely used in textiles to improve crease–resistance of the fabrics and achieve easy–care properties. Extensive work has been performed on this topic, mostly concentrating on cotton fabric by using different resin types, catalysts, treatment time and temperature. In practice, the most commonly used resin is DMDHEU. The changes of the crease angle, tensile properties and air permeability after the resin treatment has been measured, but generally there is not much literature dealing with the physiological properties of the treated fabrics. In this work, TENCEL® and cotton fabric were treated with DMDHEU at different temperatures and reaction times. Wear–comfort relevant properties such as sorption of liquid water and water vapour, drying velocity and thermal absorptivity have been measured in comparison with the untreated fabrics. The results reveal that the resin treatment does hardly affect the water vapour sorption/desorption behaviour whereas the uptake of liquid water is clearly decreased. The layer of DMDHEU on the fabric also causes an increasing in drying velocity. The thermal absorptivity measured with an Alambeta Tester is higher for TENCEL® than for cotton fabric and slightly increases after resin treatment due to a smoother surface.**

**Keywords:** *resin–treatment, cellulosic fibres, wear–comfort, water vapour sorption, thermal absorptivity*

## Introduction

Wear–comfort is an important issue in the textile science. It has been extensively explored in the last decade that man–made cellulosic fibres such as TENCEL®, Lenzing Modal® and Lenzing Viscose® show excellent physiological behaviour. All these cellulosic fibres exhibit certain properties that are favourable for the wear comfort such as a high absorbency for water vapour and liquid water and a high heat capacity resulting in a heat buffering effect. These effects are especially pronounced for TENCEL® fibres (generic fibre type Lyocell).

The outstanding wearing comfort of textiles made from TENCEL® fibres is the consequence of the fibres' nanostructure. The structural features enable a high water

absorptivity, which leads to high heat capacity and heat balancing effect for thermoregulation, comparable to the action of phase change materials [1]. The resin treatment of TENCEL® is very important for the fibrillation control. The commercial experiences in the TENCEL® resin finishing process were very inconsistent. In most of the cases the results were excellent, but from time to time the resin process seems to be out of control. The resin suppliers developed their products mainly for cotton and viscose but TENCEL® is not a main target for these companies. Because of that, Lenzing decided to investigate of the resin finishing in detail. Cellulose fibres have a different reactivity in the resin process and of course different product properties.

The curing temperature is not the only an important factor in the resin process but also the type of the resin has a big influence on the performance. The resin concentration itself influences the reactivity and performance of the fabric. The reactivity of the resin system is mainly dominated by the catalyst and curing temperature [2]. Finishing the cellulosic textiles with the resin to improve a crease–recovery has been extensively investigated over the years, but there is not much literature evidence about the effects of such treatments on the physiological properties. Generally it is perceived that the intensive treatment has a negative effect on the wear–comfort [3, 4].

In this research, the influence of the resin–treatment conditions on the physiological properties of TENCEL® and Cotton fabric has been investigated. The fabrics are treated under mild, middle (praxis relevant) and strong temperature and time conditions. The physiological properties, like absorbency of water vapour was measured by dynamic vapour sorption analysis and the absorbency of liquid water was evaluated by measuring WRV. The drying velocity was determined by a very sensitive balance and thermal absorptivity by Alambeta tester.

## Materials and Methods

### Materials

TENCEL® (1.3/38 fibres) and bleached cotton fabrics were used both with the same textile construction: yarn count Nm 50, plain weave.

### Resin Treatment

Fabrics were treated with DMDHEU / catalyst system. The treatment formulation contained 50 $gL^{-1}$ resin Fixapret CP (BASF), 15 $gL^{-1}$ catalyst $MgCl_2x6H_2O$ and 0.5 $gL^{-1}$ surfactant. The resin was applied in a pad–cure process (foulard set at 2.0 bar) under conditions summarized in Table 1.

**Table 1.** Resin–treatment conditions.

| Treatment | Conditions | |
|---|---|---|
| | | |
| | Drying | Curing |
| Mild | 120 °C / 30 min | |
| Middle | 130 °C / 30 s | 165 °C / 45 s |
| Strong | 130 °C / 30 s | 190 °C / 120 s |

The conditions of middle treatment are commonly used in industrial practise. Fabrics which were not treated with resin, were only padded in pure water at middle conditions since elevated temperature can also change the fabric structure and influence on the physiological properties. After the treatment, all samples were washed at 90 °C for 20 min to remove the uncondensed resin.

### Physiological Investigation

*Dynamic Sorption Analyser*

Dynamic water vapour sorption and desorption of the treated fabrics was performed with an automatic multisample sorption analyser SPS11 10µ (Project–Messtechnik, D–Ulm). The system is equipped with an analytical balance and sample chamber which allows the simultaneous gravimetric analysis of 11 samples [5]. The atmosphere in the analyser was set to 25 °C and 0% RH until equilibrium was achieved. Then the moisture sorption cycle was started rising

the relative humidity in 10% RH steps. The mass change of the materials was recorded every 8 min and the equilibrium conditions was set to <0.02% total mass change within 40 s. Every time this condition was fulfilled for all samples, the RH was automatically increased by 10% RH up to 90% RH and then stepwise decreased down to 0%. The full sorption/desorption cycle took 14 days and the mass change at each equilibrium condition was used to draw the moisture sorption isotherm. The hysteresis (differences between sorption and desorption) was calculated according to the equation 1 [5].

$$Hysteresis[\%] = \frac{MR(desorption) - MR(sorption)}{MR(sorption)} \times 100 \quad (1)$$

where is:
MR (sorption) [%] – moisture regain at equilibrium state at sorption process
MR (desorption) [%] – moisture regain at equilibrium state at desorption process

*Water retention value*

The water retention value (WRV) is a value, which indicates the water amount held back in fibres or textiles after total wetting and centrifuging. The measurements were performed following a Lenzing protocol using a laboratory centrifuge. The fibre sample (0.3 – 0.4 g) were weighed in the centrifuge glass and swollen for 5 minutes in deionised water. The sample was centrifuged for 15 minutes at 3000 $Rmin^{-1}$ and weighed immediately. The samples were dried for 24 h at 105 °C and weighed again. The WRV was calculated out of the measured sample weight at the wet ($m_w$) and dry ($m_d$) stage [6].

$$WRV[\%] = \frac{m_w - m_d}{m_d} \cdot 100 \quad (2)$$

where is:
$m_w$ – mass of wet sample after centrifugation
$m_d$ – mass of sample after drying

*Drying Velocity Measurements*

A 15x15 cm fabric was placed on a sensitive balance connected to the computer. An amount of 500 mg of an aqueous dye solution is applied with a syringe to the centre of a fabric. The sample was continuously weighted as it dries. The measurement takes two hours where the mass is registered every 60 seconds. The apparatus is shown in Figure 1. For each sample two parallel measurements were performed and the average curve was calculated in the OriginPro 7.5 Software.

**Figure 1.** Equipment for measuring drying velocity.

**Figure 2.** Alambeta tester.

*Alambeta Tester*

The Alambeta Measuring Device (Figure 2), developed at the Technical University of Liberec (Czech Republic) utilizes a new principle in measuring thermophysiological properties of textile fabrics. The instrument allows the measurement of a new (up to now only subjectively evaluated) instantaneous quantity of the warm/cool feeling, i.e. warm or cool sensation at the first contact of the human skin with a textile fabric. The

corresponding value (thermal absorptivity) is registered for textile fabrics in interval from 30 $Wm^{-2}s^{1/2}K^{-1}$ (raised knitted fabrics and light webs) to 300 $Wm^{-2}s^{1/2}K^{-1}$ (impregnated or coated woven fabrics). The instruments registers the heat flow through the fabric due to the different temperature of the bottom measuring plate (at ambient temperature) and the measuring head which is heated to 40 °C. The thermal absorptivity of a fabric is a measure of the amount of heat conducted away from the surface of the fabric per unit time. A fabric which does not conduct heat away from its surface will feel warm whereas one that conducts heat away will feel cooler [7].

## Results and discussion

### Sorption Properties

The water vapour sorption was measured with an automatic sorption analyser recording the mass change as function of the relative humidity at constant temperature. The equilibrium isotherms are plotted in Figure 3 and 4 and show the typical hysteresis loop of cellulose based fibres between the sorption and desorption cycle. One would expect that different coatings close the pores of the fabrics and thus prevent a direct transport of moisture through the fabric resulting in a worse wear comfort of coated textiles. However, the sorption isotherms of untreated and treated fabrics ob both TENCEL® and Cotton fabrics showed that this is not the case. The maximum absorption at 90% RH is much higher for TENCEL® (18.93%) than for Cotton fabric (11.07%). After the very strong treatment, the water uptake of the TENCEL® fabric decreased only by 1.36% at 90% RH (17.27% relative water uptake). At lower humidities (10–40%) the sorption isotherms of the fibre samples overlap which indicates no significant difference in the moisture sorption properties. The differences between untreated and resinated cotton fabrics are slightly more pronounced. Strong treatment decreases the amount of absorbed water vapour by 2%.

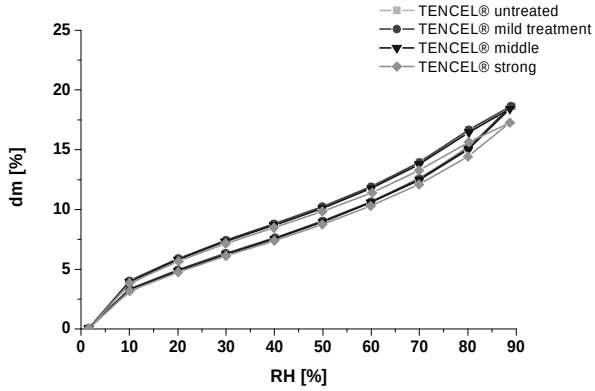


**Figure 3a.** Sorption isotherms of untreated and resinated fabrics: TENCEL®.

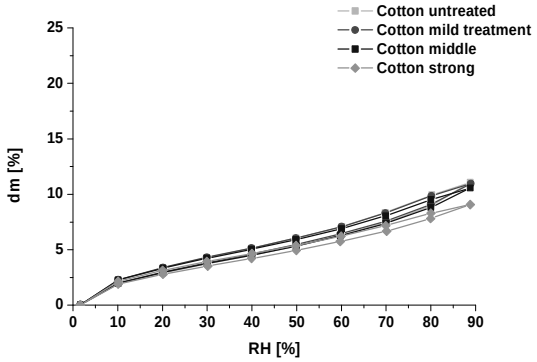


**Figure 3b.** Sorption isotherms of untreated and resinated fabrics: Cotton.

The hysteresis between desorption and sorption processes is an indicator for structural differences in the materials (Figure 4). Some earlier research on Lyocell and Cotton fibres by Okubayashi et al. showed a similar behaviour although the values for single fibres are higher [5]. The extent of hysteresis clearly decreases with increasing relative humidity, which suggest that the fibre and fabric structure changes when moisture adsorbs on the dry fibre or reversly when all moisture desorbs from the fibre. Obviously, the structural changes become smaller after some moisture has been adsorbed on the fibres. TENCEL® fabrics show a more distinct hysteresis than the cotton fabrics, especially at low RH. This result indicate that TENCEL® (Lyocell) fibre structure is less stable than that of cotton and water

can more easily invade the structure. This can be explained by the lower crystallinity, larger pore volume and larger inner surface area of Lyocell [5].
The differences in mild, middle and strong treated fabrics are more pronounced for Cotton fabric which indicated that resination causes a stronger change in the Cotton fabric structure than in TENCEL® fabric.

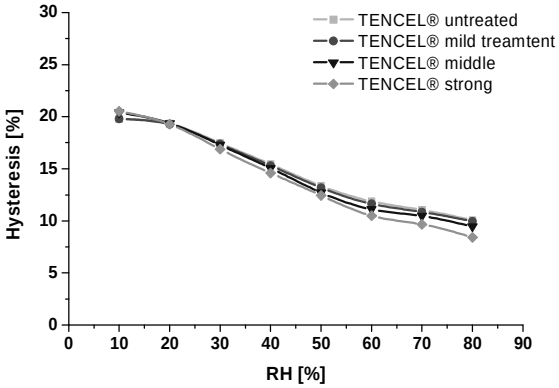


**Figure 4a.** Calculated hysteresis from the sorption data: TENCEL®.

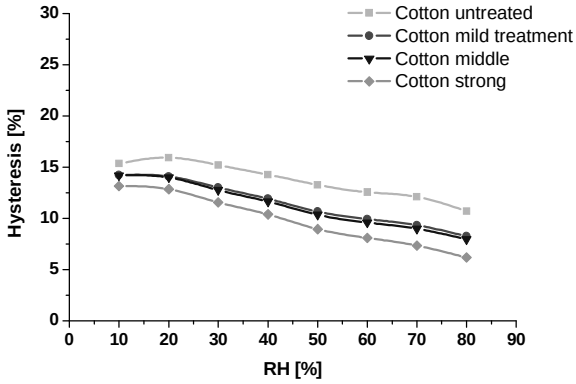


**Figure 4b.** Calculated hysteresis from the sorption data: Cotton.

The sorption of liquid water was characterised by measuring water retention values of untreated and resinated fabrics respectively, according to the Lenzing Method [6]. The resin–content was evaluated by measuring N–content. The plot in Figure 5 shows the correlation of WRV and N–content. The N–content increases as the fabrics are treated at higher temperature and the water retention value decreases with increasing N-content (amount of resin). The decrease in WRV is stronger for TENCEL® fabric than for Cotton fabric. This indicates again the different bonding ability of resin to the fabric.

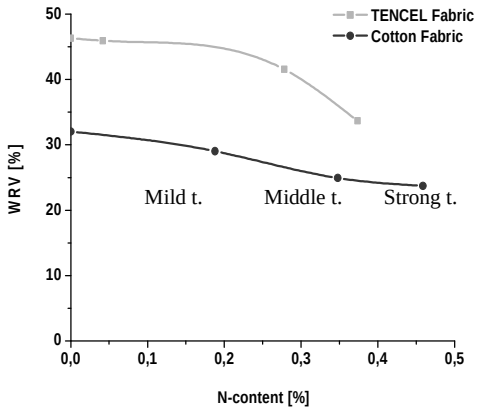


**Figure 5.** WRV versus N–content.

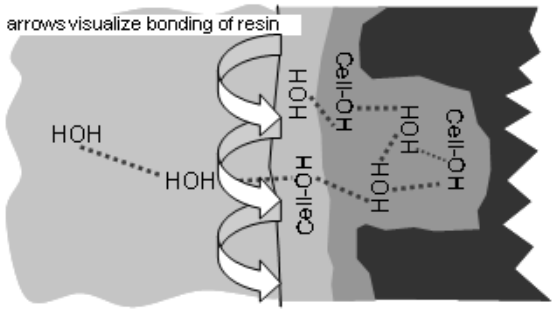


**Figure 6.** Model of porous cellulose fibre structure proposed by Ibbett, adapted from [8].

Ibbett [8] proposed a model how the resin can be bonded to the cellulose (Figure 6). Macroscopically, the resin is attached to the outer surface of pores so that accessible groups of cellulose molecules remain free for bonding of small water vapour molecules. The resin is attached to the surface of the pores decreasing therefore the Water Retention Values. In Figure 6, the arrows represent the probable distribution of the resin on the surface of pores.

## Drying Velocity

The drying velocity was measured on very sensitive balance by adding a droplet of an aqueous dye–solution and measuring the mass decrease. The comparison of the drying velocity of TENCEL® and Cotton fabric is shown in Figure 7. The first part

of the curve indicates the drying characteristics and analysed in more details. In the first 10 minutes, 140 mg of water evaporates from untreated and middle–treated TENCEL® fabric while 175 mg evaporated from mild and strongly–treated fabric. After 20 minutes 260 mg of the water evaporates from untreated and middle–treated fabric, 290 mg from mild treated and 320 mg from strongly–treated fabric. From untreated cotton fabric 110 mg evaporate in the first 10 minutes and 150 mg from all other treated cotton fabric. In 20 minutes, the evaporation exceeds to 225 mg for untreated fabric and 300 mg from treated fabric. It is obvious that the drying velocity is higher for all (untreated and treated) TENCEL® fabric than for the cotton fabrics. This behaviour originates from the smoother surface, where water spreading occurs faster resulting in a larger surface and thus a higher evaporation rate.

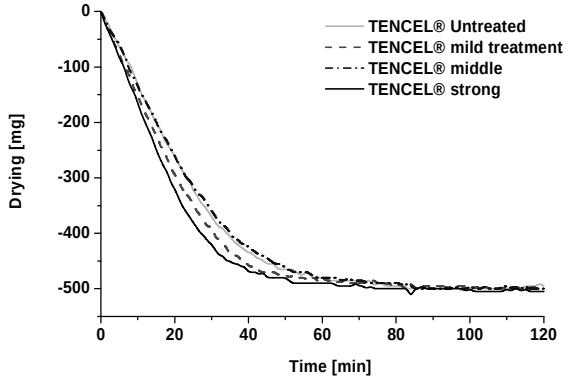


**Figure 7a.** Drying velocity measurements of: TENCEL® fabric.

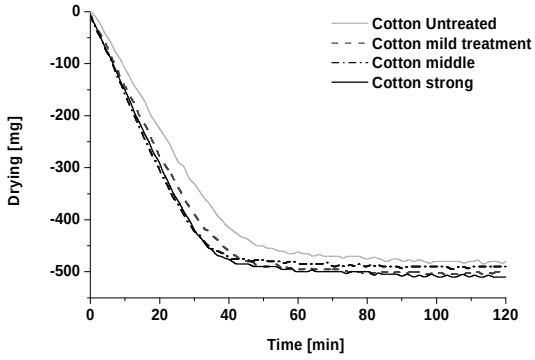


**Figure 7b.** Drying velocity measurements of: Cotton fabric.

It can be also seen that water evaporation is higher if the fabric is treated with resin. The effect is described in previous work by Firgo et al dealing with TENCEL® / Polyester sportswear [9]. The spreading of water on hydrophobic surfaces is higher so that evaporation will be also higher to some extent.

## Thermal Absorptivity

The thermal absorptivity measurements allow to calculate a so called cool–feeling factor, which represent the first sensation when textile comes in contact with skin. If the thermal absorptivity values are higher, the cool–feeling of the textiles will be better. The fibres were equilibrated before measurements for 24 hours in the laboratory with 55% relative humidity. The results in Figure 9 show that TENCEL® fabric exhibits a higher thermal absorptivity, i.e. provides a better cool–feeling than Cotton fabric. The values increase after the treatment. The fact that the resin fills the pores of the fabric makes the fabric surface smoother and less "hairy" which finally results in higher Alambeta values.

**Table 2.** Thermal absorptivity results of TENCEL® and Cotton fabric.

| Treatment | TENCEL® | Cotton |
|---|---|---|
| | Absorp<br>W $m^{-2}$ $s^{1/2}$ $K^{-1}$ | Absorp<br>W $m^{-2}$ $s^{1/2}$ $K^{-1}$ |
| untreated | 198,40 | 160,12 |
| mild | 199,20 | 162,80 |
| middle | 210,00 | 173,92 |

Finally, the crease–recovery was measured for all treated and untreated fabrics in weft and warp directions as standard test procedure in the evaluation of resinated fabrics. As expected, the values significantly increase with increasing treatment conditions.

## Conclusions

Physiological properties of resin–treated TENCEL® and Cotton fabrics were investigated. Water vapour sorption was measured by dynamic sorption analyser while sorption of liquid water was characterized by measuring Water

Retention Value. Thermal Absorptivity was determined by Alambeta Tester and Drying Velocity with the aid of a very sensitive balance. Fabrics were resin–treated by three different treatment conditions (mild, middle and strong) varying the drying and curing conditions at constant resin and catalyst concentration. The most important result of this investigation is that resin–treatment doesn't change the water vapour sorption ability whereas the sorption of liquid water decreases after the treatment. The data show that water vapour sorption decreased (at 90% RH) by 2% for Cotton fabric and by 1.36% for TENCEL® fabric. At lower RH, the differences in sorption properties between untreated and resinated fabrics are not significantly different. Calculated hystereses indicate different behaviour of resinated TENCEL® and Cotton fabric. The hysteresis of TENCEL® is practically unchanged at low relative humidities but change slightly at high values (90% RH). The hysteresis of Cotton changes stronger after the treatment. The observed decrease in the hysteresis between sorption and desorption occurs due to a structural change of the fabric that affects the invasion of water molecules into the fibres. WRV decreases with the treatment since resin is attached on the outer surface of the pores. Other physiological properties like drying velocity can be improved applying TENCEL® fabric and additionally by resination due to the better surface spreading of water. The cool–feeling factor is also increased by resination due to smoother, less hairy surface of the treated fabrics and is significantly higher in TENCEL® than in cotton.

## References


[1] Schuster, K.C., Suchomel F., Männer J., Abu–Rous M., and Firgo H.: Functional and comfort properties of textiles from TENCEL® fibres resulting from the fibres' water–absorbing nanostructure: A Review, *Macromolecular Symposia*, **244** (2006) 149–165.

[2] Schlangen, J.; Abu–Rous, M., and Liggins, J.: New aspects of TENCEL® resin finishing, *Proceedings of International Aachen–Dresden Textile Conference*, 28–29 November 2007, Aachen, Germany, (2007).

[3] Schneider, R.: Die Bedeutung von Ausrüstungen in *Funktionstextilien*, Knecht, P. (Ed.), Deutscher Fachverlag ISBN 3-87150-833-0, (2003).

[4] Mecheels, J.: *Körper – Klima – Kleidung*, Wie funktioniert unsere Kleidung?, Schiele und Schön Berlin, ISBN 3-7949-0619-5, Berlin, (1998).

[5] Okubayashi, S.; Griesser, U., and Bechtold T.: A Kinetic Study of Moisture Sorption and Desorption on Lyocell Fibres, *Carbohydrate Polymers*, **58** (2004), 293–299.

[6] Lenzing AG, TIIL – PRÜFANWEISUNG 092/00.

[7] Alambeta Measuring Device: *User' Guide* Version 2.3, Sensora Instruments Liberec, Company Brochure.

[8] Ibbett, R.N.; Schuster K.C., and Fasching M.: The Study of Water Behaviour in Regenerated Cellulosic Fibres by Low–Resolution Proton NMR, *Polymer*, **49** (2008) 5013–5022.

[9] Firgo, H., Suchomel, F., and Burrow, T.: TENCEL® High Performance Sportswear, *Lenzinger Berichte*, **85** (2006), 44 – 50.

Lenzinger Berichte 87 (2009) 143-151

# INTERACTION OF CELLULOSE WITH ALKALI METAL IONS AND COMPLEXED HEAVY METALS

Hale Bahar Öztürk[1], Hai Vu-Manh[1,2], and Thomas Bechtold[1]*

[1+]Institute of Textile Chemistry and Textile Physics, Leopold-Franzens-University of Innsbruck, Hoechsterstrasse 73, A-6850, Dornbirn, Austria
(e-mail: textilchemie@uibk.ac.at; phone: +43-5572-28533; fax: +43-5572-28629)
[2] Textiles – Garment Technology and Fashion Design Faculty, Hanoi University of Technology, Hanoi, Vietnam
[+]Member of European Polysaccharide Network of Excellence (EPNOE), www.epnoe.eu

**The interaction between cellulosic textile materials and metal ions can follow different ways such as swelling, ion-exchange and metal complexation. Uptake of alkali metal hydroxides (LiOH, NaOH, KOH, TMAH) can lead to splitting of lyocell fibres into different numbers of macrofibrils. The split number indicates the different local situation of alkali inside the fiber.Up to 5 M alkali concentration, split number is determined by the cation accessibility into the fiber. Above 5 M, no split was observed due to the homogeneous distribution of alkali inside fiber.**
**The uptake of $Ca^{2+}$ ions follows an ion exchange mechanism which is limited by the carboxyl content of cellulosic material.**
**Heavy metal complexes can be formed in the polysaccharide matrix by ligand exchange reactions. The amount of metal complexed with cellulosic material depends on co-ligand used and pH of the complex solution. Thus the amount of metal complexed with cellulose is not limited by carboxyl group content of the cellulosic material and high concentrations of metal ions can be deposited in the insoluble cellulose material.**

**Keywords:** *lyocell, alkali treatment, swelling*

## Introduction

The absorption of metal ions into cellulose fibres is of interest for many applications. While the absorption of heavy metals such as copper or manganese is of interest in the processing of cellulose fibres e.g. bleach operations, incorporation of metal ions also is of interest for dietary fibres, production of nanomaterials or for coloured fibres with high level of fastness. Dependent on the type of metal ion present, binding of ions occurs via ion-exchange e.g. in case of calcium ions or via ligand exchange e.g. in the case of heavy metals. The type of metal cation to be inserted and selection of appropriate conditions for metal insertion determine the chemical mechanism occurring and the binding capacity of the cellulose. The incorporation of metal ions via ligand exchange reaction permits to insert metal ions up to very high level e.g. copper content above 5000 mg/kg of cellulose fibre can be obtained. (Urbano and Goi 2002, Kotelnikova et al. 2007, Vainio et al. 2007, Kongdee and Bechtold 2004a, Kongdee and Bechtold 2004b, Kongdee and Bechtold 2009, Fitz-Binder and Bechtold 2009).
The methods indicate new strategies for preparation of high metal content fibres which will be useful both for improved understanding of behaviour of polysaccharide (PS) material and for production of new PS based materials.
There are three mechanisms for metal ions to bind to cellulose:

a) Sorption is the action of both absorption and adsorption taking place simultaneously. Hydrated alkali ions present in aqueous systems swell the cellulose by penetration into it and also an exchange of hydrated shell with OH groups of cellulose can occur.
b) Electrostatic interaction between metal ions and cellulose occurs in the absence of ligand in the solution. Carboxylic groups of cellulose exchange cations, i.e. hydrogen leaves carboxylic group and metal ions attaches instead.
c) Metal ion and co-ligand (ex. ethylene-diamine, ammonia, tartaric acid, etc) form complexes in solution. In the presence of cellulose which acts as ligand, competition for the metal ion occurs between ligand and co-ligand. When the stability of metal ion and co-ligand complex is sufficient weak, cellulose complexes with the metal ion are formed and the the co-ligand is released. As examples cellulose solutions FeTNa, Cuen, Cuam, etc. can be given.
In the current study, cellulose-metal ion interaction was investigated with regard to swelling, ion-exchange mechanism (electrostatic interaction) and metal complexation. Effect of various alkali metal hydroxides (LiOH, NaOH, KOH, TMAH) on lyocell fibers was investigated by alkali retention value and splitting tendency. The uptake of earth alkali metal, $Ca^{2+}$, into woven lyocell fabric was studied at pH 5 and pH 9. The uptake of $Ca^{2+}$ ions into the material was visualized by dyeing alizarin which complexes with $Ca^{2+}$. The incorporation of heavy metal ion, $Cu^{2+}$, into cotton yarns was achieved in the presence of different co-ligands e.g. D-gluconate and glycine.

## Experimental

## Materials

Lyocell staple fibers without spin finishing, with 1.3 dtex titer and 38 mm length were provided from Lenzing AG. Scoured and bleached cotton yarn (Nm 65 m/g) supplied by Getzner Textil AG (Austria). Woven fabric (135.6 g/m$^2$, yarn count 50 m/g, warp 36 y/cm, fill 29y/cm, desized) was made from 100 % lyocell fiber (1.3 dtex Tencel® Lenzing AG, Austria).
Iron (III) chloride-6 Hydrate, $FeCl_3.6H_2O$, (>99%); $NH_3$ solution (approx. 25 % w/w); gylcine (GLY) from Riedel-de Haen AG; Tartaric acid, $C_4H_6O_6$, (>99.5%) from Merck; research grade Sorbitol ($C_6H_{14}O_6$) from Serva-Feinbiochemica GmbH & Co; methylene blue (microscope quality) from Merck; $CaCl_2.2H_2O$ from Carl Roth Gmbh (Karlsruhe, Germany); sodium D-gluconate (DGL) from Merck (Darmstadt, Germany) were used. From Fluka (Buchs, Switzerland) analytical grade sodium hydroxide, NaOH, (>98 %), microscopy quality of alizarin (1,2-dihydroxy-9,10-anthra-quinone), HCl (25% w/w), analytical grade NaOAc (sodium acetate), analytical grade $CuSO_4.5H_20$ were used.
Under technical conditions for sequestering experiments of $Ca^{2+}$ containing woven lyocell fabrics, from BASF (Ludwigshafen, Germany) Trilon® TA liqu. (aqueous solution of nitrilo-tri-acetic-acid sodium salt) as complexing agent and Kieralon B® hochkonz. as surfactant were used.

## Methods

*Fiber diameter*
The lyocell fibers were swollen in alkali solutions for about 1 min and the diameter of fibers were measured by Reichert projection microscope with a magnification of 500×. Ten fibers were counted and mean value was taken for each type of alkali.

*Alkali retention value (ARV)*
The lyocell fiber samples, 0.5 g in weight, were put into alkali solutions for 2 h at room temperature. The fibers were then centrifuged at 4000× g for 10 min and weighed ($w_w$).The fibers were washed with hot water at 50°C and cold water, then

they were neutralized with the 0.01 M acetate buffer (pH 5) solution, rinsed with hot and cold water again. The fibers were dried in an oven at 105°C for 4h and the weight was measured ($w_d$). ARV was calculated by ARV = [( $w_w$- $w_d$)/ $w_d$] ×$d_{alk.}$ where $d_{alk.}$ is the density of alkaline solution. The measurement was repeated four times for each sample to obtain mean value.

*Splitting test (Öztürk et al. 2006a)*
Crockmeter is used in order to apply defined shear force onto the fiber so that swollen lyocell fiber can be splitted into its macrofibrils. Crockmeter was modified by putting a 0.5 kg weight on the rubbing arm so that total downward force on fiber was 13.9 N with a downward pressure of 34.8 kPa. The arm of tester was turned in clockwise irection between 0-90 for 10 times in 10 s so that rubbing arm moves in a straight line on the microscope slide. The photos of the fibers were taken at 500× magnification by Reichert optical microscope and the number of splitted fibers were counted. To evaluate the degree of splitted fibers, numbers were used. The number 0 means no splitting was observed. One means the fiber is unique but some line/cracks on fiber were observed. Two and more numbers represent how many splits were counted from the photos of fibers. Three fibers were tested for each type of alkali so that average was calculated.

*Impregnation and extraction of $Ca^{2+}$*
A mass of 2 g woven lyocell fabric was extracted with 50 ml 5 % HCl at 40°C for 1 h to remove $Ca^{2+}$. The samples were rinsed with water, neutralized in a solution of 1 g/l NaOAc and line dried.

Samples of 2 g mass were impregnated in 80 ml buffered $CaCl_2.2H_2O$ solution for 1 h at 40°C. The $Ca^{2+}$ concentration in the solutions ranged from 1 to 8 mM. The $Ca^{2+}$ uptake was studied at pH 5 and pH 9. A mixture of acetic acid and ammonia was used as buffer (the pH of a solution of 9 mM acetic acid was adjusted 5 or 9 by addition of 1 M $NH_3$ solution). After impregnation the samples were washed 3 times with water.

*Determination of $Ca^{2+}$*
Removal of $Ca^{2+}$ from the impregnated fabric (woven lyocell) was performed in 5 % HCl solution. A mass of 1 g fabric was treated with 25 ml 5 % HCl at 40°C for 1 h to dissolve $Ca^{2+}$. The filtered solutions were diluted with 5 % HCl and analysed by atom emission spectroscopy (AES). At least two repetitions were made for the determination of the $Ca^{2+}$ content in the woven fabric. The $Ca^{2+}$ content were determined in raw fabric and in fabrics after $Ca^{2+}$ removal with 5 % HCl.
$Ca^{2+}$ was determined by AES using a Hitachi Polarized Zeeman Absorption Spectrometer in the emission mode (wavelength 422.7 nm, Air-$C_2H_2$ flame). For calibration a 100 mg/l $Ca^{2+}$ stock solution of $CaCl_2.2H_2O$ was diluted with 5 % HCl to obtain standard solutions in the range of 0.1-1 mg/l $Ca^{2+}$.

*Color strength (K/S) (Fitz-Binder and Bechtold 2009)*
About 0.5 g of $Ca^{2+}$ impregnated woven lyocell fabric was dyed at liquor ratio of 1:100 in a solution of 0.05 g/l alizarin in 0.1 M NaOH for 1 h at room temperature. The samples were then rinsed three times in a solution of 4.7 mM $Na_2CO_3$. Exhaustion of alizarin was monitored by photometry of the dyebath, color depth of dyed samples was characterized K/S values.

K/S of the dyed fabrics was determined according to Kubelka-Munk function (Kubelka 1948, Kubelka 1954). The K/S values were calculated from the reflectance determined at the absorption maximum at 545 nm (one beam spectrophotometer Specord 50, Analytik Jena, Germany, diffuse reflectance sphere 8°/d).

*Preparation of $Cu^{2+}$-DGL complex solutions (Kongdee and Bechtold 2009)*
0.01 M stock solutions of $Cu^{2+}$ salt and 0.02 M DGL solution were prepared and mixed with 0.1 M GLY to buffer pH. Kongdee and Bechtold 2009 shows the composition of the complex solutions.
A precise weight about 0.5 g of cotton yarn was subjected to 100 ml of $Cu^{2+}$-DGL complex solution for 24 h at 60°C. The samples were then washed in distilled water and dried at room temperature. Two repetitions of each experiment were done and average values of heavy metal content are given.

*Analysis of $Cu^{2+}$ content in cotton yarns (Kongdee and Bechtold 2009)*
The $Cu^{2+}$-DGL treated samples were extracted with 25 ml of 6 M HCl at 85°C for 60 min. The extraction of $Cu^{2+}$-DGL/GLY treated samples were performed at 90°C for 30 min. The volume of the extract was made up to 50 ml with distilled water. Heavy metal content of the properly diluted solution from $Cu^{2+}$-DGL solutions was determined using inductively coupled plasma-mass spectrometer (ICP-MS) (Agilent 7500 Series). AAS (Hitachi Polarised Zeeman AAS spectrophotometer Z-8230, Inula, Vienna, Austria) was used for $Cu^{2+}$ content analysis from $Cu^{2+}$-DGL/GLY solutions.

*Preparation of FeTNa solution (Vu-Manh et al. submitted)*
FeTNa solutions were prepared with a mole ratio between $FeCl_3.6H_2O$: Tartaric acid as 1:3.275. The concentration of Fe ion varied from 0.15 M to 0.55 M. Additionally 0.4, 0.8, 1.25, 2.5, and 5 M free NaOH were used.
All solutions were prepared by following 'direct procedure' without isolation of an intermediate (Bayer 1964; Valtasaari 1957). To exclude light a weighed amount of tartaric acid was introduced into a dark bottle which contains magnetic stirring bar. Tartaric acid was dissolved in slightly more than the minimum amount of water. Ferric (III) chloride was quantitatively added to the solution with a few milliliters of water. After brief agitation, the dark bottle was introduced into a cooling bath to decrease the temperature of the mixture to about 0°C. NaOH solution was introduced dropwise to the mixture. The addition rate of NaOH was adjusted to prevent the temperature of the mixture from exceeding about 15°C.

## Results and Discussion

### Swelling of lyocell fibers in alkali metal hydroxides (Öztürk et al. 2006a, Öztürk et al. 2006b)

Figure 1 represents the optical microscope pictures of splitting of one lyocell fiber into different split numbers after swelling in different concentrations of NaOH.

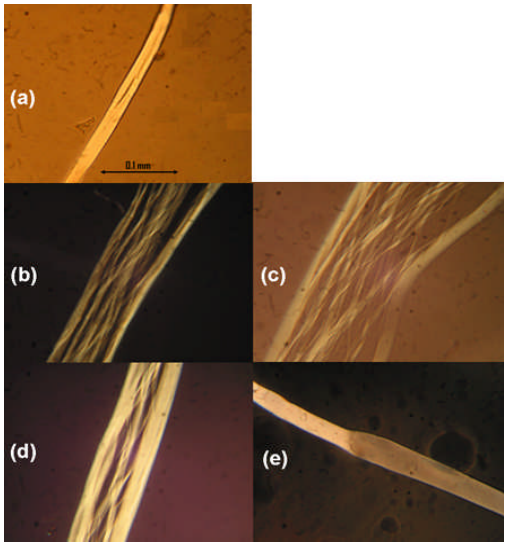


**Figure 1.** Lyocell fiber swollen and splitted in (a) 0.5 M NaOH, split number is 1 (b) 2 M NaOH, split number is 6 (c) 2.5 M NaOH, split number is 15 (d) 3 M NaOH, split number is 3 (e) 8 M NaOH, no splitting (Öztürk et al. 2006a).

Figure 2 shows the relation between split number and alkali concentration of lyocell fiber after swelling in LiOH, NaOH, KOH and TMAH. Up to 5 M different split numbers were observed depending on alkali type. This shows that at the same concentration the penetration of various alkali types into lyocell fiber is different. Above 5 M irrelevant to alkali type, no

split was observed. Above 5 M, homogeneous distribution of alkali occurs resulting in decrease in swelling stress and also no split.

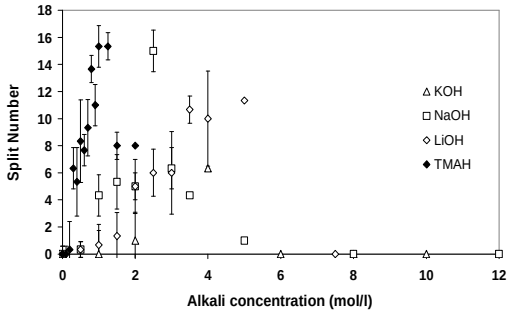


**Figure 2.** Split number of lyocell fiber as a function of concentration in different alkali solutions (Öztürk et al. 2006b).

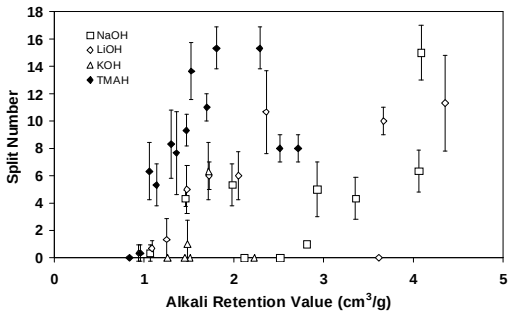


**Figure 3.** Split number of lyocell fiber as a function of alkali retention value (ARV) (Öztürk et al. 2006b).

Figure 3 shows the relation between split number and alkali retention value (ARV) of lyocell fiber. Different split numbers were found for LiOH, NaOH, KOH and TMAH at the same ARV. For example, around 1.5 $cm^3/g$ ARV the split number of lyocell was as following: TMAH>LiOH>NaOH>KOH. Same ARV of fiber in different alkali types indicates the same swelling degree but the different split numbers shows the difference in distribution of alkali inside the fiber. ARV is a bulk property indicating average swelling whereas splitting indicates the local situation of alkali due to swelling stress inside fiber. Thus up to 5 M alkali concentration, the splitting is influenced by cation modulated accessibility of alkali.

**Electrostatic interaction (Ion exchange mechanism) between a metal ion and cellulosic material (Fitz-Binder and Bechtold 2009)**

Figure 4 shows the relation between $Ca^{2+}$ amount in treatment solution and $Ca^{2+}$ amount found in woven lyocell fabric after its extraction. As the $Ca^{2+}$ concentration in the treatment solution increased, the amount of $Ca^{2+}$ found in lyocell fabric also increased. The $Ca^{2+}$ amount found in woven lyocell fabric is limited by the carboxyl group content of the material which is around 20 mmol/kg.

The basic mechanism for $Ca^{2+}$ sorption on a cellulosic material is ion exchange mechanism. The $Ca^{2+}$ amount found in woven lyocell fabric at pH 9 was found to be higher compared to that found at pH 5. This is due to the higher amount of negatively charged carboxyl groups found at higher pH. The ion exchange mechanism at pH 9 follows equation (1).

$$\text{Cell-COO}^- + Ca^{2+} + X^- \leftrightarrows \text{Cell-COO}^- Ca^{2+} X^- \quad (1)$$

At lower pH, partial protonation of cellulose occurs so that degree of carboxyl group dissociation reduces. At pH 5, both equation (1) and equation (2) occur.

$$\text{Cell-COOH} + Ca^{2+} + X^- \leftrightarrows \text{Cell-COO}^- Ca^{2+} X^- + H^+ \quad (2)$$

Alizarin marks $Ca^{2+}$ by complex formation (Fitz-Binder and Bechtold 2009). $Ca^{2+}$ and $Mg^{2+}$ ions, which arise partly from the hard water and sometimes also from soil and fabrics, should be removed during laundry. Otherwise they tend to form precipitates on the cellulosic material during laundry.

Figure 5 shows a practical example for the removal of $Ca^{2+}$ using ingredients of a detergent separately. Since the woven lyocell fabric contained a rather high amount of $Ca^{2+}$, it showed the highest color strength due to the complexation between $Ca^{2+}$ and alizarin. After washing the fabric in deionised, only a slight decrease in $Ca^{2+}$ content of the fabric was observed. Little decrease was also

observed after washing lyocell fabric with surfactant or alkali. A significant decrease in $Ca^{2+}$ amount of fabric was observed when complexing agent was used.
During household laundry usually complexing agent is present in the wash bath. Hard water is used for rinsing, thus $Ca^{2+}$ amount in the fabric increases again during the rinse operation.

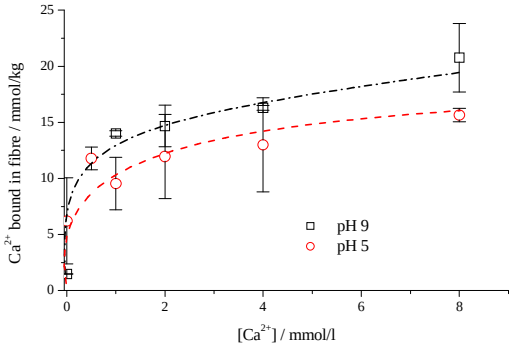


**Figure 4.** $Ca^{2+}$ binding in woven lyocell fabric as function of $Ca^{2+}$ concentration in impregnation solution (Fitz-Binder and Bechtold 2009).

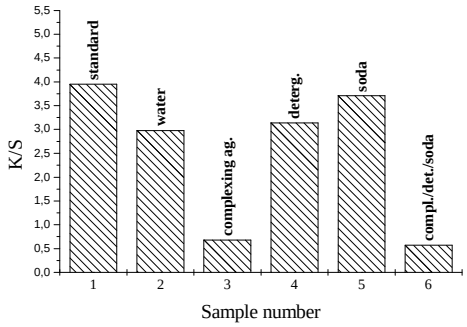


**Figure 5**. K/S values (545 nm) of the alizarin dyed woven lyocell fabric. Sample 1: desized woven lyocell fabric, 2: water treated, 3: complexing agent treated, 4: surfactant treated, 5: NaOH treated, 6: complexing agent/surfactant/NaOH treated (Fitz-Binder and Bechtold 2009).

Cation uptake via ion exchange mechanism is of importance for a wide range of applications such as:

- processing of pulp and cellulose fibers in paper and textile industry
- use of cellulose substrates as carriers for food enrichment with minerals and medical applications
- sorption of heavy metals from water on polysaccharide materials
- textile dyeing operations (dyestuff precipitates with hardness)
- household laundry
- formation of metal anchors as fixed complexing sites on the polysaccharide substrate
- mordant dyeing with natural dyes (e.g. alizarine complexes with $Ca^{2+}$)

## Metal complexation

In a first step complexes of metal ion ($Fe^{3+}$, $Cu^{2+}$, etc) and co-ligand (ammonia, ethylenediamine, tartaric acid, etc) are formed in the solution. When cellulose (ligand) is introduced into the treatment bath, a competition between insoluble polysaccharide ligand and soluble co-ligand occurs. When the metal ion is able to form a complex with the polysaccharide matrix and the stability of metal ion/co-ligand complex is sufficient weak, an metal exchange between ligand and co-ligand occurs. Equations 3 to 6 show the reaction model for metal complexation of cellulose where DGL is D-gluconate, GLY is L-glycine. Equations 3 and 4 show complex formation between metal ion and co-ligand (DGL or GLY). Equations 5 and 6 show the metal exchange reaction, which is dependent on pH (bold marked). In order to have a complex formed between metal ion and ligand (cellulose), stability of complex (metal ion/co-ligand) in the solution and pH (**bold** marked in equation 5 and 6) are important parameters.

$$p\ M^{2+}(aq)+q\ DGL \rightarrow [Mp^{2+}(DGL)_qH_{-r}]^{(q+r-2p)-}+r\ H^+ \quad (3)$$

$$p'\ M^{2+}(aq)\ +\ q'\ GLY \rightarrow [Mp'2+(GLY)_{q'}H_{-r'}]^{(q'+r-2p')-}+r'\ H^+ \quad (4)$$

$$p\ Cellulose + x\ [M_p^{2+}(DGL)_qH_{-r}] \rightarrow p\ [M_x^{2+}(Cellulose)H_{-y}]^{(y-2x)-} + qx\ DGL + \mathbf{(yp - xr)H^+} \quad (5)$$

$$p'\ Cellulose + x\ [M_{p'}^{2+}(GLY)_{q'}H_{-r'}] \rightarrow p'[M_x^{2+}(Cellulose)H_{-y}]^{(y-2x)-} + q'x\ GLY\ \mathbf{(yp' - xr')H^+} \quad (6)$$

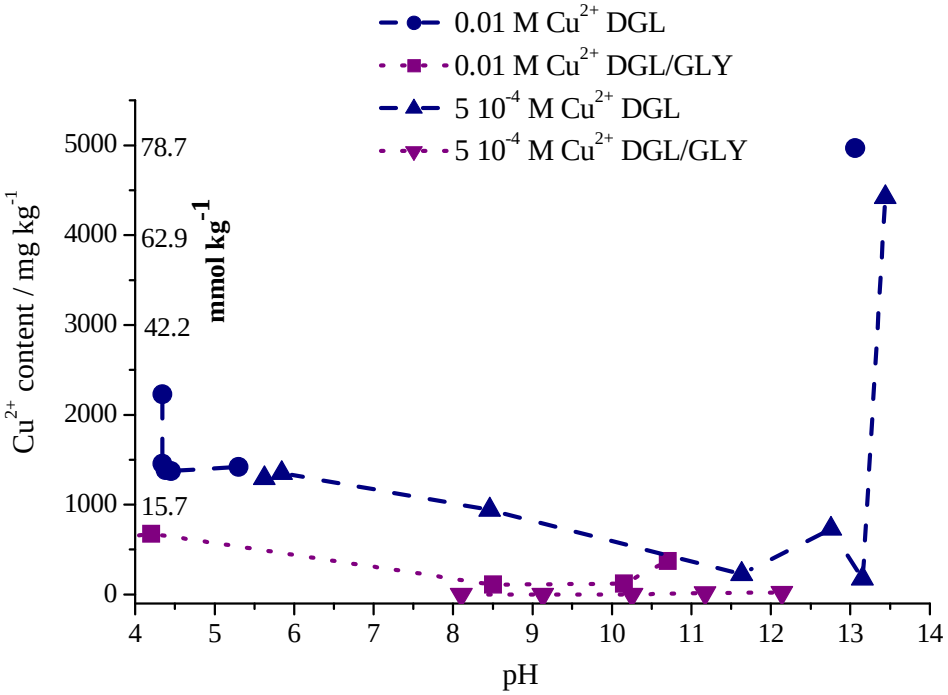


**Figure 6.** Complexation of $Cu^{2+}$ ions as function of pH (Kongdee and Bechtold 2009).

The insertion of heavy metal ions into insoluble polysaccharide matrices can be controlled by selection of:

- metal ion e.g. $Fe^{2+}$, $Co^{3+}$, $Zn^{2+}$, $Cu^{2+}$, etc.
- oxidation number of metal ion e.g. $Fe^{2+}$, $Fe^{3+}$
- polysaccharide matrix e.g. cellulose, chitosan, amylase, etc.
- co-ligand (ammonia, ethylenediamine, tartaric acid, etc) in solution
- experimental conditions e.g. pH, temperature, time, etc.

*Complexation of $Cu^{2+}$ on cotton yarns as function of pH (Kongdee and Bechtold 2009)*

Figure 6 shows $Cu^{2+}$ the amount found in cotton yarns after treatment with $Cu^{2+}$ complexes having either DGL or DGL/GLY as co-ligands. Higher amount of $Cu^{2+}$ was found in cotton when DGL was used as co-ligand which shows the complex stability of $Cu^{2+}$-DGL is lower than $Cu^{2+}$-DGL/GLY. The lower complex stability of $Cu^{2+}$-DGL compared to $Cu^{2+}$-DGL/GLY results in easier exchange of ligand (cellulose) and co-ligand (DGL).

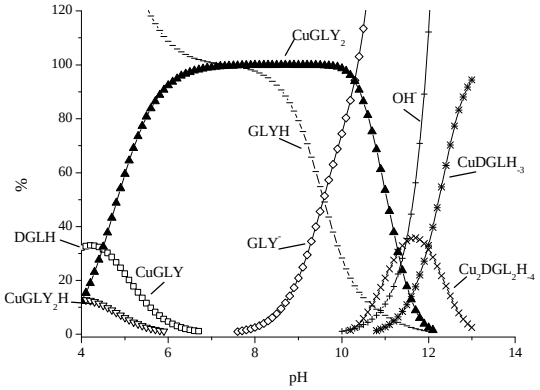


**Figure 7.** Calculated species distribution of the $Cu^{2+}$-DGL/GLY system as function of pH ($Cu^{2+}$ concentration as denominator for 100 %) (Kongdee and Bechtold 2009).

Figure 7 shows calculated species distribution of $Cu^{2+}$-DGL/GLY system as function of pH. SPE program was used to calculate species distribution while using formation constants of complexes from literature. The presence of $CuGLY_2$ increased up to pH 6, above which it leveled off up to pH 10, and got lower up to pH 12. Above pH 11, the presence of $CuDGLH_{-3}$ increased with increase in pH.

The high $Cu^{2+}$ amount found in cotton yarns at around pH 13 (Figure 6) can be attributed to the presence of Cu-DGL complex in the solution found by species distribution (Figure 7).

*Swelling and dissolution studies on lyocell fibers by using FeTNa (ferric tartaric acid complex in the presence of alkaline aqueous solution) (Vu-Manh et al. submitted)*

FeTNa is a common cellulose solvent and has many advantages such as

- it is non-toxic,
- cellulose degradation by air oxygen is very low,
- numerous variability in concentration of Fe and free NaOH is possible in order to get different phases of cellulosic material e.g. swelling, dissolution, disintegration, etc.

The optimum combining mole ratio of iron to tartrate in the FeTNa solution was found to be 1 to 4.5. The 1:3 ratio is found to be the most stable one and has a green color which is used as solvent for wood pulp and other cellulosic materials (Heinze and Wagenknecht 1998). The ligand deficiency at 1:3 ratio is filled by the glycol pair of hydroxyl groups on carbon atoms two and three on the glucopyranoside repeating unit of cellulose to fulfill 1:4.5 ratio which is the optimum one (Bayer 1964).

Figure 8 shows changes in the morphology of lyocell fibers depending on Fe and free NaOH concentration. At lower NaOH concentrations (0.4 M), limited swelling was observed which is comparable to swelling in pure water. At higher free NaOH concentrations (0.8 and 1.25 M), disintegration of fibers was observed. Around 2.5 M free NaOH, dissolution of fibers was found. At 5 M free NaOH, uneven-uniform swelling occurred when Fe concentration was 0.4-0.5 M. Excess increase in fiber diameter so that fiber diameter could not be measured by microscope (blooming) was observed at 5 M free NaOH and when Fe concentration was up to 0.45 M.

Figure 9 shows morphology of lyocell fiber *during* FeTNa treatments.

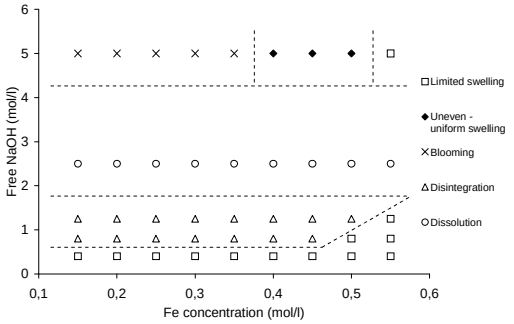


**Figure 8.** Swelling-dissolution diagramm of lyocell fibers for 10 min swelling in FeTNa solutions with varying Fe and free NaOH concentration (Vu-Manh et al. submitted).

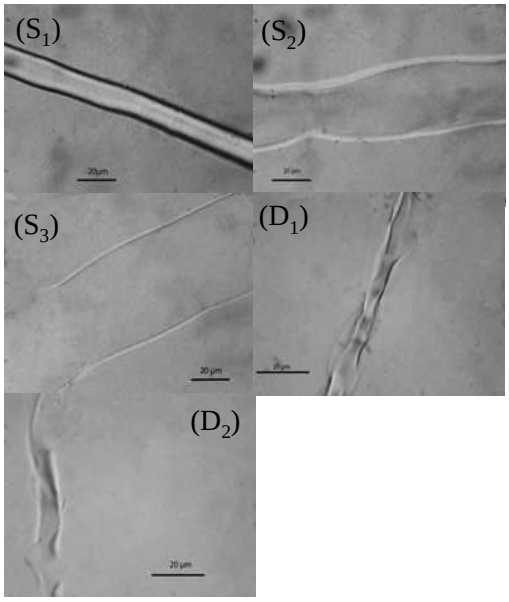


Figure 9 Morphology of lyocell fiber *during* FeTNa treatments: $S_1$ symbolizes uniform swelling at a low degree comparable to that of in pure water; $S_2$ denotes uneven swelling proceeding into $S_3$, i.e. uniform swelling at a high degree; $D_1$ and $D_2$ are time dependent disintegration of a fiber into rod-like fragments (Vu-Manh et al. submitted).

## Conclusions

A huge number of new products and applications for metal-polysaccharide interaction is available. This can be achieved by

- modification of cellulosic materials in order to modify porosity,

accessibility, sorption properties of the cellulosic material
- incorporation of metal ions at well defined conditions e.g. single metal ion insertion without precipitation, pigment coloration, catalytic properties, dietary fibers and food applications, fibers with antimicrobial acitivity ($Ag^{+}$, $Cu^{2+}$, etc), fibers containing anchors for binding of organic substances e.g. alizarine
- dissolution of cellulose by metal-ligand complexes in order to form fibers, films or amorphous precipitates.

**References**

Bayer F (1964) A study of the iron-tartrate-alkali system and its complexing reaction with cellulose-related polyhydroxy compounds, PhD Thesis, Lawrence University, Appleton, Wisconsin.

Fitz-Binder C, Bechtold T (2009) Sorption of alkaline earth metal ions $Ca^{2+}$ and $Mg^{2+}$ on lyocell fibres, *Carbohydrate Polymers* 76 123-128.

Heinze U, Wagenknecht W (1998) Comprehensive cellulose chemistry. Vol. 2, Wiley-VCH Verlag GmbH, Weinheim.

Kotelnikova N, Vainio U, Pirkkalainen K, Serimaa R (2007) Novel approaches to metallization of cellulose by reduction of cellulose-incorporated copper and nickel ions. *Macromolecular Symposia*, 254: 74-79.

Kongdee A, Bechtold T (2004a) The complexation of Fe(III)ions in cellulose fibres - A fundamental property. *Carbohydrate Polymers, 56,* 47-53.

Kongdee A, Bechtold T (2004b) In-fibre formation of $Fe(OH)_3$ - A new approach to pigment coloration of cellulose fibres. *Dyes and Pigments, 60,* 139-144.

Kongdee A, Bechtold T (2009) Influence of ligand type and solution pH on heavy metal ion complexation in cellulosic fibre: model calculations and experimental results. *Cellulose* 16 53-63.

Kubelka P (1948) New contributions to the optics of intensely light-scattering materials, Part I, *JOSA* 38 (5) 448-451.

Kubelka P (1954) New contributions to the optics of intensely light-scattering materials, Part II: non-homogeneous layers, *JOSA* 44 (4) 330-335.

Öztürk HB, Okubayashi S, Bechtold T (2006b) Splitting tendency of cellulosic fibers; part 1: the effect of shear force on mechanical stability of swollen lyocell fibers. *Cellulose* 13(4): 393-402.

Öztürk HB, Okubayashi S, Bechtold T (2006b) Splitting tendency of cellulosic fibers; part 2: effect of fibers swelling in alkali solutions. *Cellulose* 13(4): 403-409.

Urbano MG, Goi I (2002) Bioavailability of nutrients in rats fed on edible seaweeds, Nori (Porphyra tenera) and Wakame (Undaria pinnatifida), as a source of dietary fibre. *Food Chemistry*, 76/3: 281-286.

Vainio U, Pirkkalainen K, Kisko K, Goerigk G, Kotelnikova NE, Serimaa R (2007) Copper and copper oxide nanoparticles in a cellulose support studied using anomalous small-angle X-ray scattering. *European Physical Journal D*, 42/1: 93-101.

Valtasaari L (1957) The improvement of cellulose solvents based on iron-tartaric acid complex. *Paperi ja Puu* 39: 243-248.

Lenzinger Berichte 87 (2009) 152-162

# SUB-MICROMETER STRUCTURED TEXTILE COATINGS GENERATED FROM CELLULOSE BASED POLYMER BLENDS*

**Kristin Trommer[1], Bernd Morgenstern[1], Frank Gähr[2] and Frank Hermanutz[2]**

[1]Forschungsinstitut für Leder und Kunststoffbahnen gGmbH, D-09599 Freiberg, Germany
[2]Institut für Textilchemie und Textilfasern der Deutschen Institute für Textil- und Faserforschung Denkendorf, D-73770-Denkendorf, Germany

Phone: +49 3731-366-166; Fax: +49 3731-366-130; E-mail: bernd.morgenstern@filkfreiberg.de

*Parts of this work were presented during the 8th International Symposium "Alternative Cellulose", September 3-4, 2008 in Rudolstadt, Germany .

**In order to provide coated textiles with a hydrophobic and self-cleaning surface attempts were made to create structures similar to lotus leaves by generating sphere-like structures using phase separation of cellulose derivatives/poly-acrylonitrile blend solutions. Morphology of the so formed structures depends on the coagulation conditions. Resulting dimensions of this spherical structures range from 200 nm to 3,000 nm and are influenced by the cellulose derivative substituent, the polymer ratio and the coagulation medium and temperature. In general, blends with cellulose acetate and propionate form smaller spheres than those formed from cellulose carbamate.**
**The polymer blend solutions qualify for coating woven fabrics, particularly for polyamide fibre fabrics. A well-formed surface structure was obtained from CA/PAN blends. The hydrophobicity was enhanced by either adding a fluoro-carbon to the coating compound or finishing with a fluoroalkyl silane. Using the last one a surface energy of minimum 4 mN/m could be achieved.**

**Keywords:** *cellulose derivatives, polymer blends, textile coating, surface structure, hydrophobicity*

## Introduction

Textiles are coated with the goal to create materials with functional properties such as a hydrophobic and self-cleaning surface. Such a coat should prevent protective clothing, tents, tarpaulins and others from soaking by a water-repellent finish. Simultaneously, the material should be breathable and dirt-repellent. In order to provide coated textiles with a super-hydrophobic surface it is tried to generate a coat which imitates the lotus-effect. Methods for formation of surface structures in the sub-micrometer range are, for example, "embossing" [1, 2] and lithographic processes as e. g. "lasering" [3]. However, such surface structures are known to be of minor permanence. Texture formation inside the coat is to overcome this disadvantage. A well-known method is the sol-gel process [4, 5]. A new route to simulate the structure of a lotus leaf is the generation of sub-micrometer scaled spheres by controlled demixing of incompatible polymer blends. In this concept the spheres are seen as irregular structures. Therefore, they may be formed under theoretical based conditions following the mechanisms of phase separation.

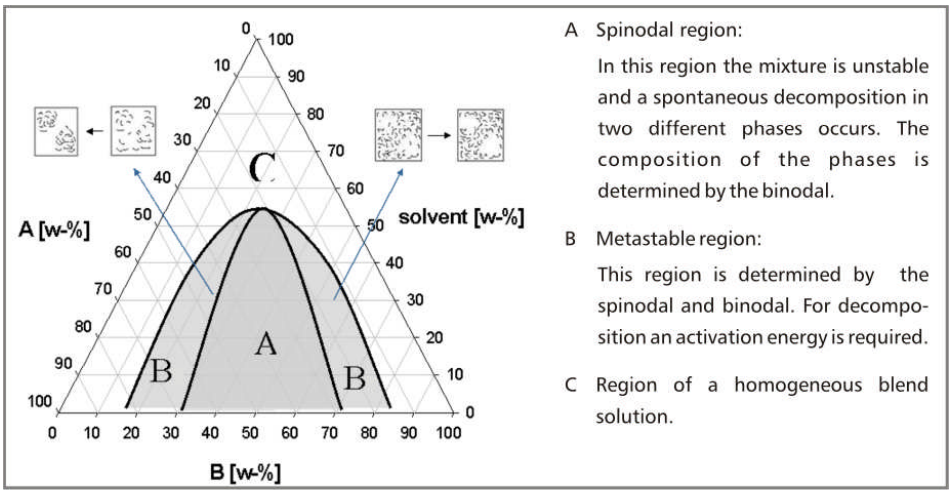


**Figure 1.** Schematic ternary phase diagram (polymer A, polymer B, solvent

A previous publication showed that foils formed by coagulation of a cellulose/polyacrylonitrile blend dissolved in dimethylacetamide/lithium chloride (DMA/LiCl) show spherical structures with an average dimension of about 200 nm over the full cross section [6]. Cellulose is a native polymer of special interest for textile coating because of its outstanding properties, for instance its high sorption capacity. However, multi-component solvents are necessary for processing of polymer blends comprising underivatized cellulose [7]. On the other hand, in a recent study cellulose esters having a low degree of substitution (DS<0.5) could be prepared [8-10]. They show good dissolution behaviour and the cellulosic character remains unchanged. Therefore, spherical structured coating films shall be formed by phase separation of blend solutions containing a low substituted cellulose derivative (CD) and polyacrylonitrile (PAN). The investigations were carried out with cellulose carbamate (CC), cellulose acetate (CA) and cellulose propionate (CP), respectively.

Thermodynamics and kinetics of phase separation are well-known. The knowledge of the phase diagram of the blend solution can be helpful for the definition of conditions of the phase separation process. Diagrams of the system cellulose/PAN/DMA/LiCl are published [6, 11]. A schematic ternary phase diagram is shown in Fig. 1.

Demixing by the nucleation and growth mechanism occurs, if the initially homogeneous polymer blend solution is transferred into the metastable state by solvent removal (evaporation or addition of a precipitating agent) or temperature change. Also, after transfer into the unstable state, irregular structures are developed, if the spinodal decomposition can run up to a late stage, i.e. up to the coalescence [12]. Demixing by this mechanism was observed and comprehensively investigated for example in blends of cellulose with PAN and an aromatic polyamide, respectively [13, 14].

Preconditions for the formation of irregular phase morphology are the existence of a sufficiently high thermodynamic driving force and a high growth rate of the developing domains [15]. These conditions have to be adjusted via the composition of the blend solution, the molar mass and the constitution of the polymers as well as the coagulation conditions (precipitation agent, evaporation temperature).

## Experimental

*Synthesis of cellulose derivatives*

An industrial available alkali cellulose was used for the synthesis of all three cellulose derivatives involved, i. e. carbamate, acetate and propionate. The alkali cellulose is characterized by an average degree of polymerization of 400 (EWN-method), a cellulose content of 32 wt-%, and a sodium hydroxide content of 17 wt-%. The alkali cellulose was stirred in an excess of methanol in order to reduce the alkaline content and to get a so-called inclusion cellulose. The cellulose was drained at 200 hPa. The resulting methanol containing matter could be taken for the synthesis of cellulose derivatives, directly.

The cellulose carbamate was synthesized as follows: Urea was melt in a kneader (135°C). Under a nitrogen atmosphere the inclusion cellulose was added in portions, whereas the formed methanol was distilled off. The ratio of cellulose and urea was 1:8 (wt-%). After a reaction time of 90 min a slightly yellow coloured cellulose carbamate could be isolated. The carbamate showed a consistency which is comparable to alkali cellulose. The carbamate was rinsed with dilute acetic acid, washed with distilled water two times and dried.

Synthesis of cellulose acetate and propionate was performed in a 2-nacked-bottom flask of 5 L. Inclusion cellulose prepared from 300 g alkali cellulose was put in portions into 1.5 L of cool (5 °C) acetic or propionic anhydride, respectively. The reaction mixture was stirred over a period of 60 min whereas the temperature should not exceed 60 °C. The resulting pulp was filtered, washed intensively with distilled water and, finally, freeze-dried.

The degree of substitution and the molecular mass of the obtained cellulose derivatives are given in Table 1.

*Solutions of the cellulose derivatives*

Ground cellulose carbamate (50 g) was slurried in water for 30 minutes. The water was then pressed out at 50 bar using a Polystat 300S filter press. The remaining water was removed completely by solvent exchange with dimethylacetamide. For this end the cellulose carbamate was suspended in DMA and pressed out again. This was repeated three times. Afterwards the cellulose carbamate was dissolved in LiCl/DMA (5 wt-%) under stirring at 50 °C until a clear solution was formed. A typical composition of a cellulose carbamate solution was 7.7 wt-% CC, 4.6 wt-% LiCl and 87.7 wt-% DMA.

Cellulose acetate and cellulose propionate, respectively, were dissolved in a solution of LiCl in DMA (5 wt-%) under anhydrous conditions. After pressure filtration a clear liquid resulted, that is storable for some weeks at low temperature (about 4 °C). Typically, the solution contained 8.7 wt-% of the cellulose derivative and 4.5 wt-% LiCl.

*Polymer blend solutions*

The required amount of powdery PAN having a weight-average molecular mass of 130 kg $mol^{-1}$ was dissolved in the solution of the cellulose derivative under stirring at 30 °C. If the resulting solution was cloudy, some LiCl/DMA (5 wt-%) was added until the solution became clear.

A hydrophobing agent was added to the

**Table 1.** Properties of the synthesized cellulose derivatives.

| ***Cellulose derivative*** | | ***Degree of substitution*** | ***Molecular mass*** |
|---|---|---|---|
| | | - | kg $mol^{-1}$ |
| cellulose carbamate | CC | 0.5 | 58 |
| cellulose acetate | CA | 0.6 | 87 |
| cellulose propionate | CP | 0.3 | 90 |

blend solution and dissolved, too, if its application was intended.

*Preparation of thin polymer films*
The polymer blend solution was cast on a glass plate to a film with a thickness of about 200 µm. The coagulation was carried out either by evaporation of the DMA at a constant temperature in the range between 35 °C and 95 °C or by immersion of the coated glass plate into a precipitation bath consisting of a DMA/water mixture or aceton. After coagulation, the films always were soaked in water for 20 minutes to wash out the LiCl. They were subsequently dried at ambient temperature. The solutions investigated exhibited no insoluble polymer particles under an optical microscope.

*Coating of fabrics*
Woven fabrics were coated using a blade coater. The textile (25x30 cm) was fixed in a pin stenter. The coating compound was applied by means of a doctor blade in a thickness of about 250 µm. The ratio of the used CD/PAN blends was 70/30 and 80/20, respectively. The coagulation was carried out by evaporation of the solvent at 60 °C, 70 °C and 85 °C, respectively. To obtain well-formed coats two layers were applied. The period of solvent evaporation of the first layer was varied between 5 min and 60 min. The second one was ‚dried' 60 min. Following, the LiCl was washed out in water. Finally, the coated textile sample was dried. The obtained coats showed a area mass of about 7.5 g/m².

*Characterization of surface structures*
For examination with a scanning electron microscope DSM 962 (Zeiss), samples were sputtered using gold-palladium. The surface profile was scanned with a Dektak 3ST (Sloan Technology). The following parameters were applied: weight of 1-40 mg, scan length 30-50,000 nm, resolution 0.5 nm.

The surface energy of films and coats was estimated by contact angle measurement of leaving drops using a drop shape analysis system G10/DSA10 (Krüss). Two test liquids were used – water and diidomethane. Calculations were made according the method of Owens.

## Results and discussion

*Structure formation in blend films*
Knowledge about the coexistence curve is fundamental to stipulate experimental parameters for demixing and structure formation in polymer blend solutions. The evaluation of the phase diagram of a cellulose carbamate/polyacylonitrile blend dissolved in dimethylacetamide (with 4 % LiCl) leads to the conclusion that for formation of well-formed sphere-like structures, a total polymer concentration of at least 6 wt-% and a CD/PAN ratio of 70/30-90/10 are recommendable.
The investigations of the basics of structure formation in CD/PAN blends were carried out by means of thin films. In that way the influence of a textile substrate was eliminated. The demixing in cast solution films was initiated by either coagulation in a precipitation bath (DMA/water, acetone) or solvent evaporation at elevated temperature (35-95 °C). A reference sample was prepared from a cast film of a cellulose carbamate solution by coagulation in DMA/water (20/80). The surface of the obtained solid film is smooth (Fig. 2 A).
The polymer blends form three different kinds of structure depending on the coagulation conditions (Fig. 2).
A honeycomb-like structure (B) resulted from coagulation of cast films in acetone. Acetone acts as a hard precipitation agent. Since a high supersaturation the phase separation runs comparatively fast and pins down at an early stage. Solvent evaporation at low temperature (35 °C) resulted in a hole-containing structure (C) which is likely to be inverse to a spheric

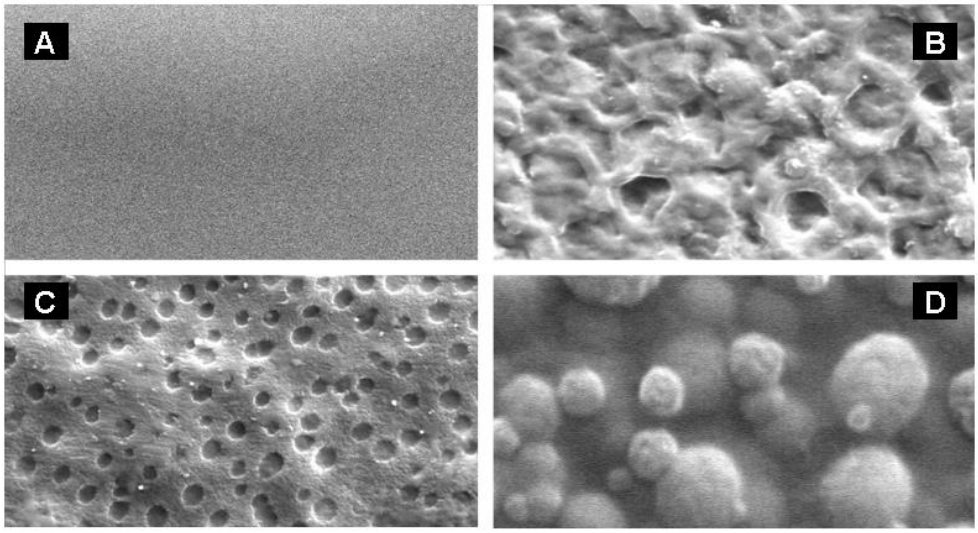


**Figure 2.** SEM photographs of surface structures of polymer films differently generated from CC/PAN solutions.

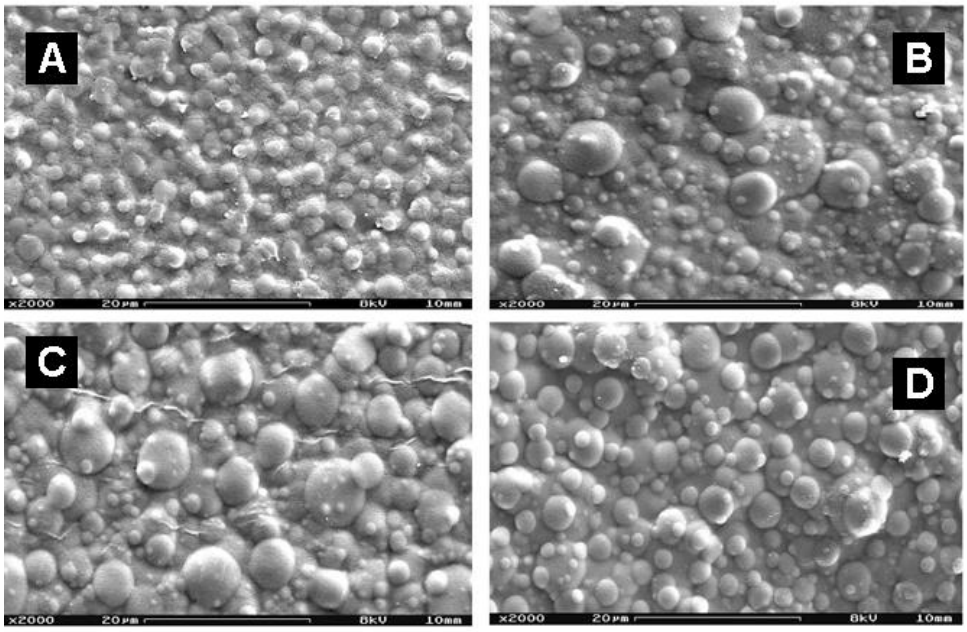


**Figure 3.** SEM photographs of surface structure of (70/30) CC/PAN films obtained after solvent evaporation at different temperature [A – 35 °C, B – 60 °C, C – 70 °C, D – 85 °C].

morphology. The aspired sphere-like structure (D) is obtained due to either coagulation of cast films of blend solutions in DMA/water mixtures, a „soft“ precipitation agent in comparison to acetone, or solvent evaporation followed by final coagulation in water.

That leads to the conclusion that the investigations have to be focussed on a controlled creation of sphere-like structures, in order to imitate a lotus effect. The general influence of the evaporation temperature on the structure dimension is shown in Fig. 3. Films made from 70/30 CC/PAN blend solutions result, at first, in raising domain sizes up to a certain evaporation temperature depending on the system. With further increasing temperature domain sizes are getting smaller. The maximum diameter for the shown 70/30 CC/PAN blend is reached at approximately 70-75 °C. For the evaluation two processes have to be taken into consideration – the growing of the domaines and the evaporation of the solvent. On the one hand a higher temperature leads to a lower viscosity and a higher mobility of the polymer molecules

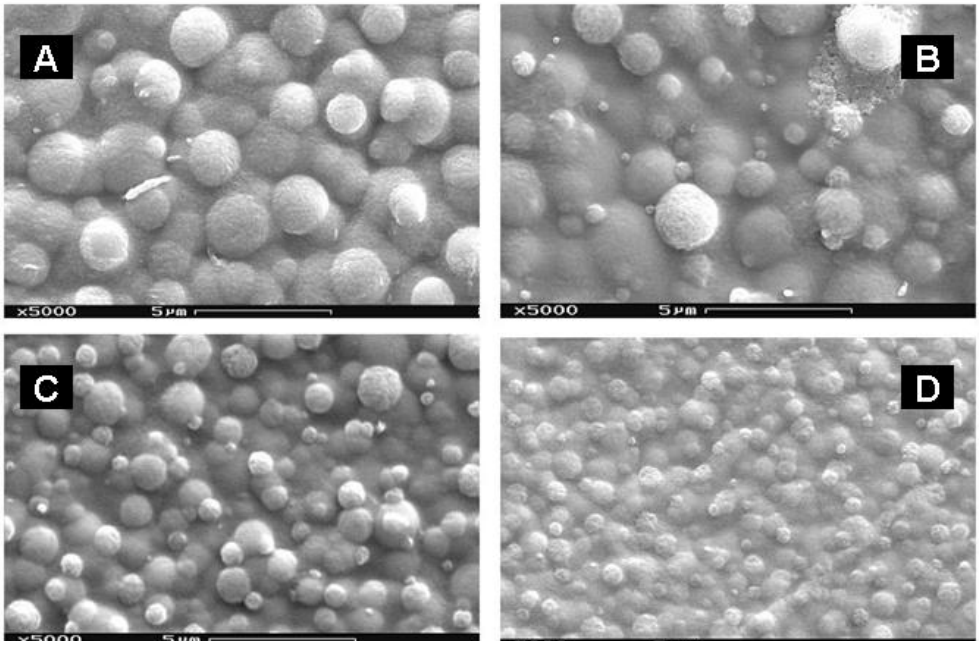


**Figure 4.** SEM photographs of surface of CC/PAN films of different polymer ratio [A - (70/30), B - (80/20), C - (85/15), D - (90/10)].

so that the growth rate of the nucleuses is high. On the other hand it leads to a faster evaporation of the solvent resulting in an increase of viscosity and decrease of mobility. Thus the maximum will be observed.

A distinct effect on the sphere dimension has the polymer ratio. Fig. 4 shows surface structures of CC/PAN films containing 70-90 % cellulose carbamate obtained after solvent evaporation at 60 °C. The higher the fraction of PAN the larger gets the sphere diameter. Blends with a ratio 70/30 led to spheric particles of about 3 µm. In case of 90/10 CC/PAN blends relatively dignified structures with a particle diameter less than 1 µm were obtained. Reason is the lowest thermodynamic driving force in this mixture compared to others having a higher PAN fraction. Last but not least the substituent of the cellulose derivative influences the structure. In the case of 70/30 blends (evaporation of DMA at 85 °C) CC/PAN forms sphere-like domains with up to 3.5 µm, whereas CA/PAN as well as CP/PAN form more dignified and more regular spheres of about 1 µm (Fig. 5).

On the basis of the results shown, so far the coagulation by solvent evaporation was chosen as the favourite method for further investigations as it also allows for easy control of structure size via temperature.

For structures showing a self-cleaning effect the third dimension is important, i. e. their altitude. In general it turned out that the higher the aspect ratio of the structure the better the dewetting behaviour. The altitude cannot be measured using SEM photography. However, a qualitative estimation is possible. Therefore, the real surface structure was measured using a profilometer that mechanically scans the surface profile. However, the profile is measured in one dimension by this method. That means that the analysis of the experimental data in this case is reasonable in connection with an image-guided method (e.g. SEM), exclusively. Figure 6 shows surface profiles and the corresponding SEM photographs of spherical structured samples obtained via solvent evaporation at various temperatures. The altitude of the surface profile depends significantly on the evaporation temperature, in a similar way as already described referring to the

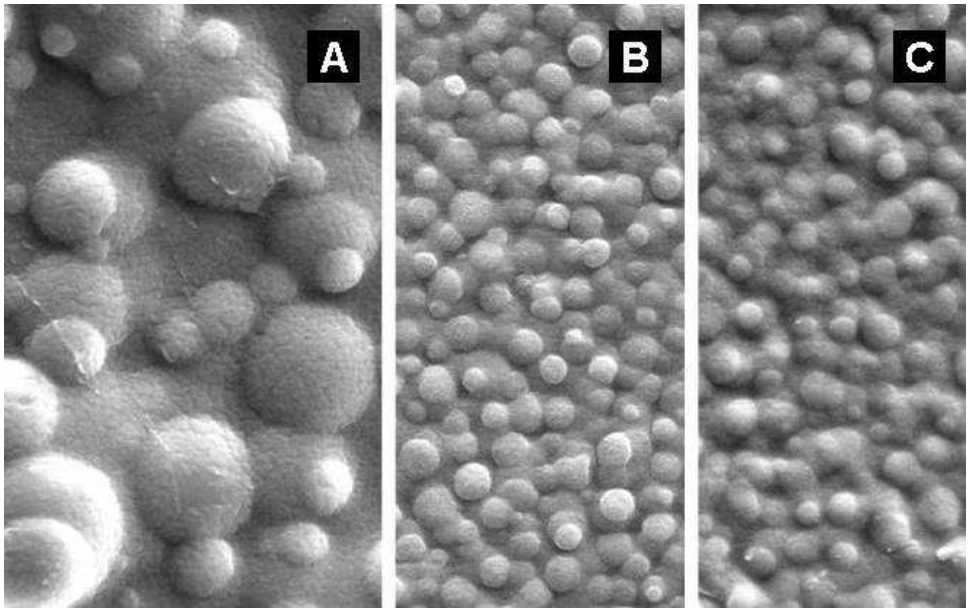


**Figure 5.** SEM photographs of surface structure of (70/30) CD/PAN films after solvent evaporation at 85° C [A - CC/PAN, B - CA/PAN, C – CP/PAN].

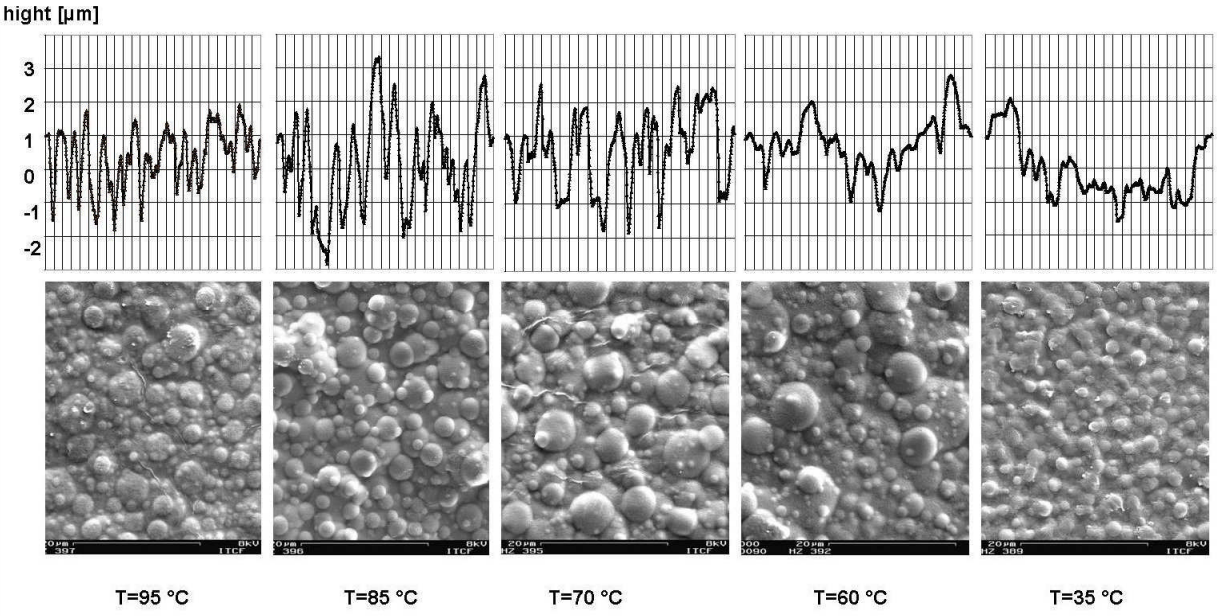


**Figure 6.** SEM photographs and surface profiles of films obtained from CC/PAN (70/30).

temperature influence on the plane structure dimension. The most structured surface and thus the most favourable altitude profile for the aspired effect was obtained at 85 °C. This evaporation temperature was optimal also for other blend compositions, so that it remained unchanged for the coating of textiles.

Surface structures having a high aspect ratio may influence the wettability. In case of a high water contact angle (>90°) dewetting properties are improved. However, the contact angle of the surface of the CD/PAN films was found to be lower than 90°. The polymer blend is not hydrophobic enough and the structured surface does not improve dewetting. Therefore, three different methods were applied to make the surface more hydrophobic: the addition of a fluorocarbon to the coating mass, the application of a fluoralkyl silane finish and

**Table 2.** Surface energy of polymer films obtained from cellulose carbamate and CC/PAN blend, respectively, after hydrophobing.

| ***Sample composition*** | ***CC*** | | ***CC/PAN (80/20)*** | |
|---|---|---|---|---|
| ***Hydrophobing method*** | ***Total surface energy*** | ***Polar part*** | ***Total surface energy*** | ***Polar part*** |
| | mN/m | mN/m | mN/m | mN/m |
| without | 58.2 | 31.2 | 48.0 | 19.7 |
| fluorocarbon additiv | 48.0 | 19.7 | 32.0 | 0.1 |
| fluoralkyl silane finish | 20.5 | 8.3 | 11.4 | 0.3 |
| plasma treatment | 30.2 | 0.1 | 27.6 | 0.0 |

the application of a hydrophobic finish via plasma treatment. Table 2 provides the results.

The surface energy of smooth reference samples (58 mN/m) was decreased after hydrophobing. The minimum surface energy of about 20 mN/m was obtained by finishing with fluoroalkyl silane. The effect is more evident in the case of the blend films (CC/PAN 80/20) showing a surface structured in the sub-micron level. The surface energy even drops from 48 mN/m to about 11 mN/m. In this case the water contact angle varies from 110° to 120°. However, the surface energy has not been significantly influenced by differences in structure dimensions, which were in the range from 0.5 µm to 4 µm.

*Coated fabrics*

The most successful coagulation conditions found out in thin film preparation were applied for the coating of woven fabrics. A polyamide fibre based fabric was chosen as the substrate from pre-tests. The coating compound was cast in two steps to provide reproducibility. Coats made from CC/PAN blends are inhomogeneous. Well-structured domains exist in cavities of the fabric, whereas on top of the filaments the structure is plain. Besides the aspired spherical shapes an inverse structure is observed (Fig. 7). Contrary, the coating with CA/PAN and CP/PAN blends, respectively, resulted in steady coats with a regular structure. The filaments are completely embedded, dewetting does not occur. The obtained structures are smaller (about 1 µm) in comparison to the CC/PAN coat. This phenomenon is caused by the higher polymer concentration of the CA/PAN and CP/PAN coating compounds (up to 9.5 wt-%) in contrast to the CC/PAN system (6 wt-%).

Looking at the increase of the hydrophobicity of the textile coats they were modified by means of a fluorocarbon additive and a fluoroalkyl silane finish, respectively. The advantage of using fluorocarbons is the easier processing. The fluorocarbon is added to the coating compound, no additional processing step is necessary. The expected structures will be formed during the coating process, too. The fluoroalkyl silane has to be applied in a downstream process. It forms a monomolecular layer on the surface, making sure that the sub-micrometer scaled structure is not levelled by the finish. A variety of evaporation conditions was applied during the investigation (see Table 3).

Both methods turned out to be efficient to enhance the hydrophobicity. However, the obtained materials show quantitatively different surface properties.

As a measure of the hydrophobing effect of the fluorocarbon additive as well as the fluoroalkyl silane the water contact angle and the surface energy of the coated fabrics were determined. Coating of the polyamide fibre based fabric with modified coating compounds resulted in coats with a surface

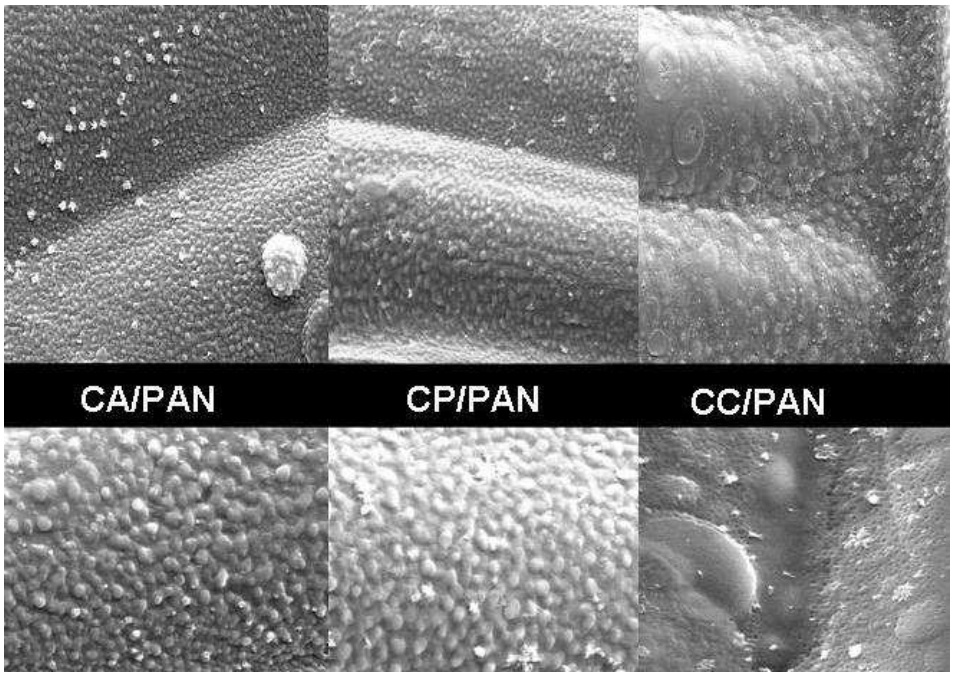


**Figure 7.** SEM photographs of CD/PAN coated polyamide fabrics. Top: evenly coated filaments in the cases CA/PAN and CP/PAN, heterogeneous structure in case of CC/PAN. Bottom (magnification): microstructure of CA/PAN and CP/PAN, inverse domains of CC/PAN.

structure (shape and size) described for the unmodified systems. The contact angles of all samples (Table 3) are much higher than the angles found for fabrics coated with a pure cellulose derivative and visibly higher than those obtained for fabrics coated with a blend without the additive. In case of 80/20 blends the water contact angle increases in the order CC/PAN < CA/PAN < CP/PAN. The surface energy was found to be in a range from 26 mN/m to 39 mN/m depending from the cellulose derivative, i. e. a relatively small decrease in comparison to the unmodified coats. The dewetting behaviour of coated fabrics modified with flourocarbon does not significantly depend from the used coagulation conditions. Solvent evapo-

**Table 3.** Surface properties of polyamide fibre based fabrics coated with CD/PAN (80/20) in dependence on the coating conditions.

| ***Sample composition*** | | ***CC/PAN*** | | ***CA/PAN*** | | ***CP/PAN*** | |
|---|---|---|---|---|---|---|---|
| ***Hydrophobing agent*** | ***Evaporation conditions*** | ***Contact angle*** | ***Surface energy*** | ***Contact angle*** | ***Surface energy*** | ***Contact angle*** | ***Surface energy*** |
| | | ° | mN/m | ° | mN/m | ° | mN/m |
| without (CD) | 5’ + 60’ at 85 °C | 37 | 59 | 67 | 42 | 79 | 37 |
| without (blends) | 15’ + 60’ at 85 °C | 87 | 38 | 91 | 35 | 75 | 39 |
| fluorocarbon | 5’ + 60’ at 60 °C | 93 | 29 | 98 | 34 | 110 | 36 |
| | 5’ + 60’ at 70 °C | 93 | 33 | 100 | 26 | 107 | 39 |
| | 5’ + 60’ at 85 °C | 97 | 30 | 103 | 24 | 110 | 36 |
| | 10’ + 60’ at 85 °C | 97 | 28 | 105 | 34 | 111 | 35 |
| | 20’ + 60’ at 85 °C | 99 | 30 | 101 | 33 | 109 | 36 |
| | 60’ + 60’ at 85 °C | 95 | 32 | 96 | 29 | 103 | 30 |
| fluoralkyl silane | 5’ + 60’ at 85 °C | 131 | 4 | 122 | 7 | 116 | 7 |

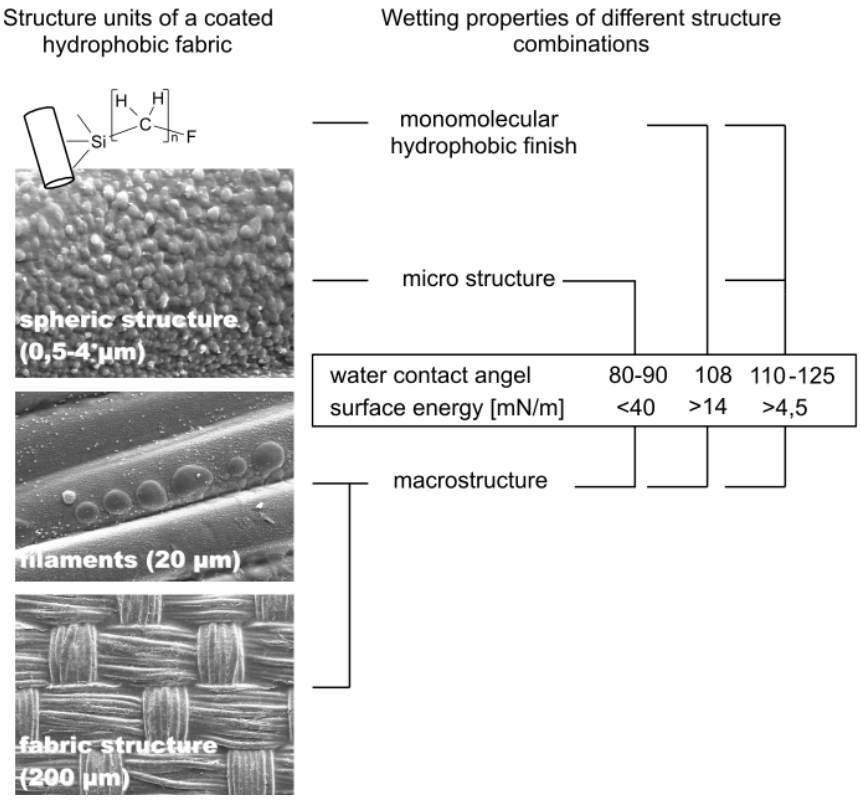


**Figure 8.** Size and wetting properties of the structure units of coated hydrophobic fabrics.

ration for 5 min at 85 °C for the first cast coat and 60 min at the same temperature for the second coat followed by a washing step turned out to be utmost suitable taking into consideration the results of surface inspection by SEM as well as the technical feasibility.

More obvious effects were observed for samples with a flouroalkyl silane finish. Water contact angels of 116-126 degree were obtained. The surface energy is very low ranging from 15 mN/m down to about 5 mN/m. In this case there is an optimal interplay of different structure units of the coated fabrics. Fig. 8 shows that only the combination of a macrostructure formed by fibres and weave texture, a microstructure formed by the CD/PAN coat, and a monomolecular layer of the flouroalkyl silane results in a high water contact angle and a minimum of surface energy. This phenomenon corresponds to constitution and wetting behaviour of a lotus leaf. In contrast to the lotus effect, water drops do not roll up. The reason is the cellulose-like behaviour of the coats. In despite of the hydrophobic finish, the water drop swells the surface and adheres to the contact area. Nevertheless, these fabrics are highly dirt-repellent against fluids like oil as well as aqueous solutions.

## Conclusions

Phase separation of polymer blend solutions comprising a cellulose derivative and polyacrylonitrile offers an attractive method to design textile coatings with a tailored surface. Shape and size of the sub-micrometer-scaled structure are influenced by the blend composition and the rate of solvent removal. Sphere-like structures with an average dimension varying from 200 µm up to 3 µm can be formed by solvent evaporation. Blends with cellulose acetate and propionate, respectively, form smaller and more regular structures than blends with cellulose carbamate. These surface structures are able to contribute to diminution of the surface energy.

Textile coating is successful using polyamide based woven fabrics. Coats with surface structures similar to the studied thin polymer films may be formed. Usually, an additional hydrophobing is necessary to obtain a low surface energy. That can be realized by addition of a fluorocarbon to the coating compound or by finishing of the surface with a fluoralkyl silane. The second method is more effective. In analogy to a lotus leaf a very low surface energy can be obtained when a smart combination of three structural levels – macrostructure, microstructure and monomolecular layer – is realized. Adequate coated fabrics are highly dirt-repellent.

## Acknowledgements

The authors are indepted to the Bundesministerium für Wirtschaft und Technologie (BMWi) for the financial support of this work (Reg.-No. BMWi / IGF 216 ZBG).

## References

[1] G. Dambacher, Kunststoffe 92, 6 (2002) 65
[2] A. Burmeister, tesa AG, Offenlegungsschrift DE 10158347 A1 (2003)
[3] C. Daniel, Laser Interferenz-Metallurgie – Biomimetische Mikro-Nano-Strukturierung von Oberflächen, in Symposium Material Innovativ, Nürnberg 10.03.2005
[4] M. Zwinzscher, U. Wienhold, S. Schwarz, Farbe+Lack 110, 5 (2004) 84
[5] W. Weigt, F. Auer-Kanellopoulos, Farbe+Lack 110, 10 (2004) 20
[6] B. Morgenstern, M. Keck, W. Berger, Acta Polymerica 41 (1990) 86
[7] D. Klemm, B. Philipp, T. Heinze, U. Heinze, W. Wagenknecht, Comprehensive Cellulose Chemistry, Fundamentals and Analytical Methods. Wiley-VCH, Weinheim NewYork Chichester Brisbane Singapore Toronto (1998)
[8] F. Hermanutz, W. Oppermann, DITF Stuttgart, Patent DE 19638319 C1 (1998)
[9] F. Hermanutz, F. Gähr, A. Haiplik, Melliand Textilber. 85 (2004) 68
[10] F. Hermanutz, F. Gähr, DITF Stuttgart, Patent DE 10344396 B4 (2005)
[11] E. Marsano, M. Tamagno, E. Bianchi, M. Terbojevich, A. Cosani, Polymer Adv. Technol. 4 (1993) 25
[12] L.A. Utracki in Polymer Alloys and Blends, Hanser Publishers, München Wien NewYork (1989)
[13] A. Schöne, B. Morgenstern, W. Berger, H.-W. Kammer, Polym. Networks Blends 1 (1991) 109
[14] T. Röder, B. Morgenstern, H.-W. Kammer, Polym. Networks Blends 3, (1993) 203
[15] H.-W. Kammer, C. Kummerlöwe, B. Morgenstern, Makromol. Chem., Macromol. Symp. 58 (1992) 131

Lenzinger Berichte 87 (2009) 163-168

# DETECTION OF COATINGS ON PAPER USING INFRA RED SPECTROSCOPY

**Eduard Gilli[1,2] and Robert Schennach[1, 2]**

[1]Graz University of Technology, 8010 Graz, Austria
[2]CD-Laboratory for Surface Chemical and Physical Fundamentals of Paper Strength, 8010 Graz, Austria

Phone: (+43) 316-873-8462; Fax: (+43) 316-873-8466; E-mail: Robert.schennach@tugraz.at

**Most of the paper used today has one or more coatings on its surface in order to tailor the surface properties according to the intended application of the paper. Such coatings range from inorganic to organic and cellulosic materials. For quality control methods to analyse such films are very important. The currently used methods range from x-ray absorption via ellipsometry to wet chemical methods. All of them have intrinsic problems like minimal thickness or time consuming measurements. Here we present a way to analyze coatings on a paper sample by using infra red spectroscopy methods. Using either attenuated total reflection or infra red reflection absorption spectroscopy together with s- and p- polarized light one can get information about both the chemical properties of the thin film and the film thickness. For the latter usually a calibration has to be made using an independent method. However, if one can measure the optical properties of the film and the substrate the thickness of the thin film can be found by simulating the IR spectra using an electrodynamics approach.**

**Keywords:** *FTIR, IRRAS, ATR – IR, paper, coating, coated paper*

## Introduction

Many different kinds of coatings on paper are used today to get the necessary surface and bulk properties of paper for different applications. Coatings are used to enhance printability, increase wet strength, decrease surface roughness, or change diffusion rates of gasses or liquids. For example the glossy surface of photographic paper for inkjet printers is made by coating the paper.

However, easy and accurate methods to measure the thickness and quality of such coatings are limited. Mostly methods like x-ray absorption and ellipsometry are used. In some cases even wet chemical methods are employed [1]. Especially the latter method is very time consuming and cannot be used as an online method. Only x-ray absorption can be used online, however it can only be used for thick enough films.

In this paper we present two methods based on Fourier Transform Infra Red Spectroscopy (FTIR) that can do both, measure the thickness of a coating (if a calibration is available) and provide chemical information at the same time.

The first method is Attenuated Total Reflection Infra Red Spectroscopy (ATR – IR) using polarized infra red light and the second method is Infra Red Reflection Absorption Spectroscopy (IRRAS) also utilizing polarized light. The physical

principles behind these methods have been described in detail before [1].

## Experimental

*ATR – IR Measurements*

FTIR measurements were made on small pieces of the pure coating materials and on about 1 x 1 cm large samples of the coated paper using a Bruker ifs66/v FTIR (Bruker Optics, Germany). Attenuated total reflection (ATR) measurements were made using a single reflection unit from Specac (MKII Golden Gate). The ATR crystal was a diamond and the incident angle was approximately 45°. A sampling rate of 100 kHz, and a recording time of 30 minutes was used unless otherwise stated.

*IRRAS Measurements*

Infra red reflection absorption spectroscopy (IRRAS) measurements were performed using a reflection unit (specular reflection) with variable angle and a polarizer from Bruker Optics. The IRRAS spectra were measured with an incidence angle of about $\Theta$ = 62°. The Brewster angle of paper is approximately 61° and it is expected that the signal – to – noise ratio is best at angles close to the Brewster angle. The spectra were recorded for 5 min at a sampling rate of 100 kHz. The manipulation function for subtracting the background is given by

$$I = (I_s - I_p)/(I_s + I_p) \qquad (1)$$

with I being the corrected signal, $I_s$, the intensity of the s- polarized spectrum and $I_p$, the intensity of the p- polarized spectrum. This correction function is commonly used for polarization modulation IRRAS and has the advantage of giving more significance to differences between the polarization directions if the over all signal is small. All FTIR measurements were done under vacuum conditions with a base pressure of about 4 mbar.

## Results and Discussion

*ATR – IR Results*

First ATR – IR spectra of the two pure coating materials were recorded. The corresponding spectra are shown in figure 1 as the green and the blue curve. It is quite clear that the inner coating on the paper sample (green curve in figure 1) has only a very limited signal in the mid infra red region. In contrast to that a clear spectrum of the outer coating of the paper sample was obtained as can be seen by the blue curve in figure 1. The red curve in figure 1 is the FTIR spectrum of the coated paper.

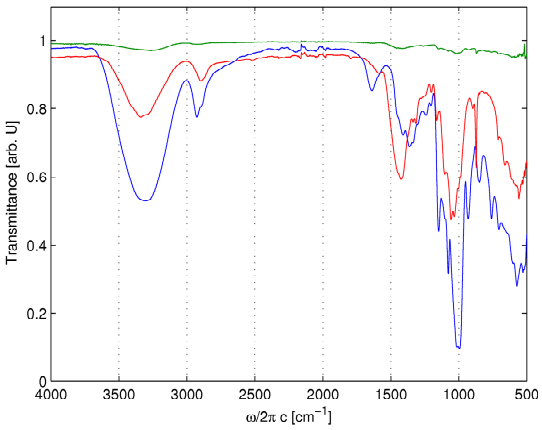


**Figure 1.** ATR – IR spectrum measured with p-polarized light. Blue is a sample of the pure outer most coating, green is a sample of the pure inner coating and red is the coated paper sample.

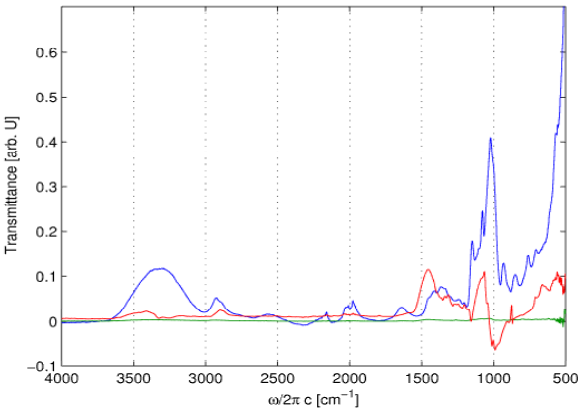


**Figure 2.** ATR – IR spectrum calculated using equation (1) from spectra measured with s- and p-polarized light. Blue is a sample of the pure outer most coating, green is a sample of the pure inner coating and red is the coated paper sample.

There are some clear differences between the outer coating and the paper sample. In the fingerprint region around 1000 $cm^{-1}$ there are mainly differences in the intensity of the peaks, which is an artefact of the ATR – IR method, as the intensity depends on the force used to press the sample against the ATR crystal.

As the hardness of the pure coating samples and of the coated paper sample is very different, even applying nominally the same pressure will result in different intensities. In addition the intensities also depend on the roughness of the sample surface, which is of course different for different samples.

At about 924 $cm^{-1}$ a peak is found in the outer coating, which is not visible in the coated paper sample. The same seems to be true for the peak at about 1640 $cm^{-1}$. However, at close inspection one can see a small peak around 1584 $cm^{-1}$ (red curve in figure 1), which might be due to the coating. Therefore, the intensity of this peak could be used to measure the thickness of the outer most coating, if a calibration with different coatings of known thickness can be made.

The region between about 1750 $cm^{-1}$ and 2750 $cm^{-1}$ shows no peaks which is simply due to the fact that the ATR crystal used in this work is a diamond, which has a large absorption band in this region [2, 3].

In the frequency range above 2750 $cm^{-1}$, the spectrum can again be measured and one can see a large OH band and a clear CH peak coming from the paper as well as from the outer most coating.

The spectra recorded with s- polarized light are very similar to the spectra recorded with p- polarized light and therefore the results with s- polarized light are not shown here.

However, the differences between measurements with s- and p- polarized light are important, when one wants to detect the effect of thin films on the measured sample. This can be done by calculating an IR spectrum out of the two measured spectra with s- and p- polarized light using equation (1). The corresponding result is shown in figure 2. The spectra of the pure coatings (blue and green curves in figure 2) hardly change due to this manipulation.

However, the spectrum of the coated paper sample shows a marked difference (see red curve in figure 2). The peak around 1044 $cm^{-1}$ from figure 1 is split in two peaks around 1075 $cm^{-1}$ and 1000 $cm^{-1}$, with the peak at lower wavenumbers pointing down instead of up. The IR peak pointing in the "wrong" direction is a clear indication that this peak is not a chemical peak, but an optical phenomenon. Such a behaviour is known as the Berreman effect [7]. This effect is basically a thin film phenomenon that leads to a peak in the mid infrared region. This peak is not due the chemistry of the thin film, but due to the optical properties of the film and the film thickness [1, 4 – 6].

It has been shown before that the intensity of the Berreman peak depends on the thickness of the thin film [5]. Therefore, this peak can be used to measure the film thickness, while the chemical peaks can be used to check the chemical properties of the film.

When the optical properties as a function of the wavelength (refractive index and real and imaginary part of the dielectric function) of the thin film and the substrate are known, one can simulate the infra red spectra [8, 9]. The results of such a simulation can be used to make a detailed interpretation of the FTIR spectra and it is possible to obtain the thickness of the thin film in principle without the need for a calibration.

Unfortunately one usually does not have the optical properties of the sample and the thin films. Therefore one would need to perform a measurement to obtain these values which can be done for example via a so called Kramers – Kronig Transformation [10 – 12]. However, also this method is limited as very pure samples

in form of a powder with an average particle size smaller than the wavelength of the light used is needed. Due to this reason no simulation of the spectra shown here could be done.

As there are two different coatings on this paper sample one would expect two such optical peaks in the spectrum. Here one has to bear in mind that the penetration depth of the infra red light in ATR – IR is very limited. This means that the outer most coating in this case is too thick for the ATR – IR measurement to also see the inner coating. The paper substrate is only seen in the ATR – IR experiment, because the coating on the paper is in form of small stripes, which leaves a part of the uncoated paper visible under the experimental conditions used in this study.

To overcome the limitation set by the ATR – IR method the same coated paper sample was also measured in the IRRAS mode. The resulting s- and p- polarized spectra are shown in figure 3. The left side in figure 3 shows the spectrum obtained with s- polarized light and the right spectrum was measured with p- polarized light. One immediately sees that in both cases all but two peaks point down in the spectrum. Therefore, one can assume that the IRRAS method actually sees both coatings, as the two peaks pointing up around 1500 $cm^{-1}$ and around 860 $cm^{-1}$ are most likely thin film peaks. The peak around 860 cm-1 has a very unusual form for an IR peak. The form of this peak would suggest that it might stem from a mechanical vibration. This peak will be discussed later.

Another advantage of the IRRAS method is also apparent from figure 3 as compared to figure 1, namely that the whole mid infra red region is measured as compared to the ATR – IR method, which has the blind region mentioned earlier. The two peaks around 1785 $cm^{-1}$ and 2500 $cm^{-1}$ seen in figure 3 could not be detected in the spectra shown in figure 1 and 2. The other chemical peaks from the ATR – IR measurement around 3000 $cm^{-1}$, around 1500 $cm^{-1}$ and around 1000 $cm^{-1}$ seen in figure 1 are also found in figure 3. At close comparison one can see that these peaks are shifted to higher wavenumbers in the IRRAS spectra as compared to the ATR – IR spectra. This difference is most likely due to the fact that the sample is pressed against the ATR – IR crystal in the ATR – IR experiment. It is a well known effect of the ATR – IR method that the peaks shift as a function of the applied pressure.

So one can conclude that the two methods show very similar spectra. The main differences are due to the blind region of the ATR – IR and due to the fact that in the IRRAS measurement the penetration depth of the infra red light is not limited, which

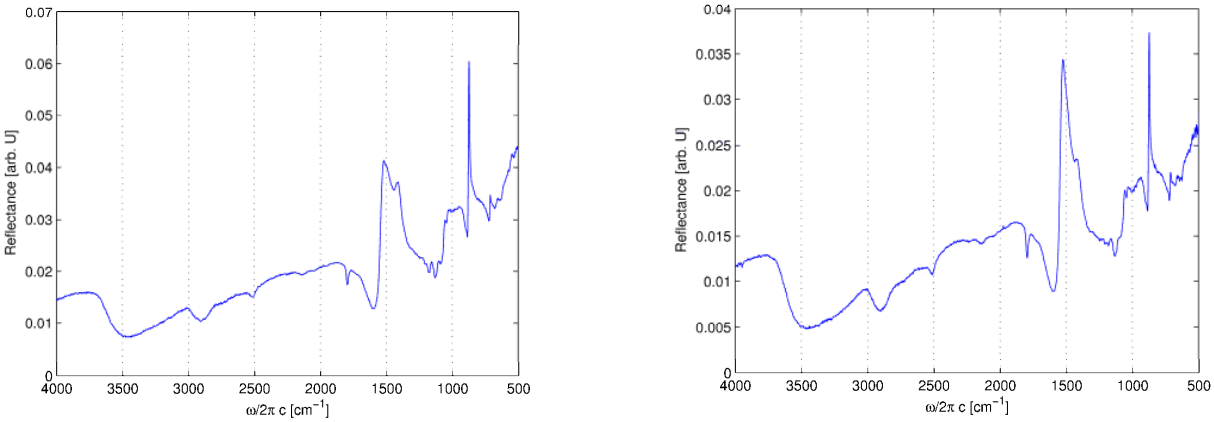


**Figure 3.** IRRAS spectrum of the coated paper measured with s- (left side) and p- polarized (right side) light.

makes it possible to detect both coatings, represented by two Berreman peaks.
An even clearer picture can again be obtained by plotting the IRRAS spectrum after application of equation (1). The result is shown in figure 4.

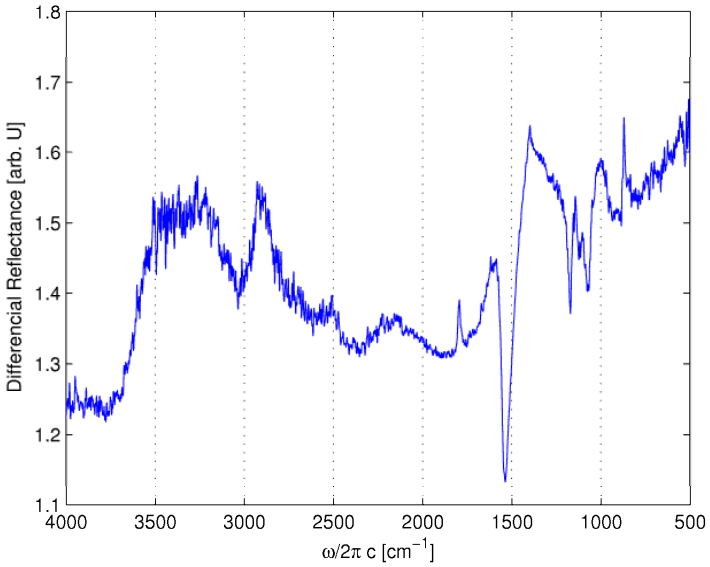


**Figure 4.** IRRAS spectrum calculated using equation (1) from spectra measured with s- and p- polarized light.

The chemical peaks point up in figure 4 according to equation (1). Therefore, one can identify four peaks pointing in the "wrong" direction at 1540 $cm^{-1}$, 1180 $cm^{-1}$, 1120 $cm^{-1}$ and 1076 $cm^{-1}$. The origin of these peaks has to be discussed in more detail.
The intense peak at 1540 $cm^{-1}$ is most likely the optical thin film peak corresponding to the inner coating on the paper sample, as this peak was not observed in the ATR – IR measurements (compare to figure 2).
The three peaks at 1180 $cm^{-1}$, 1120 $cm^{-1}$ and 1076 $cm^{-1}$ are in the fingerprint region. Therefore, one has to take into account that here an overlap between chemical peaks and optical thin film phenomena might occur. The peak at 1076 $cm^{-1}$ corresponds best to the Berreman peak observed in ATR – IR (compare to figure 2), taking the overall shift of the IR spectra between the ATR – IR and IRRAS measurements into account.
Tentatively the two peaks at 1180 $cm^{-1}$ and 1120 $cm^{-1}$ could be the result of an overlap between chemical peaks at these frequencies and the thin film peak from the top most coating. Here again only a simulation of the spectra would yield an unambiguous interpretation.
The peak at 860 $cm^{-1}$ is the only spectral feature that is at exactly the same frequency in both ATR – IR and IRRAS measurements. This fact together with the unusual shape of this peak supports the interpretation of this peak as a mechanical vibration that is detected in the IR spectrometer. The vibration most likely comes from one of the mechanical pumps connected to an ultra high vacuum chamber. The FTIR-spectrometer is connected to this ultra high vacuum chamber, as the FTIR is also used to make IRRAS measurements under ultra high vacuum conditions [13] using an external detector.

## Conclusions

A paper sample that was coated with two thin films was analyzed using ATR – IR and IRRAS with polarized light. The pure coating materials were also measured using ATR – IR.
It was shown that the outer most coating could be detected with ATR – IR due to the formation of a Berreman peak, which is an optical thin film phenomenon. The inner coating could not be detected due to the limited penetration depth of the ATR – IR method.
Using IRRAS there is no limit in the penetration depth of the infra red light and both coatings yield Berreman peaks.
The optical peaks can be used to determine the thickness of the thin films and the chemical peaks can be used to check the chemistry of the films.
For a detailed interpretation a simulation of the FTIR spectra is needed, which is possible if the optical properties of the substrate and the coatings are either known or can be measured.

## Acknowledgements

Financial support was provided by the Christian Doppler Society and by the industrial partners Mondi Packaging and Lenzing AG.

## References

[1] E. Gilli, A.E. Horvath, A.T. Horvath, U. Hirn and R. Schennach, Cellulose, (2009) .
[2] P. Thongnopkun and S. Ekgasit, Analytica Chimica Acta 576 (2006) 130.
[3] P. Thongnopkun and S. Ekgasit, Diamond and Related Materials 14 (2005) 1592.
[4] B. Harbecke, B. Heinz and P. Grosse, Applied Physics A 38 (1985) 263-267.
[5] T. Scherübl and L.K. Thomas, Applied Spectroscopy 51 (1997) 844-848.
[6] B.C. Trasferetti et.al., Applied Spectroscopy 54 (2000) 687-691.
[7] D. W. Berreman, Physical Review 130 (1969) 2193.
[8] W.N. Hansen, Journal of the optical Society of America 58 (1968) 380-390.
[9] K. Yamamoto and H. Ishida, Vibrational Spectroscopy 8 (1994) 1-36.
[10] V. Hopfe et.al., Journal of Physics D 25 (1992) 288-294.
[11] P. Grosse and V. Offermann, Applied Physics A 52 (1991) 138-144.
[12] V. Lucarini et.al., Kramers-Kronig Relations in Optical Materials Research, Springer, 2005.
[13] R. Schennach, G. Krenn, K. D. Rendulic, Vacuum 71 (2003) 89.

Lenzinger Berichte 87 (2009) 169-179

# CONSUMER PERCEPTIONS OF INNOVATIVE WOOD-POLYMER COMPOSITE DECKING WITH A FOCUS ON ENVIRONMENTAL ASPECTS

**Stefan Weinfurter[1] and Asta Eder[2]**

[1]University of Natural Resources and Applied Life Sciences, Vienna
[2]Kompetenzzentrum Holz GmbH, A-4021 Linz, Austria

Phone: (+43) 1 47654 – 4406 ; Fax: (+43) 1 47654 - 3562; E-mail: stefan.weinfurter@boku.ac.at

**Wood-polymer composites (WPCs) have entered the Austrian decking market. Their market share is growing from a low base level. Due to the fact that WPC decking is quite unfamiliar to Austrian consumers, a survey was initiated to reveal consumers' perceptions of WPCs decking, including environmental aspects. The approach chosen for the survey was product concept testing including conjoint analysis. Personal interviews were carried out with the targeted respondents, single-family home owners and "do-it-yourselfers." Deemed most important by respondents were issues related with durability followed by product handling, environmental concerns and service aspects at last. WPC decking was perceived more positively by a majority of respondents. Willingness-to-buy measures of the survey slightly speak against a "no-go" decision. The survey included conjoint analysis, revealing that the color and the kind of surface of decking planks are deemed most important for the respondents' purchase decision. Polymer share and type are of less importance and the kind of wood-fiber used is of least importance.**

**Keywords:** *wood-polymer composite decking, product concept testing, survey, environment, perceptions*

---

## Introduction

Wood-polymer composites (WPCs) clearly represent a growing market – worldwide. The most common application of WPC is decking which is one of the fasted growing markets within garden design. WPC decking recently became available in retail for Austrian consumers. However, WPC decking is still unknown by most Austrian consumers. Therefore, a survey was carried out to reveal consumer perceptions of WPC decking incorporating environmental aspects. The survey targeted single-family home owners and "do-it-yourselfers." The approach employed was product concept testing including conjoint analysis.

Although this survey is quite unique, it is not the only consumer study dealing with flooring. Studies examining consumer and customer perceptions of wood-polymer decking often included comparisons with wood [1], [2], [3], [4], [5], [6], [7], concrete [8] or laminate [9]. Generally elicitation of attributes for analyzing (prospective) consumers' purchase decisions regarding wood products is based on literature reviews and expert interviews. Johnsson et al. [10] utilized Kelly's [11] repertory grid technique and content analysis to systematically identify attribute categories that are associated by consumers with solid wood, wood-based panels and WPC composites. The most

preferred core categories associated with solid wood were naturalness, wood-likeness, living impression and value. Smoothness was specifically associated with WPC composites.

Conjoint analysis was applied in several studies as an appropriate means to more realistically simulate purchase decisions among various alternatives [3], [4], [5], [7], [9]. Based on conjoint results, market shares have been simulated for differently treated wooden decks [7]. The attributes most relevant for consumers' wood products buying decisions extracted by conjoint analysis were material, durability, and to some extent price [3], [4], [5], [7], [9]. A North American conjoint based study [5] underlined the change of consumer preferences toward WPC-decking departing from pressure treated decking from 2001 to 2003. This study further underscored the responsiveness of the conjoint method to market events.

For outdoor wood products a study by Mantau and Knauf [6] and for decking a study by Roos and Nyrud [7] showed that a green consumer segment exists. It is composed of women and married couples with higher education. Conclusions that in do-it-yourself (DYI) sector environmental considerations and eco-labels have an impact on consumer preferences for wood products such as decking may be drawn. Corresponding esthetics and quality are seen as a pre-condition for the purchase of eco-labeled products [7]. A study of laminate flooring [12] indicates that appearance is a central aspect for flooring preferences, which is supported by previous studies in German speaking countries, e.g. [13]. Roos and Hugosson [12] suggest focusing on enhanced marketing of flooring products utilizing environmental attributes.

The goal of the present study was to reveal the importance of environmental attributes in comparison to other attributes relevant in a WPC deck purchasing situation.

## Methods

### *Product concept testing*

Since WPCs are hardly at all familiar to Austrian consumers, the approach chosen for this survey was product concept testing. Precisely, product concept testing is not a method per se but a conglomerate of marketing research methods, such as willingness-to-buy measures, multi-item measures, semantic differentials, and other scales. A concept test is a means to see what potential users think about the product concept introduced to them. Typically a concept has to be screened before development can be undertaken [14]. If consumer reaction to the concept is poor, the product development project may be terminated or earlier stages of the product development cycle have to be repeated. The tests may aim at which out of several concepts to pursue, gathering information of potential consumers in the target market on how to enhance the concept, and getting a feel for the future sales potential [15].

### *Product concept statement*

A product concept test starts with a concept statement. A concept statement states a difference and how that difference benefits the consumer. Although it can be designed in different formats, the concept should make the new products variation clear. It should list the determinant attributes, specifically the ones making a difference in buying decisions. It should be realistic and credible and it should offer a certain extent of familiarity by appealing to things familiar to the consumer. Finally the concept statement should be as short as possible. For this study a combination of a verbal and a pictorial description was chosen, because a pictorial depiction has to be accompanied by a narrative statement of the concept [14].

The product concept statement of this study started with a title, "Decking planks made of WPC," succeeded by a list of benefits provided by WPC decking. A few

showcase pictures of installed decking including a close-up view of a WPC deck followed. A short comparison of prices and durability of different kinds of decking was provided next. After that a short explanation of the "mixture" of wood and polymers i.e. WPC followed. The product concept statement closed with a short series of pictures briefly showing the extrusion process comprising the wood and polymer mixture, an extruder "at work," and various extruded profiles. For consumers' ease of understanding the word the German word for plastic was used instead of polymer.

***Questionnaire design***

A purchase intention scale made up the first question, succeeded by two open-ended questions asking for the reasons for prospective purchase, respectively non-purchase. Respondents were then asked which raw material composition would be acceptable for them. The questionnaire further contained a semantic differential, revealing respondent's first impression of WPC decking. Prior knowledge respectively product category expertise was the next issue: When respondents had experience with wooden decks, they were asked how satisfied they were. In two open-ended questions respondents had the opportunity to state why they were or why they were not satisfied with wooden decks. The questionnaire pursued with the core of the questionnaire a multi-item list. The first section of the questionnaire closed with as few as possible sociodemographic questions.

***Conjoint analysis***

Conjoint analysis is very well suited for understanding consumers' evaluations of and reactions to predetermined attribute combinations that depict potential services or products. The researcher gains insight into the composition of consumers' preferences. Conjoint analysis is based on the assumption that consumers evaluate the utility or value of a product (concept) by combining the utilities contributed by each attribute. The (hypothetical) products are presented to the respondents thus simulating a more realistic purchase situation where consumer have to choose among a set of products but not rate single product attributes e.g. on importance. In conjoint analysis the importance of each product attribute and each utility of each attribute are calculated from respondents' overall product ratings according to their preference. A respondent's overall preference for a product can be called the "total worth" of the product. It can be understood as the sum of the part-worths of each level. Possible values for each attribute are called attribute levels. Each product (idea) presented to the respondents is called treatment or stimulus. It is made up by combinations of attribute levels [16], [17].

Simulation of a real buying situation calls for inclusion of price. Nevertheless, price was omitted as the number of attributes used in conjoint analysis is limited and environmental issues were added. Omitting price should not be a major drawback since the importance of price differs from study to study. What can be said is that price is less important for environmentally concerned consumers [5], [7], [18], [19]. The attributes and their levels used for the present survey are given in Figure 1.

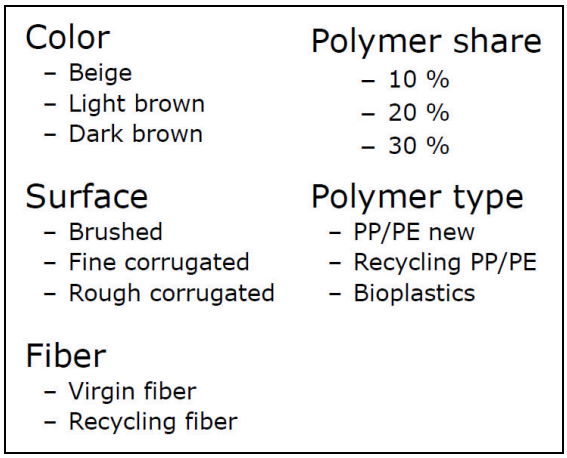


**Figure 1.** Conjoint attributes and attribute levels.

All possible combinations of the attribute levels given in Figure 1 would result in hundreds of (hypothetical) products i.e. stimuli to be presented to and evaluated by respondents. Such a factorial design is rather impractical. Therefore a fractional factorial design was used, resulting in sixteen stimuli minimum (Figure 2), still representing a challenging task for respondents.

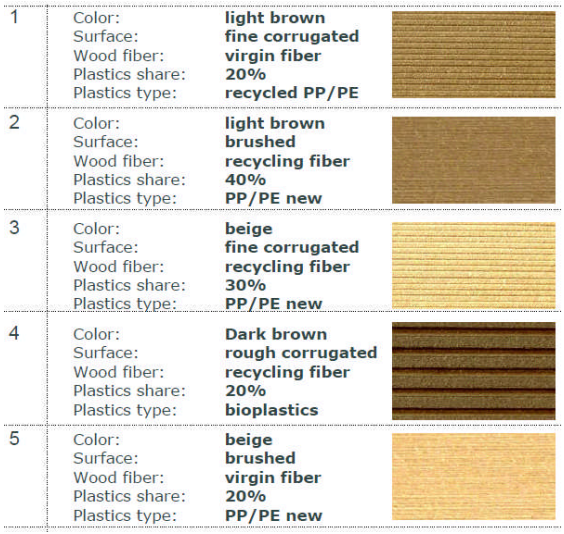


**Figure 2.** Conjoint stimuli 1 to 5 of 16.

### *Sample design and method of administration*

The samples were chosen in a way expecting they were suited best to serve the research purpose. Thus, single family home owners and do-it-yourselfers were targeted for this survey. It is also believed that they are somewhat representative of the population of interest. A sampling procedure like that is called judgment or purposive sample. There is no need that the sample elements are truly representative but they are supposed to offer the contributions sought for [20].

The method of administration was face-to-face, i.e. personal interviews. Single-family home owners were deemed to be the group for whom decks were most relevant. "Do-it-yourselfers" that did not own a single-family home but for whom decking was an option were not excluded from the survey. Being classified as "do-it-yourselfers" depended on the respondents' self-perceptions. Altogether 391 interviews were administered in Austrian private homes in the pre-garden season of 2007.

## Results and discussion

### *Sociodemographics*

To keep the questionnaire short and simple only few sociodemographic variables were questioned: (1) sex, (2) year of birth, (3) residence, i.e. province, (4) respondent's origin, i.e. rural or urban, (5) current type of community, i.e. rural or urban, (6) type of residence, and (7) monthly net household income. The sample did not perfectly represent the Austrian population. This is a minor drawback, since a target group was surveyed. The Sociodemographic variables of hardly have any influence on other variables i.e. willingness to buy WPC decking, acceptable raw material composition, and the variables of the semantic differential and the multi-item measure.

### *Willingness-to-buy measure and reasons for purchase / non-purchase*

Although it might be a "crude" measure and its results have to be interpreted with care, the willingness-to-buy question appears in almost every concept test [14]. A four-point buying intention scale was used for this study, ranging from "I would definitely not buy" to "I would definitely buy" with the intervening points "I would probably buy" and "I would probably not buy." Results of the willingness-to-buy measure (Figure 3) must be treated carefully and must not be over-interpreted. Nevertheless they provide the researcher with a direction of the respondents' preferences and support for "go – no-go" decisions. This surveys hints at a "go"-decision requiring a greater amount of consumer input for product design that is provided by subsequent questions and later conjoint analysis. The authors suspects

that part of the slightly positive willingness-to-buy measure might lie in the curiosity of respondents towards new products and that no physical decking samples were provided.

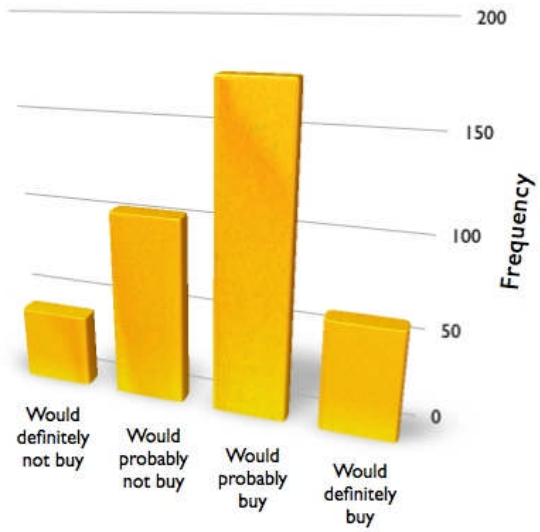


**Figure 3.** Respondents' willingness to buy WPC decking (n = 382).

Respondents named following reasons why they would by WPC decking: Durability and appearance were stated most often. Next but far less often appeared low maintenance, followed by price, natural/recyclable, and no splintering. Reasons, why respondents would not buy WPC decking, most often were the preference for wood or other materials and the "artificial" component of the material, namely polymers. Next but less often mentioned were the price and lack of knowledge caused by the newness of the material.

For further analysis the sample was split into two subgroups, (1) respondents that would definitely or probably buy WPC decking and (2) respondents that would probably not or definitely not buy WPC decking. "Non-buyers" significantly perceive WPC decking in a more negative way e.g. less innovative, less durable, less natural, colder, and more expensive (Mann-Whitney tests). Furthermore, it is obvious that "non-buyers" perceive many of the product and service attributes of the multi-item list significantly less important. All this is valuable information for communicating WPC decking to consumers not yet willing to buy.

***Raw material composition***

The ingredients of wood-polymers are of two-fold importance. From a technological point of view the type of raw materials and their shares are of particular interest for wood-polymer compound producers and for suppliers of equipment such as extruders. A vast variety of different wood-polymer compound recipes have been tested and developed globally with North America and Europe dominating. The compounds' raw materials were investigated as well as their behavior in extruding machines. Finally the wood-polymer compounds are tested for strength, weathering, fungi resistance, and UV stability. Intensive research is still going on and will continue in the future. In Europe most WPC profile producers develop their own compounds. They typically use virgin poly-propylene and virgin soft wood. However, use of other kind of fibers and polymers is increasing. That includes recycled materials and waste streams [21]. That is the technological view of raw material composition in brief.

There is still an important view missing: the consumers' view of raw material composition. Therefore, respondents were asked for the raw material composition they were willing to accept. In order not to ask too much from respondents recipes were simplified in that they were reduced to two or three main components: wood (fibers), polymers, and a specialty, namely corn starch. Corn starch was included, because at time of the survey the only Austrian wood-polymer compound producer used corn starch in addition to wood. There is no doubt that for a distinct majority of respondents, a plastics share of 30 percent is still acceptable (Figure 4). A maximum plastics share of 50 percent and minimum wood share of 50 percent were provided in the questionnaire.

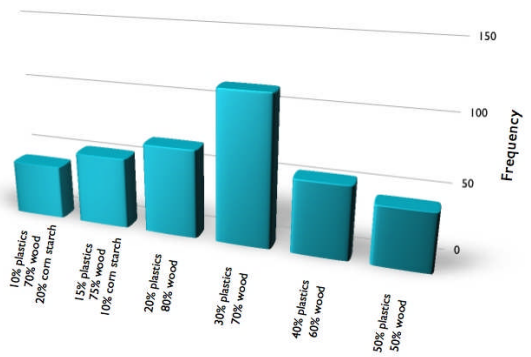


**Figure 4.** Acceptable raw material composition for respondents (n = 374).

What respondents do not know, in real world a polymer share of 30 percent is technically necessary and feasible to provide the prior benefit of WPCs, namely the extended lifetime. It seems that respondents understand this and other benefits provided by the mixture of wood particles and polymers. Interviewers reported that respondents understood the concept of WPCs without difficulties.

***Prior knowledge – product category expertise***

Prior knowledge was measured the following way: Respondents were asked if they have experience with wooden decking. If yes, they were further asked for their satisfaction with wooden decking on a four-pint Likert-type scale ranging from "very satisfied" to "not satisfied" with the two intervening points "rather satisfied" and "rather unsatisfied." Half of the respondents stated to have at least some experience with wooden decks. Only a fourth to a fifth of these was "not satisfied or "rather unsatisfied" with their wooden deck experience. About half of these respondents, was rather satisfied (Figure 5). The sample was investigated utilizing Mann-Whitney tests. Test results show that having experience in the product category or not hardly has any significant influence on other variables. (An alpha-level of 0,05 was chosen for all statistical tests applied).

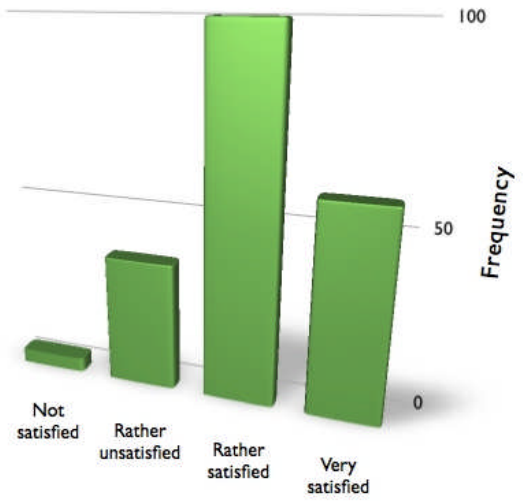


**Figure 5.** Respondents' satisfaction/experience with wooden decking (n = 202).

The closed question in form of a satisfaction rating, was complemented by two open-ended questions. The first was "why were/are you satisfied with wooden decking (planks)?" and "why were/are you not satisfied with wooden decking (planks)?" Respondents listed following factors in favor of wood: The appearance of wooden decking had the largest number of entries, followed by workability and ease of repair. These were succeeded by "naturalness" and durability. Haptics and comfort followed next with significantly fewer entries. In contrast to that lack of durability was named most often, when respondents were asked for the reasons of dissatisfaction with wooden decking, why they were/are not satisfied, followed by extensive maintenance work. Clearly less often but named next, were splintering, greying i.e. discoloration, and slippery.

Problems to the most important drawbacks of wooden decks stated by the respondents are directly addressed by WPC decking. Durability is enhanced by adding polymers for instance. This reduces maintenance. The WPC compound also prevents the creation of splinters and cracks and warping. UV-stabilizers can be added to the recipe to alleviate greying.

Applying Kruskal-Wallis test supports that respondents (rather) satisfied with wooden

decks perceived WPC decking significantly less positive than respondents (rather) unsatisfied with wooden decks. Vice versa, (rather) unsatisfied respondents perceived WPC decking significantly more positively. In addition, willingness-to-buy WPCs decking of respondents (rather) unsatisfied with wooden decks was significantly higher than that of respondents (rather) satisfied with wooden decks (Kruskal-Wallis test). Furthermore, respondents (rather) unsatisfied with wooden decks prefer and accept significantly higher plastics share in WPC decking compounds than (rather) satisfied respondents (Kruskal-Wallis test). So it is the unsatisfied fraction of consumers to focus marketing communications on first.

***Semantic differentials***

The semantic differential [22] is one of the most widely applied techniques to examine users' perceptions of product forms. This procedure investigating product semantics uses a bipolar Likert scale for quantifying the subjects' perceptions of new products. Either end of the scale is labeled with a contrasting pair of adjectives.

In general, WPC decking was perceived positively by respondents. It was perceived clearly innovative and durable, rather comfortable, but a little expensive and artificial (Figure 6). For marketing, that means innovativeness and durability do not have to be thoroughly communicated to consumers any more. Though stressing that WPCs are recyclable might help overcoming their lack of naturalness.

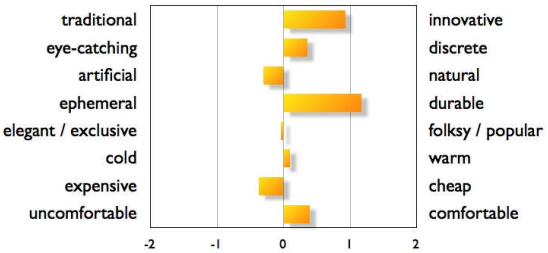


**Figure 6.** Semantic differential; respondents' mean perceptions of WPC decking (n = 381).

When splitting the sample of both surveys a priori in two subgroups, (1) respondents that would definitely or probably buy WPC decking and (2) respondents that would probably not or definitely not buy WPC decking, significant differences were revealed as follows with Mann-Whitney tests: "Non-buyers" perceive WPC decking in a more negative way e.g. less innovative, less durable, less natural, colder, and more expensive. The same counts for respondents satisfied with wooden decks. They perceive WPC decking more negatively, too. All this can be considered valuable information for marketing communication.

***Multi-item measure***

"Multi-item" paraphrases a "simple" list of attributes "independently" evaluated by the respondents. Developing the multi-item list of this study was far from simple. It is based on a large number of studies concerning forest products including decking. Most of these studies either deal with b-to-b or b-to-c customer perceptions [19]. A large number of marketing scientists and practitioners was consulted to adopt the list and to ensure completeness of the measure. The practitioners comprised WPC experts and wholesalers and retailers of forest products and outdoor (garden) applications of wood. The goal was to design a multi-item measure of overall WPC decking quality. According to Garvin et al. [23] this instrument ought to circumvent sufficient aspects of product and service quality. Respondents had to rate the items of the measure on importance. In the case of this study the 4-point scale ranged from "very important" (3) to "not important at all" (0) The items respectively attributes covered technical product features comprising several items associated with durability and materials handling. Other attributes covered information, service, and ecology (Figure 7). Items associated with durability were rated most important followed by ease of product handling and finally

service. Price and environmental issues are found in the midfield and the lower midfield, respectively.

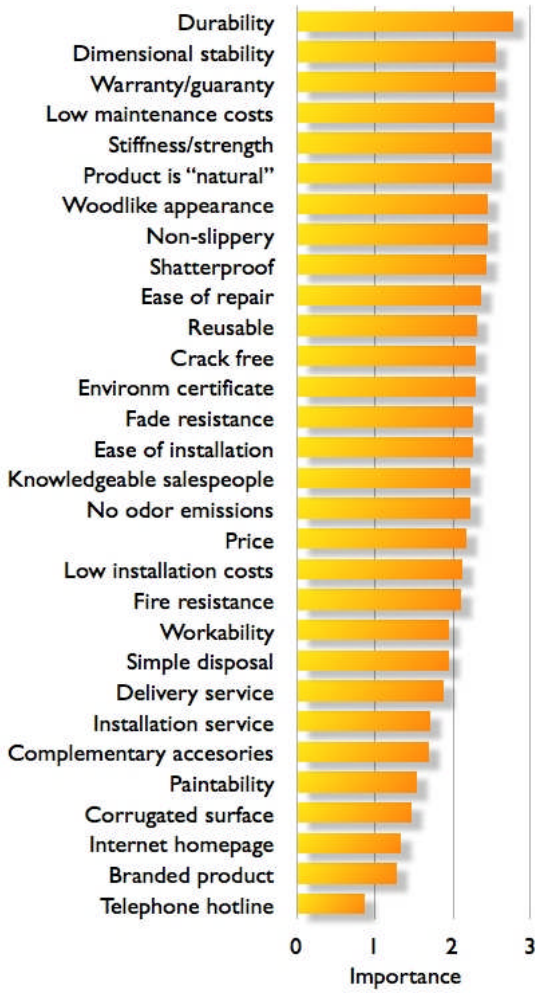


**Figure 7.** Mean importance ratings of attributes describing product and service quality of WPC decking (n = 380; 0 = not important, 3 = very important).

High reliability has a positive impact on the validity of the interpretation of data analysis results and the conclusions drawn from them. Coefficient alpha [24] is a widely used measure of reliability in marketing scales such a multi-item measures [25], [26], [27]. Coefficient alpha was calculated for the three dimensions, extracted by factor analysis, of this research's multi-item construct, which proofed highly reliable.

***Results of full-profile rankings-based conjoint analysis***

For several reasons, ease of design, administration, and data analysis a full-profile rankings-based conjoint method was selected. Full-profile in conjoint analysis means that each stimulus incorporates a level of each (of the five) attributes. The full-profile method allows the use of fractional factorial design described above. Rankings-based means that respondents had to rank-order the 16 stimuli from the most to the least preferred. The full profile method is used most often in comparison to others such as trade off and pairwise comparison methods, because it offers to reduce the number of comparisons by fractional factorial design [17].

In this survey, significant Kendall's tau and Pearson's R values close to one indicate that empirically derived data is well represented by conjoint results.

On one hand, conjoint analysis results provide the part-worths (utilities) of all attribute levels and the importance of all attributes for each respondent. That is called disaggregate analysis. On the other hand, results of conjoint analysis provide the levels' utilities and the attributes' importance aggregated for all respondents [17].

In Figure 8, it can be easily recognized that the attributes most important to respondents are the WPC deck's color and its surface. So, appearance seems to be the major purchase criterion followed by the plastics share and plastics type.

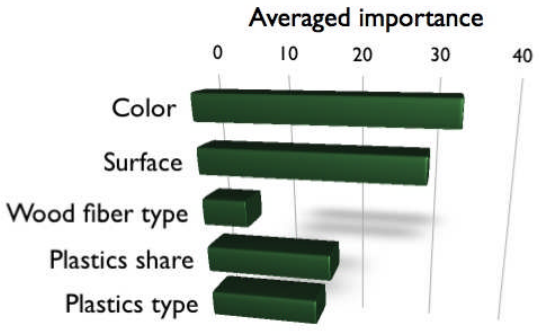


**Figure 8.** Conjoint analysis – attribute importance (n = 374).

Having a closer look at the attribute levels, a fine-corrugated surface seems to provide the highest utility to the respondents followed by a brushed surface. Rough surface had the lowest utility value (Figure 9). It is also quite obvious that respondents prefer light brown colored decks most followed by dark brown and beige at least (Figure 10).

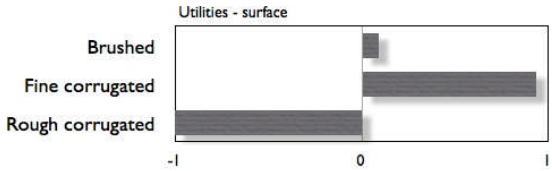


**Figure 9.** Conjoint analysis – utilities surface (survey 06/07, n = 374).

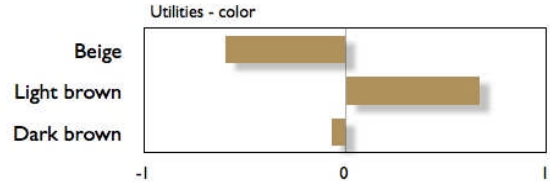


**Figure 10.** Conjoint analysis – utilities color (n = 374).

Respondents clearly prefer bioplastics and recycled plastics in contrast to virgin polypropylene and polyethylene (Figure 11). Care has to be taken when interpreting the utilities for plastics type because they might not be based on true behavior but socially desired behavior. That might bias results. Furthermore, the development of **bio-**composites is just under way. The respondents' preference for a low plastics share (Figure 12) corresponds with the results of the first section of the questionnaire.

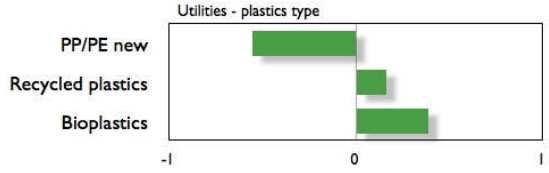


**Figure 11.** Conjoint analysis – utilities plastics type (n = 374).

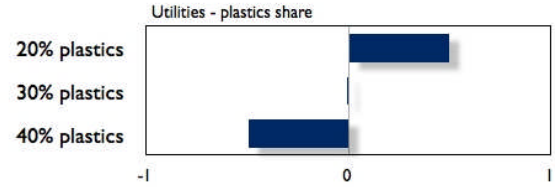


**Figure 12.** Conjoint analysis – utilities plastics share (n = 374).

At last it doesn't seem to matter to respondents if either virgin fiber or recycled fiber is used in the WPC compound (Figure 13).

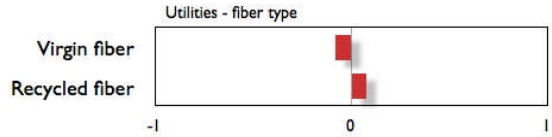


**Figure 13.** Conjoint analysis – utilities fiber type (n = 374).

## Closing remarks

The WPC market is growing worldwide. Extensive technical research is continuing specifically in Europe. Nevertheless, WPC still is an unfamiliar material to European consumers, including Austrians. Therefore, consumer perceptions of WPC decking were investigated in a survey with a focus on environmental aspects. Main reasons named by respondents in favor of buying WPC decking were durability, appearance, and low maintenance. The importance appearance is underlined by previous studies considering wood products, especially floors. This is also true for durability. Environmental issues range in the midfield. An additionally performed conjoint analysis, focusing on environmental issues as well, revealed that the attributes most important to respondents are the WPC deck's color and its surface. Again, appearance is the major purchase criterion, whereas polymer share and type are of "average" importance. Main reasons for denial of buying wood-plastic composite decking were the preference for wood or other materials and WPC's artificial character. Corresponding to that, a majority of respondents prefer a

low polymer share in the compound. Respondents named following factors for their satisfaction with wooden decks: appearance, comfort, naturalness and workability. Reasons provided by respondents for dissatisfaction were: lack of durability, extensive maintenance work, warp, splintering and cracks, greying i.e. discoloration, and slipperiness. These issues can be addressed and improved by WPC. Respective attributes are the ones to communicate the unique selling proposition (USP) of WPC decks in marketing strategies activities. Least important are various kind of services. That reduces the opportunity for distinguishing WPCs decking through services. Of "average" importance to consumers are ecological matters, which generally play a certain role when consumers purchase wood products. Concerning the environmental issues of WPC, respondents would prefer bioplastics and recycled plastics in contrast to virgin polymers. In general, WPC decking was perceived positively by respondents. It was perceived clearly innovative and durable, rather comfortable, but a little expensive and artificial.

## References


[1] Fell, D. and C. Gaston. 2001. Material Selection for Outdoor Projects in Western Canada. Forintek Canada Corporation. Project 2523.42. Vancouver, Canada.

[2] Thomas, J., D. Fell, and E. Hansen. 2004. Consumer Preferences for Decking Products: North America. Report for Project No. 1055. Forintek Canada Corporation. Vancouver, BC.

[3] Eder, A. and S. Weinfurter. 2005. Industrial Buyer and Consumer Requirements for Selected Wood-Plastic Composite Applications. Wood Fibre Polymer Composites International Symposium**,** 24-25 March 2005**,** Bordeaux, France

[4] Weinfurter, S. 2007. Consumer perceptions of wood-plastic composite decking. WOOD K plus - Kompetenzzentrum für Holzverbund-werkstoffe und Holzchemie, unpublished study.

[5] Fell, D., J. Thomas, and E. Hansen. 2006. Evolving consumer preferences for residential decking markets. The Forestry Chronicle, 82 (2):253-257.

[6] Mantau, U. and M. Knauf. 2008. Einmal Gartenholzkäufer immer Gartenholzkäufer. Befragung in Bau- und Fachmärkten zur Verwendung von Holz in der Außenanwendung – Teil 2. Holz-Zentralblatt, 15:413-414.

[7] Roos, A. and A.Q. Nyrud. 2008a. Preferences for pressure-treated wooden deck materials. Wood and Fiber Science, 40(3):436-447.

[8] Smith, P. and K. Bright. 2002. Perceptions of new and established waterfront materials: U.S. port authorities and engineering consulting firms. Wood and Fiber Science, 34(1):28-41.

[9] Roos, A. and A. Q. Nyrud. 2008b. Description of green versus environmentally indifferent consumers of wood products in Scandinavia: flooring and decking. Journal of Wood Science, 54: 402-407.

[10] Jonsson, O., S. Lindberg, A. Roos, M. Hugosson, and M. Lindström. 2008. Consumer perceptions and preferences on solid wood, wood-based panels and composites: A repertory grid study. Wood and Fiber Sience, 40:663-678.

[11] Kelly G.A. 1963. A Theory of personality : the psychology of personal constructs. Norton & Company, New York, NY

[12] Roos, A. and M. Hugosson. 2008. Consumer preferences for wooden and laminate flooring. Wood

Material Science and Engineering, 3(1):29-37.

[13] Eder, A. 2005. Marktchancen für innovative Holzwerkstoffe. Ergebnisse einer Business-to-Business Befragung in der Bau-, Innenausbau,- Möbel- und Autoindustrie. Dissertation. BOKU – University of Natural Resources and Applied Life Sciences Vienna.

[14] Crawford, C.M. and C.A. Di Benedetto. 2003. New Products Management. McGraw-Hill, Boston, MA.

[15] Ulrich, K.T. and S.D. Eppinger. 2004. Product Design and Development. 3rd ed. McGraw-Hill/Irwin, Boston, MA.

[16] Backhaus, K., B. Erichson, W. Plinke, and R. Weiber. 2000. Multivariate Analysemethoden. Eine Anwendungsorientierte Einführung. Springer, Berlin.

[17] Hair, J.F., Jr., R.E. Anderson, R.L. Tatham, and W.C. Black. 1995. Multivariate data analysis. 4th ed. Prentice Hall, Upper Saddle River, NJ.

[18] Cohen, D. H., C. Xie, and J. Ruddick. 1992. Retailer perceptions of treated Wood products in Vancouver, Britisch Columbia. Forest Product Journal, 42(3): 41-44.

[19] Shook, S.R. and I.L. Eastin. 2001. A characterization of the U.S. residential deck material market. Forest Products Journal, 51(4):28-36.

[20] Churchill, G.A., Jr. 1991. Marketing Research : Methodological Foundations. 5th ed. The Dryden Press, Chicago, IL.

[21] Eder, A., S. Weinfurter, P. Schwarzbauer, and S. Strobl. 2007. WPCs – An Updated Worldwide Market Overview Including a Short Glance at Final Consumers. Wood Fibre Polymer Composites International Symposium 2007. 26-27 March 2007. Bordeaux, France

[22] Osgood, C.E., C.J. Suci, and P.H. Tannenbaum. 1957. The Measurement of Meaning. University of Illinois Press, Urbana, IL.

[23] Garvin, D.A. 1984. What does product quality really mean? Sloan Management Review 26(Fall):25-43.

[24] Cronbach, L.J. 1951. Coefficient alpha and the internal structure of tests. Psychometrika, 31: 93-96.

[25] Bearden, W.O. and R.G. Netemeyer. 1999. Handbook of Marketing Scales : Multi-Item Measures for Marketing and Consumer Behavior Research. 2nd ed. Sage Publications, Thousand Oaks, CA.

[26] Bruner, G.C. and P.J. Hensel. 1992. Marketing scales handbook : a compilation of multi-item measures. American Marketing Association, Chicago, IL.

[27] DeVellis, R.F. 2003. Scale Development : Theory and Applications. 2nd ed. Sage Publications, Thousand Oaks, CA.